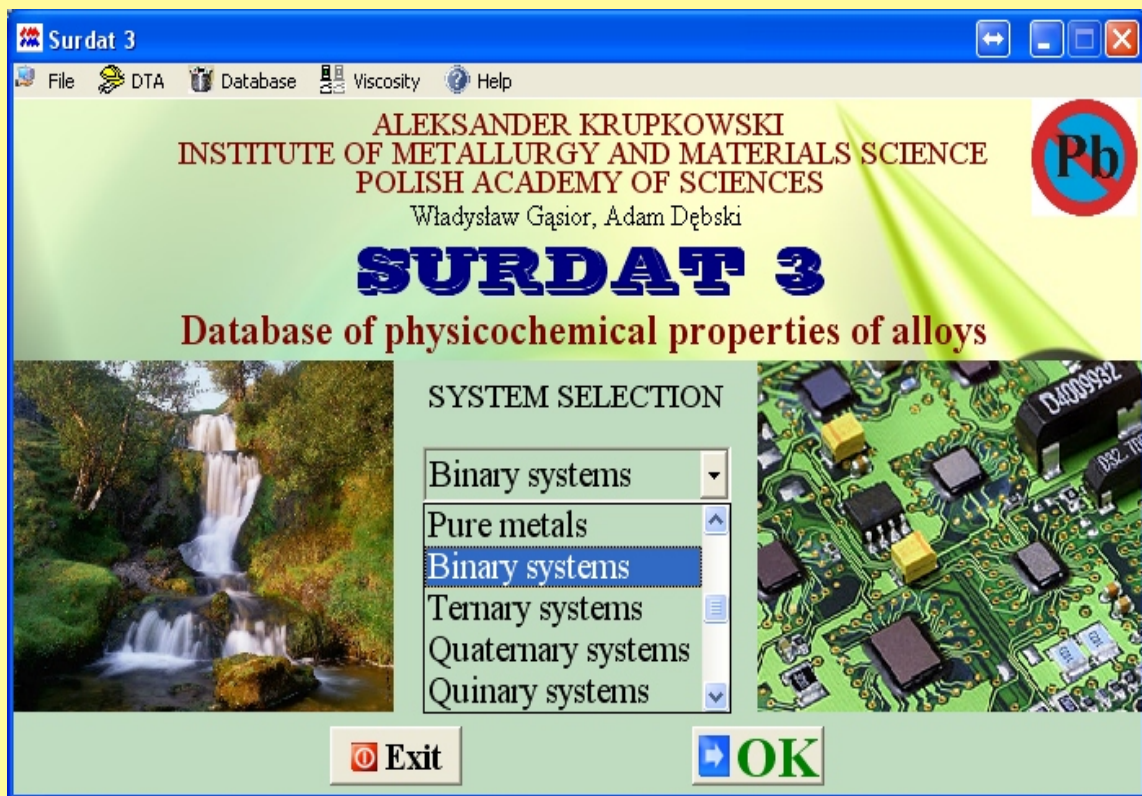


Władysław Gašior, Adam Dębski

SURDAT 3

Database of physicochemical properties
of alloys



Density, surface tension, molar volume,
viscosity, electrical properties, mechanical properties,
meniscographic data, DTA (liq, sol),
phase diagrams, NIST database



Institute of Metallurgy and Materials Science
Polish Academy of Sciences

Kraków 2019

SURDAT 3

Database of physicochemical properties of alloys

**Density, surface tension, molar volume, viscosity,
electrical properties, mechanical properties,
meniscographic data, DTA (liq, sol), phase diagrams,
NIST database**

W. Gąsior, A. Dębski

w.gasior@imim.pl
a.debski@imim.pl

Institute of Metallurgy and Materials Science
Polish Academy of Sciences
30-059 Kraków, 25 Reymonta Street, Poland

Kraków 2019

Reviewer:

John F. Smith[†], Professor Emeritus, Iowa State University, Ames, IA

Copyright © 2019 by Institute of Metallurgy and Materials Science Polish Academy of Sciences

ISBN 978-83-60768-08-2

SURDAT 3 – database of physicochemical properties of alloys is available on website <http://www.imim.pl>

All rights reserved. No part of this book may be reproduced or transmitted in any form or by any means, electronic or mechanical, including photocopying or by any information storage and retrieval system, without permission in writing from the publisher.

POLISH ACADEMY OF SCIENCES

Institute of Metallurgy and Materials Science

30-059 Kraków, ul. W. Reymonta 25, Poland

<http://www.imim.pl>

Issue I, 50 copies of issue, Kraków 2019

Printed in Poland

Contents

<i>Preface</i>	5
1. Introduction	8
2. Basics of solder material wetting	21
2.1. Wettability	21
2.2. Wettability forming factors	26
2.3. Wettability as technological property – wetting dynamics	27
2.4. Wetting time	28
2.5. Wetting force	29
2.6. Structure of solder-substrate joint	30
3. Experimental methods	31
3.1. Maximum bubble pressure method	31
3.2. Dilatometric method	33
3.3. Meniscographic method	34
3.3.1. Physical bases for meniscographic measurements	34
3.3.2. Surface and interfacial tension measurements by the Miyazaki method [1997Miy]	37
3.3.3. Measurement of wetting time and wetting force	39
3.4. Sessile drop method	42
3.4.1. Apparatus for wetting test by sessile drop method	42
3.5. Viscosity measurement by capillary flow method	47
3.6. Measurement of viscosity, density and surface tension by liquid outflow through the container orifice	57
4. Modeling of surface tension and viscosity	64

4.1. Surface tension modeling	64
4.1.1. Temperature relations of surface tension calculated from Butler's model	76
4.2. Monoatomic surface layer	88
4.2.1. Polarized atom model	88
4.2.2. Excess free energy of monoatomic phase	98
4.3. Modeling of metal alloy viscosity from thermodynamic and physical properties	104
5. NIST database	119
6. Presentation of SURDAT 3 database	123
6.1. Program installation	123
6.2. Application example	126
7. References	184
8. The abstracts of the most important publications	213

Preface

The idea of creating a database for the physico-chemical properties of metals and alloys came to life at the turn of the 20th and 21st century, after a few years of studies of the metallic systems which could potentially be applied as new lead-free solders in power and electronic engineering. The research performed at that time at A. Krupkowski Institute of Metallurgy and Materials Science of the Polish Academy of Sciences (IMMS PAS) focused on measurements of the physical properties of alloys, such as: surface tension and density as well as, sporadically, viscosity. At the same time, computer programs were being designed for the modelling of surface tension and viscosity in binary and multi-component solutions, which made it possible to analyze the agreement of the modelled values with the measured values, which, in turn, led to the development of own models.

After some significant experimental data for over a dozen systems and metals had been collected, the creation of an electronic database for lead-free solder materials began, which was to be commonly accessible, free of charge and successively expanded with new systems and properties. This way, the „*SURDAT. Database of Pb-free soldering materials*” came to life in the form of an electronic computer program, constituting a CD supplement to a book of the same title, which, in retrospect, can now be named SURDAT 1. Its authors were: Prof. Zbigniew Moser, PhD. Eng. (coordinator and co-author of several chapters), Władysław Gąsior, PhD. Eng, a PAS professor (author of a computer program for surface tension modelling as well as a few chapters), Adam Dębski, M.Sc. Eng. (author of the electronic version of the database as well as the installation guidelines and manual) and Janusz Pstruś, M.Sc. Eng. (executor of the experimental

studies). The first edition of the SURDAT database was issued in 2007. It contained the experimental and calculated surface tension data as well as the results of density and molar volume measurements for 10 metals and 17 binary, ternary and quaternary systems and, according to the previous plans, it was available at www.imim.pl, with the option of being installed at a PC.

The studies of lead-free metal alloys as potential substitutes for lead containing solders were continued and, as previously planned, the material for the expansion of SURDAT with new properties and systems was successively collected. The new database named „*SURDAT 2. Physico-chemical properties database for selected solders*” was issued in 2012 by the initiative of W. Gašior and A. Dębski, already after the passing of Prof. Z. Moser (2011). Compared to SURDAT 1, it contained experimental data for a larger number of physico-chemical properties as well as a much bigger group of systems (from binary to quinary ones). The collected experimental material was the effect of the research projects realized by the Polish Government and also within European funds such as: COST Action 531, COST Action MP0602 – HISOLD - Advanced solder materials for high temperature applications, the scientific network ELFNET and the MSWN Project 4582/BT08/2007/33. Some of the projects were implemented in cooperation with Tele-and Radio Research Institute in Warsaw (K. Bukat, J. Sitek, S. Korolewski, I. Rafalik) and Non-Ferrous Metal Institute (S. Księżarek), as well as Warsaw University of Technology (R. Kisiel, R. Biaduń, K. Szyłko). What is more, within the agreement with T. Siewert, PhD. from National Institute of Standards and Technology (NIST) in Boulder, Colorado, USA, SURDAT 2 was supplemented by the NIST database as well as other studies realized at A. Krupkowski Institute

of Metallurgy and Materials Science of the Polish Academy of Sciences (IMMS PAS). A book version of the SURDAT 2 database was issued in Polish, reaching out to a Polish user. Some of the chapters were elaborated in cooperation with Przemysław Fima, PhD. Eng., Tomasz Gancarz, PhD. Eng. and Janusz Pstruś, PhD. Eng.

After the issue of SURDAT 2, a decision was made by W. Gašior and A. Dębski to expand the scope of the presented data and create a new database, SURDAT 3, in English. The changes referred to viscosity modelling (new models were discussed, the computer program was modified and calculations for new systems were made) as well as surface tension modelling (the correction parameters for the calculation of the surface area of the mono-atomic surface layer and the excess free energy of the surface phase were determined). These steps greatly expanded the database of the binary systems, for which it was possible to acquire information on the cited quantities. The works on the new version were twofold. On the one hand, an English translation was prepared, with a big help of J.F. Smith, PhD, who provided assistance in the proofreading and the substantive aspect, and on the other hand, the viscosity and surface tension modelling programs were modernized, and the physical properties for new systems were calculated. In this way, the database has been significantly enlarged. Similarly to the older versions, a CD is attached to the book, which includes the database installation program as well as an electronic version of the book in English. The database is accessible free of charge and commonly available at the A. Krupkowski Institute of Metallurgy and Materials Science of the Polish Academy of Sciences website: www.imim.pl, to be installed on a PC.

1. Introduction

Experimental studies of the physical properties of lead-free solders were begun at IMIM PAS in 1998. These solders were of a type that is in the process of replacing the traditional but more toxic Sn-Pb solders. These lead-free solders were based mainly on the Sn-Ag and Ag-Sn-Cu eutectics with additions of In, Bi, or Sb. By 2007 enough data had been determined [2007Mos3] for surface tension, density, and molar volume of pure metals, binary alloys, and selected multi-component alloys to justify organization into a database.

The initial form (Fig 1.1) of this database is now known as SURDAT-1 and was made accessible free of charge at <http://www.imim.pl>. The numerical values presented in SURDAT were obtained during the implementation of:

- The COST 531 program,
- The ELFNET network, participated in by the members of the Associated Phase Diagram and Thermodynamics Committee,
- The research programs, projects and networks participated in by IMIM PAN, in cooperation with the industrial institutes: Tele and Radio Research Institute in Warszawa and Institute of Non-Ferrous Metals in Gliwice.

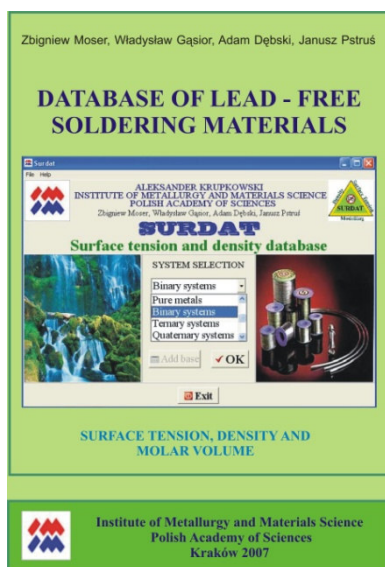


Fig. 1.1. The SURDAT database issued in 2007 as a monograph, together with installation software [2007Mos3]

In 2006, the SURDAT database was presented at the 16th Symposium on Thermophysical Properties, Boulder, CO, USA, and interest in the database was shown by personnel of the National Institute of Standards and Technology at Boulder Colorado, USA (NIST) [2006Mos4]. After the issuing of the monograph in 2007, the database was presented at the 2nd International Scientific and Technology Conference “Progress in Soldering Technologies” in Wrocław [2007Deb1, 2007Deb2]. Since 2007, the studies developing the database were continued within the scope of the research program “Project MSWN 4582/BT08/2007/33”, and modifications of the database were published and presented at foreign and local conferences [2007Mos4, 2007Gas1, 2008Gas1, 2009Gas1-3].

As suggested in [2010Gas1] and with cooperation between the authors of SURDAT and people at NIST, the SURDAT and NIST databases were combined in the new edition of SURDAT 2 and SURDAT 3.

SURDAT 3 has also been expanded by adding meniscographic test results obtained here at IMIM PAS and by relevant data generously contributed by Polish industrial institutes. It also includes the elaborated software for the modeling of the surface tension and viscosity of multi-component alloys with the application of their thermodynamic properties as well the physical properties of pure metals. New models have been developed here at IMIM PAN which allow the obtaining of a better correlation with experimental values than the correlation previously obtained [2009Gas3]. The cooperation with the local industrial institutes made it possible to expand the database with wetting characteristic such as wetting angle, wetting time and force, interfacial tension, as well as the eutectic and mechanical properties of solders and the joints of the soldered elements. The SURDAT 3 database was supplemented by the new test results obtained during the implementation of the COST MP0602 – HISOLD – Advanced Solder Materials for High Temperature Applications program, as well as by the wettability test results for the Sn-Zn eutectic alloys, with Bi, Sb and Li additions.

In the option scheme of SURDAT 3 presented in Fig. 1.2, the new physico-chemical properties as well as the new component elements, which were not present in the base published in 2007, are denoted by the * symbol.

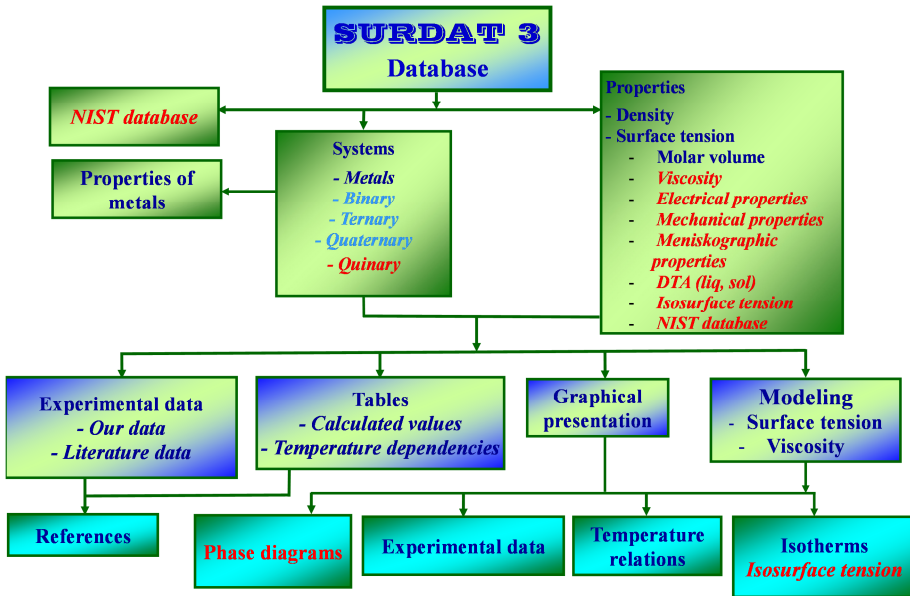


Fig. 1.2. Scheme of the options available in the SURDAT 3 database

SURDAT 3 includes data concerning the following:

- density (D),
- surface tension (ST),
- molar volume (MV),
- viscosity (V),
- electrical properties (RE, RY),
- mechanical properties (H, SS, TS, YM),
- meniscographic characteristics (WT, WA, IT),
- DTA (liq, sol),
- phase diagrams,

for the metals and alloys presented in Table 1.1. Table 1.1 presents data for 10 metallic elements, 29 binary alloys, 20 ternary alloys, 6 quaternary systems, and 1 quinary system. The red entries with the red * symbol denotes data for systems which were not available in the original SURDAT base of 2007.

Table 1.1. Metals and alloys in the SURDAT 3 database

Metals	Binary system		Ternary system		Quaternary and quinary systems
Pb Sn In	Pb - Sn	Ag - Sn	(Sn-Ag) _{ext} + In	(Sn-Ag) _{ext} + Bi	(Sn-Ag) _{ext} + Cu + Sb (Sn-Ag) _{ext} + Cu + Bi Ag-Cu-In-Sn * Bi-In-Sn-Zn * Bi-Cu-Sn-Zn * Bi-Sb-Sn-Zn * (Sn-Ag) _{ext} + Cu + Bi + Sb *
	Ag - In	Bi - Sn	(Sn-Ag) _{ext} + Cu	(Sn-Ag) _{ext} + Sb	
	In - Sn	Ag - Bi	Ag-Bi-In *	Ag-Cu-In *	
	Sb - Sn	Sn - Zn	Ag-Sn-Zn *	Ag-Bi-In *	
	Ag - Sb	Cu - Sn	Al-Sn-Zn *	Au-In-Sn *	
		Cu - Sb	Au-Sn-Zn *	Bi-Cu-Sn *	
	Ag	Ag-Au *	Bi-In-Sn *	Bi-Sb-Sn *	
	Bi	Al-In *	Bi-Sn-Zn *	Cu-Sn-Ti *	
	Sb	Al-Zn *	Cu-Sn-Zn *	Ga-In-Sn *	
	Cu	Au-In *	In-Sb-Sn *	In-Sn-Zn *	
Zn	Bi-Cu *				
Al	Bi-Zn *				
Au	Cu-Ti *				
	Ga-Sn *				
	In-Sb *				
	In-Zn *				
	Sn-Ti *				

Tables 1.2 ÷ 1.6 present the information on the availability of the data for the particular systems. The + symbol in the given system does not denote the set of data for the given property, but it only points to the fact that the base includes the selected data for the selected property. The – symbol denotes a lack of any data for the given property.

Table 1.7 shows the systems for which the DTA test results are available.

Index of symbols:

D – Density,

ST – Surface tension,

MV – Molar volume,

V – Viscosity,

RE – Resistance,

RY – Resistivity,

H – Hardness,

SS – Shear strength,

TS – Tensile strength,

YM – Yang modulus,

WT – Wetting time,

WF – Wetting force,

CA – Contact angle,

IT – Interfacial tension.

Table 1.2. Metals in the SURDAT 3 database

No	Metals	Properties									
		Physicochemical				Electrical		Mechanical			
		D	ST	MV	V	RE	RY	H	SS	TS	YM
1	Ag	+	+	+	+	-	-	-	-	-	-
2	Al	+	+	+	+	-	-	-	-	-	-
3	Au	+	+	+	+	-	-	-	-	-	-
4	Bi	+	+	+	+	-	-	-	-	-	-
5	Cu	+	+	+	+	-	-	-	-	-	-
6	In	+	+	+	+	-	-	-	-	-	-
7	Pb	+	+	+	+	-	-	-	-	-	-
8	Sb	+	+	+	+	-	-	-	-	-	-
9	Sn	+	+	+	+	-	-	-	-	-	-
10	Zn	+	+	+	+	-	-	-	-	-	-

The base also includes selected data for metals, such as: the atomic mass, the melting and boiling point, the crystalline structure (at room temperature) and the covalent and atomic radius.

Table 1.3. Binary systems in the SURDAT 3 database

No	System	PhD	Properties															
			Physicochemical				Electrical		Mechanical				Miscographic					
			D	ST	MV	V	RE	RY	H	SS	TS	YM	WT	WF	CA	IT		
1	Ag-Au	+	-	+	-	+	-	-	-	-	-	-	-	-	-	-	-	
2	Ag-Bi	+	+	+	+	-	-	-	-	-	-	-	-	-	-	+	-	
3	Ag-Cu	+	+	+	+	-	-	-	-	-	-	-	-	-	-	-	-	
4	Ag-In	+	+	+	+	-	-	-	-	-	-	-	-	-	-	-	-	
5	Ag-Sb	+	+	+	+	-	-	-	-	-	-	-	-	-	-	-	-	
6	Ag-Sn	+	+	+	+	+	+	-	+	-	+	-	+	-	+	+	+	
7	Al-In	+	-	+	-	-	-	-	-	-	-	-	-	-	-	-	-	
8	Al-Sn	+	+	+	-	-	-	-	-	-	-	-	-	-	-	-	-	
9	Al-Zn	+	+	+	+	-	-	-	-	-	-	-	-	-	-	-	-	
10	Au-Cu	+	+	+	+	-	-	-	-	-	-	-	-	-	-	-	-	
11	Au-In	+	+	+	+	-	-	-	-	-	-	-	-	-	+	-	-	
12	Au-Sn	+	+	+	+	-	-	-	-	-	-	-	-	+	-	+	-	
13	Bi-Cu	+	+	-	+	-	-	-	-	-	-	-	-	-	-	-	-	
14	Bi-In	+	+	+	+	-	-	-	-	-	-	-	-	+	-	-	-	

No	System	PhD	Properties														
			Physicochemical									PhD					
			D	ST	MV	V	RE	RY	H	SS	TS	YM	WT	WF	CA	IT	
15	Bi-Sn	+	+	+	+	-	-	-	-	-	-	-	-	-	-	-	-
16	Bi-Zn	+	-	-	+	-	-	-	-	-	-	-	-	-	-	-	-
17	Cu-In	+	+	+	-	-	-	-	-	-	-	-	-	-	-	-	-
18	Cu-Sb	+	+	+	-	-	-	-	-	-	-	-	-	-	-	-	-
19	Cu-Sn	+	+	+	+	-	-	-	-	-	-	-	-	-	+	-	-
20	Cu-Ti	+	+	-	-	-	-	-	-	-	-	-	-	-	-	-	-
21	Ga-In	+	+	-	-	-	-	-	-	-	-	-	-	-	-	-	-
22	Ga-Sn	+	+	-	-	-	-	-	-	-	-	-	-	-	-	-	-
23	In-Sb	+	+	-	+	-	-	-	-	-	-	-	-	-	-	-	-
24	In-Sn	+	+	+	+	-	-	-	-	+	-	-	-	-	-	+	-
25	In-Zn	+	+	+	+	-	-	-	-	-	-	-	-	-	-	-	-
26	Pb-Sn	+	+	+	+	-	-	-	-	-	-	-	-	-	+	-	-
27	Sb-Sn	+	+	+	-	-	-	-	-	-	-	-	-	-	-	-	-
28	Sn-Ti	+	+	-	-	-	-	-	-	-	-	-	-	-	-	-	-
29	Sn-Zn	+	+	+	+	-	-	-	-	-	-	-	-	-	+	-	-

No	System	PhD	Properties																
			Physicochemical				Electrical		Mechanical					Meniscographic					
			D	ST	MV	V	RE	RY	H	SS	TS	YM	WT	WF	CA	IT			
15	Bi-Sn-Zn	+	+	-	-	-	-	-	-	-	-	-	-	-	-	-	-	-	
16	Cu-Sn-Ti	-	+	-	-	-	-	-	-	-	-	-	-	-	-	-	-	-	
17	Cu-Sn-Zn	+	+	-	-	-	-	-	-	-	-	-	-	-	+	+	+	-	
18	Ga-In-Sn	-	+	-	-	-	-	-	-	-	-	-	-	-	-	-	-	-	
19	In-Sb-Sn	+	+	-	+	-	-	-	-	-	-	-	-	-	-	-	-	-	
20	In-Sn-Zn	+	+	+	+	-	-	-	-	-	-	-	-	-	+	+	-	-	

Table 1.5. Quaternary systems in the SURDAT 3 database

No	System	PhD	Properties																
			Physicochemical				Electrical		Mechanical					Meniscographic					
			D	ST	MV	V	RE	RY	H	SS	TS	YM	WT	WF	CA	IT			
1	Ag-Bi-Cu-Sn	-	+	+	-	+	+	-	+	+	-	-	-	-	+	+	+	+	
2	Ag-Cu-In-Sn	-	+	-	-	-	-	-	-	-	-	-	-	-	-	-	-	+	
3	Ag-Cu-Sb-Sn	-	+	+	-	-	-	-	-	-	-	-	-	-	-	-	-	-	
4	Bi-Cu-Sn-Zn	-	-	-	-	-	-	-	-	-	-	-	-	-	-	-	-	-	
5	Bi-In-Sn-Zn	-	+	-	-	-	-	-	-	-	-	-	-	-	-	-	-	-	
6	Bi-Sb-Sn-Zn	-	+	+	-	-	-	-	-	-	-	-	-	-	-	-	-	-	

Table 1.6. Quinary systems in the SURDAT 3 database

No	System	PhD	Properties													
			Physicochemical			Electrical		Mechanical				Micrographical				
			D	ST	MV	V	RE	RY	H	SS	TS	YM	WT	WF	CA	IT
1	Ag-Bi-Cu-Sb-Sn	-	+	+	+	-	+	+	-	+	+	+	-	+	+	+

Table 1.7. DTA results available in the SURDAT 3 database

No	Binary systems	Ternary systems	Quaternary systems	Quinary systems
1	Ag-Sn	Ag-Cu-Sn	Ag-Bi-Cu-Sn	
2	Sn-Zn	Bi-Sn-Zn	Ag-Cu-In-Sn	-
3	-	Li-Sn-Zn	Bi-Sb-Sn-Zn	

2. Basics of solder material wetting

2.1. Wettability

Wettability is the property describing the character of the connection between the liquid and the solid phase in a system of three phases, of which one is solid (often treated as the so-called substrate), one is liquid and one is gaseous or liquid. The system of the surface forces at the point situated on the contact line of the three phases (Fig. 2.1.1.) determines the shape of the liquid phase's surface and the force of the connection. Wettability is not a measurable physical quantity; it presents the system of the surface forces in a descriptive manner. We can thus designate the wettability as good or constant, and these qualifications can merely be utilized for the technological purposes.

Wettability is characterized by the so-called wetting angle θ , which is a measurable physical quantity. Figure 2.1.1 presents the system of the surface forces existing in the case of a drop of liquid resting on a horizontal chemically inert and non-deformable substrate, in the atmosphere of an inert gas. The forces are referred to the unitary surface and, in this form, they are called interfacial tensions. They are denoted as follows:

- for solid phase in contact with gas: σ_{SV} ,
- for liquid phase in contact with gas: σ_{LV} ,
- for contact of solid and liquid phase: σ_{SL} .

The first two quantities also refer to surface tensions.

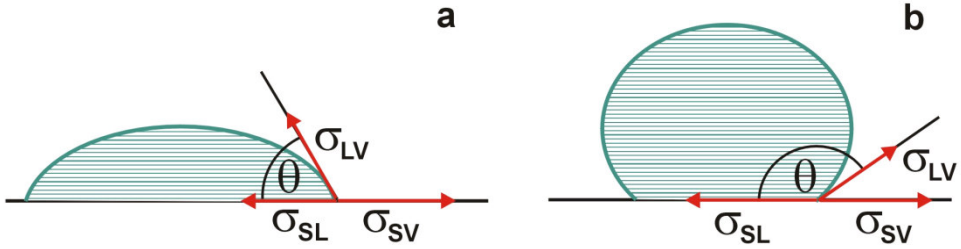


Fig. 2.1.1. Surface forces for the system: drop of liquid-horizontal substrate-gas. **a)** good wettability, **b)** lack of wettability

Interfacial tension is connected with the Gibbs free energy of the system of two phases, in the following manner:

$$\sigma_{ij} = \left(\frac{\partial G_{ij}}{\partial A} \right)_{T,P} \quad (2.1.1)$$

where **A** designates the surface area of the phase boundary.

From the system of the interfacial tensions presented in Fig. 2.1.1 we obtain the following relation, called the Young equation:

$$\sigma_{SV} - \sigma_{SL} = \sigma_{LV} \cdot \cos \theta \quad (2.1.2)$$

where: θ is the wetting angle.

The work needed to create a connection with a unitary surface of two phases, that is the work of adhesion W_a , is described by the Dupré equation:

$$W_a = \sigma_{SV} + \sigma_{LV} - \sigma_{SL} \quad (2.1.3)$$

where W_a is the work of adhesion.

The result of a combination of formulae (2.1.2) and (2.1.3) is formula (2.1.4), called the Young–Dupré equation.

$$W_a = \sigma_{LV} \cdot (1 + \cos \theta) \quad (2.1.4)$$

Equation (2.1.4) implies that with the increase of the wetting angle θ , the work of adhesion decreases, which is understood as the drop of wettability. It is assumed that the wettability is weak for the wetting angles exceeding 90° , and it is good for those significantly lower than this border value.

The Young equation (2.1.2) implies that:

$$\cos(\theta) = \frac{\sigma_{SV} - \sigma_{SL}}{\sigma_{LV}} \quad 2.1.5)$$

Fig. 2.1.2. illustrates the relation between the quantity of the difference ($\sigma_{SV} - \sigma_{SL}$) and the surface tension of liquid σ_{LV} , and the wetting angle θ . It can be seen that the occurrence of wettability ($\theta < 90^\circ$) depends on the sign of the difference ($\sigma_{SV} - \sigma_{SL}$), and not on the surface tension of the liquid.

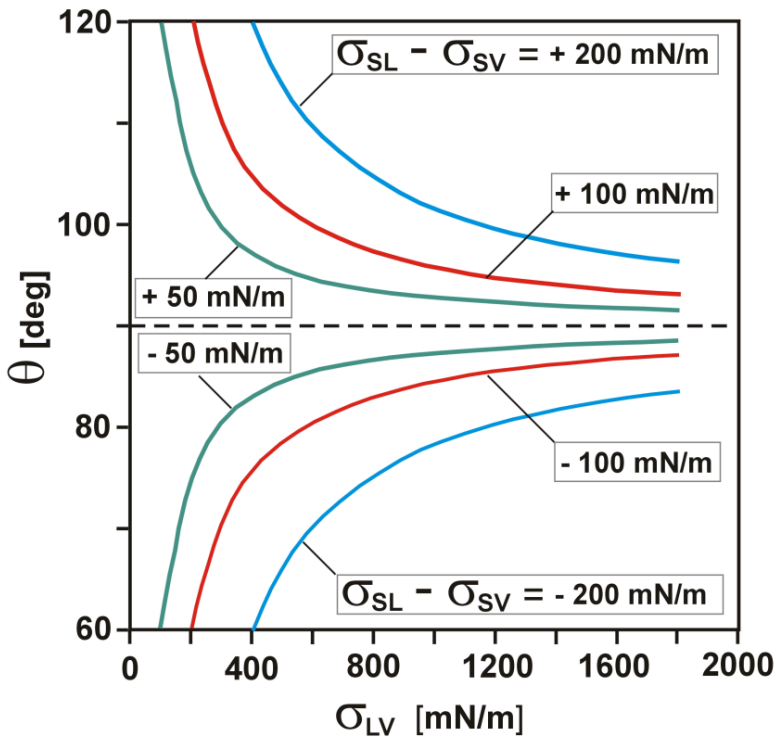


Fig. 2.1.2. Relation of the wetting angle value on the surface tension and interfacial tension values in a system of three phases s-l-g, determined by the Young equation

However, with higher values of the liquid's surface tension, a slight change in the value of the difference ($\sigma_{SV}-\sigma_{SL}$) can result in a transition from the state of wetting to the state of no wetting, or vice versa. The σ_{SV} value does not change with the change of the liquid in the systems of the given substrate, and so the wettability is determined by the σ_{SL} value. The higher it is, the better the wetting.

In the practical aspect, the concept of wettability is connected with its application in material technologies. The latter mostly relates to the creation of stable connections of different phases, mainly soldered joints. Coating steel products with a protective layer of zinc (hot-dip galvanizing) also requires achieving a high quality wetting of the steel by the zinc-based liquid alloy. In the production of various composites, e.g. fibres of a ceramic material in metal (Al/Al₂O₃), good wettability determines the proper mechanical properties.

Wettability is also a very significant element determining the course of high temperature metallurgical processes. In the first place, one can mention the effect typical for the steel metallurgy, that is interaction between fine (normally 1 – 100 μm in diameter) particles of non-metallic precipitates, mainly of the oxide- and more seldom of the nitride- and sulfide type, which are the product of steel deoxidation. The low wettability of these particles makes them tend to create interconnections under the effect of the surface forces. Such connection of two particles in liquid metal is stable. The result is a progressing agglomeration of particles, which facilitates their outflow, according to the Stokes law [1992Muk].

The same mechanism is also responsible for the adhesion of non-metallic precipitates into ceramic surfaces of metallurgical aggregates. This phenomenon is usually advantageous from the point of view of the

steel purity; however, it sometimes causes the overgrowth of the canals of small sections, e.g. of the nozzle in a crystallizer of continuous steel casting. Similar problems are also typical for the aluminium metallurgy.

The above description implies that, in realistic processes, the interlocation of 2 or 3 phases in the system where the wetting takes place, can be very diverse. The surface of the solid phase can have a flat, oval or cylindrical shape and it can be situated at different angles with reference to the horizontal. The actual wetting conditions of the phases in the processes of material technologies divert from the ideal case, for which one can apply equations (2.1.2 – 2.1.4). The most significant differences are related to the following:

- The presence of impurities which physically modify the conditions of the phase contact, such as the layer of the adsorbed gas on a solid or liquid surface, the layer of the substance being the result of oxidation (e.g. Al_2O_3 on the surface of Al), or minor outside impurities.
- The effect of the components of the liquid phase, consisting in the lowering of the surface tension σ_{LV} by one or more elements, which accumulate in the surface layer. Especially strong is the effect of oxygen and sulphur, which are typical surface-active components.
- The occurrence of a chemical reaction between the solid and liquid phase, which can result in:
 - a) a change in the chemical composition of the phases (especially the liquid one) in the area of their contact surface,
 - b) a change of the character of the solid phase's surface by the reaction products, and in consequence, a change in the surface tension values σ_{SV} , and σ_{SL} .

- The occurrence of porosity and irregularity of the surface.

The work of adhesion is equivalent to the change in the Gibbs free energy, in the process in which, in the initial state, two phases – solid and liquid – are separated, and in the final state, they create a connection. This work consists of a physical and a chemical part. The physical part is exclusively connected with the surface energy balance, and the chemical one – with the sequence of the chemical processes, which leads to the creation of one or more new phases. The Young–Dupré equation describes the ideal case, when the chemical part does not occur. However, under the conditions of a real experiment, even when the chemical part can be negligible, additional effects take place, such as the porosity of the surface or the presence of fine solid particles or gases.

2.2. Wettability forming factors

An additional factor which modifies the state of equilibrium at the contact point of three phases is the presence of a flux. The job of a flux is to prepare the surface of the substrate, which, through the elimination of the impurities, should cause the lowering of the σ_{SV} value, and also the improvement of wettability, that is the lowering of the wetting angle's value. A liquid flux, providing that it is introduced in a proper amount, constitutes the third phase in the system, together with a solid substrate and a liquid solder. In this case, the Young equation assumes the following form:

$$\sigma_{SF} - \sigma_{SL} = \sigma_{LF} \cdot \cos \theta \quad (2.2.1)$$

where σ_{SF} and σ_{LF} designate the interfacial tensions between, respectively, the solid substrate and the flux, and the liquid solder and the flux. The interfacial tension between the substrate and the flux is described by the ability of the flux to dissolve impurities.

A significant element modifying the wettability is the presence of surface-active elements in the liquid metal, mainly oxygen, which change the value of the surface tension σ_{LV} , and also, the application of a flux, σ_{LF} . Such situation causes the lowering of the wetting angle. On the other hand, with high partial pressures of oxygen, the surface of the liquid solder becomes impure because of the oxide in the liquid or solid form, which drastically lowers the wettability. For example, the work [2007Sob1] presents the results of the tests of the behaviour of liquid tin placed on a copper substrate. Under the atmospheric pressure, which means a significant degree of oxidation of both surfaces forming the connection, the wetting angle equaled 136° . Here we can state a lack of wettability. However, if the test is conducted under a much lower pressure, $2 \cdot 10^{-4}$ Pa, the wetting angles' value will drop to 52° . In the case of the application of a feeder which mechanically removes the outer oxidized tin layer, and under a lower pressure, one can obtain the wetting angle equaling 23° .

2.3. Wettability as technological property – wetting dynamics

One of the conditions for the applicability of the Young equation is an ideally smooth and clean surface of the substrate. It is also assumed that there are no chemical interactions between the phases. Under such conditions, the shape of the drop of liquid resting on the substrate, and so the contact angle θ as well, should not change in time. In fact, when the

time of the liquid's (liquid alloys') contact with the base increases, one can observe a change in the shape of the drop and a decrease of the value of the contact angle θ . The work of Moser et al. [2011Mos1] presents the results of an experimental determination of the wetting angle by the sessile drop method (experiment performed according to the scheme in Fig. 2.1.1), which imply that, for tin alloys containing about 3% Ag, about 0.5% Cu and 2 – 14 % In, on a Cu substrate and at 250°C, the wetting angle significantly decreases with time:

- 1) After 4 s from the beginning of the experiment, the wetting angle values equaled 69-81, whereas after 600 s, they were 25° – 32°.
- 2) A significant change in the wetting angle value takes place in a time shorter than 100 s.

As the effect described above is commonly observed, one can pose the question whether to treat the initial value of the wetting angle as the equilibrium one, or rather the final value thereof. The former concerns a system in which the surface impurities, e.g. the adsorbed gases, play an important role. As for the latter, it can include the effect of the chemical reaction between the liquid metal and the substrate. From the point of view of the quality of the connection, the final value of the wetting angle is more significant.

2.4. Wetting time

The concept of wetting time as a characteristic measurable quantity refers to the procedure of the meniscographic measurement which in fact directly determines the value of the vertical component of the surface force ($\mathbf{P} \cdot \sigma_{LV} \cdot \cos\theta$), where \mathbf{P} designates the length of the contact line of the liquid

with the immersed solid material. This concept concerns the initial stage of the process, when, after the immersion of the solid element in the liquid alloy, the surface force counterbalances the buoyant force. The tin-based lead-free solders, such as 91.4Sn/4.1Ag/0.5Cu/4In and 88Sn/3.5Ag/4.5Bi/4In, examined at 245 °C demonstrate the wetting time values of 0.7 – 0.8 s, which are only slightly higher than those for the 63Sn37Pb alloy. It is considered that in the case of wave soldering, the wetting time should be less than 1 s, and these conditions are fulfilled by the alloys of a quite diverse composition. With reflow soldering, the required wetting time must be lower than 2 s.

The effect of temperature on the wetting time is very strong. Glazer [1995Gla] states that the Sn-eutectic wets the tin 5 times faster at 210 °C than at 170°C. In the case of the Sn-Zn-Ag-Al-Ga alloy, gallium in the amount of 2 % significantly shortens the wetting time at 220 °C (by 1/3). At higher temperatures, this influence is weaker.

2.5. Wetting force

Wetting force is determined in the meniscographic experiment. It operates on the line of contact of three phases: the liquid alloy, the gas and the sampler, which is a homogeneous bar with a constant surface of the horizontal section and the perimeter **P**. The value of the vertical component of the wetting force is given as:

$$\mathbf{F}_w = \sigma_{LV} \cdot \mathbf{P} \cdot \cos\theta \quad (2.4.1)$$

The meniscographic test records the vector sum of the vertical component of the sampler's wetting force and the buoyant force operating on the sampler. The zero value of the wetting force refers to the beginning of the

experiment – the zero immersion of the sampler. The course of the wetting curve for the given type of soldering alloy and sampler, at a constant temperature, depends on the perimeter of the sampler and the depth of the immersion. Thus it is difficult to compare the wetting force values for different materials. The results of the wetting force tests presented in the literature are usually of the order of a few mN.

2.6. Structure of solder-substrate joint

The creation of a soldered joint above all requires the wetting of the substrate by the liquid phase. Next, as a rule, a joining layer is formed, built of intermetallic compounds, and this requires a partial dissolution of the substrate material by the liquid solder. This layer becomes thicker at a rate which is determined by the diffusion of the components of the forming compound. The growth rate is proportional to $t^{1/2}$ or $t^{1/3}$. The temperature effect on the layer's growth rate depends on the diffusion's activation energy.

In the case of the application of tin and the eutectic Sn-Cu, Sn-Ag and Sn-Bi alloys, as well as one such as Sn-Ag-Cu, the same intermetallic compounds are formed: Cu_3Sn on the side of the Cu substrate and Cu_6Sn_5 on the side of the solder. Ag and In do not form intermetallic compounds in this case. With a Ni substrate, Ni_3Sn_2 and Ni_3Sn_4 compounds are created. In the case of the Sn-Zn or Sn-Zn-Bi alloys, the formation of the Cu_5Zn_8 compound is observed, which forms a layer on the copper substrate [2006Liu2].

3. Experimental methods

3.1. Maximum bubble pressure method

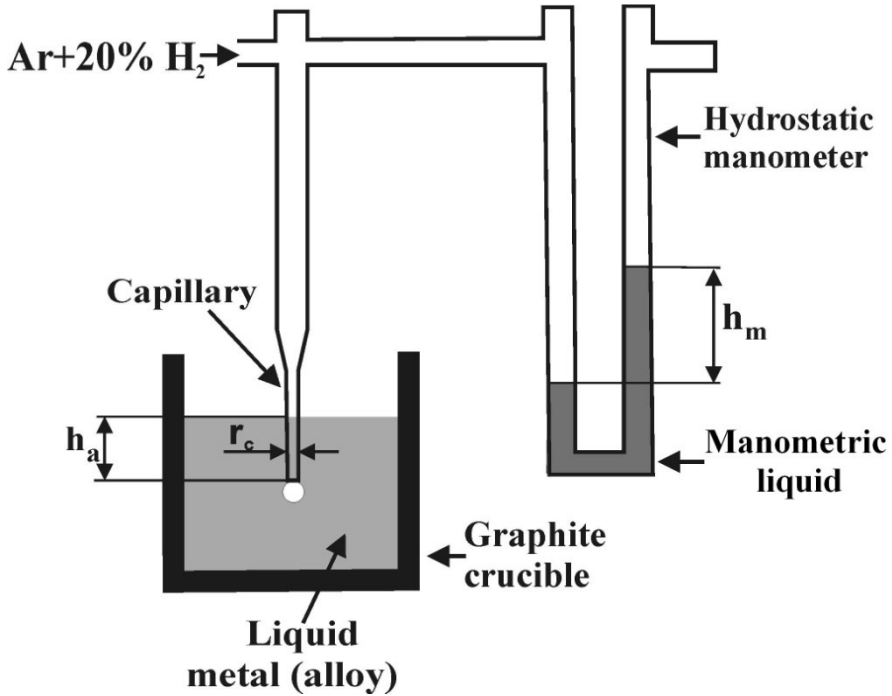


Fig. 3.1. . Experimental arrangement for the surface tension measurements by the maximum bubble pressure method

The maximum bubble pressure method was used in the surface tension measurements. The method is based on the known capillarity equation:

$$\sigma = \frac{1}{2} r \Delta p \quad [N/m] \quad (3.1.1)$$

describing the relation between the surface tension σ , the radius of the capillary r and the pressure Δp necessary to form and to detach

the gas bubble from the end of the capillary. The Δp is, in fact, the pressure difference between the gas pressure and the hydrostatic pressure of the liquid alloy and it is given by the following equation:

$$\Delta p = p_g - p_a \quad [N/m^2] \quad (3.1.2)$$

$$\Delta p = g(\rho_m h_m - \rho_a h_a) \quad [N/m^2] \quad (3.1.3)$$

where: p_g - the gas pressure, p_a - the hydrostatic pressure, g - the acceleration of gravity, ρ_a and ρ_m - the density of the investigated liquid alloy and manometric liquid, h_a - the immersion depth of the capillary and h_m - the height of the manometric liquid. The scheme for measuring the surface tension is shown in Fig.3.1. The surface tension calculated from Eq.3.1.1 presents the approximate value; thus, the exact values of surface tensions were calculated using the procedure proposed by Sugden [1922Sug].

3.2. Dilatometric method

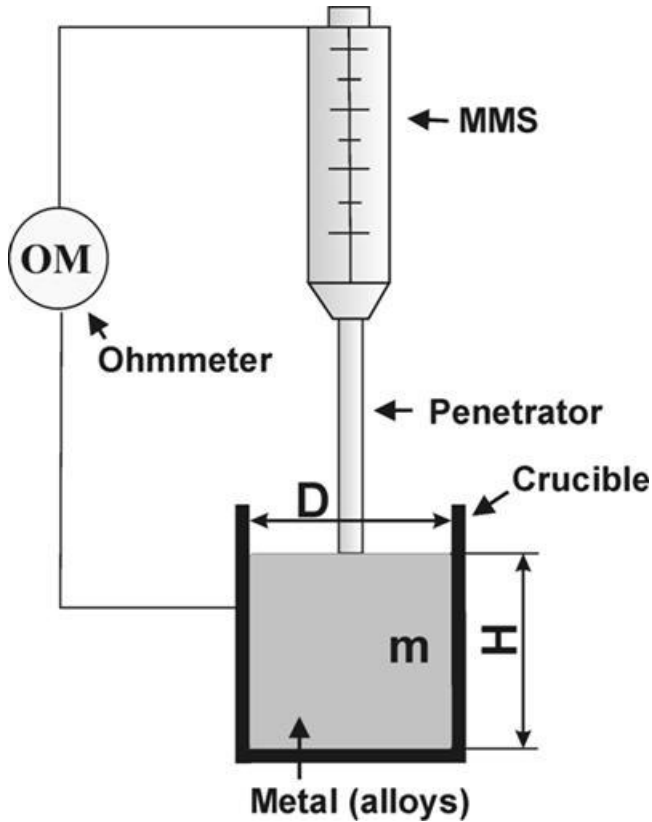


Fig. 3.2. Experimental set - up for density measurements by the dilatometric method. MMS denotes the screw micrometer

The densities were measured by the dilatometric method (shown schematically in Fig. 3.2) based on the measurement of the height of the constant weight of the alloy in the crucible of the diameter **D**. The density is calculated from the following equation:

$$\rho = \frac{m}{V} \quad (3.2.1)$$

$$V = \frac{\pi D^2 H}{4} \quad (3.2.2)$$

In equation (3.2.1) and (3.2.2) ρ is the density, m - the weight of alloy, V - the volume of the alloy, D - the crucible diameter and H - the height of the alloy in the crucible. The correction on the thermal expansion of the crucible was made at each measured temperature.

3.3. Meniscographic method

The meniscographic studies are applied in the observation of the dynamic process of wetting through the measurement of the force which operates between the immersed sampler and the liquid solder, in the given time. In a sense, they constitute a simulation of the first stage of soldering, when the soldering alloy is still liquid.

3.3.1. Physical bases for meniscographic measurements

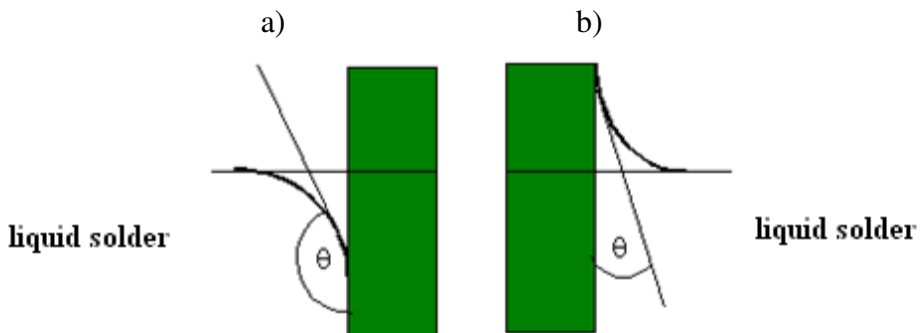


Fig. 3.3.1. Wetting cases **a)** non-wetted surface $\theta > 90^\circ$,
b) wetted surface $\theta < 90^\circ$

Figure 3.1.1 presents two cases when the sampler is immersed in the liquid alloy. In Fig. 3.1.1a, the solid surface of the sampler is not wetted by the alloy, whereas in Fig. 3.1.1b, the wetting takes place. The character of the interaction between the solid surface and the alloy depends on the set of the surface (or interfacial) tensions which are formed as a result of the molecular interaction between:

- The solid and the liquid phase - σ_{SL} ,
 - The solid and the gaseous phase - σ_{SV} ,
 - The liquid and the gaseous phase - σ_{LV} ,
- or σ_{SF} and σ_{LF} , when the flux replaces the gaseous phase.

The state of equilibrium of this system is described by the Young equation:

$$\sigma_{SV} + \sigma_{SL} + \sigma_{LV} = 0 \quad (3.3.1)$$

where: σ_{SV} - the interfacial tension between the substrate and the gaseous phase,

σ_{SL} - the interfacial tension between the liquid alloy and the substrate,

σ_{LV} - the surface tension between the liquid alloy and the gaseous phase.

When a flux is applied, the equation describing the state of equilibrium assumes the following form:

$$\sigma_{SF} + \sigma_{SL} + \sigma_{LF} = 0 \quad (3.3.2)$$

where: σ_{SF} - the interfacial tension between the substrate and the flux,

σ_{LF} - the interfacial tension between the liquid alloy and the flux.

If the sampler is wetted by the alloy, the meniscographic method determines

and records in a continuous manner the difference of the vertical component's value of the wetting force, originating from the surface tension F_w , and the buoyant force F_g :

$$F_r = F_w - F_g \quad (3.3.3)$$

where: F_r - the measured resultant force,
 F_w - the vertical component of the wetting force,
 F_g - the buoyant force.

In the state of equilibrium, the above relation can be noted by means of the Laplace's equation [1989Kle]:

$$F_r = \sigma_{LV} \cdot l \cdot \cos \theta - \rho \cdot V \cdot g \quad (3.3.4)$$

Or, in the case of the flux application:

$$F_r = \sigma_{LF} \cdot l \cdot \cos \theta - \rho \cdot V \cdot g \quad (3.3.5)$$

where:

F_r – the value of the force measured by the meniscographic system,
 σ_{LV} – the surface tension between the liquid alloy and the gaseous phase (air),
 σ_{LF} – the interfacial tension between the liquid alloy and the flux,
 L – the perimeter of the sample (in the horizontal section),
 ρ - the density of the soldering alloy at the measurement temperature,
 P – the surface area of the sample's horizontal section,
 h – the depth of the sample's immersion,

g – the gravitational constant (9.81 m/s^2).

The above relations (3.3.3-3.3.5) constitute the basis for the two most important applications of the meniscographic method:

- The measurement of the surface or interfacial tension (when a flux is used) of the liquid alloy,
- The measurement of the wetting time and force in an experiment simulating the real soldering process.

3.3.2. Surface and interfacial tension measurements by the Miyazaki method [1997Miy]

This method is dynamic in character, and it consists in vertical immersion of the sampler made of a material non-wettable by the liquid alloy, such as Al_2O_3 or Teflon, at a constant rate, in the liquid solder. The wetting angle of the sampler θ is initially slightly smaller than π (180°), but after exceeding a certain critical immersion value, it reaches the π value, which corresponds to a complete decline of wettability. The force operating on the sampler, which originates from the surface tension, from this moment on, is directed vertically up. In the system: sampler-liquid solder-atmosphere, the following vertical forces operate:

- the sampler's weight,
- the buoyant force,
- the force originating from the surface tension.

The weight of the sampler is usually counterbalanced through the calibration of the meniscograph, which is a device recording the forces in the wetting process, and so, it is not considered during the measurement. The values of the two remaining forces depend on the depth of the sampler's

immersion, its perimeter and the surface tension between the liquid alloy and the air, or the interfacial tension between the liquid alloy and the flux, in the case when a flux is applied. When there is a complete lack of wettability, the force operating on the sampler is directly proportional to the immersion depth. In diagram $F_r = f(h)$, this is indicated by a straight line (Fig. 3.3.2). It can thus be inferred that the ordinate of the conventional point of transition of diagram $F_r = f(h)$ into a straight line (described by extrapolation) determines the value of the surface tension of the liquid alloy in air or of the interfacial tension: liquid alloy/flux, if the measurements include the use of the latter.

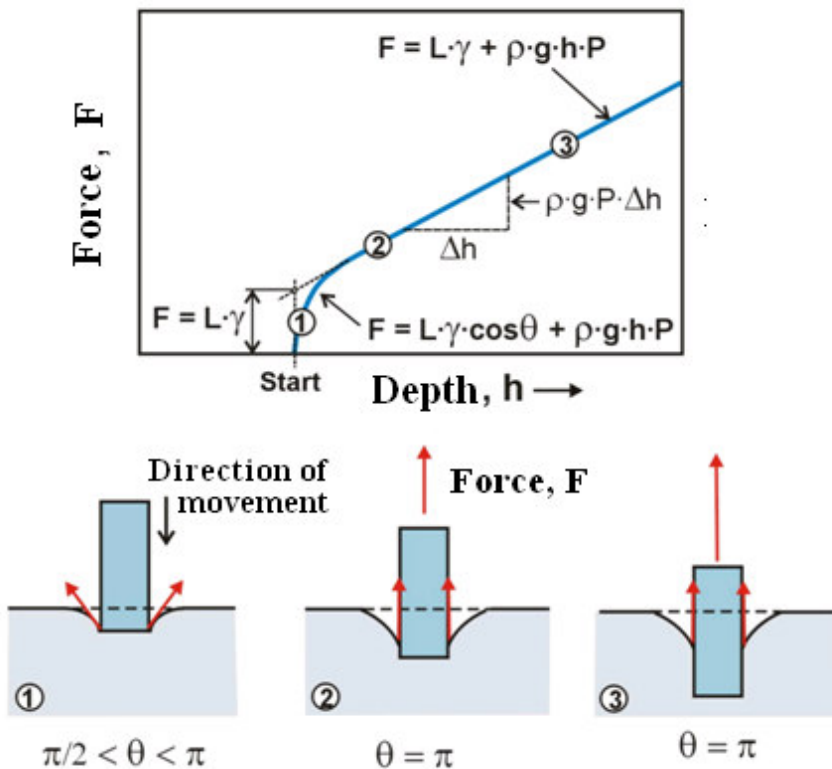


Fig.3.3.2. Scheme of meniscographic method according to Miyazaki [1997Miy]

The basic condition for a proper measurement of the surface (or interfacial) tension, when this method is used, is the achievement of the state of complete non-wettability of the sampler by the alloy. This is determined by both the surface properties of the sampler material and the properties of the applied flux; as for direct determination of the wetting degree, it is practically impossible in a meniscographic experiment. The latter results from the fact that the measurement of the surface tension requires the selection of the optimal sampler material and flux for the given alloy. The tests presented in Mizayaki's work [1997Miy] imply that when a flux is not applied, there is the case of an undesirable wetting for five tested sampler materials, and the only exception is the behavior of Al_2O_3 .

The effect of the use of different fluxes has been shown in publication [2004Gas2], which describes the measurement of the surface tension of the Sn-Ag eutectic and additionally, also of the Sn-Pb eutectic, with 8 different fluxes. The selection criterion for the best flux was a relatively low value of the interfacial tension obtained in the measurement and a small scatter of results.

3.3.3. Measurement of wetting time and wetting force

Another application of the meniscographic method is a simulation of the soldering process and it consists in determining the wetting curve for an immobile sampler immersed in a liquid alloy. The wetting curve represents the change of the force operating on the immersed sampler from the side of the liquid alloy. The sample's weight is counterbalanced through the calibration of the meniscograph and it is not considered in the analysis. An exemplary wetting curve can be seen in Fig.3.3.3. The vertical

component of the non-wetting force, that is the repulsive force ($\cos\theta < 0$), assumes negative values in the diagram, whereas the wetting force assumes positive values.

The experiment begins with constituting a contact between the sampler and the surface of the liquid alloy (point **a**). Next, the sampler is immersed in the alloy down to the determined level.

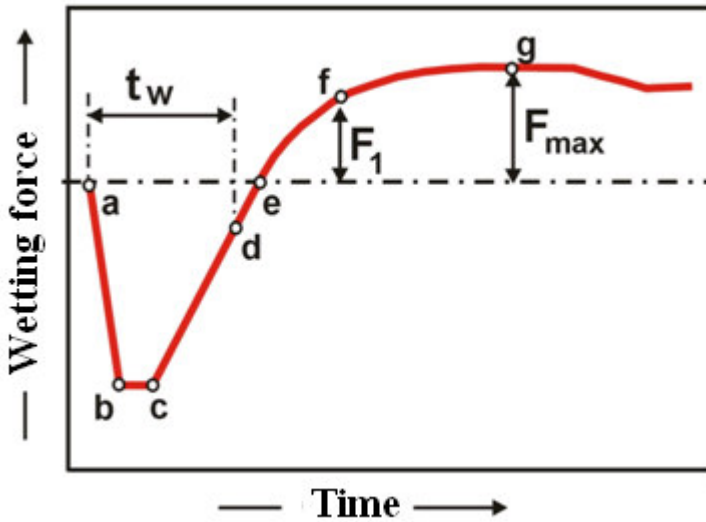


Fig.3.3.3. Typical wetting curve obtained during a meniscographic test with the sampler immersed down to the predetermined depth

The **b-c** interval with a constant value of the wetting force corresponds to the time needed to obtain the alloy temperature by the sampler, as well as the time required for the activation of the flux (among others, the flux evaporation). Depending on the thermal properties of the sampler and the type of the flux, this time can be significantly reduced; the soldering process can even begin already during the sampler's immersion.

Next, the solder starts to wet the surface of the sampler, and so the

wetting angle decreases. At point **d**, the alloy's surface comes back to the horizontal and the angle θ reaches the value of 90° . In the vertical direction, only the buoyant force is operating at that time. The time which has lasted from the beginning of the immersion to that point is called the wetting time (t_w). At point **e**, the measured resultant force reaches the value of zero, which means that the buoyant force counterbalances the wetting force.

Point **f** describes the force F_1 which has been reached after the time of 1 s. At point **g**, the wetting force achieves the maximum value, and so the wetting angle assumes the minimal value. In the further course of the experiment, the wetting force can slightly decrease, e.g. as a result of the alloy's reaction with the sampler.

The meniscographic test results, which will be presented in this study, have been obtained with the use of two devices installed at the Tele and Radio Research Institute: the Solderability Tester MENISCO ST 60 produced by Metronelec (France) and the Solderability Tester Mk6^A made by General Electric (USA). The former was applied in the determination of the values of the surface and interfacial tension by the Miyazaki method [1997Miy] with the use of a non-wettable sampler. The second device, as well as copper wettable samples, were used to determine the wetting force and time, and through the application of the interfacial tension value obtained earlier, the wetting angles were calculated.

3.4. Sessile drop method

3.4.1. Apparatus for wetting test by sessile drop method

The device used in the wetting tests is schematically presented in Fig.3.4.1. The apparatus consists of a pipe furnace in a horizontal system equipped with a loading mechanism making it possible to transfer the sample from the loading („cold”) zone of the furnace to the measuring („hot”) zone, in which the test is conducted, as well as a video camera for the image recording. The furnace and the video camera are connected with a computer equipped with image recording software as well as furnace temperature controlling software.

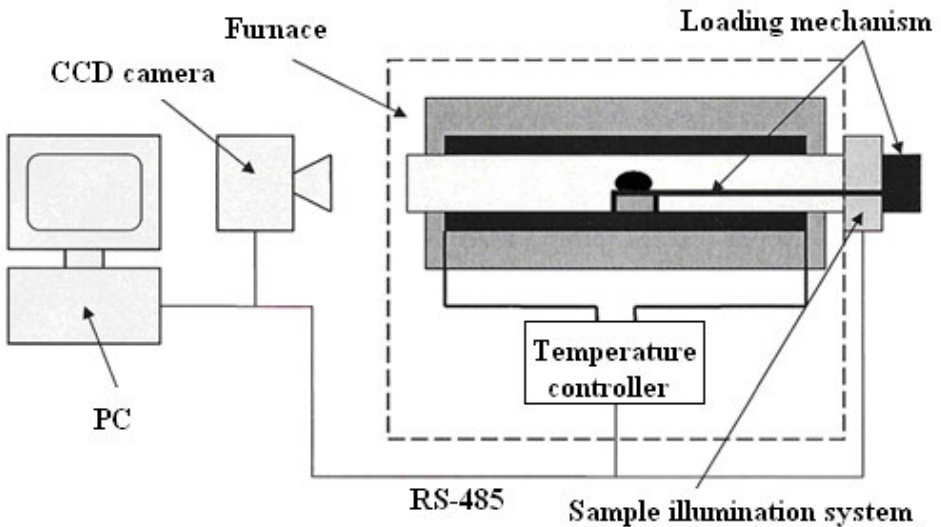


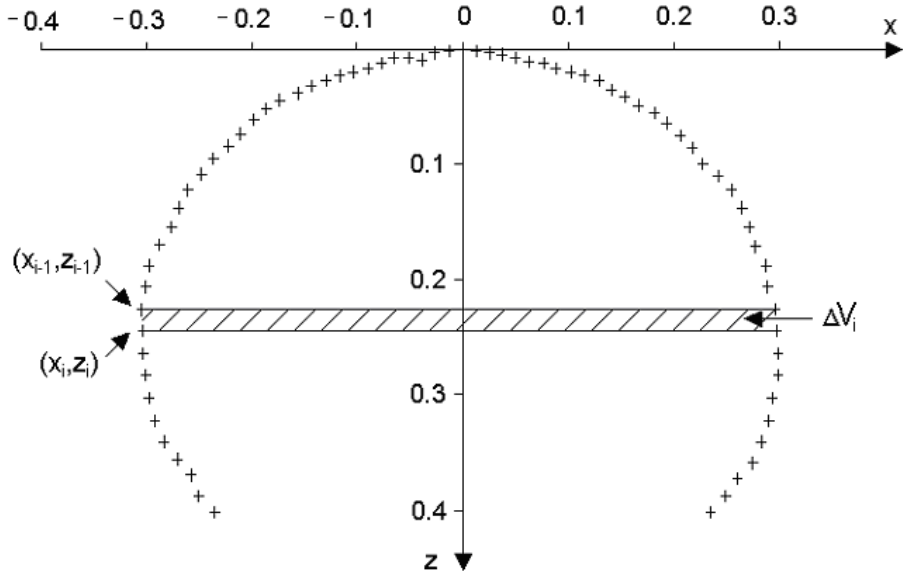
Fig. 3.4.1. Scheme of wetting angle test apparatus

Next to the wetting tests (the wetting angle measurement), the device makes it possible to measure the density and surface tension by the sessile drop method. The measurements are possible to be conducted within the temperature range up to 500 °C, under the conditions of low pressure, in the atmosphere of a protective gas (Ar and N₂), or in air, with or without the presence of a flux. Before the measurement, the tested metal or alloy sample, previously mechanically cleansed and degreased with acetone, is next placed on a smooth horizontal substrate. The sample, together with the substrate, is placed in the loading part of the furnace. Depending on the needs, the heating of the sample can be conducted in two variants, that is the “slow” and the “quick” one. In the „slow” variant, after the sample has been placed in the loading part, the furnace has been tightly closed and the proper protective atmosphere has been determined, the sample is relocated to the central measuring part and it is heated uniformly with the heating of the furnace. In the “quick” variant, after the closing of the furnace, the heating of the measuring part is performed at the time when the sample remains in the loading part. After the measuring part has reached the predetermined temperature, with the use of the loading mechanism, the sample is relocated from the “cold” loading part to the “hot” measuring part. The heating of the sample up to the previously determined temperature is possible during a few seconds, instead of tens of minutes in the “slow” variant. The element affecting the improvement of the sample’s heating rate is a special block made of copper, placed in the measuring part of the furnace, which serves as a heat reservoir. In this method of heating, the transport of the heat into the substrate and the sample takes place not only by way of convection and radiation, but also through conductivity.

The measurement is controlled by special computer software, which makes it possible to:

- program the measurement temperatures by assigning the so called step temperature profile, in which the temperature changes in the furnace can be performed upwards and downwards;
- program the measurement duration time, as well as determine the duration time of the measurement at the particular temperatures;
- program the number of the pictures shot in the particular stages – at intervals of 1s or longer;
- record the time and temperature of the measurement (temperature measured at the sample, close to the heating elements of the furnace).

After the measurement has been completed (the temperature profile has been implemented and the images have been recorded), the program performs the analysis of the images (the treatment of the recorded shots). Such collection of coordinates describing the shape of the drop (considering that a drop is a rotary figure with one vertical symmetry axis crossing the highest point of the drop) is applied in the calculation of the density and the surface tension.



$$\Delta V_i = \pi/3 |z_{i-1} - z_i| (x_i^2 + x_{i-1}^2 + x_i x_{i-1})$$

Fig. 3.4.2. Scheme illustrating the method of calculating the density of the sessile drop [2004Kuc1]

Figure 3.4.2 explains the idea of the assumed method for the density calculations. The density is calculated on the basis of the sum of the elementary volumes between the planes of the circles determined through a rotation of the pairs of the opposite points around the drop's axis symmetry, according to the relation:

$$\rho = \frac{m}{\sum_i \Delta V_i} \quad (3.4.1)$$

where: m – mass of the sample, $\sum_i \Delta V_i$ - volume of the drop.

The surface tension is calculated with the use of special computer software which numerically solves the Laplace's equation for a set of points

describing the shape of the drop. The value of the surface tension is connected with the drop's shape by way of the Laplace's equation:

$$\sigma \left(\frac{1}{R_1} + \frac{1}{R_2} \right) = \frac{2\sigma}{R_0} + \rho g z \quad (3.4.2)$$

R_0 - the radius of the drop's curvature in its highest point, R_1 and R_2 - the radii of the drop's curvature in two perpendicular planes crossing the vertex of the drop, ρ - the density, g – the gravitational constant, z – the vertical coordinate.

The surface tension was calculated with the use of computer software based on the method developed by Rotenberg et al. 1983[Rot1]. The authors of this study have proposed a numerical solution of the Laplace's equation, consisting in adjusting the generated curve to the points obtained in the experiment. The measure of the curve's adjustment to the experimental data is the sum squares of the distance of the experimental points from the generated curve.

3.5. Viscosity measurement by capillary flow method

The viscosity measurement by the method of the liquid flowing through the capillary tube is based on the Hagen-Poiseuille's law, which states that the rate of the laminar flow of the liquid is inversely proportional to the viscosity coefficient and the capillary's length and directly proportional to the difference of pressure between the capillary's end and the surface of the liquid in the reservoir, as well as the capillary's radius to the fourth power. This equation is expressed by the formula below:

$$\frac{V}{t} = \frac{\pi \Delta p r^4}{8 \eta l} \quad (3.5.1)$$

V - the volume of the liquid [m^3] which has outflown after the time t [s],
 Δp - the pressure difference [Pa], r - the capillary radius [m],
 η - the viscosity coefficient [mPa·s], l - the capillary's length [m].

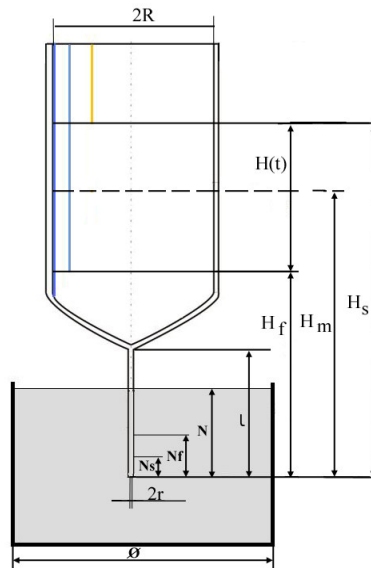


Fig.3.5.1. Scheme of the viscosity measurement method

By measuring the V , t and Δp and after reformulating equation (3.5.1), one can calculate the dynamic viscosity coefficient from the following equation:

$$\eta = \frac{\pi r^4}{8 l v} \Delta p \quad (3.5.2)$$

The Hagen-Poiseuille's law in the form of (3.5.2) can be applied for the determination of η only in the case when the liquid flows out of the capillary tube under the effect of the constant pressure difference Δp between the capillary's end and the surface of the liquid in the reservoir. One should thus make sure that the pressure in the reservoir is much higher than in the hydrostatic one. What is more, the reservoir's diameter should be as big so as the outflow of very little amounts of liquid will not cause a significant change in the pressure Δp , as a result of the change of the hydrostatic pressure.

In the case of the free flow of the liquid under the effect of the changing hydrostatic pressure (lowering of the height of the liquid's column H in the reservoir), both the volume V and the pressure Δp as well as the liquid's height in the reservoir H are functions of time: $V=V(t)$, $\Delta p=\Delta p(t)$ and $H=H(t)$, and equation (3.5.1) assumes the following form:

$$\frac{dV(t)}{dt} = \frac{\pi \Delta p_1(t) r^4}{8 \eta l} \quad (3.5.3)$$

where $\Delta p_1(t)$ is the pressure in the time t .

As the hydrostatic pressure changes together with the height of the liquid's column $H(t)$ in the reservoir (Fig. 3.5.1), equation (3.5.3) should be noted in the form below:

$$\frac{\pi R^2 dH(t)}{dt} = \frac{\pi \rho g r^4}{8\eta l} H(t) \quad (3.5.4)$$

which implies that:

$$\frac{dH(t)}{H(t)} = \frac{\pi \rho g r^4}{8\eta l R^2} dt \quad (3.5.5)$$

After introducing the constant α equaling:

$$\alpha = \frac{\pi \rho g r^4}{8\eta l R^2} \quad (3.5.6)$$

into equation (3.5.5), the latter is brought to the following form:

$$\frac{dH(t)}{H(t)} = \alpha dt \quad (3.5.7)$$

From the above one can determine the height of the column of liquid H_f in the reservoir (Fig.3.5.1), that is the hydrostatic pressure at a random time t during the free flow of the liquid from the reservoir. By integrating equation (3.5.7) in the time range from 0 to t and from H_s to H_f ,

$$\int_{H_s}^{H_f} \frac{dH(t)}{H(t)} = \int_0^t \alpha dt \quad (3.5.8)$$

one can obtain the following relation (3.5.9):

$$\ln \frac{H_f}{H_s} = -\alpha t \quad (3.5.9)$$

and next (3.5.10)

$$\mathbf{H}_f = \mathbf{H}_s \exp(-\alpha t) \quad (3.5.10)$$

which makes it possible to calculate the height of the column of liquid in the reservoir after the time t (Fig. 3.5.1). By determining the time of the flow of different liquid volumes from the reservoir on the capillary tube, one can assume the parameter α for equation (3.5.10) and next calculate the viscosity from relation (3.5.6).

As the experiment is performed by way of measuring the outflow time of the particular liquid volume which is contained between the heights \mathbf{H}_s and \mathbf{H}_f of the reservoir (Fig. 3.5.1), one can substitute the change of the height from \mathbf{H}_s to \mathbf{H}_f at the time t by a mean value \mathbf{H}_m , which is calculated as the surface area \mathbf{S} under the curve (3.5.10) divided by the time of the liquid's flow t . By first calculating \mathbf{S} as the below integral:

$$\mathbf{S} = \int_0^t \mathbf{H}_s \exp(-\alpha t) dt = -\frac{\mathbf{H}_s}{\alpha} e^{-\alpha t} - \frac{\mathbf{H}_s}{\alpha} \quad (3.5.11)$$

and after dividing it by t , one obtains the mean (substitute) value of the height \mathbf{H}_m :

$$\mathbf{H}_m = \frac{\mathbf{S}}{t} = \frac{\mathbf{H}_s}{\alpha t} (1 - e^{-\alpha t}) \quad (3.5.12)$$

After the introduction of relations (3.5.9) and (3.5.10) into equation (3.5.12), the equation for the substitute height \mathbf{H}_m is determined:

$$\mathbf{H}_m = \frac{\mathbf{H}_s - \mathbf{H}_f}{\ln \mathbf{H}_s - \ln \mathbf{H}_f} \quad (3.5.13)$$

which is the function of the initial height - H_s ($t=0$) and the final height - H_f after the time t in which the liquid's volume V flows out of the reservoir into the lower container, under the changing hydrostatic pressure $\Delta p_1(t)$:

$$\Delta p_1 = \rho g \frac{H_s - H_f}{\ln H_s - \ln H_f} \quad (3.5.14)$$

When expression (3.5.14) is substituted into (3.5.2) and the Hagenbach correction η_H [1983Sch] is considered for the drop of the kinetic energy of the stream of liquid, calculated from the formula below:

$$\eta_H = - \frac{V\rho}{8\pi l t} \quad (3.5.15)$$

one obtains the following equation:

$$\eta = \frac{\pi r^4 t \rho g (H_s - H_f)}{8 l V (\ln H_s - \ln H_f)} - \frac{V\rho}{8\pi l t} \quad (3.5.16)$$

This allows for the calculation of the dynamic viscosity coefficient of the liquid of density ρ on the basis of the experiment, in which the liquid volume V occupying the space between the height H_s and H_f flows out, at the time t , of the capillary of radius r and length l .

When the capillary tube is immersed in the liquid accumulating in the lower container, one should consider the correction for the change of the pressure $\Delta p_2(t)$ connected with the increase of the liquid's level in the lower container.

By conducting such analysis as that for the reservoir, one can express the change of the pressure $\Delta p_2(t)$ by means of the following relation:

$$\Delta p_2 = \rho g \frac{N_s - N_f}{\ln N_s - \ln N_f} \quad [\text{Pa}] \quad (3.5.17)$$

in which: N is the depth of the capillary's immersion before the liquid suction in the reservoir [m], $N_s = V_s / (\pi \Phi^2 / 4)$ is the depth of the capillary's immersion at the beginning of the measurement, that is after the suction of the liquid of volume V into the reservoir ($t=0$) [m], $N_f = N - N_s$ is the depth of the capillary's immersion at the end of the measurement [m] that is after the outflow of the liquid of volume V , V_s is the volume of the liquid sucked into the reservoir [m³], Φ is the diameter of the lower container (crucible) [m] (Fig. 3.5.1), and the depth of the capillary N 's immersion, when the liquid flows in time t from the reservoir to the container. It is given by the relation below:

$$N(t) = N - N_s e^{-\beta t} \quad [m] \quad (3.5.18)$$

where

$$\beta = -1/t \ln N_s/N \quad (3.5.19)$$

Ultimately:

$$\Delta p = \Delta p_1 - \Delta p_2 = \rho g \left(\frac{H_s - H_f}{\ln H_s - \ln H_f} - \frac{N_s - N_f}{\ln N_s - \ln N_f} \right) \quad (3.5.20)$$

Another equation for the pressure change caused by the increase of the liquid's level in the lower container, as a result of the liquid's outflow from the reservoir through the capillary tube, can be derived with the consideration of the fact that the volume of the liquid flowing out of the reservoir of diameter $2R$ and that flowing into the lower container of diameter Φ is the same. Then, the increase of the liquid's level at the time t can be expressed by the ratio of the volume of liquid which has flown into the lower container to the latter's surface area. This leads to the dependence

on the capillary's immersion depth after time t and next to its substitution by the mean value N_m given in the equation:

$$N_m = N - (4V_s / \pi \Phi^2) + (2R / \Phi)^2 \quad [m] \quad (3.5.21)$$

where: N_s – the depth at the beginning of the measurement [m] - equals:

$$N_s = N - 4V_s / \pi \Phi^2 \quad [m] \quad (3.5.22)$$

V_s is the volume of liquid sucked into the reservoir during the initiation of the measurement, expressed experimentally [m³], Φ is the diameter of the crucible [m] and N_m is the substitute measurement depth [m].

Ultimately, the pressure difference Δp , which was substituted in equation (3.5.1), can be calculated from the formula below:

$$\Delta p = \rho g \left(\frac{\Phi^2 - 4R^2}{\Phi^2} \frac{H_s - H_f}{\ln H_s - \ln H_f} - N + \frac{4V_s}{\pi \Phi^2} \right) \quad (3.5.23)$$

The derived relations were verified in the viscosity measurement for carbon tetrachloride, water, methyl alcohol and the model liquid produced by Brookfield. First, the measurements of the change in the height of the liquid in the reservoir after time t were performed, and the results are presented in Figure 3.5.2.

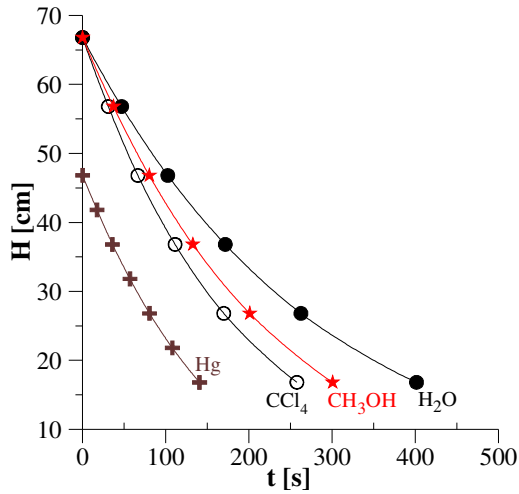


Fig.3.5.2. Relation of the liquid column's height on the effect of the outflow time for different liquids [2004Smi]

The measurements fully confirm relation (3.5.12) which describes the height of the column of liquid in the container after time t , as such curve can be represented by the equation of the following form:

$$H(t) = Ae^{-\alpha t} \quad (3.5.24)$$

in which A is the initial height H_s of the liquid in the reservoir (Fig.3.5.1). From the determined value of parameter α one can then calculate the viscosity, by applying equation (3.5.6). The measurement results for the mentioned liquids (except for Hg) are presented in Figure 3.5.3 (crosses) in reference to the literature data (full line).

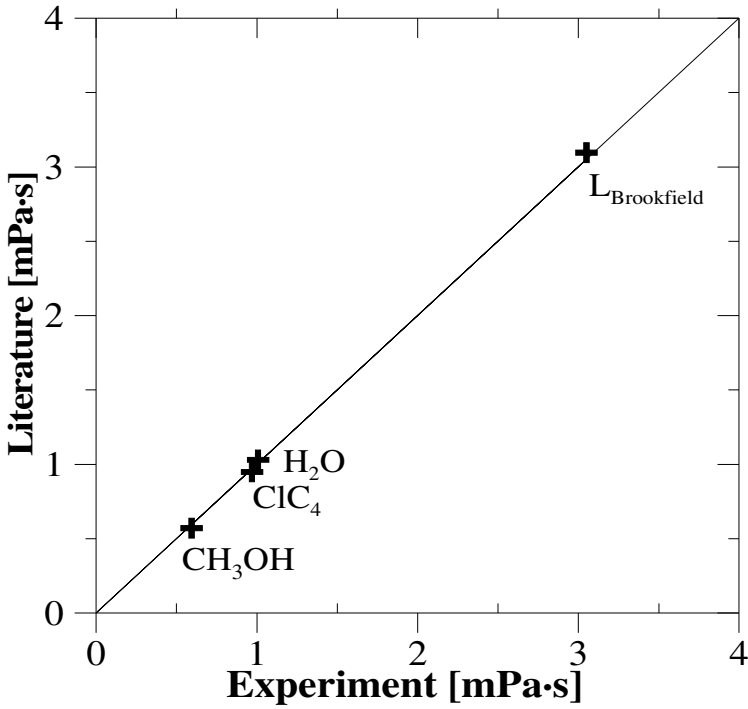


Fig. 3.5.3. Literature values of the viscosities of different liquids in the function of their experimental values (H₂O, CCl₄, CH₃OH) [1986Wea], (L_{Brookfield}) model liquid

Figure 3.5.3 shows very good agreement of the experimental data with previously published literature values. This verifies the correctness of the whole deduction and of the derived relations for the case of the laminar liquid outflow through the capillary tube, that is for the Reynolds number $Re < 2300$, under the effect of the time-dependent change of hydrostatic pressure. In the tests, the value of the Reynolds number Re oscillated within the range of 1600-2000. In the case of mercury, the obtained viscosity value was burdened with a large error due to the significantly larger value of the Reynolds number (turbulent outflow) and thus it was not plotted into the diagram (Fig. 3.5.3).

Before the initiation of the tests, the metal or alloy was placed in the lower graphite crucible, on which a container with a capillary of known dimensions was installed, and both elements were placed in the alundum pipe of the furnace with winding. Next, the apparatus was tightly closed and the air was pumped out with a vacuum pump from the measuring space and the latter was then filled with protective gas (argon-hydrogen mixture). At the time of the heating of the measuring apparatus, protective gas was let through the latter for the period of over a dozen hours. With the use of a micrometric screw, the lower crucible was raised up to the moment when the liquid became in contact with the capillary, which was signaled by the rapid increase of the pressure of the gas flowing out of the capillary. Next, the capillary was immersed to the required depth and the system was thermostated for approximately 1 hour. As the further step, the liquid (alloy) was sucked from the crucible into the reservoir and the measurement of the time of outflow for the particular volume of liquid through the capillary was initiated.

3.6. Measurement of viscosity, density and surface tension by liquid outflow through the container orifice

Roach and Heinein [2003Roa, 2004Roa, 2005Hen] proposed the method of a simultaneous measurement of the surface tension, viscosity and density. The equation which they derived originates from the well-known Bernoulli flow equation for inviscid liquids:

$$Q = \pi r^2 \sqrt{2gh} \quad (3.6.1)$$

This equation states that the maximal volumetric capacity of the liquid's outflow Q (the volume V of the liquid flowing out at the time t) through the orifice of radius r , from the container (Fig. 3.6.1), in which the liquid's meniscus is at height h , is proportional to the section area of the orifice r_o and the rate of the outflowing liquid $\sqrt{2gh}$.

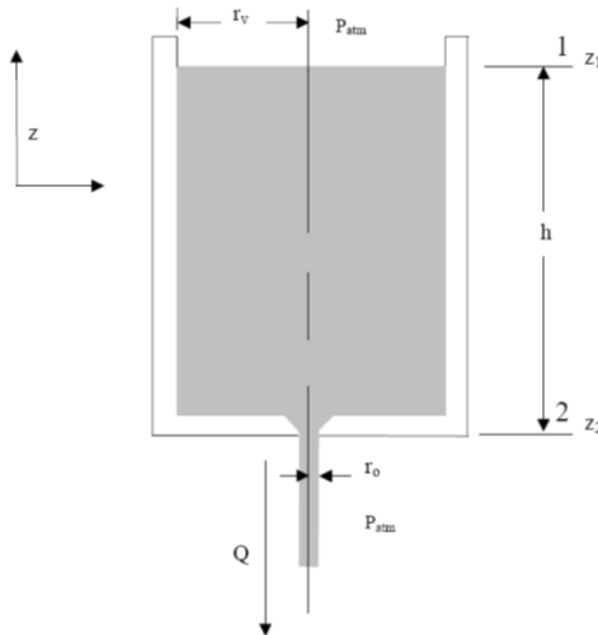


Fig. 3.6.1. Scheme of liquid's discharge from the crucible of radius r_o

In the case of viscid liquids, equation (3.6.1) is modified by the introduction of the discharge coefficient C_d , which is defined as the ratio of the actual (experimental) rate u_e of the liquid in the orifice of radius r_o to the theoretical one:

$$C_d = \frac{u_e}{\sqrt{2gh}} \quad (3.6.2)$$

Under the conditions of volumetric flow, the coefficient expressed by equation (3.6.2) assumes the following form:

$$C_d = \frac{Q_e}{\pi r_o^2 \sqrt{2gh}} \quad (3.6.3)$$

The Bernoulli equation for the actual discharge:

$$Q_e = \pi r_o^2 C_d \sqrt{2gh} \quad (3.6.4)$$

Taking into consideration also the effect of the pressure originating from the surface tension σ , the authors [2003Roa, 2004Roa, 2005Hen] proposed the relation below:

$$Q_e = \pi r_o^2 C_d \sqrt{2g \left(h - \frac{\sigma}{\rho g r_o} \right)} \quad (3.6.5)$$

The parameter C_d is indirectly connected with the Reynolds number Re by the equation which, beside viscosity η and density ρ of the liquid flowing through the orifice of radius r_o , also includes Q_e :

$$Re = \frac{2\rho u_e}{\eta} = \frac{2\rho Q_e}{\pi r_o \eta} \quad (3.6.6)$$

The comparison of equations (3.6.5) and (3.6.6) shows that the parameter C_d is connected with the Reynolds number by Q_e , which is clearly seen after the rearrangement of formula (3.6.6) into the following form:

$$\mathbf{Q}_e = \frac{\pi r_0 \eta \mathbf{Re}}{2\rho} \quad (3.6.7)$$

\mathbf{C}_d is the function of the height of the meniscus \mathbf{h} . By experimentally determining \mathbf{Q}_e for a liquid of known viscosity, one can establish, for the particular diameter of the orifice $2\mathbf{r}$, the relation between \mathbf{C}_d and \mathbf{Re} in the form of a linear, parabolic or polynomial relation, and next apply it to calculate the surface tension, density and viscosity.

To that end, we determine the height of the column of liquid \mathbf{h}_e from equation (3.6.5):

$$\mathbf{h}_e = \frac{1}{2g} \left(\frac{\mathbf{Q}_e}{\mathbf{C}_d \pi r_0^2} \right)^2 + \frac{\sigma}{\rho g r_0} \quad (3.6.8)$$

and next, after we insert into 3.6.8 an equation describing the dependences of \mathbf{C}_d on \mathbf{Re} , which is determined on the basis of the results of the reservoir calibration, e.g. in the form of a third degree polynomial:

$$\mathbf{C}_d = \mathbf{a}_4(\mathbf{Re})^3 + \mathbf{a}_3(\mathbf{Re})^2 + \mathbf{a}_2(\mathbf{Re}) + \mathbf{a}_1 \quad (3.6.9)$$

where: \mathbf{a}_i are the coefficients calculated from the calibration results. We obtain a relation describing \mathbf{h}_e as the function of the Reynolds number:

$$\mathbf{h}_e = \frac{1}{2g} \left(\frac{\mathbf{Q}_e}{(\mathbf{a}_4(\mathbf{Re})^3 + \mathbf{a}_3(\mathbf{Re})^2 + \mathbf{a}_2\mathbf{Re} + \mathbf{a}_1) \pi r_0^2} \right)^2 + \frac{\sigma}{\rho g r_0} \quad (3.6.10)$$

After the insertion of expression 3.6.6 defining \mathbf{Re} into equation 6.6.10, a further equation is obtained:

$$\mathbf{h}_e = \frac{1}{2g} \left(\frac{Q_e}{\left(a_4 \left(\frac{2\rho Q_e}{\pi r_0 \eta} \right)^3 + a_3 \left(\frac{2\rho Q_e}{\pi r_0 \eta} \right)^2 + a_2 \frac{2\rho Q_e}{\pi r_0 \eta} + a_1 \right) \pi r_0^2} \right)^2 + \frac{\sigma}{\rho g r_0} \quad (3.6.11)$$

As the measurements provide information on the mass of the liquid which flows out through the orifice in the bottom, whose density is unknown, one should replace the volumetric outflow Q_e with the mass stream outflow V_e , defined by the equation:

$$V_e = \frac{\rho Q_e}{\pi r_0^2} \quad (3.6.12)$$

from which one can calculate Q_e from the following relation:

$$Q_e = \frac{\pi r_0^2 V_e}{\rho} \quad (3.6.13)$$

After the insertion in equation (3.6.11), one obtains a new equation, in which the height of the meniscus is expressed by the stream of the liquid's mass V_e which flows out of the container:

$$\mathbf{h}_e = \mathbf{f}(V_e) = \frac{1}{2g} \left(\frac{V_e}{\rho \left(a_4 \left(\frac{2r_0 V_e}{\eta} \right)^3 + a_3 \left(\frac{2r_0 V_e}{\eta} \right)^2 + a_2 \left(\frac{2r_0 V_e}{\eta} \right) + a_1 \right)} \right)^2 + \frac{\sigma}{\rho g r_0} \quad (3.6.14)$$

The measurement is used to determine the accumulated liquid mass C_m that is the mass of the liquid which has flown out after the given time t , i. e. one obtains a curve in the form of $C_m = \mathbf{f}(t)$, which can be approximated by the third degree polynomial:

$$C_m = \sum_{i=1}^4 C_i t^{i-1} \quad (3.6.15)$$

By calculating the derivative from (3.6.15) and by dividing it by the section area of the container's orifice of radius r_o , one obtains an equation describing the stream of the outflowing liquid V_e :

$$V_e = \frac{1}{\pi r_o^2} \frac{dC_m}{dt} = \frac{1}{\pi r_o^2} (3C_4 t^2 + 2C_3 t + C_2) = \frac{3C_4 t^2 + 2C_3 t + C_2}{\pi r_o^2} \quad (3.6.16)$$

By then inserting relation (3.6.16) into equation (3.6.13), one obtains a dependence for Q_e expressed by the experimentally measured quantity of the accumulated liquid mass C_m , described by equation (3.6.15):

$$Q_e = \frac{\pi r_o^2 V_e}{\rho} = \frac{3C_4 t^2 + C_3 t + C_2}{\rho} \quad (3.6.17)$$

which, after being inserted in equation (3.6.11), creates a dependence of Q_e on the parameters describing the mass liquid outflow from the container through the orifice of radius r_o . By substituting equation (3.6.16) into (3.6.15), or (3.6.17) into (3.6.11), one obtains a dependence of the liquid column's height in the container after time t on the viscosity, density and surface tension. If the height in the function of time is expressed by an equation in the parabolic form:

$$h(t) = h_0 + h_1 t + h_2 t^2 \quad (3.6.18)$$

then, in order to minimize the difference between the left and the right sides of equation (3.6.11) or (3.6.15), one can select such values of parameters h_i (3.6.18), density ρ , surface tension σ and viscosity η so that the sum square of the differences for a few tens of time values t will be lower. This solves the problem in the determination of density, viscosity and surface tension from the measurements of the liquid mass which flows out of the container through the orifice of diameter $2r_o$.

Another method of solving relation (3.6.15) has been proposed by the authors of the method [2003Roa, 2004Roa, 2005Hen]. Their basis

was a series expansion of equation (3.6.15) and next the creation of a proper system of linear equations, which are solved by the iteration method, with the specified accuracy δh_e . The calculations of the surface tension, density and viscosity performed for the same parameter values C_i of equation (3.6.15) and a_i of equation (3.6.10), for liquid tin at 723 K, and with the application of the procedure given by the creators of method [2003Roa, 2004Roa, 2005Hen] and the minimization method presented above, resulted in values differing by about 2 %. They equal, respectively, 509 and 511.5 mN/m for surface tension, 6.8 and 6.781g/cm³ for density and 1.26 and 1.23 mP s for viscosity.

The obtained exemplary calibration curve $C_d=f(Re)$ can be seen in the Figure below:

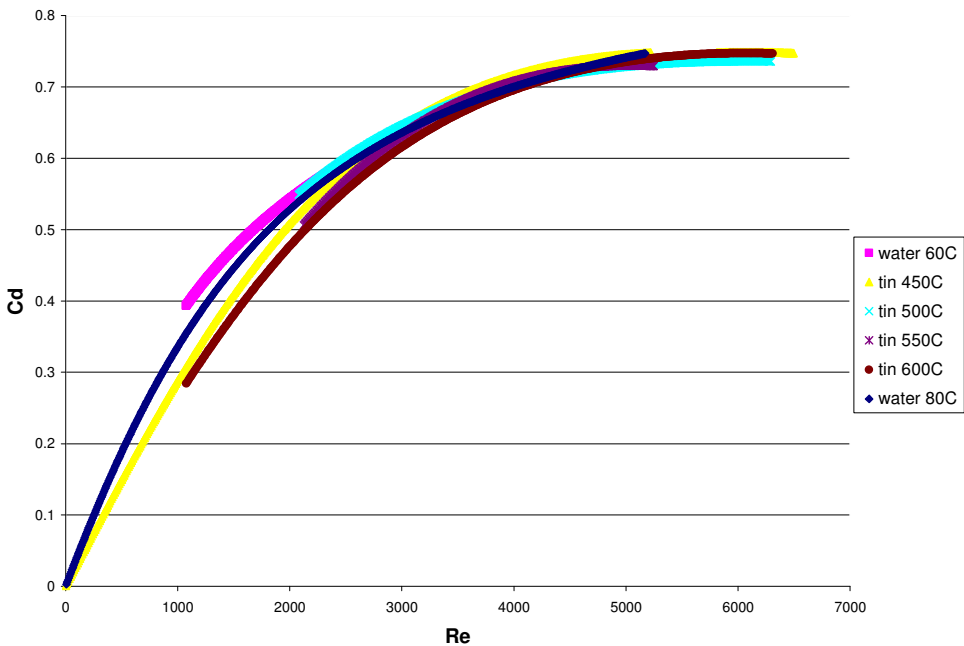


Fig. 3.6.2. Calibration curve of a crucible with a 0.0002 orifice [m], obtained from the measurements for water and tin, for different temperatures and heights of the tested liquid

The equation obtained from the measurements, describing the dependence of coefficient C_d on the Reynold's number Re assumes the following form:

$$C_d = 2 \cdot 10^{-12} Re^3 - 4 \cdot 10^{-08} Re^2 + 0.0003 Re - 0.0114 \quad (3.6.19)$$

The calculated standard deviation, according to the relation:

$$\partial C_d = \sqrt{\frac{\sum (C_{d,poly} - C_{d,exp})^2}{n - 4}} \quad (3.6.20)$$

equals 0.018.

It should be noted that, in the measurement of density ρ by the dylatometric method, in the same experiment, when the mass of the applied liquid alloy in the container is known and the apparatus is equipped with a penetrator measuring the height of the liquid column, the problem of optimization is somewhat simplified, as one of the parameters is previously known and the number of selectable parameters is reduced by 1. Thus, in the case of the parabolic description of the height of the column of liquid in the container (3 parameters) after time t , the number of selectable parameters equals 5.

Further improvement of the method consisting in the calibration of the container to the set volume occupied by the liquid makes it possible to directly determine the relation of the height of the column of liquid in the container on the particular outflow time, as well as to apply equations (3.6.5), (3.6.15) and (3.6.14) or (3.6.11) for the calculation of the surface tension and viscosity of the examined liquid (metal alloy).

4. Modeling of surface tension and viscosity

4.1. Surface tension modeling

The Butler's equations introduced in 1932 in [1932But], are unquestionably one of the earliest relations making a connection between the surface tension of liquid solutions with molar surfaces and the activity of the elements in the liquid phase, which, with the correct assumptions, makes it possible to calculate the surface tension. When introducing the equations, the author assumed that the monatomic surface layer is a separate phase and that the molar surface of the monoatomic surface layer has the properties of an ideal solution, which comes down to the assumption that the partial molar surfaces are equal to the molar surfaces of the solution's pure components. The relation derived by Butler for n-component solutions, is of the following form:

$$\sigma = \sigma_1 + \frac{RT}{S_1^0} \ln \left(\frac{a_1^S}{a_1^B} \right) = \sigma_1 + \frac{RT}{S_1^0} \ln \left(\frac{X_1^S}{X_1^B} \right) + \frac{RT}{S_1^0} \ln \left(\frac{\gamma_1^S}{\gamma_1^B} \right)$$

----- (4.1.1)

$$\sigma = \sigma_n + \frac{RT}{S_n^0} \ln \left(\frac{a_n^S}{a_n^B} \right) = \sigma_n + \frac{RT}{S_n^0} \ln \left(\frac{X_n^S}{X_n^B} \right) + \frac{RT}{S_n^0} \ln \left(\frac{\gamma_n^S}{\gamma_n^B} \right)$$

The symbols present in equation (4.1.1) designate as follows: R – the gas constant, T – the temperature, σ – the surface tension of the n – component solution (alloy) and σ_i , S_i^0 , a_i^B , a_i^S , γ_n^B , γ_i^S , X_i^B , X_i^S , ($i=1, n$) – the surface tension, the molar surface, the activity, the activity coefficient and the concentration of component „ i ” in the surface layer (phase) (index S) or the volumetric phase (index B).

Depending on the number of components forming the solution, the number of independent equations (4.1.1) equals $i=(1, n)$. The determination of the surface tension from equations (4.1.1) is possible if, beside the activity coefficient in the volumetric and surface phase, one also knows the molar surface of pure components „i”. In his work, Butler [1932But] does not suggest any way of calculating the molar surface, yet in the following years, to that end, the molar volume of liquid components began to be used, by the application of the following equation:

$$A = LV^{2/3}N^{1/3} \quad (4.1.2)$$

In equation (4.1.2), V designates the component’s molar volume, N is the Avogadro number and L is the geometrical parameter which, depending on the assumed atomic structure in the monoatomic surface phase (layer), takes different values.

In 1957, Hoar and Melford [1957Hoa] performed an analysis of the change in the free energy connected with the creation of monoatomic surface layer of binary solutions, by way of:

- a) mixing, under the conditions of the monoatomic layer, X_1' and X_2' moles of pure components 1 and 2 and next placing them on the surface of the solution (volumetric phase) and,
- b) introducing X_1' and X_2' moles of components into the solution, allowing for an intrinsic creation of the surface layer.

The analysis of the change in the free energy connected with the above processes has led the authors to the following equations:

$$\begin{aligned}\sigma &= \sigma_1 \frac{S_1^0}{S_1} + \frac{RT}{S_1} \ln \left(\frac{a_1^S}{a_1^B} \right) = \sigma_1 \frac{S_1^0}{S_1} + \frac{RT}{S_1} \ln \left(\frac{X_1^S}{X_1^B} \right) + \frac{RT}{S_1} \ln \left(\frac{\gamma_1^S}{\gamma_1^B} \right) \\ &= \sigma_2 \frac{S_2^0}{S_2} + \frac{RT}{S_2} \ln \left(\frac{a_2^S}{a_2^B} \right) = \sigma_2 \frac{S_2^0}{S_2} + \frac{RT}{S_2} \ln \left(\frac{X_2^S}{X_2^B} \right) + \frac{RT}{S_2} \ln \left(\frac{\gamma_2^S}{\gamma_2^B} \right)\end{aligned}\quad (4.1.3)$$

With the assumption that the change in the molar surface of the surface phase equals zero $\Delta S=0$, the partial molar surfaces S_1 and S_2 become equal to the molar surfaces of pure components, and the relation (4.1.3) becomes identical to the Butler's relation (4.1.1). Equation (4.1.3) is the most general form of the relation which allows for the calculation of the surface tension of binary solutions with the application of the physical and thermodynamic properties of the volumetric phase (solution). It should be emphasized that Hoar and Melford [1957Hoa] were the first to propose a different structure of the surface phase than that of the volumetric phase, assuming a close packing of atoms in the monoatomic surface phase, which corresponds to the value $L=1.091$ in equation 4.1.2. In 1972, Randles from the University of Birmingham and Behr from the Institute of Physical Chemistry PAN in Warsaw [1972Ran] derived equations which made it possible to model the surface tension from the thermodynamic properties of the volumetric phase, with the arbitrarily assumed thickness τ and the rectilinear change of the alloy surface depending on the concentration:

$$\begin{aligned}\sigma &= \sigma_1 + \frac{RT}{A_1} \ln \left(\frac{a_1^S}{a_1^B} \right) = \sigma_1 + \frac{\tau RT}{V_1} \ln \left(\frac{X_1^S}{X_1^B} \right) + \frac{\tau RT}{V_1} \ln \left(\frac{\gamma_1^S}{\gamma_1^B} \right) \\ &= \sigma_2 + \frac{RT}{A_2} \ln \left(\frac{a_2^S}{a_2^B} \right) = \sigma_2 + \frac{\tau RT}{V_2} \ln \left(\frac{X_2^S}{X_2^B} \right) + \frac{\tau RT}{V_2} \ln \left(\frac{\gamma_2^S}{\gamma_2^B} \right)\end{aligned}\quad (4.1.4)$$

Relations (4.1.4), when the discussion is limited to the monoatomic layer, become identical to Butler's equations [1932But] (Eq. (4.1.1)), and they make it possible to determine the thermodynamic properties of the surface phase for its given thickness. By performing calculations for different thicknesses of the surface phase, one can prove that already with the thickness equal to two atomic diameters, the excess free energy of the surface layer reaches values very close to those for the volumetric phase, which point to the fact that the discussion on the surface phase should in fact be limited to the case of monoatomic layer.

As mentioned above, the Butler relations (4.1.1) have been the most extensively used for calculating surface tension. This results from their form which from the assumption that the partial molar surfaces are identical to those of the pure metals and equal to those calculated from the relation (4.1.2).

The relation between the excess free energy of the monoatomic surface layer and that of the volumetric phase, expressed parameter $\beta=0.83$ was introduced by Tanaka et al. [1996Tan]. The latter set the value β from the thermodynamic analysis of the free energy of the surface phase and the volumetric phase. As a result, they obtained the following relation between the surface tension and the heat of evaporation referred to a unit of the surface area of the monoatomic surface layer (Eq. 4.1.2):

$$A_i \sigma_i = LN^{1/3} V_i^{2/3} \sigma_i = (1 - \beta) \Delta H_{m,i}^g \quad (4.1.5)$$

The values β calculated by [1996Tan] for a few tens of metals are graphically presented in Figure 4.1.1, and the mean value established by the authors equals $\beta=0.83$ (0.833). This parameter connects the excess

free energy of the components in the volumetric and the surface phase by the equation:

$$G_{S,i}^{\text{ex}}(\mathbf{X}_i^S, \mathbf{T}) = \beta G_{B,i}^{\text{ex}}(\mathbf{X}_i^S, \mathbf{T}) \quad (4.1.6)$$

Relation (4.1.6) means that the partial excess free energy of component „i” in the surface phase of concentration \mathbf{X}^S is equal to the free energy of this component in the volumetric phase of the same concentration multiplied by coefficient β .

It should be noted that the value of parameter β calculated by the least square method as the slope of a straight line $\sigma=(1-\beta)Y$, that is with the assumption that the surface tension equals zero and in the case when heat of evaporation equals zero, determines the value β slightly higher and equal to $\beta=0.85$ (0.847).

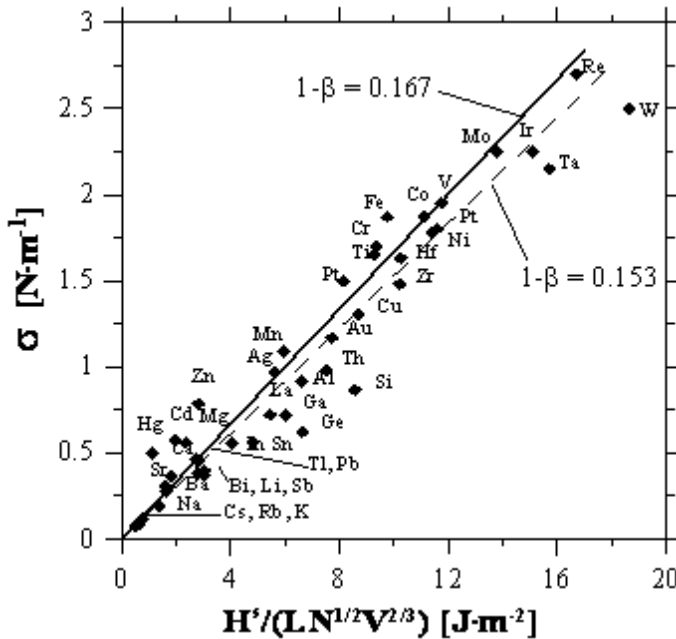


Fig. 4.1.1. Relation of surface tension of metals on their heat of evaporation from the surface of monoatomic surface layer of a mole of atoms at melting point. [1996Tan]

The isotherms of surface tension presented in [1996Tan], [1999Tan], [1987Spe], [1989Yeu], [1992Lee], [1997Lee], [2001Tan], [1999Tan], [1999Yoo1] and [2005Kuc], for over z dozen binary systems, calculated from relation (4.1.1), with constant values of $L=1.091$ and $\beta=0.83$, (usually, 1 isotherm per system), show quite good agreement of the experimental values with the calculated ones. However, none of the mentioned works performed an analysis of the temperature relations for selected concentrations, which would give a full picture of the correlations between the experimental and the calculated data. The studies of the surface tension conducted at IMIM PAN by the maximum bubble pressure method have allowed for a more detailed comparative analysis of the calculated and the experimental values of the surface tension in a wide temperature range. A graphical presentation of both sets of data, that is the experimental ones and those calculated from (4.1.1), is shown in Figure 4.1.2 on the example of a bismuth-silver system [2003Gas2], for which two basic discrepancies have been most clearly demonstrated.

One of the above concerns the calculated curvilinear temperature relations of the surface tension for alloys of a higher content of Ag ($X_{Ag} = 0.5, 0.75, 0.95$), and the other – the plus value of the temperature coefficient, that is the increase of the surface tension together with the temperature increase. It should be emphasized that the change in the value of parameter β cannot change the sign of the temperature coefficient of the surface tension for the opposite one, but it can merely heighten or lower the values of the surface tension at a given calculation temperature, with the preservation of the identical tendency of changes. A verification of this fact are the calculation results for the Ag – Bi and Ag – Sn alloys presented in Tables 4.1.1 and 4.1.2. The calculations assumed different values of β , the concentration

of $X_{Ag} = 0.25$, the thermodynamic parameters given in the work [1993Kar], and the surface tension and molar volume data taken from the own measurements of [2003Gas2] and [2001Mos1].

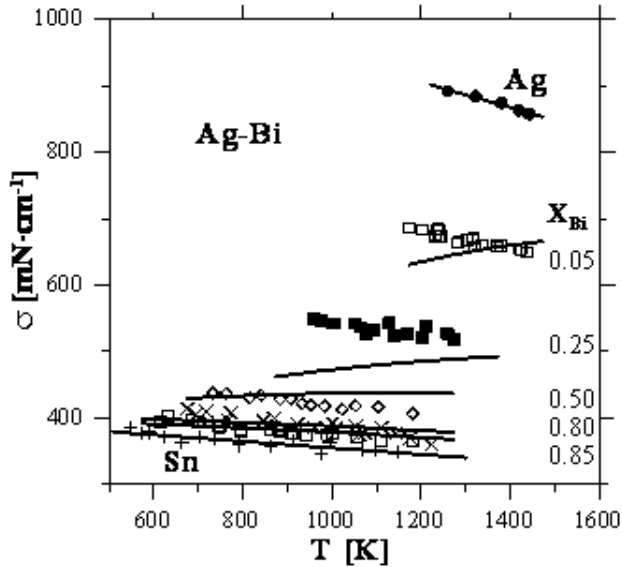


Fig. 4.1.2. Temperature relations of surface tension for liquid Ag – Bi alloys, calculated with the use of thermodynamic parameters [1993Kar]. Symbols used to denote the experimental values and lines – the values calculated from the Butler’s relation (4.1.1)

Table 4.1.1. Surface tension calculated from Butler’s relation (Eq. 4.1.1) for Ag – Bi alloys of concentration $X_{Ag} = 0.25$, different values of β and

$$L = 1.091$$

β	$\sigma_{973\text{ K}}$ [mN·cm ⁻¹]	$\sigma_{1073\text{ K}}$ [mN·cm ⁻¹]	$\sigma_{1173\text{ K}}$ [mN·cm ⁻¹]	$\sigma_{1273\text{ K}}$ [mN·cm ⁻¹]	$\sigma_{1373\text{ K}}$ [mN·cm ⁻¹]
0.75	470.87	478.47	484.68	489.56	493.15
0.83	470.59	478.1	484.23	489.03	493.56
0.9	470.35	477.78	483.84	488.57	492.04

Table 4.1.2. Surface tension calculated from Butler's relation (Eq. 4.1.1) for Ag – Sn alloys of concentration $X_{Ag} = 0.3$ and different values of β and $L = 1.091$

β	$\sigma_{873\text{ K}}$ [mN·cm ⁻¹]	$\sigma_{973\text{ K}}$ [mN·cm ⁻¹]	$\sigma_{1073\text{ K}}$ [mN·cm ⁻¹]	$\sigma_{1173\text{ K}}$ [mN·cm ⁻¹]	$\sigma_{1273\text{ K}}$ [mN·cm ⁻¹]	$\sigma_{1373\text{ K}}$ [mN·cm ⁻¹]
0.75	653.87	659.80	662.47	662.01	659.01	654.04
0.83	653.95	659.75	662.09	661.20	657.75	652.37
0.9	654.01	659.69	661.73	660.45	656.61	650.87

Another parameter applied in the surface tension modeling is the partial molar surface of the components (metals). The calculation procedure assumes (Eq. 4.1.1) that the molar surface of the solution (alloy) changes linearly between the molar surfaces of pure components, which comes down to the assumption that the partial molar surfaces of the components are equal to their molar surfaces calculated from Eq. 4.1.2. By analyzing the effect of the molar surfaces on the value of the calculated surface tension, with constant values of the remaining parameters, one can state its significant influence on the calculation results. The results of such simulation for an alloy from the system Ag - Bi, of concentration $X_{Bi} = 0.25$, are presented in Table 4.1.3 for the molar surfaces differing by $\pm 10\%$ from the values calculated from equation (4.1.2).

Table 4.1.3. Effect of the molar surface value **S** on the surface tension calculated from the Butler's relation (4.1.1) for an alloy from the system Ag-Bi, with the bismuth concentration of 0.25 (in molar fractions)

S	$\sigma_{973\text{ K}}$ [mN·cm ⁻¹]	$\sigma_{1073\text{ K}}$ [mN·cm ⁻¹]	$\sigma_{1173\text{ K}}$ [mN·cm ⁻¹]	$\sigma_{1273\text{ K}}$ [mN·cm ⁻¹]	$\sigma_{1373\text{ K}}$ [mN·cm ⁻¹]
0.9*S	480.35	488.36	494.81	499.78	503.35
1.0*S	470.59	478.10	484.23	489.03	492.56
1.1*S	462.50	469.68	475.63	480.37	483.93

The data presented in Table 4.1.3 imply that the changes in the molar surfaces, in a similar range as in the case of parameter β , cause much more significant changes in the modeled surface tension than those observed in the case of parameter β which sets the relation between the excess free energy of the volumetric phase and the surface phase. Thus, one can suggest that, in the case of large discrepancies between the calculated and the experimental values of the surface tension, one should look for the cause in the different values of the components' molar surface than those concluded from equation (4.1.2).

A very important factor affecting the calculated surface tension values (4.1.1) is the excess free energy of liquid alloys (of volumetric phase), calculated with the use of the coefficient of the equation describing the dependences of the excess free energy on the temperature and the content, that is, the so called thermodynamic parameters. As the literature analysis shows, their values established by different authors very often differ from each other, sometimes quite significantly, which will be demonstrated in the further part of the work.

The calculated parameters can be treated as subjective, as, during the phase diagram calculations, different authors give different weight to the same test

results or reject some of them. Thus, very similar phase diagram calculation results presented by various research groups do not necessarily prove similar values of the developed and proposed thermodynamic parameters of the liquid phase. An example of this can be the elaboration of phase diagrams performed by [1996Xie] and [1988Che] et al., which, for the Ag – Sn system, showed good agreement of the equilibrium lines with the experimental results obtained by different research methods, with a large difference among the excess free energies for a mole of liquid alloy (Fig. 4.1.3). The surface tension values calculated with the application of the thermodynamic parameters [1996Xie] and [1988Che], in some concentration ranges, show differences which equal up to a few tens of $\text{mN}\cdot\text{cm}^{-1}$ (Table 4.1.4).

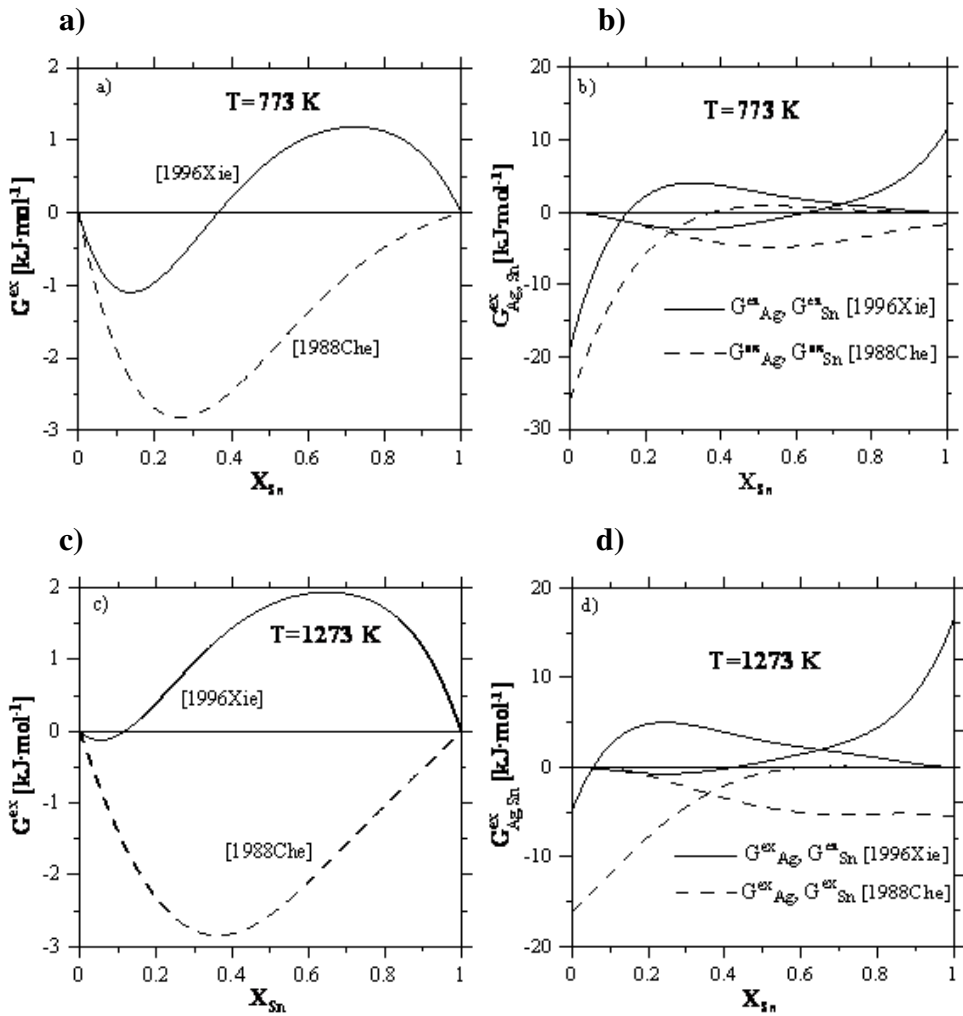


Fig. 4.1.3. Molar excess free energy of liquid Ag – Sn alloys at 773 K (a) and 1273 K (c) and excess free energies of Ag and Sn (b, d) calculated with the use of the thermodynamic parameters from the works [1996Xie] and [1988Che]

Table 4.1.4. Calculation results for the surface tension of an alloy from the Ag–Sn system, with concentration $X_{Sn} = 0.3$, obtained with the use of the thermodynamic parameters of the excess free energy of the liquid phase, coming from the works [1996Xie] and [1988Che]

	$\sigma_{873\text{ K}}$ [mN·cm ⁻¹]	$\sigma_{973\text{ K}}$ [mN·cm ⁻¹]	$\sigma_{1073\text{ K}}$ [mN·cm ⁻¹]	$\sigma_{1173\text{ K}}$ [mN·cm ⁻¹]	$\sigma_{1273\text{ K}}$ [mN·cm ⁻¹]
[1996Xie]	582	596	589	590	591
[1988Che]	674	680	683	682	678

Due to the significant discrepancies between the experimental data on the thermodynamic properties of the liquid phase obtained by different measuring methods and elaborated by different authors, it seems that good agreement, in a wide range of temperatures and concentrations, of the model and the experimental surface tension values can, on the one hand, be a criterion for the assessment of their correctness, and, on the other hand, the surface tension measurements can be used for the determination of the thermodynamic properties providing additional data to be applied in the thermodynamics of alloys, as it was presented in the works [2006Gas3] and [2011Gas].

The comparative analysis of the calculated and experimental values of surface tension makes it possible to draw the following conclusions:

1. The parameter set, $\beta = 0.83$ i $L = 1.0901$, proposed by the authors of [1996Tan] [1956Hoa], for surface tension modeling does not always provide results which are comparable with the experimental ones.
2. For some binary systems, the discrepancies concern not only the big differences between the measured and calculated values of the surface tension, but also the opposite values of the temperature

coefficient of surface tension, which is expressed by the increase of the surface tension together with the temperature increase, as opposed to the measured values, which present the opposite tendency (drop of surface tension together with temperature).

3. The change of the value of parameter β does not alter the character of the surface tension change for one similar to the experimental one, but merely raises or lowers its values within the whole temperature range of the calculations by a certain constant value.
4. The strong curvilinear temperature relations of surface tension, observed for some alloys, often with its maximum at higher temperatures, do not find their confirmation in the experimental results.

Due to the presented discrepancies between the model and experimental values of surface tension, work [2006Gas2] proposed new expressions for the calculation of parameter β and the molar surface of the monoatomic surface phase, whose application increases the correlation between the experimental data and the ones calculated from relation (4.1.1, 4.1.3).

4.1.1. Temperature relations of surface tension calculated from Butler's model

This chapter presents the temperature dependences of surface tension calculated from the Butler's model together with the standard deviation for binary systems and the Ag-Cu-Sn system. The surface tension calculations included the application of the own data on the surface tension of pure components, presented in the form of equations:

$$\sigma_{\text{Ag}} = 1133.9541 - 0.1904719 \cdot T \quad [2001Mos2]$$

$\sigma_{Au} = 1503.00 - 0.25000 \cdot T$	[2004Smi]
$\sigma_{Bi} = 405 - 0.0492 \cdot T$	[2001Mos3]
$\sigma_{Cu} = 1475.6 - 0.1422 \cdot T$	[2005Mos2]
$\sigma_{In} = 593.8 - 0.09421 \cdot T$	[2001Mos2]
$\sigma_{Pb} = 497.5 - 0.1096 \cdot T$	[2001Gas2]
$\sigma_{Sb} = 419 - 0.0561 \cdot T$	[2004Gas2]
$\sigma_{Sn} = 582.826 - 0.083361 \cdot T$	[2001Gas2]
$\sigma_{Zn} = 892.5 - 0.1246 \cdot T$	[2004Pst]

The temperature relations of the surface tension calculated from the Butler's model were presented in the form the following equation:

$$\sigma_{AB} = \sigma_A X_A + \sigma_B X_B + \Delta\sigma_{AB} =$$

$$\sigma_{AB} = \sigma_A X_A + \sigma_B X_B + X_A X_B \sum_{i=0}^n (a_i + b_i T + c_i T \ln T + d_i T^2) (X_A - X_B)^i$$

or

$$\sigma_{AB} = \sigma_A X_A + \sigma_B X_B + X_A X_B \sum_{i=0}^n (a_i + b_i T + c_i T^2) (X_A - X_B)^i$$

where:

X_A, X_B – mole fraction of A and B,

σ_A, σ_B – surface tension of A and B,

$a_i, b_i,$ and c_i – function parameters.

Ag-Au

$$\sigma = \sigma_{Ag} \cdot X_{Ag} + \sigma_{Au} \cdot X_{Au} + X_{Ag} \cdot X_{Au} \cdot$$

$$[(-128.79 + 0.045836 \cdot T + 0.00680219 \cdot T \cdot \ln T - 0.00001833 \cdot T^2) +$$

$$(243.86 - 0.060170 \cdot T - 0.00965926 \cdot T \cdot \ln T + 0.00002163 \cdot T^2) \cdot (X_{Ag} - X_{Au}) +$$

$$(-455.82 + 0.185348 \cdot T + 0.02786783 \cdot T \cdot \ln T - 0.00011934 \cdot T^2) \cdot (X_{Ag} - X_{Au})^2 +$$

$$\begin{aligned}
& (328.02-0.215276\cdot T-0.03058366\cdot T\cdot\ln T+0.00020777\cdot T^2) \cdot (X_{Ag} - X_{Au})^3 + \\
& (-696.90+0.305482\cdot T+0.05253429\cdot T\cdot\ln T-0.00011031\cdot T^2) \cdot (X_{Ag} - X_{Au})^4 + \\
& (767.94 -0.247998\cdot T-0.05354872\cdot T\cdot\ln T-0.00008074\cdot T^2) \cdot (X_{Ag} - X_{Au})^5 + \\
& (-783.30+0.034526\cdot T+0.03251694\cdot T\cdot\ln T-0.00010342\cdot T^2) \cdot (X_{Ag} - X_{Au})^6 + \\
& (622.05+0.151679\cdot T-0.01182360\cdot T\cdot\ln T+0.00010878\cdot T^2) \cdot (X_{Ag} - X_{Au})^7 + \\
& (-265.20+0.568632\cdot T+0.09529815\cdot T\cdot\ln T-0.00048490\cdot T^2) \cdot (X_{Ag} - X_{Au})^8 + \\
& (146.14 -0.777307\cdot T-0.11440099\cdot T\cdot\ln T+0.00066111\cdot T^2) \cdot (X_{Ag} - X_{Au})^9]
\end{aligned}$$

Standard deviation = 0.24 mN/m.

Temperature range: 1123 K – 1773 K.

Ag – Bi

$$\begin{aligned}
\sigma &= \sigma_{Ag}\cdot X_{Ag} + \sigma_{Bi}\cdot X_{Bi} + X_{Ag}\cdot X_{Bi}\cdot \\
& [(-0.149287E+04 + 0.761469E+00\cdot T - 0.121620E-03\cdot T^2) + \\
& (0.173843E+04 - 0.137566E+01\cdot T + 0.403969E-03\cdot T^2) \cdot (X_{Bi}-X_{Ag}) + \\
& (-0.190420E+04 + 0.233459E+01\cdot T - 0.959588E-03\cdot T^2) \cdot (X_{Bi}-X_{Ag})^2 + \\
& (0.441925E+04 - 0.374690E+00\cdot T - 0.161773E-02\cdot T^2) \cdot (X_{Bi}-X_{Ag})^3 + \\
& (-0.513947E+04 - 0.424837E+01\cdot T + 0.511611E-02\cdot T^2) \cdot (X_{Bi}-X_{Ag})^4 + \\
& (-0.138488E+05 + 0.443033E+01\cdot T + 0.339766E-02\cdot T^2) \cdot (X_{Bi}-X_{Ag})^5 + \\
& (0.164233E+05 + 0.462766E+01\cdot T - 0.107320E-01\cdot T^2) \cdot (X_{Bi}-X_{Ag})^6 + \\
& (0.253252E+05 - 0.178596E+02\cdot T + 0.943579E-03\cdot T^2) \cdot (X_{Bi}-X_{Ag})^7 + \\
& (-0.276606E+05 + 0.128574E+02\cdot T + 0.356715E-02\cdot T^2) \cdot (X_{Bi}-X_{Ag})^8]
\end{aligned}$$

Standard deviation = 2.6 mN/m.

Temperature range: T=523 K-1473 K.

Ag-Cu

$$\sigma = \sigma_{Ag} \cdot X_{Ag} + \sigma_{Au} \cdot X_{Au} + X_{Ag} \cdot X_{Cu}$$

$$\begin{aligned} & [(-982.68 + 0.262677 \cdot T + 0.04028137 \cdot T \cdot \ln T - 0.00013536 \cdot T^2) + \\ & (1625.72 - 0.693760 \cdot T - 0.09772514 \cdot T \cdot \ln T + 0.00039080 \cdot T^2) \cdot (X_{Ag} - X_{Cu}) + \\ & (-1142.64 - 0.084365 \cdot T + 0.14883052 \cdot T \cdot \ln T - 0.00030951 \cdot T^2) \cdot (X_{Ag} - X_{Cu})^2 + \\ & (884.43 + 0.115910 \cdot T - 0.13503940 \cdot T \cdot \ln T + 0.00031221 \cdot T^2) \cdot (X_{Ag} - X_{Cu})^3 + \\ & (-1834.68 - 0.167029 \cdot T + 0.32995081 \cdot T \cdot \ln T - 0.00064483 \cdot T^2) \cdot (X_{Ag} - X_{Cu})^4 + \\ & (786.99 + 0.928588 \cdot T - 0.22033146 \cdot T \cdot \ln T - 0.00004961 \cdot T^2) \cdot (X_{Ag} - X_{Cu})^5 + \\ & (-503.91 - 2.227133 \cdot T + 0.30070463 \cdot T \cdot \ln T - 0.00010432 \cdot T^2) \cdot (X_{Ag} - X_{Cu})^6 + \\ & (427.52 + 2.150896 \cdot T - 0.24607041 \cdot T \cdot \ln T + 0.00010187 \cdot T^2) \cdot (X_{Ag} - X_{Cu})^7 + \\ & (-304.05 - 1.644333 \cdot T + 0.52676684 \cdot T \cdot \ln T - 0.00098027 \cdot T^2) \cdot (X_{Ag} - X_{Cu})^8 + \\ & (195.10 + 1.125710 \cdot T - 0.50464926 \cdot T \cdot \ln T + 0.00113689 \cdot T^2) \cdot (X_{Ag} - X_{Cu})^9] \end{aligned}$$

Standard deviation = 0.30 mN/m

Temperature range: T = 1223 K – 1773 K.

Ag-In

$$\sigma = \sigma_{Ag} \cdot X_{Ag} + \sigma_{In} \cdot X_{In} + X_{Ag} \cdot X_{In}$$

$$\begin{aligned} & [(-0.118379E+04 + 0.937811E+00 \cdot T - 0.236329E-03 \cdot T^2) + \\ & (0.542148E+03 - 0.845177E+00 \cdot T + 0.244210E-03 \cdot T^2) \cdot (X_{In} - X_{Ag}) + \\ & (0.117512E+04 - 0.604659E+00 \cdot T + 0.198968E-03 \cdot T^2) \cdot (X_{In} - X_{Ag})^2 + \\ & (-0.126368E+04 + 0.279646E+00 \cdot T + 0.582528E-03 \cdot T^2) \cdot (X_{In} - X_{Ag})^3 + \\ & (-0.301611E+03 + 0.207517E+00 \cdot T - 0.760798E-03 \cdot T^2) \cdot (X_{In} - X_{Ag})^4 + \\ & (0.108103E+04 + 0.108580E+01 \cdot T - 0.141289E-02 \cdot T^2) \cdot (X_{In} - X_{Ag})^5 + \\ & (-0.976049E+03 + 0.892292E-02 \cdot T + 0.105965E-02 \cdot T^2) \cdot (X_{In} - X_{Ag})^6] \end{aligned}$$

Standard deviation = 1.2 mN/m.

Temperature range: T = 523 K - 1473 K.

Ag – Sb

$$\sigma = \sigma_{Ag} \cdot X_{Ag} + \sigma_{Sb} \cdot X_{Sb} + X_{Ag} \cdot X_{Sb} \cdot$$

$$\begin{aligned} & [(-0.184869E+04 + 0.119478E+01 \cdot T - 0.230032E-03 \cdot T^2) + \\ & (0.192438E+04 - 0.166853E+01 \cdot T + 0.402689E-03 \cdot T^2) \cdot (X_{Sb} - X_{Ag}) + \\ & (-0.178450E+04 + 0.198100E+01 \cdot T - 0.409537E-03 \cdot T^2) \cdot (X_{Sb} - X_{Ag})^2 + \\ & (0.228498E+04 - 0.329140E+01 \cdot T + 0.813957E-03 \cdot T^2) \cdot (X_{Sb} - X_{Ag})^3 + \\ & (0.186812E+04 + 0.269826E+01 \cdot T - 0.255553E-02 \cdot T^2) \cdot (X_{Sb} - X_{Ag})^4 + \\ & (-0.521756E+04 + 0.223883E+00 \cdot T + 0.263498E-02 \cdot T^2) \cdot (X_{Sb} - X_{Ag})^5 + \\ & (0.127895E+04 - 0.736562E+01 \cdot T + 0.413016E-02 \cdot T^2) \cdot (X_{Sb} - X_{Ag})^6 + \\ & (0.530285E+02 + 0.835367E+01 \cdot T - 0.576077E-02 \cdot T^2) \cdot (X_{Sb} - X_{Ag})^7] \end{aligned}$$

Standard deviation = 0.9.

Temperature range: T = 873 K-1473 K.

Ag-Sn

$$\sigma = \sigma_{Ag} \cdot X_{Ag} + \sigma_{Sn} \cdot X_{Sn} + X_{Ag} \cdot X_{Sn} \cdot$$

$$\begin{aligned} & [(-1196.52 - 1.28986 \cdot T + 0.319539 \cdot T \cdot \ln(T) - 0.000332752 \cdot T^2) + \\ & (-2288.32 + 10.2823 \cdot T - 1.19297 \cdot \ln(T) - 9.46879E-005 \cdot T^2) \cdot (X_{Sn} - X_{Ag}) + \\ & (-4736.38 + 51.3672 \cdot T - 7.0256 \cdot T \cdot \ln(T) + 0.00218277 \cdot T^2) \cdot (X_{Sn} - X_{Ag})^2 + \\ & (508.949 + 21.2309 \cdot T - 3.36837 \cdot T \cdot \ln(T) + 0.002235732 \cdot T^2) \cdot (X_{Sn} - X_{Ag})^3 + \\ & (5470.9 - 31.5738 \cdot T + 3.86967 \cdot T \cdot \ln(T)) \cdot (X_{Sn} - X_{Ag})^4 + \\ & (-277.125 - 0.373722 \cdot T) \cdot (X_{Sn} - X_{Ag})^5 - 910.691 \cdot (X_{Sn} - X_{Ag})^6] \end{aligned}$$

Standard deviation = 1.4 mN/m.

Temperature range: T = 523 K-1473 K.

Au-Cu

$$\sigma = \sigma_{\text{Au}} \cdot X_{\text{Au}} + \sigma_{\text{Cu}} \cdot X_{\text{Cu}} + X_{\text{Au}} \cdot X_{\text{Cu}}$$

$$\begin{aligned} & [(94.97 + 0.002865 \cdot T - 0.00050101 \cdot T \cdot \ln T - 0.00002177 \cdot T^2) + \\ & (-43.72 - 0.009243 \cdot T - 0.00094336 \cdot T \cdot \ln T + 0.00000558 \cdot T^2) \cdot (X_{\text{Au}} - X_{\text{Cu}}) + \\ & (-9.72 - 0.008609 \cdot T - 0.00071243 \cdot T \cdot \ln T + 0.00002569 \cdot T^2) \cdot (X_{\text{Au}} - X_{\text{Cu}})^2 + \\ & (0.08 - 0.000511 \cdot T - 0.00003730 \cdot T \cdot \ln T + 0.00000219 \cdot T^2) \cdot (X_{\text{Au}} - X_{\text{Cu}})^3 + \\ & (27.03 - 0.021334 \cdot T - 0.00300341 \cdot T \cdot \ln T + 0.00000035 \cdot T^2) \cdot (X_{\text{Au}} - X_{\text{Cu}})^4 + \\ & (8.85 - 0.003558 \cdot T - 0.00059567 \cdot T \cdot \ln T - 0.00000411 \cdot T^2) \cdot (X_{\text{Au}} - X_{\text{Cu}})^5 + \\ & (88.17 - 0.006967 \cdot T - 0.00129433 \cdot T \cdot \ln T + 0.00000026 \cdot T^2) \cdot (X_{\text{Au}} - X_{\text{Cu}})^6 + \\ & (3.16 + 0.001416 \cdot T + 0.00011203 \cdot T \cdot \ln T + 0.00000061 \cdot T^2) \cdot (X_{\text{Au}} - X_{\text{Cu}})^7 + \\ & (-46.64 - 0.024473 \cdot T - 0.00243680 \cdot T \cdot \ln T + 0.00002911 \cdot T^2) \cdot (X_{\text{Au}} - X_{\text{Cu}})^8 + \\ & (-5.45 - 0.001065 \cdot T - 0.00015061 \cdot T \cdot \ln T + 0.00000215 \cdot T^2) \cdot (X_{\text{Au}} - X_{\text{Cu}})^9] \end{aligned}$$

Standard deviation = 0.06 mN/m.

Temperature range: T= 1323 K – 1773 K.

Au-Sn

$$\sigma = \sigma_{\text{Au}} \cdot X_{\text{Au}} + \sigma_{\text{Sn}} \cdot X_{\text{Sn}} + X_{\text{Au}} \cdot X_{\text{Sn}}$$

$$\begin{aligned} & [(-1308.74 + 0.337166 \cdot T + 0.06473997 \cdot T \cdot \ln T - 0.00017182 \cdot T^2) + \\ & (-167.61 + 0.249078 \cdot T + 0.03450839 \cdot T \cdot \ln T - 0.00021232 \cdot T^2) \cdot (X_{\text{Au}} - X_{\text{Sn}}) + \\ & (539.07 + 0.376942 \cdot T - 0.06569887 \cdot T \cdot \ln T - 0.00013672 \cdot T^2) \cdot (X_{\text{Au}} - X_{\text{Sn}})^2 + \\ & (813.94 - 0.840101 \cdot T - 0.12356500 \cdot T \cdot \ln T + 0.00082397 \cdot T^2) \cdot (X_{\text{Au}} - X_{\text{Sn}})^3 + \\ & (522.70 - 1.459313 \cdot T - 0.19136750 \cdot T \cdot \ln T + 0.00179447 \cdot T^2) \cdot (X_{\text{Au}} - X_{\text{Sn}})^4 + \\ & (-1579.78 + 0.716893 \cdot T + 0.08940023 \cdot T \cdot \ln T - 0.00054143 \cdot T^2) \cdot (X_{\text{Au}} - X_{\text{Sn}})^5 + \\ & (-1858.58 + 1.486399 \cdot T + 0.18602332 \cdot T \cdot \ln T - 0.00165612 \cdot T^2) \cdot (X_{\text{Au}} - X_{\text{Sn}})^6 + \\ & (-73.31 + 1.629518 \cdot T + 0.36997327 \cdot T \cdot \ln T - 0.00230965 \cdot T^2) \cdot (X_{\text{Au}} - X_{\text{Sn}})^7 + \\ & (-31.90 + 2.600040 \cdot T + 0.42347484 \cdot T \cdot \ln T - 0.00300577 \cdot T^2) \cdot (X_{\text{Au}} - X_{\text{Sn}})^8 + \\ & (-232.50 - 4.312586 \cdot T + 0.13173129 \cdot T \cdot \ln T + 0.00192850 \cdot T^2) \cdot (X_{\text{Au}} - X_{\text{Sn}})^9 + \\ & (-349.57 - 4.214777 \cdot T - 0.07544004 \cdot T \cdot \ln T + 0.00285428 \cdot T^2) \cdot (X_{\text{Au}} - X_{\text{Sn}})^{10}] \end{aligned}$$

Standard deviation = 0.20 mN/m.

Temperature range T= 673 K – 1473 K.

Bi – Sn

$$\sigma = \sigma_{Bi} \cdot X_{Bi} + \sigma_{Sn} \cdot X_{Sn} + X_{Bi} \cdot X_{Sn} \cdot$$

$$\begin{aligned} & [(-0.305468E+03 + 0.299480E+00 \cdot T - 0.947360E-04 \cdot T^2) + \\ & (0.247886E+03 - 0.299949E+00 \cdot T + 0.102698E-03 \cdot T^2) \cdot (X_{Sn} - X_{Bi}) + \\ & (-0.412439E+03 + 0.658512E+00 \cdot T + -0.268636E-03 \cdot T^2) \cdot (X_{Sn} - X_{Bi})^2 + \\ & (0.425522E+03 - 0.736134E+00 \cdot T + 0.314682E-03 \cdot T^2) \cdot (X_{Sn} - X_{Bi})^3] \end{aligned}$$

Standard deviation = 0.7 mN/m.

Temperature range: T =523 K-1373 K.

Cu – Sb

$$\sigma = \sigma_{Cu} \cdot X_{Cu} + \sigma_{Sb} \cdot X_{Sb} + X_{Cu} \cdot X_{Sb} \cdot$$

$$\begin{aligned} & [(-0.254453E+04 + 0.869491E+00 \cdot T - 0.525369E-04 \cdot T^2) + \\ & (0.303829E+04 - 0.236892E+01 \cdot T + 0.702098E-03 \cdot T^2) \cdot (X_{Sb} - X_{Cu}) + \\ & (-0.439107E+04 + 0.604184E+01 \cdot T - 0.242030E-02 \cdot T^2) \cdot (X_{Sb} - X_{Cu})^2 + \\ & (-0.170621E+04 + 0.106854E+02 \cdot T - 0.591391E-02 \cdot T^2) \cdot (X_{Sb} - X_{Cu})^3 + \\ & (0.776173E+04 - 0.272121E+02 \cdot T + 0.141186E-01 \cdot T^2) \cdot (X_{Sb} - X_{Cu})^4 + \\ & (0.451172E+04 - 0.285694E+02 \cdot T + 0.162044E-01 \cdot T^2) \cdot (X_{Sb} - X_{Cu})^5 + \\ & (-0.861627E+04 + 0.498186E+02 \cdot T - 0.280224E-01 \cdot T^2) \cdot (X_{Sb} - X_{Cu})^6 + \\ & (0.129271E+05 + 0.776027E+01 \cdot T - 0.910825E-02 \cdot T^2) \cdot (X_{Sb} - X_{Cu})^7 + \\ & (-0.152099E+05 - 0.133876E+02 \cdot T + 0.134642E-01 \cdot T^2) \cdot (X_{Sb} - X_{Cu})^8] \end{aligned}$$

Standard deviation = 2.6 mN/m

Temperature range: T =873 K-1473 K.

Cu – Sn

$$\sigma = \sigma_{Cu} \cdot X_{Cu} + \sigma_{Sn} \cdot X_{Sn} + X_{Cu} \cdot X_{Sn} \cdot$$

$$\begin{aligned} & [(-0.238198E+04 + 0.104937E+01 \cdot T - 0.126049E-03 \cdot T^2) + \\ & (0.203605E+04 - 0.862612E+00 \cdot T - 0.186603E-04 \cdot T^2) \cdot (X_{Sn} - X_{Cu}) + \\ & (-0.122393E+04 + 0.104175E+01 \cdot T - 0.155827E-03 \cdot T^2) \cdot (X_{Sn} - X_{Cu})^2 + \\ & (0.241711E+04 - 0.421994E+01 \cdot T + 0.162659E-02 \cdot T^2) \cdot (X_{Sn} - X_{Cu})^3 + \\ & (-0.229390E+04 + 0.358032E+01 \cdot T - 0.148493E-02 \cdot T^2) \cdot (X_{Sn} - X_{Cu})^4 + \\ & (0.103584E+03 - 0.212607E+01 \cdot T + 0.112093E-02 \cdot T^2) \cdot (X_{Sn} - X_{Cu})^5 + \\ & (-0.696978E+02 + 0.310262E+01 \cdot T - 0.104502E-02 \cdot T^2) \cdot (X_{Sn} - X_{Cu})^6 + \\ & (0.434818E+02 + 0.169575E+01 \cdot T - 0.583009E-03 \cdot T^2) \cdot (X_{Sn} - X_{Cu})^7 + \\ & (-0.148976E+03 - 0.194523E+01 \cdot T - 0.122857E-03 \cdot T^2) \cdot (X_{Sn} - X_{Cu})^8] \end{aligned}$$

Standard deviation = 1.3 mN/m.

Temperature range T = 523 K-1473 K.

In – Sn

$$\sigma = \sigma_{In} \cdot X_{In} + \sigma_{Sn} \cdot X_{Sn} + X_{In} \cdot X_{Sn} \cdot$$

$$[(0.190681E+01 + 0.460633E-02 \cdot T) + 0.377716E+01 \cdot (X_{Sn} - X_{In})]$$

Standard deviation = 0.05 mN/m.

Temperature range: T = 523 K-1233 K.

In-Zn

$$\sigma = \sigma_{In} \cdot X_{In} + \sigma_{Zn} \cdot X_{Zn} + X_{In} \cdot X_{Zn} \cdot$$

$$\begin{aligned} & [(-746.06 - 0.391066 \cdot T + 0.16179879 \cdot T \cdot \ln T - 0.00031034 \cdot T^2) + \\ & (153.56 + 10.487036 \cdot T - 1.63402043 \cdot T \cdot \ln T + 0.00094829 \cdot T^2) \cdot (X_{In} - X_{Zn}) + \\ & (1805.95 - 10.878760 \cdot T + 1.02694740 \cdot T \cdot \ln T + 0.00164930 \cdot T^2) \cdot (X_{In} - X_{Zn})^2 + \\ & (3020.64 + 5.064608 \cdot T - 2.00025118 \cdot T \cdot \ln T + 0.00588519 \cdot T^2) \cdot (X_{In} - X_{Zn})^3 + \\ & (-23912.52 + 24.775854 \cdot T + 3.89660696 \cdot T \cdot \ln T - 0.02736033 \cdot T^2) \cdot (X_{In} - X_{Zn})^4 + \end{aligned}$$

$$\begin{aligned}
& (1935.45-27.880448\cdot T+5.62818385\cdot T\cdot\ln T -0.01268307T\cdot T^2) \cdot (X_{\text{In}}-X_{\text{Zn}})^5+ \\
& (48946.89+141.832275\cdot T-40.9315708\cdot T\cdot\ln T+0.09020524\cdot T^2) \cdot (X_{\text{In}}-X_{\text{Zn}})^6+ \\
& (-7524.56-163.739836\cdot T+27.82890413\cdot T\cdot\ln T-0.02045047\cdot T^2) \cdot (X_{\text{In}}-X_{\text{Zn}})^7+ \\
& (-52789.77-15.194208\cdot T+20.30734426\cdot T\cdot\ln T-0.07108110\cdot T^2) \cdot (X_{\text{In}}-X_{\text{Zn}})^8+ \\
& (30268.77 +4.429380\cdot T -9.31929265\cdot T\cdot\ln T+0.02910028\cdot T^2) \cdot (X_{\text{In}}-X_{\text{Zn}})^9]
\end{aligned}$$

Standard deviation = 0.70 mN/m.

Temperature range: 673 K – 1173 K.

Pb-Sn

$$\begin{aligned}
\sigma &= \sigma_{\text{Pb}}\cdot X_{\text{Pb}}+\sigma_{\text{Sn}}\cdot X_{\text{Sn}}+X_{\text{Pb}}\cdot X_{\text{Sn}}\cdot \\
& [(-190.005 + 0.139122\cdot T -4.71105\text{E-}005\cdot T^2) + \\
& (-249.947+0.264891\cdot T - 7.06023\text{E-}005\cdot T^2)\cdot(X_{\text{Sn}}-X_{\text{Pb}}) + \\
& (-303.309 + 0.594119\cdot T - 0.000289183\cdot T^2)\cdot(X_{\text{Sn}}-X_{\text{Pb}})^2 + \\
& (-183.532 +0.496143\cdot T -0.000289061\cdot T^2)\cdot(X_{\text{Sn}}-X_{\text{Pb}})^3]
\end{aligned}$$

Standard deviation = 0.4 mN/m.

Temperature range: T=573 K-1273 K.

Sb – Sn

$$\begin{aligned}
\sigma &= \sigma_{\text{Sb}}\cdot X_{\text{Sb}}+\sigma_{\text{Sn}}\cdot X_{\text{Sn}}+X_{\text{Sb}}\cdot X_{\text{Sn}}\cdot \\
& [(-0.118699\text{E}+03 + 0.111200\text{E}+00 \cdot T - 0.270760\text{E-}04\cdot T^2) + \\
& (- 0.299993\text{E}+01 + 0.290997\text{E-}01\cdot T - 0.175259\text{E-}04\cdot T^2) \cdot (X_{\text{Sn}}-X_{\text{Sb}}) + \\
& (-0.254475\text{E}+03 + 0.364843\text{E}+00\cdot T - 0.143034\text{E-}03\cdot T^2) \cdot (X_{\text{Sn}}-X_{\text{Sb}})^2 + \\
& (-0.169695\text{E}+03 + 0.179507\text{E}+00\cdot T - 0.439113\text{E-}04\cdot T^2) \cdot (X_{\text{Sn}}-X_{\text{Sb}})^3]
\end{aligned}$$

Standard deviation = 0.3 mN/m.

Temperature range: T =573 K-1473 K.

Sn – Zn

$$\sigma = \sigma_{\text{Sn}} \cdot X_{\text{Sn}} + \sigma_{\text{Zn}} \cdot X_{\text{Zn}} + X_{\text{Sn}} \cdot X_{\text{Zn}} \cdot$$

$$\begin{aligned} & [(-0.727759\text{E}+03 + 0.595108\text{E}+00 \cdot T - 0.151107\text{E}-03 \cdot T^2) + \\ & (0.144075\text{E}+04 - 0.248597\text{E}+01 \cdot T + 0.130529\text{E}-02 \cdot T^2) \cdot (X_{\text{Sn}} - X_{\text{Zn}}) + \\ & (-0.279219\text{E}+04 + 0.649153\text{E}+01 \cdot T - 0.406738\text{E}-02 \cdot T^2) \cdot (X_{\text{Sn}} - X_{\text{Zn}})^2 + \\ & (-0.997136\text{E}+03 + 0.852386\text{E}+01 \cdot T - 0.782555\text{E}-02 \cdot T^2) \cdot (X_{\text{Sn}} - X_{\text{Zn}})^3 + \\ & (0.510303\text{E}+04 - 0.240004\text{E}+02 \cdot T + 0.199273\text{E}-01 \cdot T^2) \cdot (X_{\text{Sn}} - X_{\text{Zn}})^4 + \\ & (0.190041\text{E}+04 - 0.197816\text{E}+02 \cdot T + 0.194024\text{E}-01 \cdot T^2) \cdot (X_{\text{Sn}} - X_{\text{Zn}})^5 + \\ & (-0.474652\text{E}+04 + 0.374526\text{E}+02 \cdot T - 0.354238\text{E}-01 \cdot T^2) \cdot (X_{\text{Sn}} - X_{\text{Zn}})^6 + \\ & (0.101937\text{E}+05 - 0.603384\text{E}+01 \cdot T - 0.515570\text{E}-02 \cdot T^2) \cdot (X_{\text{Sn}} - X_{\text{Zn}})^7 + \\ & (-0.116980\text{E}+05 + 0.361051\text{E}+01 \cdot T + 0.976749\text{E}-02 \cdot T^2) \cdot (X_{\text{Sn}} - X_{\text{Zn}})^8] \end{aligned}$$

Standard deviation = 2.1 mN/m.

Temperature range: T = 523 K-973 K.

Ag – Cu – Sn

$$\sigma_{\text{Ag}} = 1133.9541 - 0.1904719$$

$$\sigma_{\text{Cu}} = 1656.1 - 0.26$$

$$\sigma_{\text{Sn}} = 582.826 - 0.083361$$

$$X_{\text{Ag}} = X_1$$

$$X_{\text{Cu}} = X_2$$

$$X_{\text{Sn}} = X_3$$

$$C_{\text{Ag}} = X_{\text{Ag}} / (X_{\text{Ag}} + X_{\text{Cu}})$$

$$C_{\text{Cu}} = 1 - C_{\text{Ag}}$$

$$C_{\text{Ag}} = X_{\text{Ag}} / (X_{\text{Ag}} + X_{\text{Sn}})$$

$$C_{\text{Sn}} = 1 - C_{\text{Ag}}$$

$$C_{\text{Cu}} = X_{\text{Cu}} / (X_{\text{Cu}} + X_{\text{Sn}})$$

$$C_{\text{Sn}} = 1 - C_{\text{Cu}}$$

Ag-Cu

$$C_{Ag} = X_{Ag} / (X_{Ag} + X_{Cu})$$

$$C_{Cu} = 1 - C_{Ag}$$

$$\begin{aligned} \sigma_{Ag-Cu} = & \sigma_{Ag} \cdot C_{Ag} + \sigma_{Cu} \cdot C_{Cu} + \\ & C_{Ag} \cdot C_{Cu} \cdot [(-1575.78 + 1.1426 \cdot T - 0.000264833 \cdot T^2) + \\ & (-2105.05 + 1.85056 \cdot T - 0.000485818 \cdot T^2) \cdot (1 - 2 \cdot C_{Ag}) + \\ & (-1395.73 + 0.431049 \cdot T + 0.000245942 \cdot T^2) \cdot (1 - 2 \cdot C_{Ag})^2 + \\ & (-353.358 - 2.12909 \cdot T + 0.0016628 \cdot T^2) \cdot (1 - 2 \cdot C_{Ag})^3 + \\ & (-2902.95 + 4.5745 \cdot T - 0.00201852 \cdot T^2) \cdot (1 - 2 \cdot C_{Ag})^4 + \\ & (-5138.84 + 12.6341 \cdot T - 0.00683891 \cdot T^2) \cdot (1 - 2 \cdot C_{Ag})^5 + \\ & (-3886.24 + 6.47157 \cdot T - 0.00255543 \cdot T^2) \cdot (1 - 2 \cdot C_{Ag})^6 + \\ & (-4399.98 - 0.131168 \cdot T + 0.00272847 \cdot T^2) \cdot (1 - 2 \cdot C_{Ag})^7 + \\ & (-2514.85 - 0.834288 \cdot T + 0.00196306 \cdot T^2) \cdot (1 - 2 \cdot C_{Ag})^8] \end{aligned}$$

Ag-Sn

$$C_{Ag} = X_{Ag} / (X_{Ag} + X_{Sn})$$

$$C_{Sn} = 1 - C_{Ag}$$

$$\begin{aligned} \sigma_{Ag-Sn} = & \sigma_{Ag} \cdot C_{Ag} + \sigma_{Sn} \cdot C_{Sn} + \\ & C_{Ag} \cdot C_{Sn} \cdot [(-1350.69 + 0.931166 \cdot T - 0.000190183 \cdot T^2) + \\ & (1300.76 - 1.39459 \cdot T + 0.000420192 \cdot T^2) \cdot (1 - 2 \cdot C_{Ag}) + \\ & (-1063.49 + 1.91129 \cdot T - 0.000617902 \cdot T^2) \cdot (1 - 2 \cdot C_{Ag})^2 + \\ & (1020.03 - 1.6385 \cdot T + 0.000233688 \cdot T^2) \cdot (1 - 2 \cdot C_{Ag})^3 + \\ & (1286.77 + 0.417819 \cdot T - 0.00112704 \cdot T^2) \cdot (1 - 2 \cdot C_{Ag})^4 + \\ & (-3289.67 - 1.96031 \cdot T + 0.00392327 \cdot T^2) \cdot (1 - 2 \cdot C_{Ag})^5 + \\ & (1252.75 - 1.1378 \cdot T + 7.22516E-005 \cdot T^2) \cdot (1 - 2 \cdot C_{Ag})^6 + \\ & (-620.138 + 10.388 \cdot T - 0.00765225 \cdot T^2) \cdot (1 - 2 \cdot C_{Ag})^7 + \end{aligned}$$

$$(996.961-7.41334 \cdot T+0.00494539 \cdot T^2) \cdot (1-2 \cdot C_{Ag})^8]$$

Cu-Sn

$$C_{Cu}=X_{Cu}/(X_{Cu}+X_{Sn})$$

$$C_{Sn}=1-C_{Cu}$$

$$\mathbf{dstCuSn}=C_{Cu} \cdot C_{Sn} \cdot$$

$$\begin{aligned} & [(-2381.98+1.04937 \cdot T-0.000126049 \cdot T^2) + \\ & (2036.05-0.862612 \cdot T-1.86603E-005 \cdot T^2) \cdot (1-2 \cdot C_{Cu}) + \\ & (-1223.93+1.04175 \cdot T-0.000155827 \cdot T^2) \cdot (1-2 \cdot C_{Cu})^2 + \\ & (2417.11-4.21994 \cdot T+0.00162659 \cdot T^2) \cdot (1-2 \cdot C_{Cu})^3 + \\ & (-2293.9+3.58032 \cdot T-0.00148493 \cdot T^2) \cdot (1-2 \cdot C_{Cu})^4 + \\ & (103.584-2.12607 \cdot T+0.00112093 \cdot T^2) \cdot (1-2 \cdot C_{Cu})^5 + \\ & (-69.6978+3.10262 \cdot T-0.00104502 \cdot T^2) \cdot (1-2 \cdot C_{Cu})^6 + \\ & (43.4818+1.69575 \cdot T-0.000583009 \cdot T^2) \cdot (1-2 \cdot C_{Cu})^7 + \\ & (-148.976-1.94523 \cdot T-0.000122857 \cdot T^2) \cdot (1-2 \cdot C_{Cu})^8] \end{aligned}$$

$$\begin{aligned} \mathbf{ter}(X_{Ag}, X_{Cu}, X_{Sn}) = & X_1 \cdot X_2 \cdot X_3 \cdot [(47185 - 69,9172 \cdot T) \cdot X_3 + \\ & (-65853,8+46,2144 \cdot T) \cdot X_3^2 + (-81607.3+799,227 \cdot T) \cdot X_1^3 + \\ & (-23868.2+51,5619 \cdot T) \cdot X_2^3 + (-31119.8+87,1466 \cdot T) \cdot X_3^3 + \\ & (37960-4211,29 \cdot T) \cdot X_1^4 + (1419.67-1,38848 \cdot T) \cdot X_2^4 + \\ & (72680.1-20,2167 \cdot T) \cdot X_3^4 + (67133+10244,7 \cdot T) \cdot X_1^5 + \\ & (26826.6-45,4089 \cdot T) \cdot X_2^5 + (31210.8-175,318 \cdot T) \cdot X_3^5 + \\ & (10817-9874,39 \cdot T) \cdot X_1^6 + (-11438.9+13,4692 \cdot T) \cdot X_2^6 + \\ & (-47062.2+114,528 \cdot T) \cdot X_3^6] \end{aligned}$$

$$\sigma_{Ag-Cu-Sn} = \sigma_{Ag-Cu} \cdot (C_{Cu}/(C_{Cu}+C_{Sn})) +$$

$$\sigma_{Ag-Sn} \cdot (1-C_{Cu}/(C_{Cu}+C_{Sn})) + \mathbf{dstCuSn} \cdot (1-C_{Ag}-C_{Sn}) \cdot \mathbf{ter}(X_{Ag}, X_{Cu}, X_{Sn})$$

Standard deviation = 1.0.

$$X_{Sn} \geq 0.65$$

Temperature range: T=500 K-1373 K.

4.2. Monoatomic surface layer

4.2.1. Polarized atom model

The previous chapter, which included the analysis of the effect of parameters β and the molar surface of the surface layer, implies that even significant changes in the value of β do not cause a change of the calculated surface layer big enough to explain its increase with temperature, which is observed e.g. for the silver-bismuth system. Another unexpected property of the calculated surface tension is, sometimes observed, its strong curvilinear character of changes together with temperature change. Faced with the incapability to correct these anomalies, or at least to significantly weaken them by way of rendering parameter β variable, one can draw an obvious conclusion that the only quantity which can significantly change this tendency is a new model of the monoatomic structure of the surface layer, other than that applied so far, expressed by relation (4.1.3). It is because, according to the relations connecting the surface tension with the thermodynamic properties in Figures (4.1.1) and (4.1.2), the molar surface is another variable which has an effect on the value of the calculated surface tension, with the particular relation between the excess free energies of the surface and volumetric phase.

4.2.1.1. Model assumptions

In comparison with the monoatomic surface phase presented in Fig. 4.2.1, resulting from the assumption of dense atomic packing (Eq. (4.1.3)), it is postulated that in [2006Gas2], the atom distribution visible in Figs. 4.2.2a and 4.2.2b, in relation to the effect of the interaction between the atoms of the gaseous and volumetric phase with those of the monoatomic surface phase, as well as a very high pressure (compressive stress) in the mono-layer (according to the Laplace's definition), the surface tension σ is a product of the thickness of layer h and the compressive stress δ).

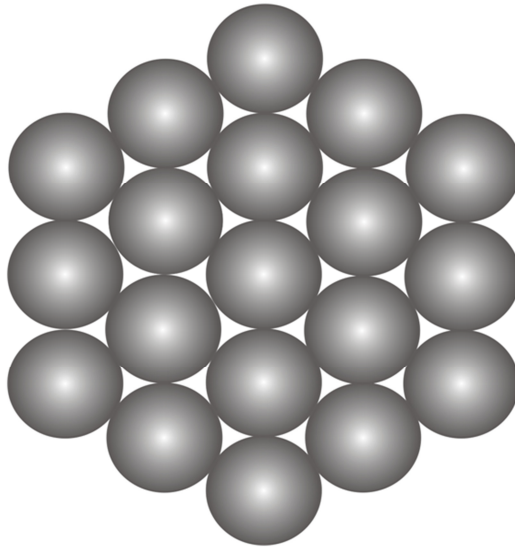


Fig. 4.2.1. Structure of monoatomic surface layer of the densest atomic packing

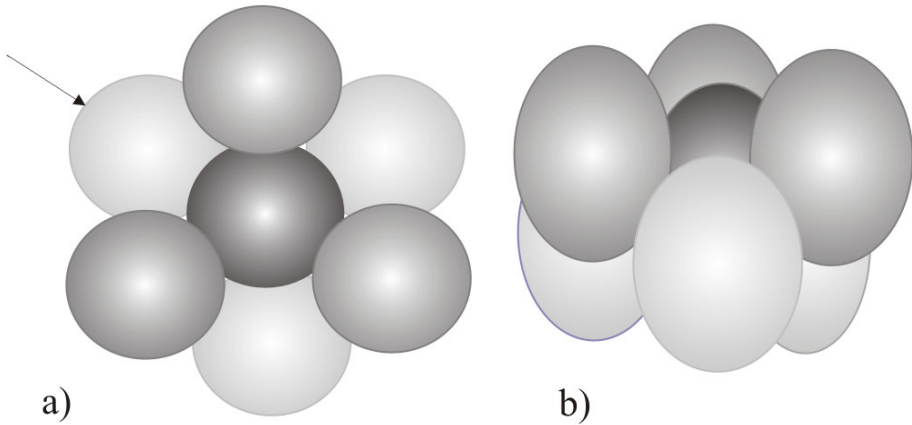


Fig. 4.2.2 A possible atomic packing in the monoatomic surface phase, which is a result of the atom reaction of the volumetric and gaseous phase, the asymmetrical electrostatic reaction (no atoms over the mono-layer) and the high pressure in the surface phase

The derived relation for the molar surface of the monoatomic surface layer is implied by the electron theory and by the different energy state of the metal atoms of the monoatomic surface layer, compared to those in the volumetric phase, which is the effect of the lack of atoms over the surface of the monoatomic layer. The assumptions made are as follows:

- The asymmetrical distribution of the potential field around the atoms in the surface layer, caused by the lack of neighbours over the monoatomic surface, causes the existence of a resultant force which operates on the atoms' electrons.
- This force causes shifts of the valence electrons, rendering the atoms in the surface layer polarized (Fig. 4.2.2).

- The strongest operation effect is demonstrated by the valence electrons, which are the most remote from the atomic nucleus. As a result, one observes an approximation of the atoms in the surface layer, and thus a change of the interatomic distance in relation to that in the volumetric phase.
- The effect of the approximation is the most transparent at the temperatures lower than a certain characteristic temperature T_C , corresponding to a certain constant value of the pressure of the metal vapours over the solution, at which once observes an equalization of the interatomic distances (D_{sr}) with those calculated from equation (4.1.2).
- Beyond temperature T_C , the increase of the inter-atomic distances is higher than it is implied by equation (4.1.2), as a result of an intense bombardment (effect) of the surface layer atoms by those in the gaseous phase (over the surface layer) and those from the volumetric phase. Although the interaction of the gaseous phase with the surface layer (phase) takes place at every temperature above the melting point, only beyond temperature T_C is the interaction strong enough to cause an additional growth of the molar surface of the surface layer beyond that calculated from relation (4.1.2).

Due to the made assumption about the change in the inter-atomic distance in the monoatomic surface layer, the next point presents the relation which makes it possible to determine the molar surface of the surface layer with the application of equation (4.1.2) and the introduced correction coefficient k_r .

4.2.1.2. Relation between molar surfaces of different atomic ion radii

The molar surface of a metal's (solution's) surface layer is calculated from the molar volume, according to the following relations:

$$D_{sr} = \sqrt[3]{\frac{V}{N}} \quad (4.2.1)$$

$$S = ND_{sr}^2 = V^{2/3} N^{1/3} \quad (4.2.2)$$

where: D_{sr} is the mean atom diameter (distance between the atom centres), N is the Avogadro number, and S is the molar surface with the same structure as the metal (solution) occupying the molar volume V . When we assume that the structure of the surface layer is one which is densely packed, the molar surface S is corrected by the introduction of coefficient L into relation (4.1.2) or (4.2.2), which equals 1.091. Relation (4.1.2) then assumes the following form:

$$S = L V^{2/3} N^{1/3} = 1.091 V^{2/3} N^{1/3} = 1.091 N D_{sr}^2 \quad (4.2.3)$$

If we denote the molar surfaces of two metals of different atomic radii by S_1 and S_2 , they will be expressed by the following relations:

$$S_1 = 1.091 V_1^{2/3} N^{1/3} = 1.091 N D_{sr}^2 \quad (4.2.4)$$

$$S_2 = 1.091 V_2^{2/3} N^{1/3} = 1.091 N D_{sr}^2 \quad (4.2.5)$$

By dividing equation (4.2.4) by (4.2.5) and substituting $D_{sr} = D = 2R$, where R denotes the atomic radius, we obtain the following relation:

$$\frac{S_1}{S_2} = \frac{V_1^{2/3}}{V_2^{2/3}} = \frac{D_1^2}{D_2^2} = \frac{R_1^2}{R_2^2} \quad (4.2.6)$$

It allows to calculate one of the molar surfaces, when the ratio of the atomic diameters 1 and 2 is known, and to calculate the other molar surface or determine it from the atomic diameters, when the molar volumes and the other atomic diameter are known.

By denoting the atomic diameter (radius) ratio with \mathbf{k}_r , after rearranging equation (4.2.6), one obtains the equation for the molar surface of component 1 in the following form;

$$\mathbf{S}_1 = \mathbf{k}_r^2 \mathbf{S}_2 = \frac{\mathbf{R}_1^2}{\mathbf{R}_2^2} \mathbf{S}_2 \quad (4.2.7)$$

Equation (4.2.7) is also correct when the metal can be converted from state „S” into state „B”, and it has the same structure as in state **S**, but a different atomic radius (inter-atomic distance), e.g. as a result of high pressure. By denoting the molar surface in state **S** by \mathbf{S}_S and that in state **B** by \mathbf{S}_B , one can write relation (4.2.7) in the following way:

$$\mathbf{S}_S = \frac{\mathbf{R}_S^2}{\mathbf{R}_B^2} \mathbf{S}_B = \mathbf{k}_r^2 \mathbf{S}_B \quad (4.2.8)$$

where \mathbf{R}_S and \mathbf{R}_B are the atomic radii in state „S” and „B”.

With the assumption that the inter-atomic distances ($2\mathbf{R}_S$) in the surface phase are different than those in the volumetric phase ($2\mathbf{R}_B$), from equation (4.2.8) we can calculate \mathbf{S}_S , if we know the molar volume of the volumetric phase (**V**) and the inter-atomic distance ($2\mathbf{R}_S$) in the surface phase, that is the correction parameter \mathbf{k}_r .

4.2.1.3. Correction parameter of metal surface layer structure

According to the presented model of the surface layer of liquid metals, the knowledge of the correction parameter k_r is necessary for the determination of the molar surface of the surface layer from the molar volume of the metals forming the solution (4.2.8). The model's assumptions state that the mathematical formalism should include two quantities which allow to determine the correction parameter k_r . One is the characteristic temperature T_C and the other is the atomic radius R of the metal in the surface phase. The mean atomic radius in the volumetric phase is calculated with the use of relation (4.2.1). The work makes the following assumptions with regard to the mentioned quantities:

- The characteristic temperature T_C is the temperature at which the saturated vapour pressure of the metal is equal to one thousandth of an atmosphere ($p_n = 0.001 \text{ atm}$), as a result of the comparative analysis of the calculated and experimental values of surface tension for several binary systems.
- The atomic radius in the surface layer of the liquid metal in the state cooled down to room temperature ($T=298.14 \text{ K}$) is equal to its radius in the ion crystals with the coordination number of 6 and the ion valency equaling the number of electrons filling the furthest subshell. For a big majority of metals, this number equals 3, for antimony and bismuth, it is 1 or 2, and only for one, that is polonium, it equals 4 (subshells s and p).
- The correction parameter k_r is a linear function of temperature.

In order to determine the linear dependence of k_r on temperature, it is necessary to know at least two values of k_r at two different temperatures T . One value of k_r , at room temperature, is calculated from the definition of k_r in equation (4.2.8) and the data on metals included in Table 4.2.1. The other value of k_r , according to the assumed model (chapter 4.2.1.3), equals 1 at temperature T_C , that is such at which the metal vapour pressure $p=0.001\text{atm}$ ($k_r = 1$ for $T = T_C$). Temperature T_C is calculated from the equilibrium between the gaseous and the liquid phase, as well as from the thermochemical data on the given metals.

The calculations of k_r involved the use of the mean values of atomic radii calculated on the basis of the data from [1923Gol], [1967Tea] and that of Żdanow cited in [1987Boj], as well as the metal ion radii developed by Shanon [1976Sha] for the coordination number of 6 and for different valencies (Table 4.2.1).

The characteristic temperatures T_C were determined on the basis of the thermodynamic data and the vapour pressure data given in the book by Barrin and Knacki [1973Bar], and the determined equations of coefficient k_r are compiled in Table 4.2.2.

Table 4.2.1. Mean atomic and ion radii of selected metals for their different valencies W and their ratio $R_J/R_A = k_r$ for $T = 298 \text{ K}$

Metal	W	R [m ⁻¹⁰]	R _J /R _A	T _C [K]	Metal	W	R [m ⁻¹⁰]	R _J /R _A	T _C [K]
Ag	0	1.38	0.84 78	1582	Pb	0	1.68	0.7083	1229
	+1	1.15				+2	1.19		
Bi	0	1.71	0.60 23	1155	Sb	0	1.54	0.4935	1000
	+3	1.03				+3	0.76		
In	0	1.57	0.84 08	1486	Sn	0	1.53	0.6078	1858
	+1	1.18				+2	0.93		

Table 4.2.2. Temperature dependences of correction coefficients k_r of the molar surface of selected metals

Metal	$k_r = a + bT$	Metal	$k_r = a + bT$
Ag	$= 0.8125 + 0.0001186T$	Pb	$= 0.6149 + 0.0003134T$
Bi	$= 0.4639 + 0.0004641T$	Sb	$= 0.2784 + 0.0007217T$
In	$= 0.8008 + 0.0001340T$	Sn	$= 0.5328 + 0.0002514T$

4.2.1.4. Surface of monoatomic surface layer of solutions

Chapter 4.2.1.2 proposed a correction of the size of the monoatomic molar surface of metal surface layer through an introduction of parameter k_r , which takes into account the change of the inter-atomic distance in relation to that in the volumetric phase (Table 4.2.2). in the case of binary solutions, due to the different metals and different values of parameters k_r , for the alloy of the surface phase composition equaling X_1^S and X_2^S ,

the parameter's value should be within the range of the values for pure metals. Work [2006Gas1] proposes a rectilinear concentration dependence which binds the values of k_{r1} and k_{r2} of the metals constituting the solution and their concentrations in the surface phase with parameter k_r of the solution:

$$\mathbf{k}_r = \mathbf{k}_{r1}^2 \mathbf{X}_1^S + \mathbf{k}_{r2}^2 \mathbf{X}_2^S \quad (4.2.9)$$

When the molar volume of the solutions is denoted by V_m and equation (4.1.2) is applied, the monoatomic molar surface, with the consideration of equation (4.2.9), is expressed by the following relation:

$$S_m = 1.091(\mathbf{k}_{r1}^2 \mathbf{X}_1^S + \mathbf{k}_{r2}^2 \mathbf{X}_2^S) V_m^{2/3} \mathbf{N}^{1/3} = 1.091 \mathbf{k}_r V_m^{2/3} \mathbf{N}^{1/3} \quad (4.2.10)$$

from which one can calculate the partial molar surfaces of the components of a binary solution. The calculations also assume that:

$$V_m = V_1 \mathbf{X}_1^S + V_2 \mathbf{X}_2^S \quad (4.2.11)$$

Equations (4.2.9), (4.2.10) and (4.2.11) can be easily expanded by multicomponent solutions and applied in the calculations.

With the assumption that the molar surface of the monoatomic surface phase changes additively with the components' concentration, equation (4.2.10) takes the following form:

$$S_m = L \mathbf{k}_{r1}^2 V_1^{2/3} \mathbf{N}^{1/3} \mathbf{X}_1^S + L \mathbf{k}_{r2}^2 V_2^{2/3} \mathbf{N}^{1/3} \mathbf{X}_2^S \quad (4.2.12)$$

The first and the second term of equation (4.2.12) are represented by the molar surfaces of components 1 and 2.

As it is implied by the observations, the surface tensions calculated with the use of equations (4.2.10) and (4.2.12), in some cases, have similar values.

4.2.2. Excess free energy of monoatomic phase

4.2.2.1. Dependence of β on metal, temperature and concentration

The values of parameter β calculated for various metals, presented in Figure 4.1.2, show that latter's value is different for each metal. The use of one mean value is an approximation which simplifies the calculation procedures, as the same concentration relation is applied for the description of the excess free energy of the volumetric and the surface phase. The introduction of variation β involves different relations for the description of the thermodynamic properties in the volumetric phase than those in the surface phase, as then, the excess free energy of the volumetric phase is multiplied not by a constant value (Eq. 4.2.9) but, in the simplest case, by a linear function, which assumes values from β_1 to β_2 , depending on the concentration of the surface layer. For similar values of β_1 and β_2 and small values of excess free energy, one should expect slight differences in the calculated surface tensions. Due to the different values of β for different metals, the author of work [2006Gas2] considered this fact in the calculations and varied the values of β depending on the component concentration in the surface phase.

The surface tension calculations also assume that parameter β describing the relation of the thermodynamic properties of the surface and the volumetric phase is independent of temperature. When equation (4.2.10) is applied for the calculation of the surface area of the solution, it seems that parameter β should be the function of temperature, as the higher the temperature, the stronger the effect of the correlation coefficient k_r of the molar surface of the surface layer, as parameters k_{r1} and k_{r2} are raised to the second power. This causes that, after exceeding the characteristic

temperature T_C , in which $k_{ri} = 1$, the molar surface of the monoatomic surface layer increases much more rapidly (parabolically) with the temperature increase than the molar surface calculated from equation (4.1.2) without the correlation coefficient k_r . As a result, the inter-atomic distances in the surface layer increase more rapidly than it is implied by formula (4.1.2), the energy of interaction between the atoms decreases and the thermodynamic properties of the surface layer become close to the properties of ideal solutions more rapidly than the volumetric phase. Thus, in relation (4.1.6), the parameter should be a decreasing function of temperature. Work [2006Gas2] assumed that β decreases linearly together with temperature and that at the temperature at which the surface tension equals zero $\sigma = 0$, parameter $\beta = 0$. In this way, the coordinates of one of the points were established, and they will be used to determine the temperature dependence β in the form of a linear equation. The coordinates of the other one are determined from the modification of equation 4.1.5 presented in work [1996Tan], where it was assumed that the isotheric-isobaric work needed to create a surface unit of the monoatomic layer is proportional to the energy of the bonds of the atoms which form it, and the energy, in turn, is approximately equal to the vapourization heat at the melting point. Work [2006Gas2] proposed a proportionality between the free energy needed to create a surface containing 1 mole of metal atoms and the standard change of the free energy connected with the vaporization of one mole of metal into the form of monoatomic gas at its melting point. Equation (4.1.5) assumes then the following form:

$$S\sigma = (1 - \beta)(G_g^\circ - G_c^\circ) \quad (4.2.13)$$

where: S and σ are the molar surface and the surface tension, and $G_g^\circ - G_c^\circ$ is the standard change of the free energy of 1 mole of liquid metal vapourized into monoatomic gas at the melting point.

The determined equations describing the dependence of parameter β on temperature for selected metals are included in Table 4.2.3 and in Figure 4.2.3, and they were calculated on the basis of the monograph by Barrin and Knacki [1973Bar] and the own data on surface tension and density [2001Mos1, 2001Mos2, 2001Mos3, 2001Gas2, 2002Liu, 2003Gas2, 2004Mos2, 2009Mos2] with the consideration of correlation coefficient k_r of the molar surface of the surface layer (Table4.2.2).

Table 4.2.3. Physical and thermodynamic properties of Ag, Bi, In, Pb, Sb and Sn with calculated temperature dependences of parameter $\beta = A + BT$.

β_t is the parameter β calculated at the metal's melting point

Metal	T_i [K]	σ [mN m ⁻¹]	S [m ² mol ⁻¹]	$G_g^0 = G_c^0$ [J mol ⁻¹]	β_t	T_{kr} [K]	$\beta = A + BT$
Ag	1233.9 5	898.9	42475.82	128272	0.6969	5953	= 0.879 - 0.000148T
Bi	545.00	377.7	36842.56	138883	0.903	8222	= 0.967 - 0.000118T
In	429.76	553.3	36836.30	194843.	0.8758	6032	= 0.943 - 0.000156T
Pb	600.58	432.1	42606.83	131066	0.8586	4429	= 0.993 - 0.000224T
Sb	904.00	368.2	56326.05	145375	0.8566	7475	= 0.974 - 0.000130T
Sn	505.06	540.7	27338.93	246692	0.942	6988	= 1.015 - 0.000145T

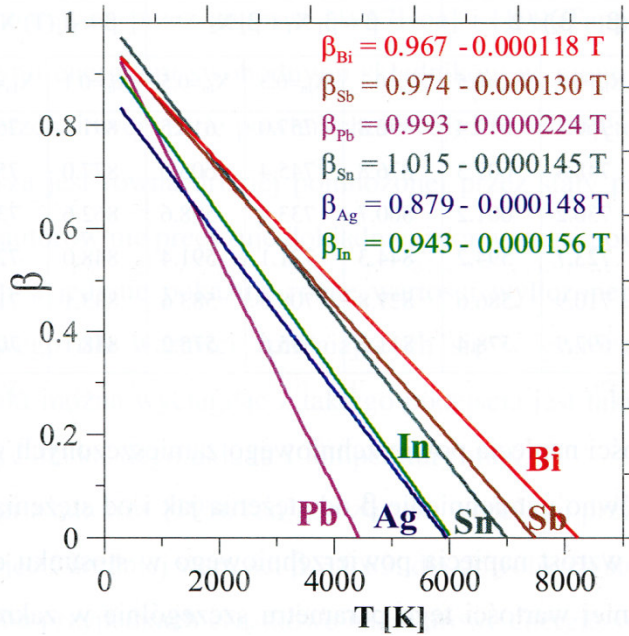


Fig. 4.2.3. Temperature dependences of parameter β for selected metals

The assumption of the variability of parameter β together with the change of the alloy concentration necessitates the determination of the relation between the coefficients of the excess free energy of the volumetric and the surface phase. It should be noted that making β variable according to temperature causes the fact that, in the case of a rectilinear temperature dependence of the excess free energy of the volumetric phase, the excess free energy of the surface phase becomes its curvilinear function of temperature.

4.2.2.2. Thermodynamic properties of components in surface layer

The relation proposed by the authors of [1957Hoa] and [1996Tan] between the excess free energies of the components in the monoatomic surface layer (surface phase) and the volumetric phase states that the former is equal to the latter multiplied by the constant parameter β (4.2.9). The first of the authors does not specify the value of this parameter, but merely points to the different values of the calculated surface tensions for the values 0.5 and 0.75 and for different temperatures. From this approach one can draw the conclusion that the authors were inclined to accept the variability of parameter β according to temperature and the metals forming the solution. The other author [1996Tan], as it was presented earlier, proposes the assumption of one mean value of $\beta = 0.83$ for any metal alloy.

In both cases, the partial excess free energies of the components in the surface layer are equal to those in the volumetric layer multiplied by the constant parameter β . This is, however a simplification, as equation (4.1.1) implies that this parameter assumes different values for different metals at different temperatures, and its effect on the calculated values of the surface tension can be significant, especially for the systems characterizing in big differences in the surface tensions of the metals forming the alloy. Also, the constant value of parameter β does not cause the necessity to introduce an additional dependence on the excess free energy of the component in the surface layer, which also simplifies the calculation procedures.

By accepting the fact that for different metals the values of β are different, in the relation between the excess free energies of the volumetric and the surface phase, one should apply the function describing the

dependence of this parameter on the concentration, in the form of the following equation:

$$\mathbf{G}_S^{\text{ex}} = [\beta_1(1 - \mathbf{X}_S) + \beta_2\mathbf{X}_S] \mathbf{G}_B^{\text{ex}}(\mathbf{X}_S) \quad (4.2.14)$$

where \mathbf{X}_S is the concentration of component 2 in the surface layer. Next, from (4.2.14) one should calculate the partial excess free energies of the components from the relations, known in the thermodynamics, between the functions of a mole of solution and their partial functions.

4.3. Modeling of metal alloy viscosity from thermodynamic and physical properties

The measurements of physical properties of metals and alloys at elevated temperatures are troublesome, time-consuming and expensive. Therefore, when designing and solving metallurgical processes estimated values of different physical properties are often used. They are calculated based on the thermodynamic properties of solutions and the alloy components. The viscosity of liquid alloys is one of such properties.

The scientific literature provides models which allow predicting the viscosity of liquid metal alloys using thermodynamic properties such as excess molar free enthalpy (\mathbf{G}^E), molar free enthalpy or enthalpy of mixing changes ($\Delta\mathbf{G}' = \Delta\mathbf{G}_{id} + \mathbf{G}^E$, $\Delta\mathbf{H}_m$) as well as, in some cases, using physical properties like viscosity of components, density or molar volume of alloys (\mathbf{V} , ρ), atomic masses (\mathbf{M}_i) and diameter (\mathbf{d}_i).

The earliest and the simplest equation was derived by **Moelwyn-Hughes** and reported in [1961Moe]:

$$\eta = (\eta_1 X_1 + \eta_2 X_2) \left(1 - 2 \frac{\Delta H_m}{RT} \right) \quad (4.3.1)$$

In which: X_1 , X_2 represent molar fractions of metals; R is gas constant; T temperature. Equation (4.3.1) is valid only for the binary alloys.

In 1977 **Iida, Ueda and Morita** [1977Iid] presented the following model given by the equation below:

$$\eta = (\eta_1 X_1 + \eta_2 X_2) \left\{ 2 \left[1 + \frac{X_1 X_2 (\sqrt{M_1} - \sqrt{M_2})^2}{(X_1 \sqrt{M_1} + X_2 \sqrt{M_2})^2} \right]^{\frac{1}{2}} - 1 - \frac{5X_1 X_2 (d_1 - d_2)^2}{X_1 d_1^2 + X_2 d_2^2} - \Delta \right\} \quad (4.3.2)$$

$$\Delta = 0.12 \frac{\Delta H_m}{RT}, \quad \Delta = 0.12 \frac{\Delta G^E}{RT} \quad (4.3.3)$$

It connected the viscosity of components (except for the thermodynamic functions and composition) also with the atomic masses and Pauling's ionic radii. Authors of work [1977Iid] suggested to apply excess free energy or enthalpy of mixing change in the calculations. The parameters R and T denote gas constant and absolute temperature, respectively.

Ten years after Iida et al. [1977Iid], **Kucharski** [1987Kuc] in his DSc work derived the relation for the calculation of multicomponent system viscosity η in which activity coefficients γ_i , partial molar volumes V_i , molar volume V and viscosity of metals η_i were used. In the case of binary alloys the equation was given as follows:

$$\eta = X_1 \frac{V_1}{V} \left(\frac{\beta}{\beta_1} \right)^2 \gamma_1^a \eta_1 + X_2 \frac{V_2}{V} \left(\frac{\beta}{\beta_2} \right)^2 \gamma_2^a \eta_2 \quad (4.3.4)$$

In Eq. (4) β and β_i are the relations described by the equations below:

$$\beta = X_1 V_1^{1/3} + X_2 V_2^{1/3} \quad (4.3.5)$$

$$\beta_1 = X_1 V_1^{1/3} + X_2 V_2^{4/3}/V_1 \quad (4.3.6)$$

$$\beta_2 = X_2 V_2^{1/3} + X_1 V_1^{4/3}/V_2 \quad (4.3.7)$$

The α parameter in (4.3.4) is calculated from the experimental data to improve the correlation between the calculated and measured values of viscosity. If the α parameter is equal unity the system of equations (4.3.4-4.3.7) allows obtaining the viscosity of binary alloys basing only on the thermodynamic and molar volume data. Additionally, assuming that V depends linearly on the composition, the viscosity calculations can be conducted following the equation (4.3.4) without additional investigations of the density or molar volume. In this work the calculations with Kucharski model were performed for $\alpha = 1$.

The model of **Kozlov, Romanov and Petrov** [1983Koz] applied the mixing enthalpy change of liquid solutions for the prediction of viscosity, similarly to that of **Moelwyn-Hughes**. It was represented for the binary alloys with the following logarithmic equation:

$$\ln(\eta) = \sum_{i=1}^2 X_i \ln(\eta_i) - \frac{\Delta H_m}{3RT} \quad (4.3.8)$$

The transformation of equation (4.3.6) gives the expression, which describes the viscosity of binary alloys in the form of exponential function:

$$\eta = \exp \left[\sum_{i=1}^2 X_i \ln(\eta_i) - \frac{\Delta H_m}{3RT} \right] \quad (4.3.9)$$

All symbols in equations (4.3.6) and (4.3.7) have the same meaning as in the models presented earlier.

In year 1994 **Du Sichen, Bygden and Seetharaman** [1994Sic] proposed equations, which comprised the thermodynamic properties of liquid solutions, their densities, activation energies and viscosities of components, to the viscosity calculations of multi-component solution. For the case of binary system it is of the following form:

$$\eta = A \exp\left(\frac{G^*}{RT}\right) \quad (4.3.10)$$

$$A = \frac{hN\rho}{M} \quad (4.3.11)$$

$$G^* = \sum_{i=1}^2 X_i G_i^* + RT \sum_{i=1}^1 \sum_{k=i+1}^2 X_i X_k + \Delta G' \quad (4.3.12)$$

In (4.3.10-4.3.12): G^* denotes Gibbs activation energy, $\Delta G'$ change of Gibbs activation energy, T temperature, G_1^* and G_2^* activation energy of components, R gas constant, ρ alloy density, N Avogadro number, h Planck constant and M atomic mass of alloy.

In the same year, **Seetharaman and Du Sichen** [1994See] modified the relationship describing the activation energy to the following form for the binary alloys:

$$G^* = \sum_{i=1}^2 X_i G_i^* + 3RT \sum_{i=1}^1 \sum_{k=i+1}^2 X_i X_k + \Delta G' \quad (4.3.13)$$

The author of this paper will present the calculations of both variants; since as it followed from his observations, the substitution of relation (4.3.5) in equation (4.3.2) not always gave the results complementary with experimental data.

In 2003, **Kaptay** [2003Kap], proposed a modification of **Seetharaman and Sichen** expression for the viscosity calculation (4.3.13), which consists in substituting two last expressions of sum in Eq. (4.3.12, 4.3.13) of Gibbs activation energy G^* into the equation with the enthalpy of mixing multiplied by an α coefficient, which, according to the author amounts to **0.155±0.015**. The proposed equation of viscosity for binary alloys is of the following form:

$$\eta = \frac{hN}{\sum_{i=1}^2 X_i V_i + \Delta V^E} \exp \left(\frac{\sum_{i=1}^2 X_i \Delta G_i^* - \alpha \Delta H_m}{RT} \right) \quad (4.3.14)$$

All the symbols in relation (4.3.14) have the same meaning as in the earlier presented models (eq. 4.3.10 - 4.3.13), while the new expressions in V_i and ΔV^E refer to the molar volume of alloy components and the excess molar volume of alloy. It should be noticed that the molar volume in the denominator of equation (4.3.14) is identical with the expression M/ρ in the equation (4.3.11).

A new equation for the modeling of viscosity of alloys was proposed in the work of Budai et al. [2007Bud] based on the viscosity equation of liquid metals given by Kaptay [2005Kap]:

$$\eta = A \frac{\left(\sum_{i=1}^n X_i M_i \right)^{1/2}}{\left(\sum_{i=1}^n X_i V_i + \Delta V^E \right)^{2/3}} T^{1/2} \exp \left[\frac{B}{T} \left(\sum_{i=1}^2 X_i T_{m,i} - \frac{\Delta H_m}{qR} \right) \right] \quad (4.3.15)$$

where: $A = (1.8 \pm 0.39) \cdot 10^{-8} \text{ (J/Kmol}^{1/3})^{1/2}$, $B = 2.34 \pm 0.2$, $q = 25.4 \pm 2$ and $T_{m,i}$ is melting temperature of metal i . Using Eq. 4.3.15 one can

estimate either the viscosity of metals or alloys. Therefore it is different from these presented in this work in which the viscosity of metals must be known for.

Another model for the viscosity calculation of alloys has been lately proposed by Schick et al. [2012Sic] and it is represented by the equation 4.3.16:

$$\eta = A' \exp \left(\frac{\sum_{i=1}^2 X_i Q_i - \Delta H_m}{RT} \right) \quad (4.3.16)$$

$$A' = \sum_{i=1}^2 A_i X_i \ln(X_i) \quad (4.3.17)$$

Where: Q_i is the activation energy and A_i is the pre-exponential parameter in the Arrhenius' equation describing the dependence of viscosity on temperature. The meaning of the remaining symbols is the same as in the models presented above.

In 2011 **Sato** [2011Sat] proposed a new model for the prediction of alloy viscosity given for binary alloys by the equations below:

$$\eta_{\text{alloy}} = \eta_{\text{alloy}}^0 \exp \left(\frac{E_{\text{alloy}}}{RT} \right) \quad (4.3.18)$$

$$\ln(\eta_{\text{alloy}}^0) = X_1 \ln(\eta_1^0) + X_2 \ln(\eta_2^0) \quad (4.3.19)$$

$$\ln(E_{\text{alloy}}) = \frac{1}{T} (X_1 \frac{E_1}{R} + X_2 \frac{E_2}{R}) \quad (4.3.20)$$

In Eqs 4.3.18-4.3.20 E_i is the activation energy of metal i and η_i^0 is the pre-exponential coefficient of the Arrhenius equation. This model is based only

on the viscosity data of metals neglecting the part concerned with thermodynamic properties of alloys.

In 2010 Gaşior and Moser [2010Gas2] based on the analysis of calculated and experimental viscosity values for many binary metallic systems noticed firstly, that the viscosity values calculated from some models described above were in a weak correlation with the experimental data, secondly, that the viscosity models not always showed the same deviation of the excess viscosity (positive or negative) as the measured one and thirdly that when the excess entropy was positive the experimental excess viscosity was always negative and on the contrary, when the excess entropy was positive the measured excess viscosity was negative. Additionally, it was noticed that the similar values of excess entropy caused directly proportional deviations to the absolute values of viscosity difference and inversely proportional to the sum of viscosity.

The equation proposed for the viscosity calculation is given below:

$$\eta = (\eta_1 X_1 + \eta_2 X_2) \left(1 - k_s \frac{S^{ex}}{R} \right) \quad (4.3.21)$$

$$k_s = 1 + 2 \frac{|\eta_1 - \eta_2|}{\eta_1 + \eta_2} = 1 + 2 \sqrt{\frac{(\eta_1 - \eta_2)^2}{(\eta_1 + \eta_2)^2}} \quad (4.3.22)$$

In Eq. 4.3.21 S^{ex} is the molar excess entropy of binary system. The other symbols have the same meanings as above. The relation for k_s coefficient was found basing on the experimental data and Eq. 4.3.21. It is shown in Fig.4.3.1, in which apart from the dots calculated from experimental data two different linear equations describing k_s as the function of quotient of the difference and the sum of 1 and 2 metals are shown. The R-squared coefficient calculated and shown in Fig. 4.3.1 is low and equal about 0.07

because the great dispersion its value calculated on the base of experimental data at different temperatures and for different systems. However, even for systems with great difference between experimental and calculated k_s data the calculated viscosity from Eq. 4.3.21 differs not so much from that measured. Taking into consideration the Bi-Sb system [1993Iid1] for example one can find that the k_s coefficient calculated using experimental data at 973K is equal about 8 and the calculated and experimental viscosity for 0.5 mole fraction of Sb is equal 1,16 and 1,07 mPa·s, respectively. In the case of for Bi-Pb system [1954Sat] at 573 K and for $X_{Sb}=0.4$, the calculated k_s (using experimental data) is equal 7.14 and the calculated and experimental viscosity is equal 2.16 and 1.8 mPa·s, respectively.

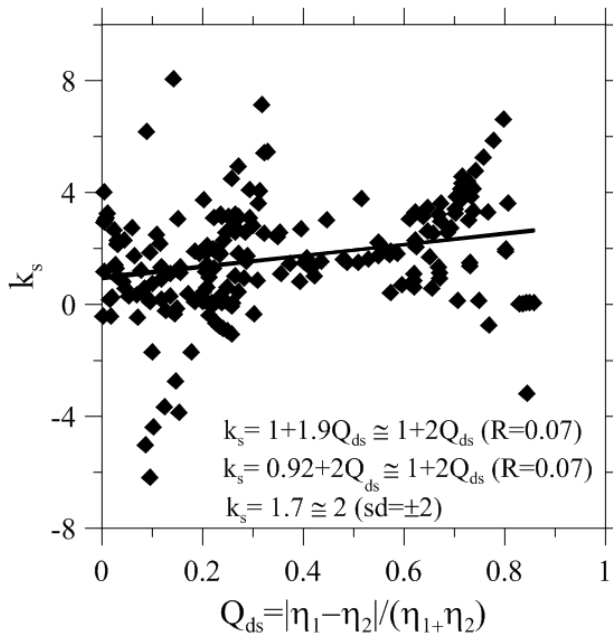


Fig. 4.3.1. Correlation between k_s and Q_{ds} parameter for binary systems. Dots show the k_s values which were calculated basing on the experimental data. R denotes R-squared and sd is the standard deviation

Another model was proposed by Gaşior in the course of TOFA 2012 Meeting [2012Gas1] and in [2014Gas1]. It was the result of the observations that the average value of k_s coefficient in Eq. 4.3.21 is nearly equal 2 (Fig. 4.3.1) for many systems. So, the new simpler model was proposed in the form as follows:

$$\eta = (\eta_1 X_1 + \eta_2 X_2) \left(1 - 2 \frac{S^{ex}}{R} \right) \quad (4.3.23)$$

The k_s average value is equal 1.7 (Fig. 4.3.1) however the author proposed to assume it as equal 2 because of two reasons. First: because of full analogy to the model of Moelwyn-Hughes (Eq. 4.3.1) which is only equation for the viscosity prediction of binary solutions derived on the base on the thermodynamic definition of the resistant force and Stock's equation of the viscosity and second that the difference 0.3 in k_s gives the difference in the viscosity much lower than 0.1 mPa·s (Pb-Sn at 573 K and $X_{Sn}=0.5$: $k_s= 1.619$, $\eta= 2.643$ mPa·s and for $k_s= 2$, $\eta=2.703$ mPa·s). Eqs 4.3.21 and 4.3.23 can stand for the entropy or, rather, the excess entropy models because they contain that thermodynamic function.

4.3.1. Isolines of viscosity in Ag – Cu – Sn system

Figures 4.3.2–4.3.6 present the isolines of viscosity in the Ag–Cu–Sn system, calculated from models [1961Moe, 1994Sic, 1994See, 1983Koz, 2003Kap]. It can be seen that all the models show very distinct or slight viscosity extrema.

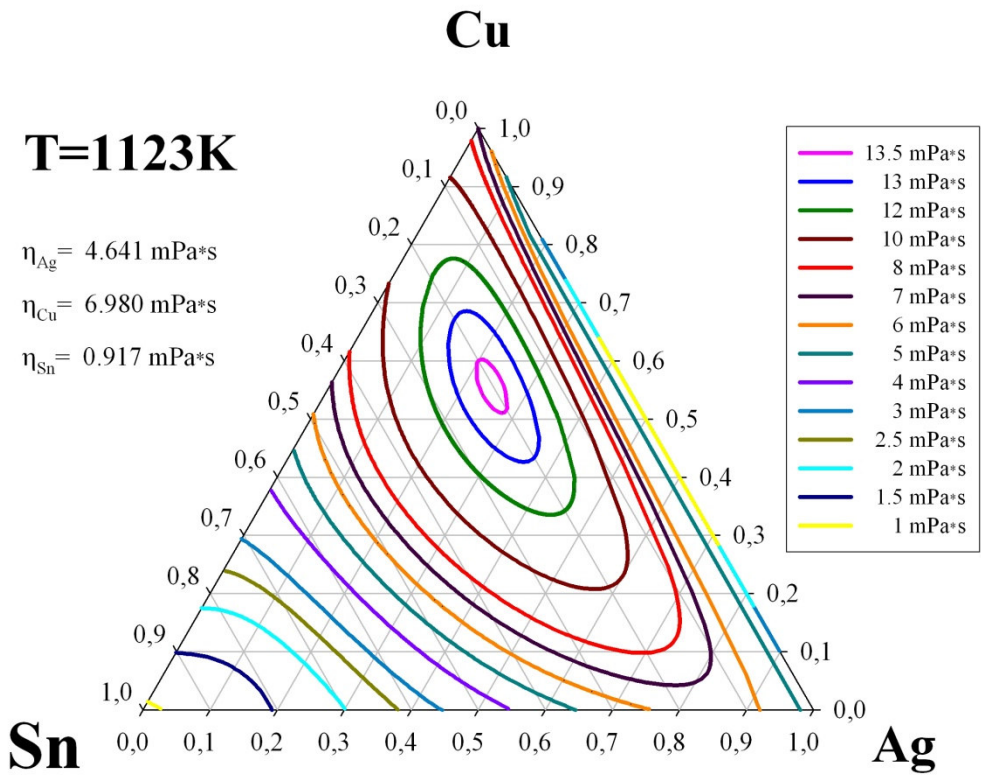


Fig. 4.3.2. Isolines of viscosity calculated from the Moelwyn-Hughes model [1961Moe] at T=1123 K

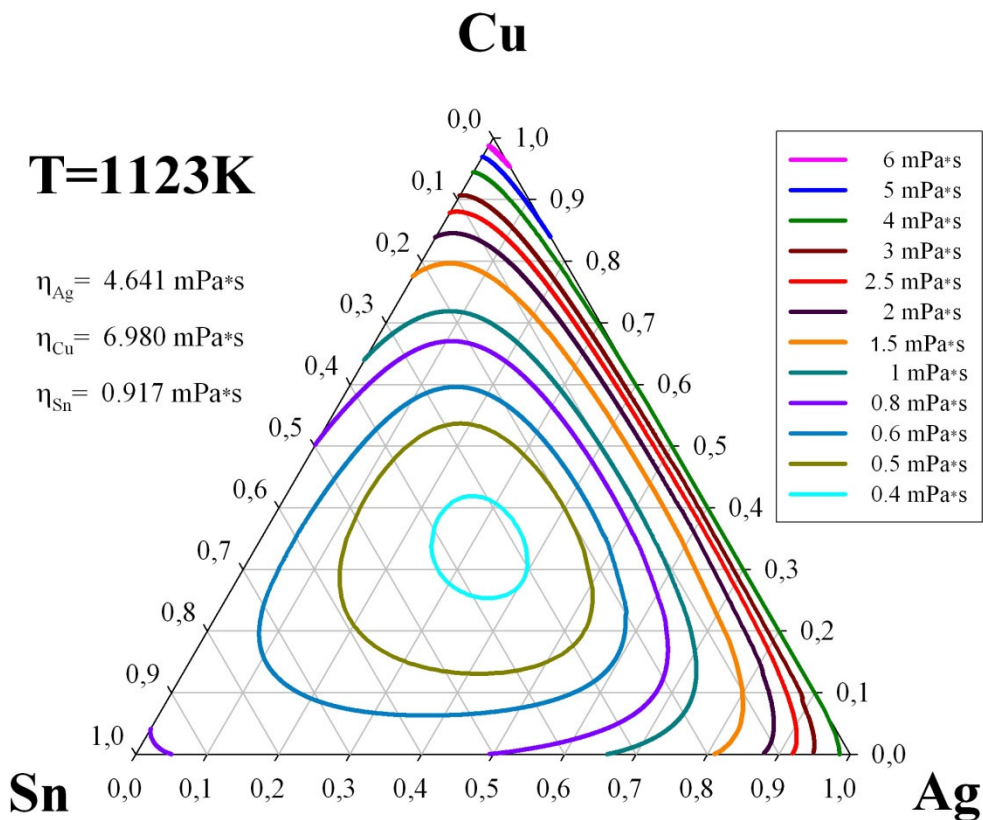


Fig. 4.3.3. Isolines of viscosity calculated from the Du Sichen, Bygden and Seetharaman model [1994Sic] at T=1123 K

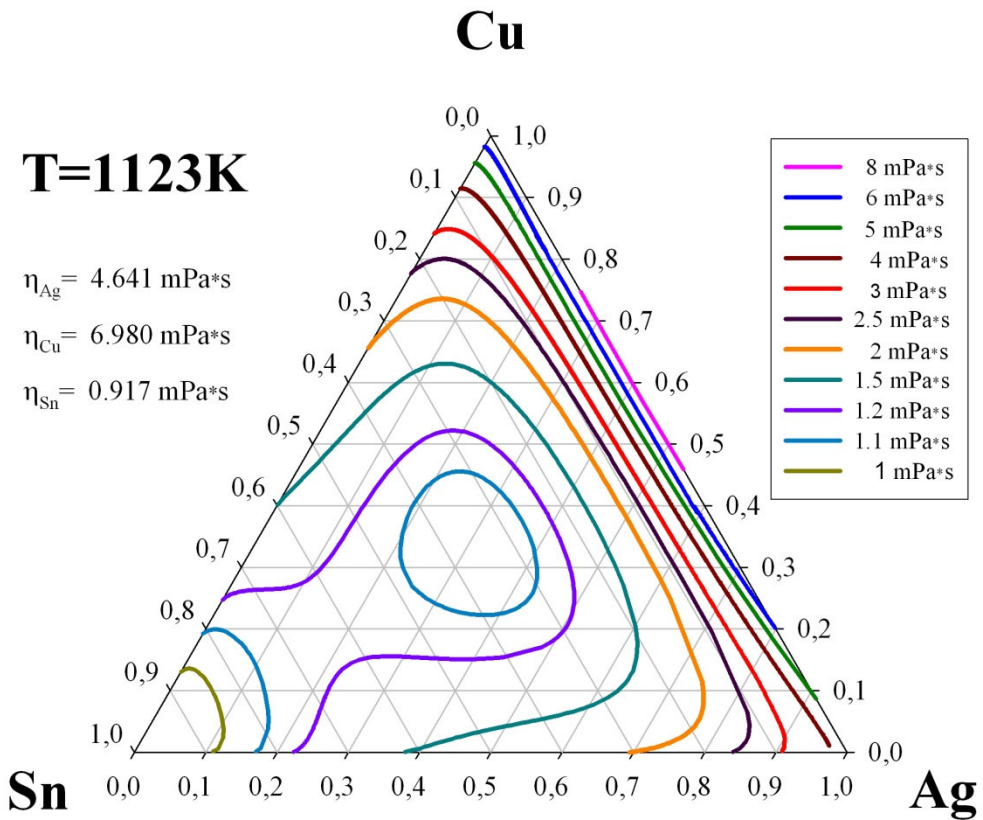


Fig. 4.3.4. Isolines of viscosity calculated from the Seetharaman and Du Sichen model [1994See] at T=1123 K

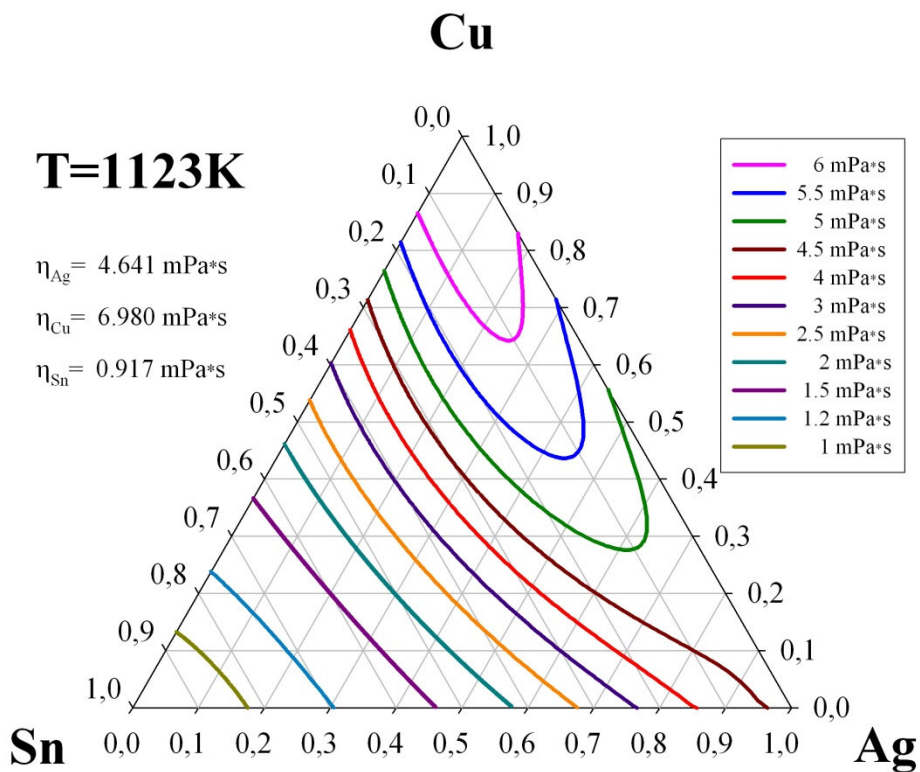


Fig. 4.3.5. Isolines of viscosity calculated from the Kozlov, Romanov and Petrov model [1983Koz] at T=1123 K

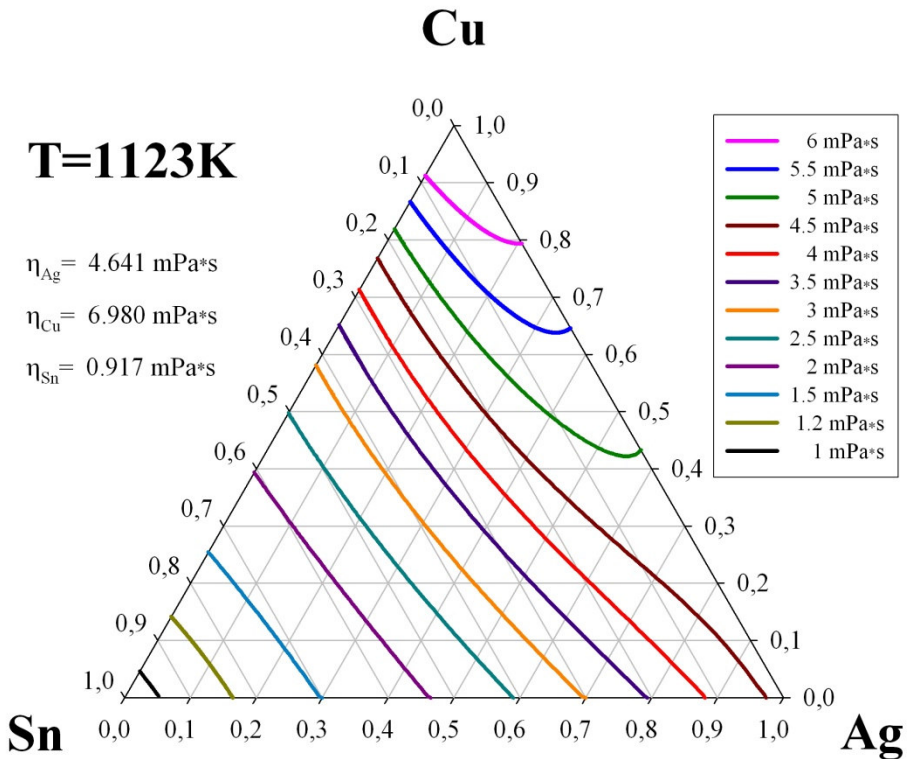


Fig. 4.3.6. Isolines of viscosity calculated from the Kaptay model [2003Kap] at T=1123 K

The Moelwyn-Hughes model [1961Moe] (Fig. 4.3.1) gives a distinct maximum of viscosity slightly over 13.5 mPa·s, which nearly twice exceeds the viscosity of copper - the metal of the highest viscosity from those forming the ternary solution. What is more, in quite a wide range of concentrations very close to the binary Ag-Cu system, the viscosity assumes values lower than 1 mPa·s (similarly to the Ag-Cu system) and it rapidly increases together with the content of tin, assuming the maximum values for the concentration of Sn, which equals about 0.2 mole fraction, and the ratio $X_{\text{Cu}}/(X_{\text{Cu}}+C_{\text{Ag}})=0.7$.

In the case of the model of Sichen et al. [1994Sic] (Fig. 4.3.2) and that of Seetharaman and Sichen [1994See] (Fig. 4.2.3), the calculated viscosity of liquid Sn-Ag-Cu alloys, contrary to the Moelwyn-Hughes model [1961Moe], shows the minima in the central part of concentration with the viscosity values slightly below 0.4 mPa·s [1994Sic] and 1.1 mPa·s [1994See].

The isolines shown in Fig. 4.3.4 calculated from the Kozlov-Romanov and Petrov relation [1983Koz] change in the range of big concentrations of tin almost linearly between the equal viscosity values for the systems Sn-Cu and Sn-Ag. With the tin concentrations over 0.25 mole fraction and for the cuttings of constant values $X_{Cu}/(X_{Cu}+X_{Ag})$ increasing from 0.38 to 1, weak maxima are observed on the viscosity curves, increasing from about 5 mPa·s to the viscosity of copper, with the increase of the copper concentration in the alloy.

The viscosity isolines determined from the Kaptay model [2003Kap] (Fig. 4.3.5), in the range of large concentrations of tin, show almost rectilinear changes between the identical values for the systems Sn-Cu and Sn-Ag, and for higher tin contents, these changes are weakly curvilinear.

5. NIST database

National Institute of Standards and Technology (NIST) includes at its website:

www.boulder.nist.gov/div853/lead_free/solders.html



a database of lead-free solders in the 4.0 version. It is a database in the HTML format (for direct viewing in the form of internet pages) or in the Microsoft Word format (for download). The access to the database and the available internet links can be gained through the NIST home page (Fig. 5.1).

NIST is receiving applications for granting the information which is not included in the database. These data can be generated at research centres all over the world which work in the field of soldering. The links to those centres as well as to the universities from all over the world which work on projects focused on lead-free solders have been included at the NIST home page.

The site also provides links to the related research programs, such as „New technology for Environment” National Science Foundation, so that the viewers of the website can gain information on other programs which contribute to the development of the lead-free solder database.



As a result of the undertaken action, a preliminary version of the lead-free solder database was developed, which consisted of the 4.0 version of NIST, complemented by the SURDAT database (edition 2007 r.). The common version of the combined SURDAT+NIST databases (Database for Solder Properties with Emphasis on New Lead-free Solders Release 5.0) was presented at the 17th Symposium on Thermophysical Properties

(Boulder, Colorado, June 21-26, 2009). The start-up window of the new version is presented in Fig. 5.2.





**Lead-Free Solders
Research Programs at
Universities**

The following are established research centers with Lead-Free Solders programs:

- [Alabama Microelectronics Science and Technology Center - Auburn University](#)
- [Packaging Research Center - Georgia Institute of Technology](#)
- [Reliable Microelectronics Packaging Program - University of California at Berkeley](#)
- [Center for Welding, Joining and Coatings Research - Colorado School of Mines](#)
- [Integrated Electronics Engineering Center - State University of New York at Binghamton](#)
- [Ames Laboratory and Iowa State University](#)
- [CALCE Electronic Products and Systems Center - University of Maryland](#) 
- [Centre for Microelectronics Assembly and Packaging - University of Toronto](#) 

The following is a list of universities also involved in this research. The contact person would be a faculty member:

- [Purdue University](#)
- [University of Wisconsin - Madison](#)
- [Michigan State University](#)
- [Northwestern University](#)
- [University of Toronto](#)
- [University of Michigan - Dearborn](#)
- [University of California at LA](#)
- [University of Colorado](#)
- [University of Connecticut](#)
- [Cornell University](#)
- [Lehigh University](#)
- [University of Massachusetts at Lowell](#)
- [Marquette University](#) 

Database for Solder Properties with Emphasis on New Lead-free Solders Release 4.0

National Institute of Standards & Technology and Colorado School of Mines

OBJECTIVE

The purpose of this web site is to provide an on-line database for solder properties emphasizing new lead-free solders. Lead-free solder data are being developed rapidly, but are still difficult to find. (See the Alloy Database section in the August 29, 2000 press release on the NEMI web site - www.nemi.org). Therefore, we hope this web site will allow us to collect this information in one place, and update it frequently. If you have additional data to contribute, please send it to the contact at the bottom of this page. The data reported in this site has been collected from reliable sources and orderly put together. There is no restriction to access the datafile. The user is able to read the data on HTML format and download in WORD format, which then can be formatted in EXCEL for easier manipulation.

DATAFILES

The datafiles are ordered by the date in which they were placed on-line, to see them click on one of the links below. If you would like to download the file, click on WORD FORMAT, then go to file and save the document.

HTML FORMAT

- [Properties of Lead-free Solders, RELEASE 4.0](#)
2002 February 11 8:30:50 am

MS WORD FORMAT

- [Properties of Lead-free Solders, RELEASE 4.0](#)
2002 February 11 8:30:50 am

"NEMI" DATA REQUEST

The NATIONAL ELECTRONICS MANUFACTURING INITIATIVE - NEMI is very interested in contacting university centers and professors that are involved in the characterization of lead free solders. If you are interested on this information click here: "[NEMI Data Request](#)".

RELATED LINKS

NSF INTEREST IN LEAD FREE SOLDERS

The National Science Foundation and its program New Technologies for the Environment has shown interest in the research of Lead-Free Solders and welcomes proposals in this subject. If you would like more information, visit the following sites:

- [Office of Multidisciplinary Activities](#)
- [New Technologies for the Environment](#)

or contact:

Dalea Durham
Director of the Program New Technologies for the Environment
Engineering Division of Design, Manufacture and Industrial

Fig. 5.1. Home page of NIST solder database, edition 4.0

Lead-Free Solders Research Programs at Universities	OBJECTIVE				
<p>The following are established research centers with Lead-Free Solders programs:</p> <ul style="list-style-type: none"> - Alabama Microelectronics Science and Technology Center - Auburn University - Packaging Research Center - Georgia Institute of Technology - Reliable Microelectronics Packaging Program - University of California at Berkeley - Center for Welding, Joining and Coatings Research - Colorado School of Mines - Integrated Electronics Engineering Center - State University of New York at Binghamton - Ames Laboratory and Iowa State University - CALCE Electronic Products and Systems Center - University of Maryland NEW - Centre for Microelectronics Assembly and Packaging - University of Toronto NEW 	<p>The purpose of this web site is to provide an on-line database for solder properties emphasizing new lead-free solders. Lead-free solder data are being developed rapidly, but are still difficult to find. (See the Alloy Database section in the August 29, 2000 press release on the NEMI web site - www.nemi.org). Therefore, we hope this web site will allow us to collect this information in one place, and update it frequently. If you have additional data to contribute, please send it to the contact at the bottom of this page. The data reported in this site has been collected from reliable sources and orderly put together. There is no restriction to access the datafile. The user is able to read the data on HTML format and download in WORD format, which then can be formatted in EXCEL for easier manipulation.</p>				
Lead-Free Solders Research Programs at Universities	DATAFILES				
	<p>The datafiles are ordered by the date in which they were placed on-line, to see them click on one of the links below. If you would like to download the file, click on WORD FORMAT, then go to file and save the document.</p>				
	<table border="1" style="width: 100%; border-collapse: collapse;"> <tr> <td style="background-color: #e0e0e0; text-align: center; padding: 5px;"> HTML FORMAT </td> <td style="background-color: #e0e0e0; text-align: center; padding: 5px;"> MS WORD FORMAT </td> </tr> <tr> <td style="padding: 5px;"> <ul style="list-style-type: none"> • Properties of Lead-free Solders, RELEASE 5.0 2009 April 9 </td> <td style="padding: 5px;"> <ul style="list-style-type: none"> • Properties of Lead-free Solders, RELEASE 4.0 2002 February 11 8:30:50 pm </td> </tr> </table>	HTML FORMAT	MS WORD FORMAT	<ul style="list-style-type: none"> • Properties of Lead-free Solders, RELEASE 5.0 2009 April 9 	<ul style="list-style-type: none"> • Properties of Lead-free Solders, RELEASE 4.0 2002 February 11 8:30:50 pm
HTML FORMAT	MS WORD FORMAT				
<ul style="list-style-type: none"> • Properties of Lead-free Solders, RELEASE 5.0 2009 April 9 	<ul style="list-style-type: none"> • Properties of Lead-free Solders, RELEASE 4.0 2002 February 11 8:30:50 pm 				

Fig. 5.2. Home page of combined SURDAT + NIST databases, edition 5.0

The integrated SURDAT-NIST-CSM database provides the possibility to view the data included in SURDAT (edition 2007) in the form of internet pages. SURDAT, in the combined database version, has been divided into the following sections:

1. Properties of metals used as lead-free solder materials,
2. Property isotherms of lead-free solder binary systems,
3. Temperature dependences of properties of lead-free solder binary systems,

4. Property isotherms of lead-free solder ternary systems,
5. Temperature dependences of properties of lead-free solder ternary systems,
6. Property isotherms of lead-free solder quaternary systems,
7. Temperature dependences of properties of lead-free solder quaternary systems.

6. Presentation of SURDAT 3 database

6.1. Program installation

SURDAT 3 is a program which requires an installation procedure. To install the program, the installation file SETUP.EXE should be started. After the installation has been run, the window shown in Fig. 6.1 is activated.

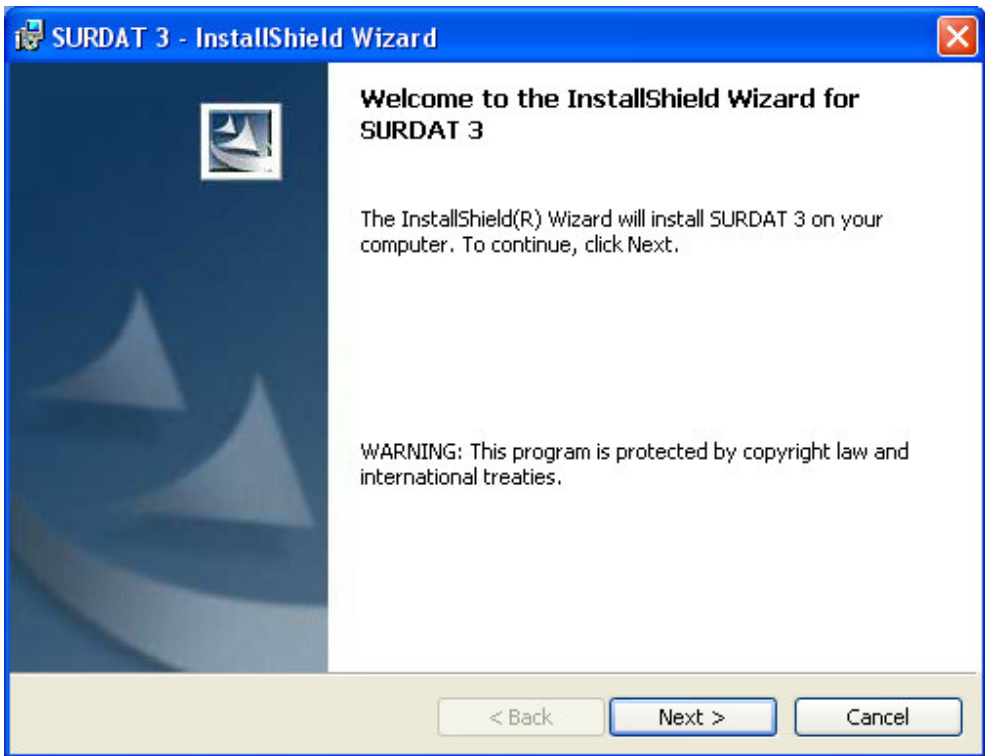


Fig. 6.1. First installation window

Pushing the „Next” button opens the second installation window, which includes the already filled-in fields: „User Name” and „Organization” (Fig. 6.2).

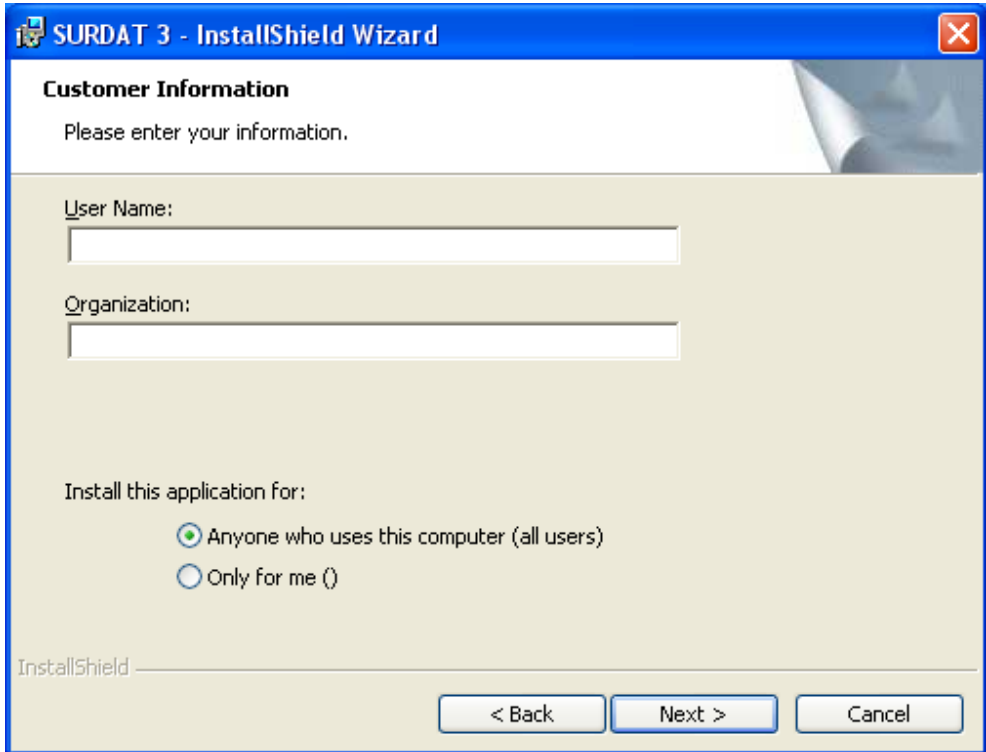


Fig. 6.2. Second installation window

Pushing the „Next” button opens the following installation window. The installation window in Fig. 6.3. shows where the program will be installed.

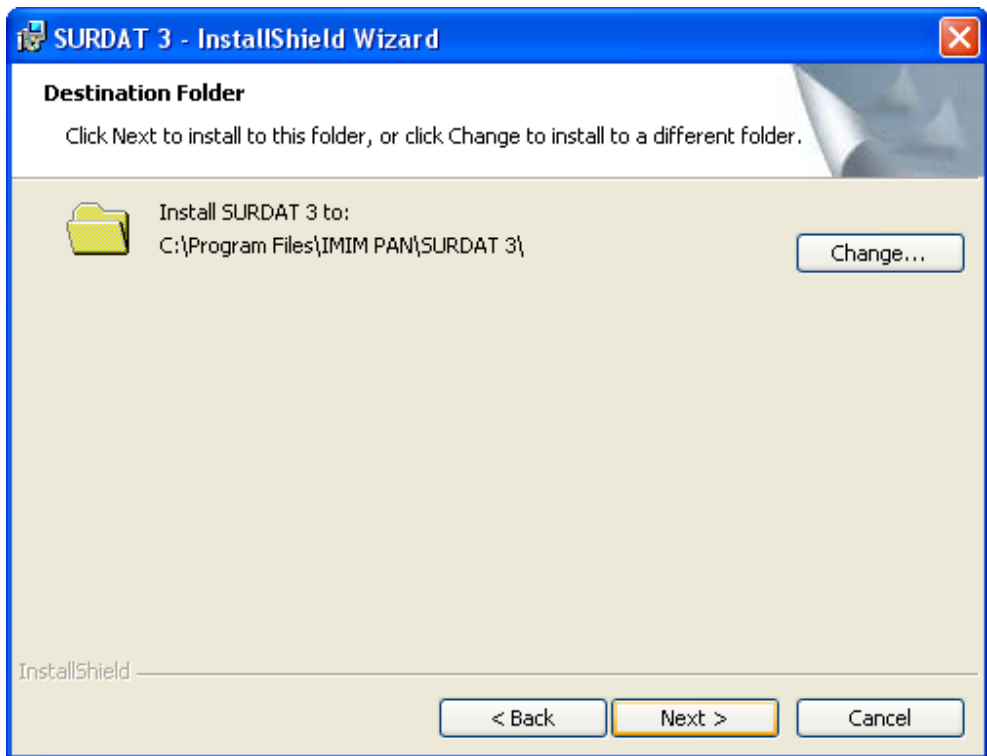


Fig. 6.3. Third installation window

It is possible to change the installation directory by pushing the „Change...” button and manually select the folder where the program should be installed. After „Next” has been pushed, the installation program will go through the successive windows to the last installation window presented in Fig. 6.4. Pressing the „Finish” button finalizes the program installation process.

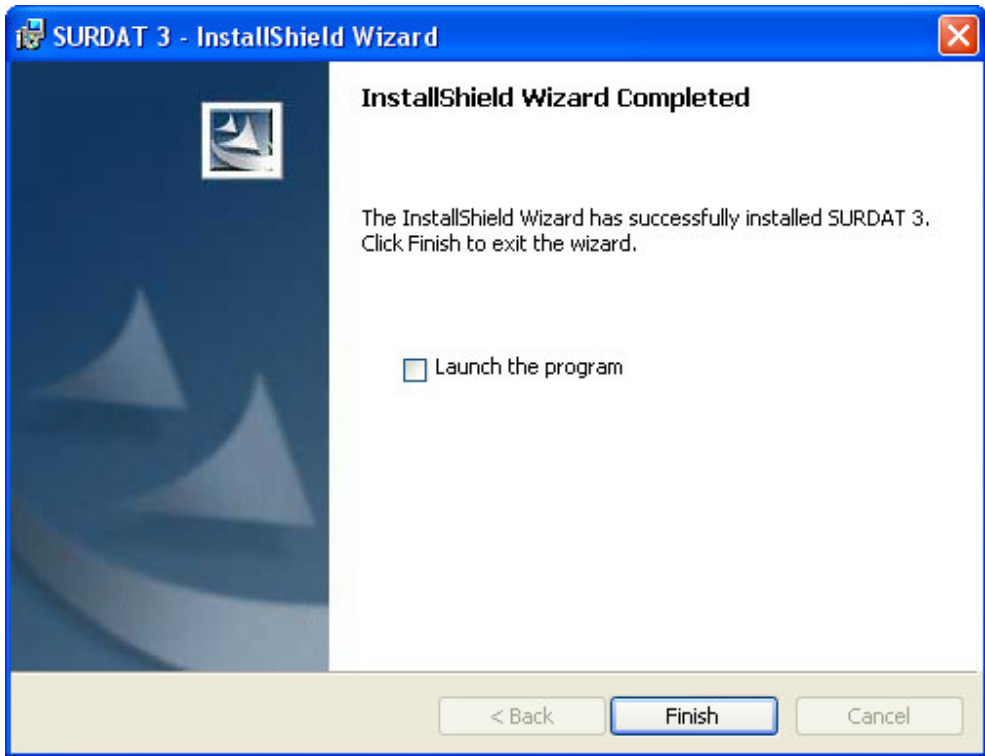


Fig. 6.4. Final installation window

6.2. Application example

The capabilities of the SURDAT 3 database will be presented on the example of the binary Ag – Sn and the ternary Ag – Cu – Sn (SAC) systems.

After the activation of the SURDAT 3 computer database, the first window appears (Fig. 6.5), which informs about the place where the base was created, what it refers to and next the selection window for the system type opens. To go to the further options of the database operation, in section

„SYSTEM SELECTION”, one should select the system type (unary, binary or multi-component).

For example, selecting option „Pure metals” and pressing „OK” directs the program to the next window (Fig. 6.6), where it is possible to select the metal („SELECT SYSTEM”) and its physical properties „SELECT PROPERTIES”.

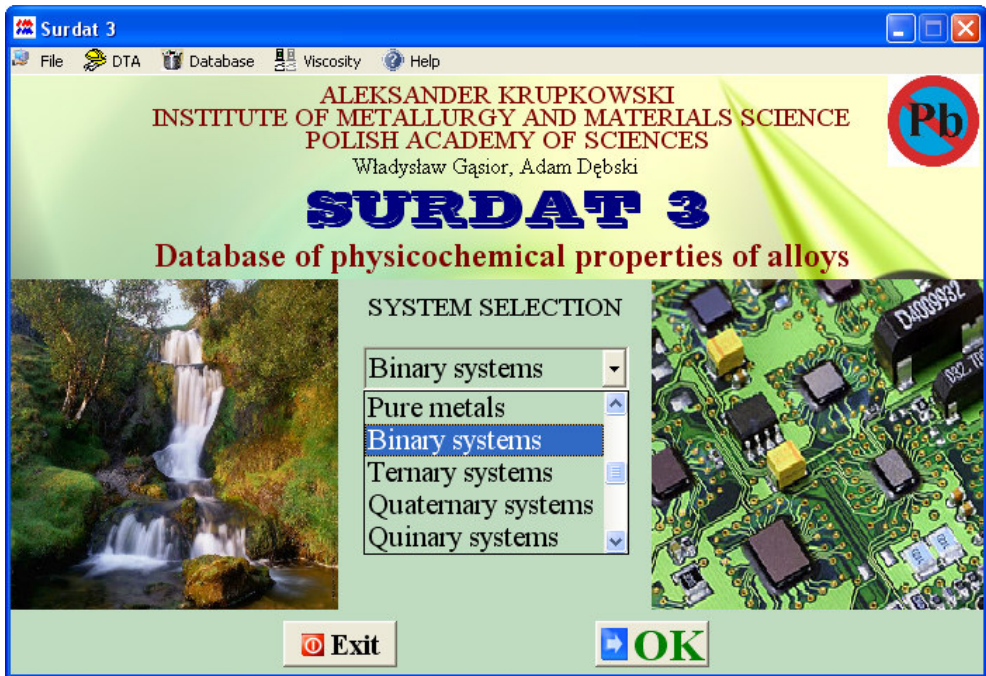


Fig. 6.5. First window of SURDAT 3 database. System type selection window.

If, in the unfoldable window „SELECT SYSTEM”, we select „Ag” and press „Show”, the program will show the given data from the periodic system for silver, such as: atomic weight (ATOMIC WEIGHT), melting point (MELTING POINT), boiling point (BOILING POINT), crystalline structure at room temperature (CRYSTAL STRUCTURE) and – not

demonstrated in Fig. 6.6 – covalent radius (COVALENT RADIUS) and atomic radius (ATOMIC RADIUS).

Next to the „Show” button, there are the „Fig”, „Solid sim”, „Menisc” and „Ph Diag” buttons, which represent the following:

- „Fig” – browsing through the published data in the form of images,
- „Solid sim” – solidification simulations (option currently unavailable),
- „Menisc” – meniscographic data,
- „Ph Diag” – phase diagrams (only binary and ternary systems).

The presented options will be discussed in the further part of the chapter.

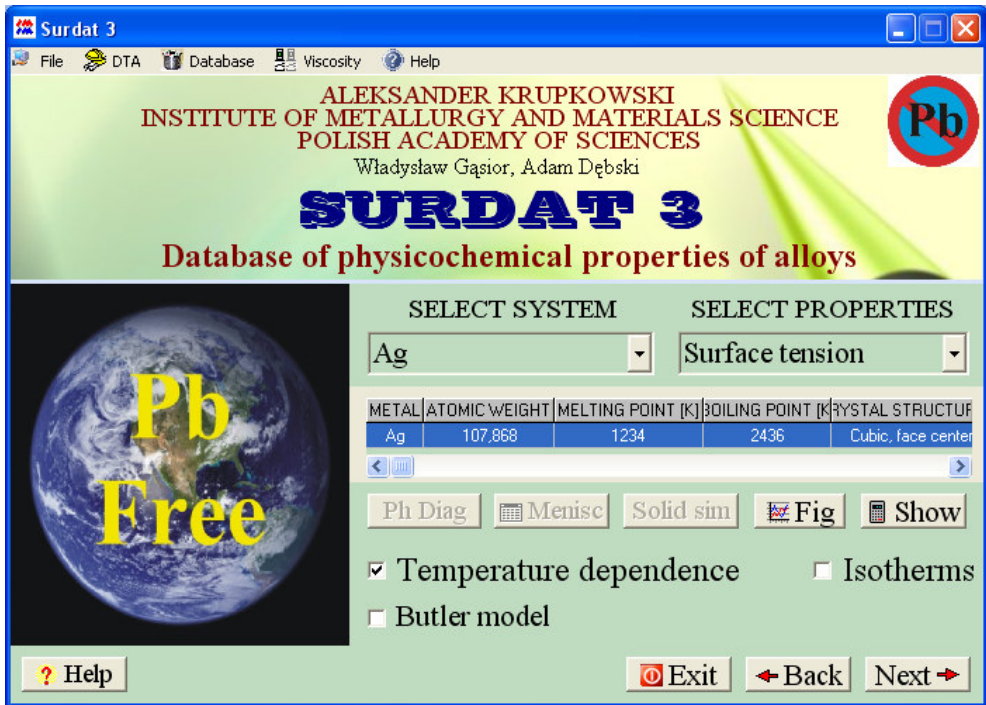


Fig. 6.6. Second window of SURDAT 3 database. System and property selection window

The „Fig” option allows to browse through the temperature dependences and isotherms developed and presented by a given author, in a given publication.

For metals, only the temperature dependences are available. Selecting, successively, the „Surface tension” property and the „temperature relation” presentation mode in the „SELECT PROPERTIES” window and next pressing the „Fig” button directs the program to a window with the possibility to select the author and the property (Fig. 6.7.). The „Select Properties” window presented in Fig. 6.7 is activated only in the case when the „Electrical properties” or „Mechanical properties” option is selected in the window presented in Fig. 6.6. For example, selecting the data author [2001Mos2] and pressing the „OK” activates a display of the diagram of the surface tension dependence on temperature, presented by the author of [2001Mos2] (Fig. 6.8). What is more, pressing the „References” button opens the window with a list of publications on the Ag surface tension (Fig. 6.9).

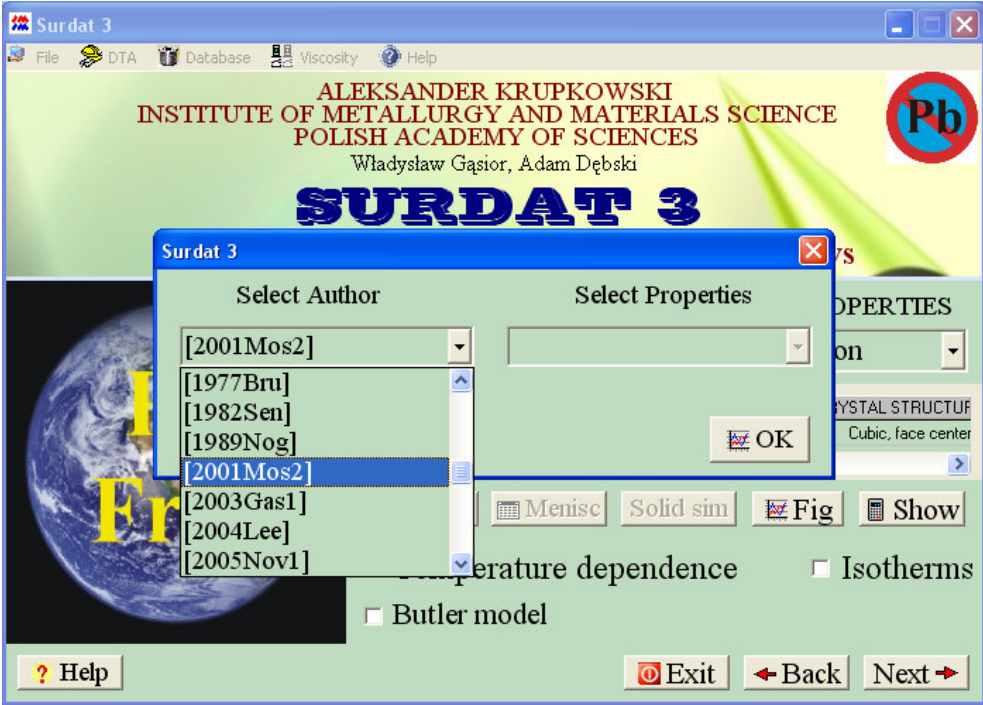


Fig. 6.7. Window for author and property selection

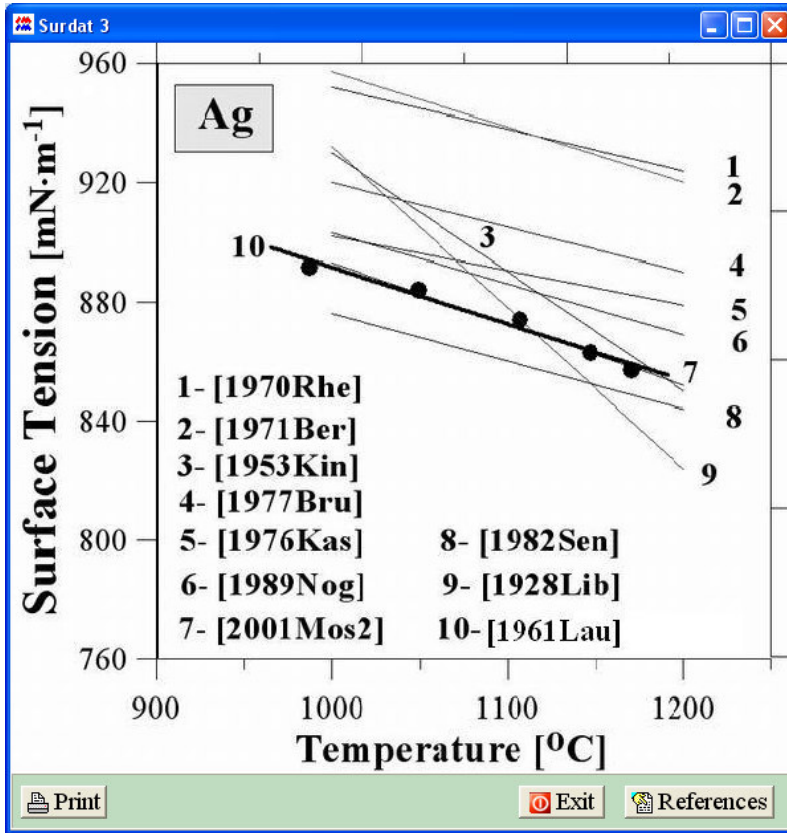


Fig. 6.8. Comparison of literature available temperature dependences of silver surface tension with experimental data. Experimental points from [2001Mos2]

REFERENCES	AUTHORS	TITLE	JOURNAL	VOL	YEAR	PAGES
[1928Lb]	E.E. Libman		Bull. III Univ. Eng. Exp. Sta.		1928	187
[1953Kin]	W.D. Kingey, M. Humenik	Surface Tension at Elevated Temperatures. I. Furnace and Method for	J. Phys. Chem.	57	1953	359-363
[1961Lau]	I. Lauerman, G. Metzger, F.	Surface tensions of molten silver, tin and silver-tin alloys	Z. Phys. Chem.	216	1961	42-49
[1970Rhe]	S.K. Rhee	Wetting of Au and Ti by Liquid Ag and Liquid Cu	J. Am. Ceram. Soc.	53	1970	639-641
[1971Ber]	G. Bernard, C.H.P. Lupis	The Surface Tension of Liquid Silver Alloys: Part I. Silver - Gold Alloys	Metal. Trans.	2	1971	555-559
[1976Kas]	A. Kasama, T. Iida, Z. Mori	Temperature Dependence of Surface Tension of Liquid Pure Metals	J. Japan. Inst. Metals	40	1976	1030-1038
[1977Bru]	M. Brunet, J.C. Joud, N. Et	Surface Tension of Germanium and Silver - Germanium Alloys in the Liquid	J. Less Common Met.	51	1977	69-77
[1982Sen]	R. Sengozgi, M.L. Muolo, J.	Surface Tension and Adsorption in Liquid Silver - Oxygen Alloys	Acta Metall.	30	1982	1597-1604
[1989Nog]	K.Nogi, K.Oshino, K.Ogino	Wettability of Solid Oxides by Liquid Pure Metals	Mater. Trans. JIM	30	1989	137-144
[2001Mos2]	Z. Moser, W.Gastor, J.Patin	Density and surface tension of the Ag-In liquid alloys	J. Electron. Mater.	30	2001	1120-1128
[2003Gas1]	Gastor W., Moser Z., Pstru	Surface Tension and Thermodynamic Properties of the Liquid Ag-Bi	Sci. J. Phase Equilib.	24	2003	21-39
[2004Lee]	J. Lee, W. Shimoda, and T	Surface Tension and its Temperature Coefficient of Liquid Sn-X (X=Ag, Mater. Trans.	45, No.9	2004	2864-2870	
[2005Nov1]	R. Novakovic, E. Ricci, D.	Surface and transport properties of Ag-Cu liquid alloys.	Surf. Sci.	576	2005	175-187
[2006Kuc]	M. Kucharski, P. Fima, P.	Surface Tension and Density of Cu-Ag, Cu-In and Ag-In Alloys	Archs. Metall. and Mater.	51	2006	389-397

Fig. 6.9. The references for the surface tension of Ag

Selecting the „Binary systems” option (Fig. 6.6), the „Ag-Sn” system, the „Density” option and the author of [2001Mos1] makes it possible to display, by means of the „Fig” option, the temperature dependences („Temperature relation”, Fig. 6.10) and the density isotherms („Isotherms”) determined on the basis of the experimental data (Fig. 6.11).

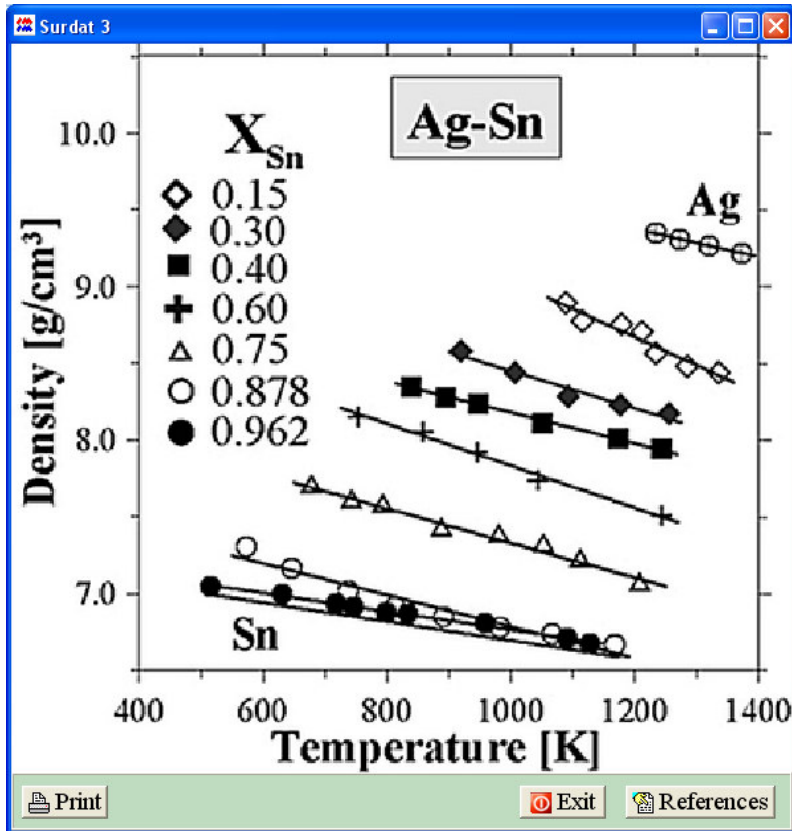


Fig. 6.10. Density temperature dependences of liquid Ag-Sn alloys

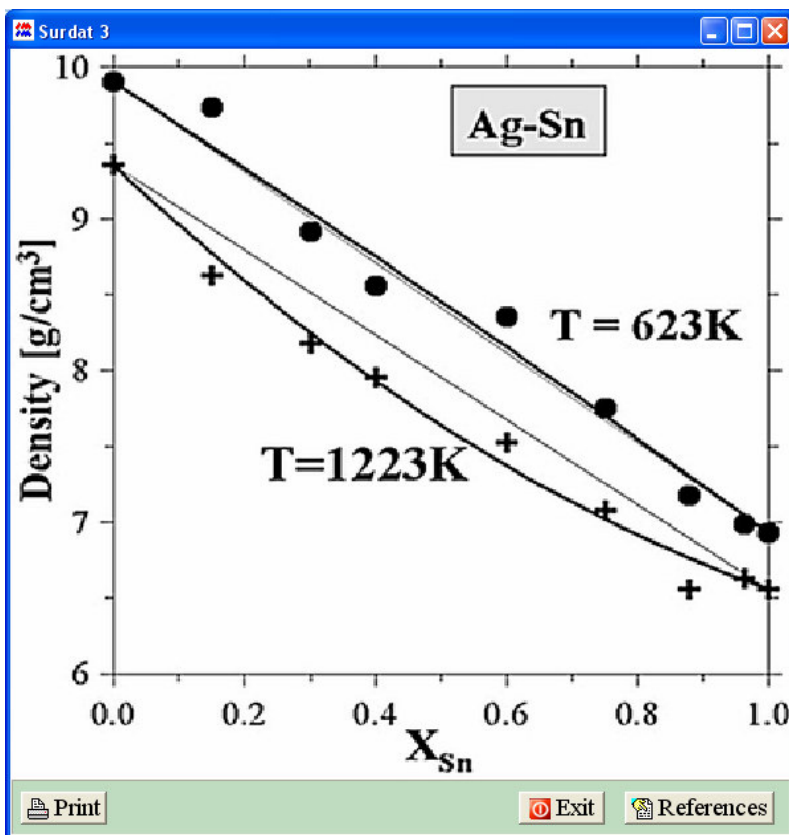


Fig. 6.11. Density isotherms of liquid Ag-Sn alloys

The idea of the „Fig” option in reference to surface tension and molar volume will be presented on the example of the data from [2001Mos1]. If, in the „SELECT PROPERTIES” window, the user selects „Surface tension” as the property, he or she can browse through the temperature dependences (Fig. 6.12) and the isotherms of surface tension (Fig. 6.13). Checking the „Butler model” option displays the temperature dependences (Fig. 6.14) and the isotherms of the surface tension (Fig. 6.15) calculated from the Butler’s relation [1932But].

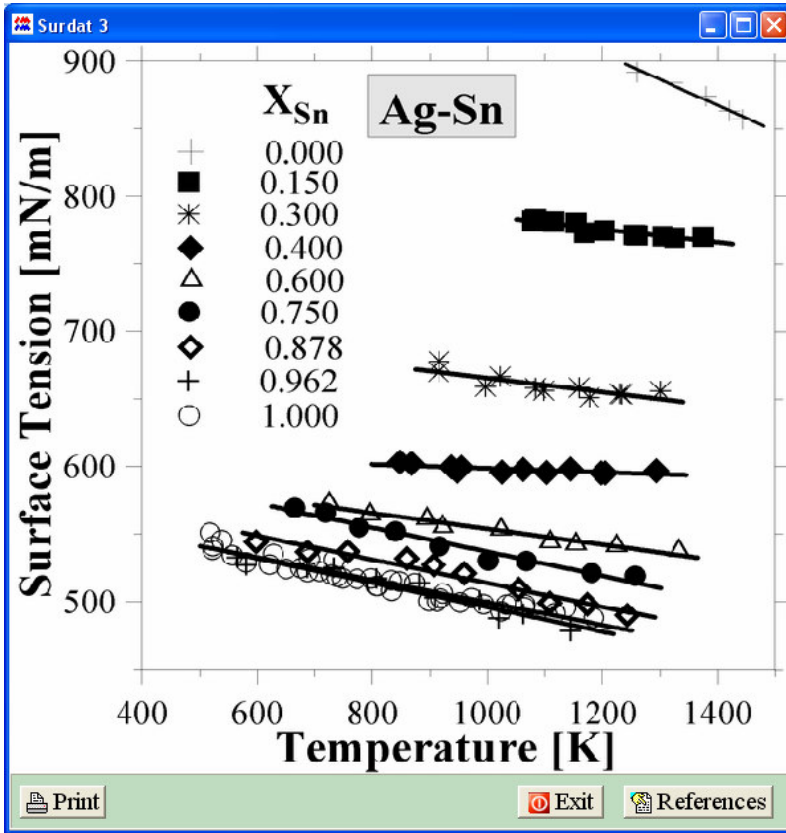


Fig. 6.12. Surface tension temperature dependences of liquid Ag-Sn alloys

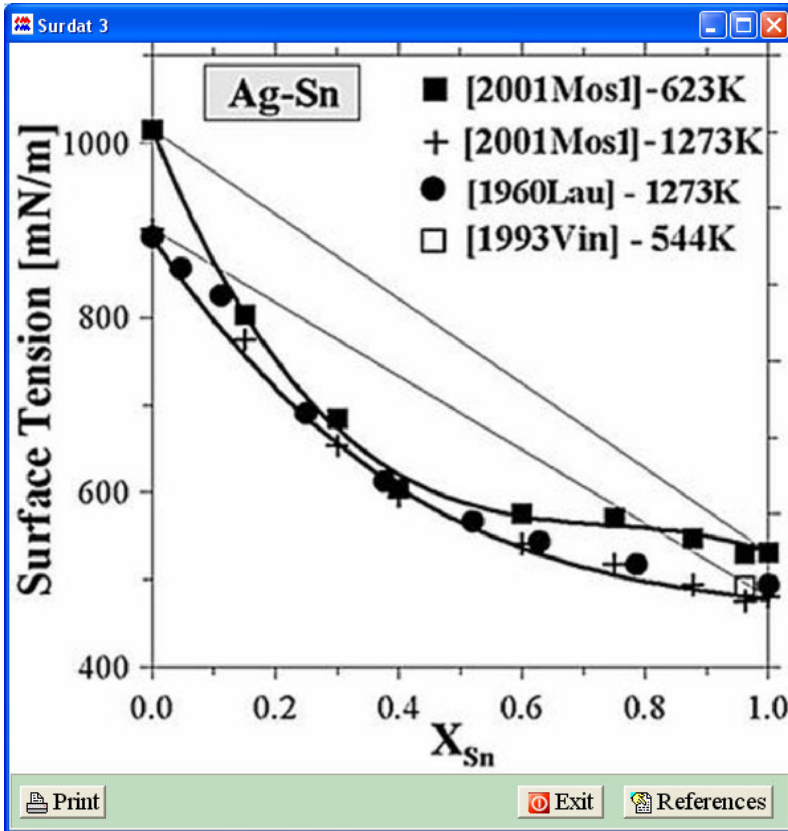


Fig. 6.13. Surface tension isotherms of liquid Ag-Sn alloys

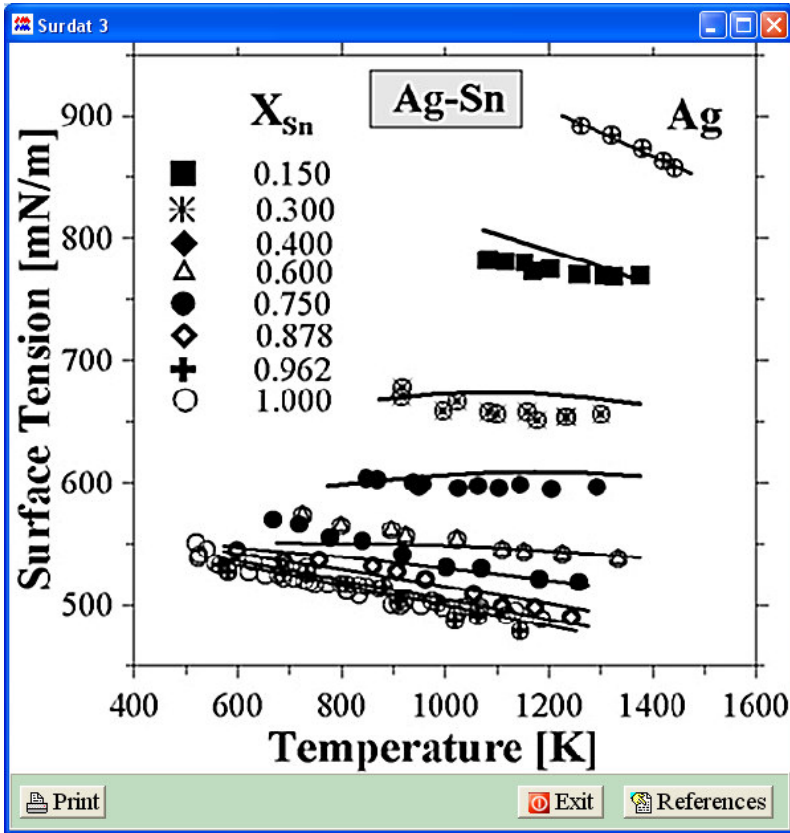


Fig. 6.14. Surface tension temperature dependences of liquid Ag-Sn alloys calculated from Butler's model (lines) on the background of experimental data (symbols)

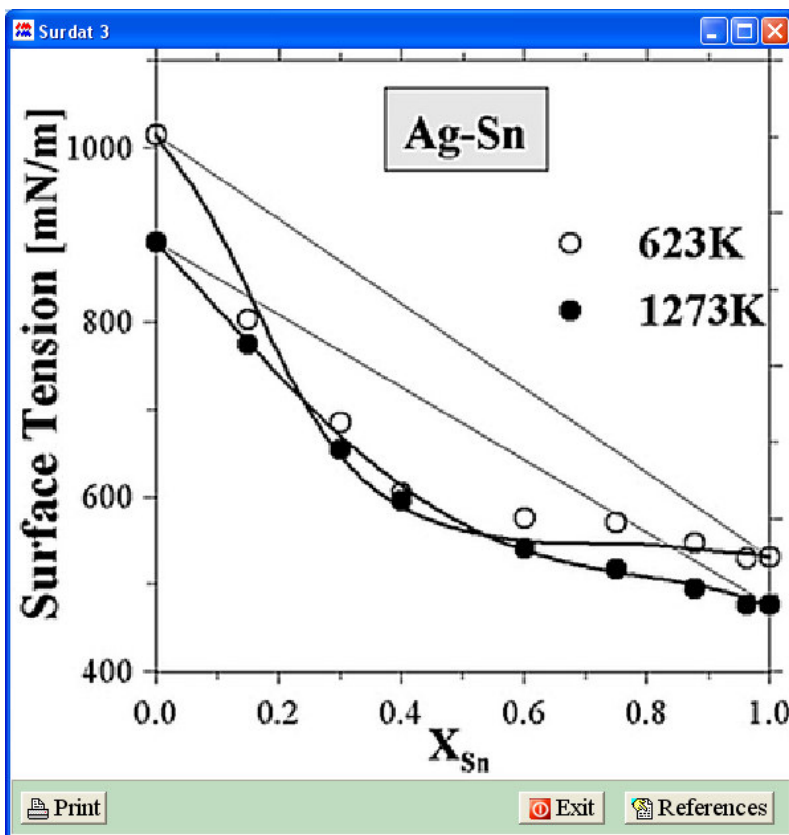


Fig. 6.15. Surface tension isotherms in Ag-Sn system calculated by Butler’s model for 2 selected temperatures: 623 K and 1273, on the background of experimental points [2001Mos1]

For molar volume, only the „Isotherms” option is available in the database (Fig. 6.16), where the experimental values, represented by graphic symbols (black squares and circles), are the properties recalculated from the temperature dependences of the density and the molecular mass of the alloy.

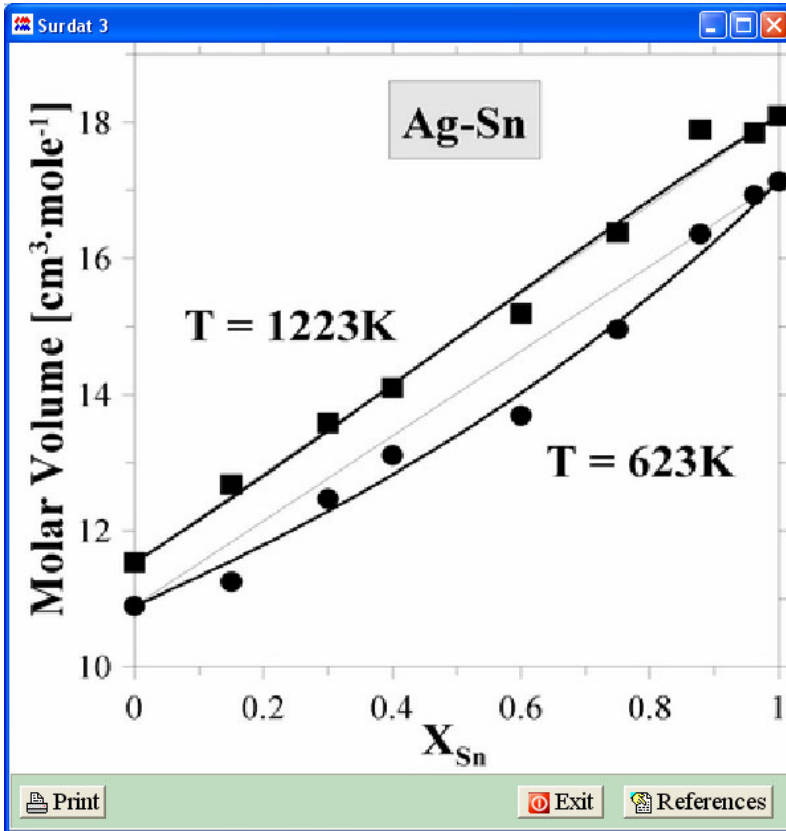


Fig. 6.16. molar volume isotherms of liquid Ag-Sn alloys

Selecting the „Viscosity” property and the presentation mode in the „SELECT PROPERTIES” window and activating the „Fig” button opens the window designed to select the author and the property (Fig. 6.17.). And so, selecting, e.g. the author of [2001Lee1] and pressing the „OK” button displays the viscosity isotherms presented in the selected work (Fig.6.18).

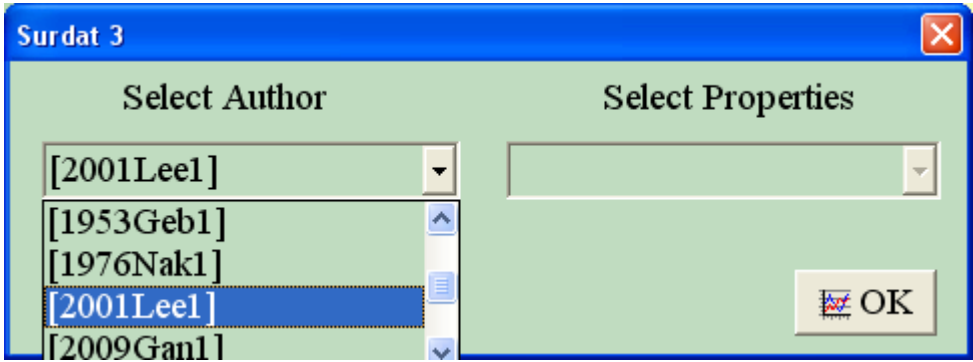


Fig. 6.17. Author and property selection window

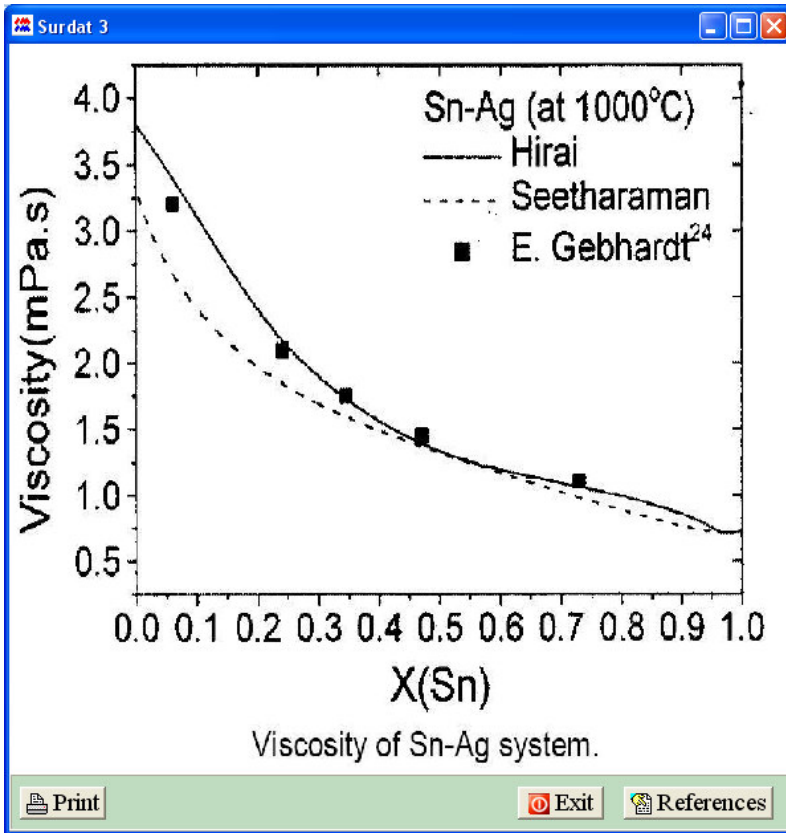


Fig. 6.18. Viscosity isotherms presented in [2001Lee1]

If the temperature dependences are selected as the presentation mode, taking the analogical path to that for the molar volume will result in a display of the window shown in Fig.6.19.

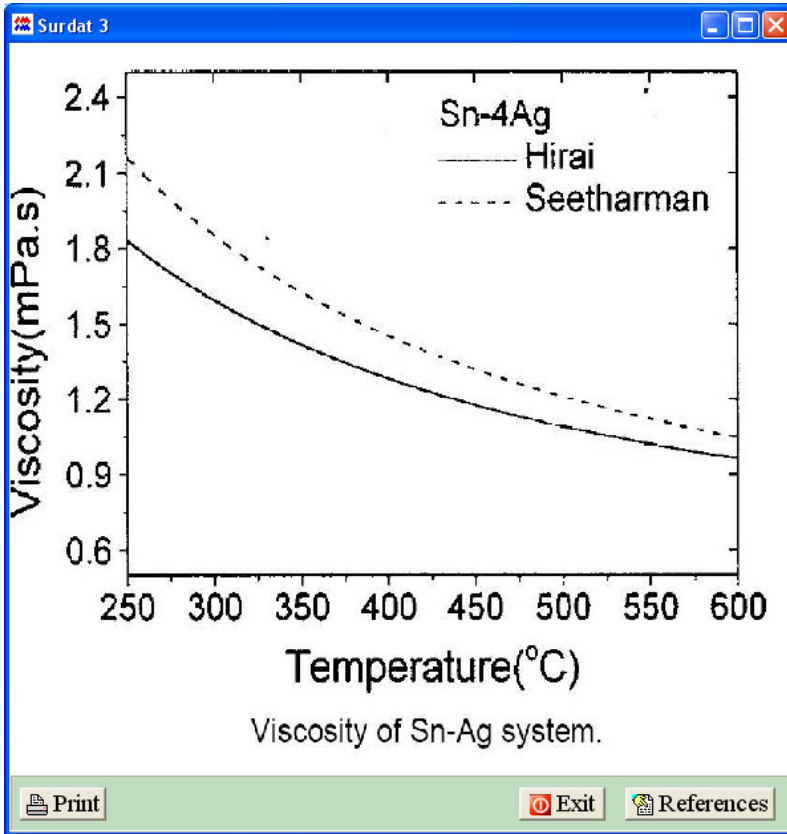


Fig. 6.19. Temperature dependences devolved in [2001Lee1]

The SURDAT 3 database also includes selected data on electrical and mechanical properties. In the case of electrical properties, the following are available:

- Resistance,
- Resistivity.

For example, selecting the author of [2005Gas1] and the „Resistance” property in the window shown in Fig. 6.20 displays a drawing with the information on the effect of the Cu and Bi addition to the SnAg_{eut} alloy on the resistance of the selected solders (Fig. 6.21).

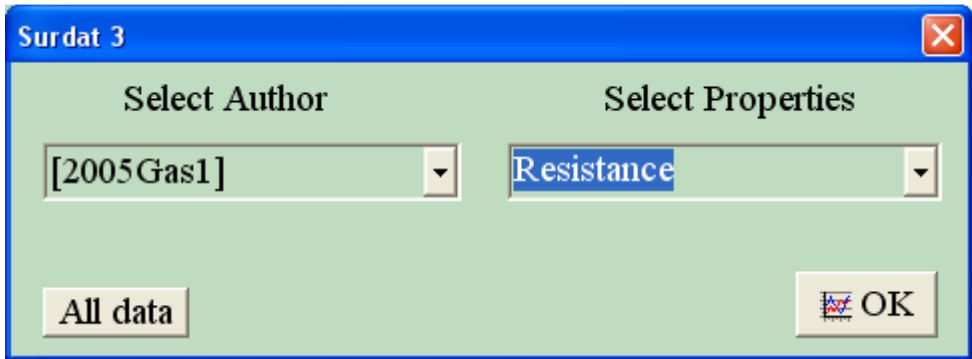


Fig. 6.20. Author and property selection window

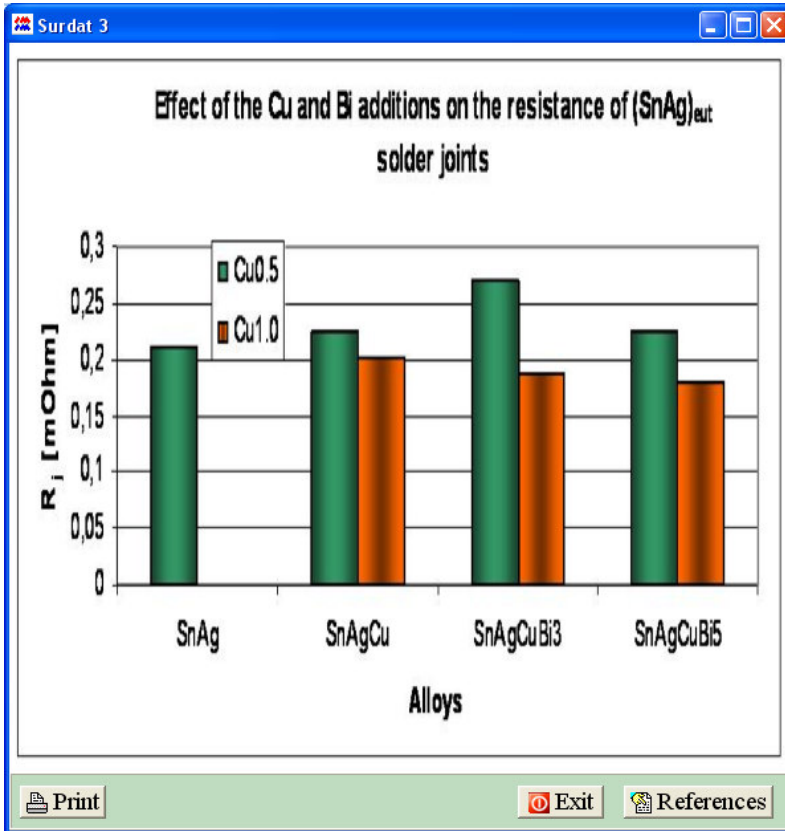


Fig. 6.21. Effect of Cu and Bi on SnAg_{eut} resistance

If, for the given author, we select a property not included in the database, the program will display the window shown in Fig. 6.22 informing on the available graphic presentations for the elected author, which can be displayed with the use of the „Fig” option.

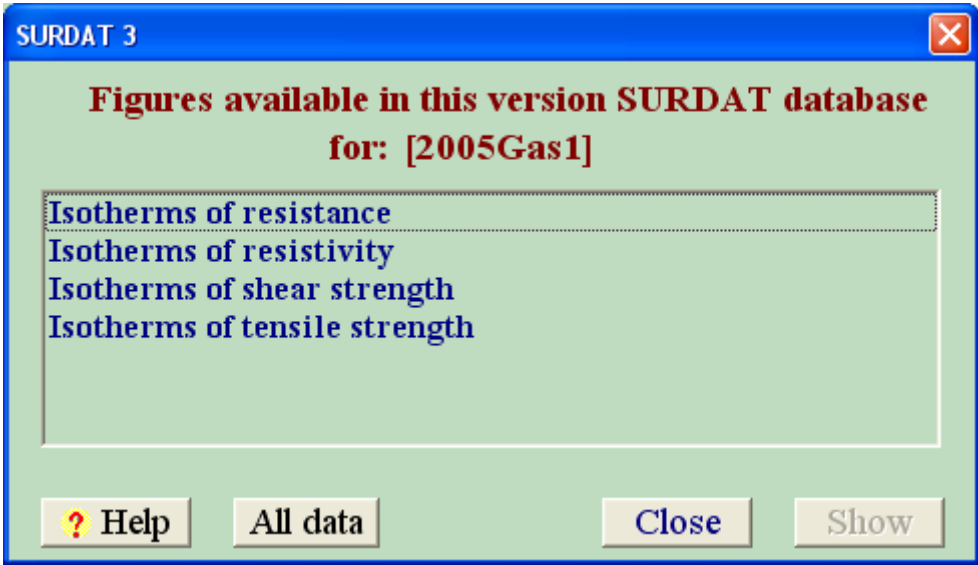


Fig. 6.22. Information window – available graphic presentations of results in [2005Gas1]

In the case of the selection of the „Mechanical properties” option, it is possible to obtain the following property data:

- Hardness,
- Shear Strength,
- Tensile Strength,
- Young’s Modulus.

Selecting the „Mechanical properties” option, the author of [2005Gas1] („Select Author”) and the „Shear Strength” property (“Select Properties”) (Fig. 6.23) in the window shown in Fig. 6.6 will display the window with the information on the effect of the Cu and Bi addition to the SnAg_{eut} alloy on the shear strength of solders (Fig. 6.24).

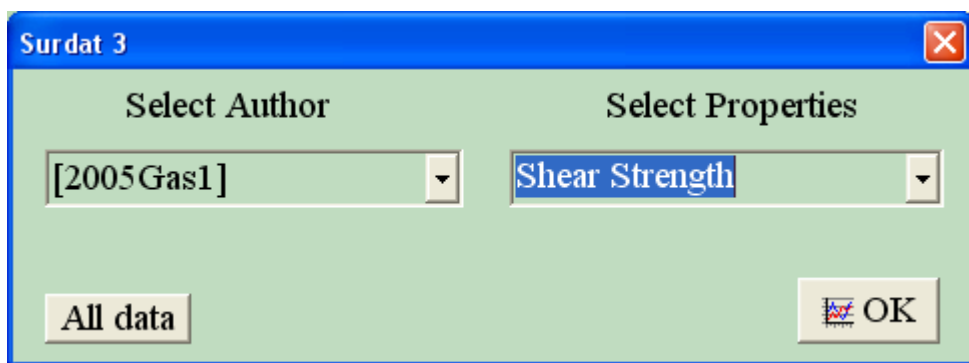


Fig. 6.23. Author and property selection window

If the „All data” button is pressed (Fig. 6.23), the program will display all the collected physicochemical data for the given system in the form of diagrams or a table.

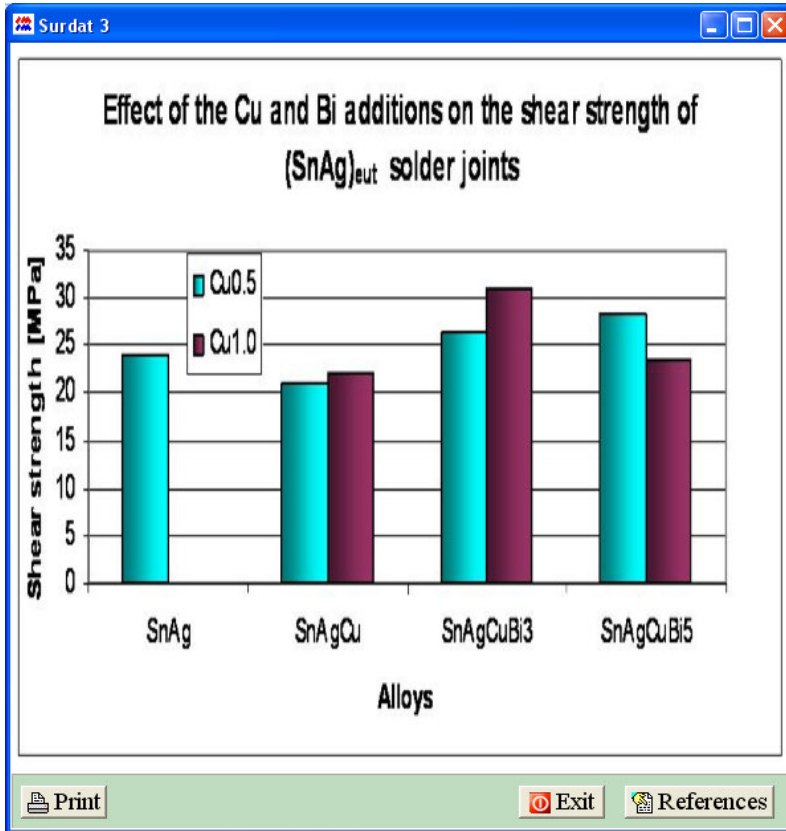


Fig. 6.24. Cu and Bi effect on shear strength of SnAg_{eut}

Browsing the physical properties with the use of the „Fig” option proceeds identically for all the systems available in the SURDAT 3 database.

Another option provided by the database is the possibility to display the phase diagram for a binary system and the liquidus line projection for ternary systems. For example, selecting binary systems, then the „Ag-Sn system (Fig. 6.6) and next pressing the „Ph Diag” button in the window shown in Fig. 6.5 will display the phase diagram for the Ag-Sn system (Fig.

6.25). The bottom of the window provides the data on the phase diagram's origin.

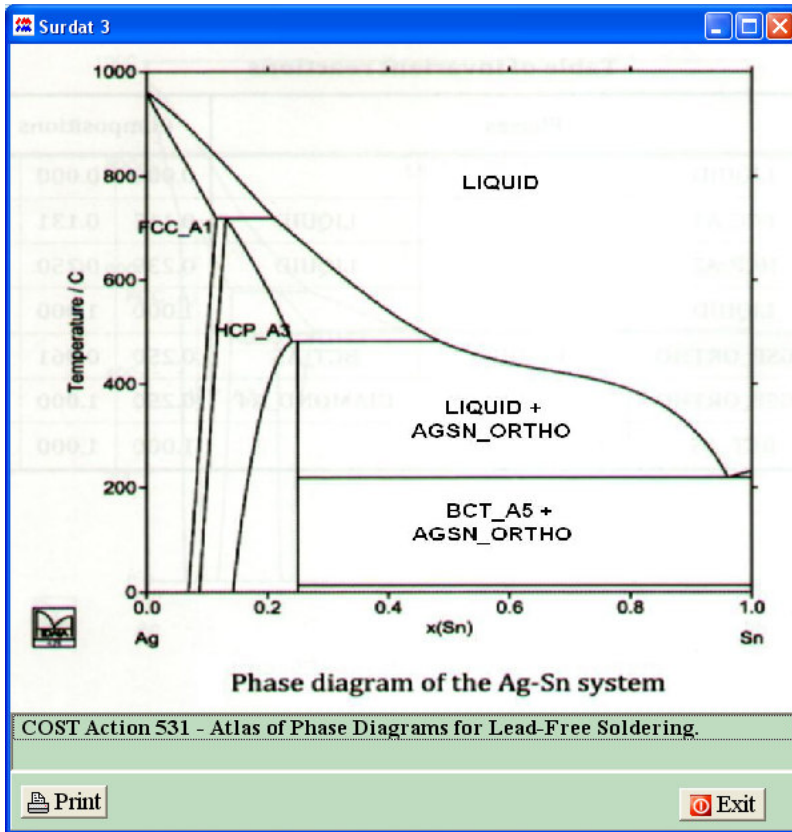


Fig. 6.25. Phase diagram for Ag-Sn developed within COST 531 program

If, in the window in Fig.6.5, we select the option of ternary systems („Ternary systems”), then the „Ag-Cu-Sn system (Fig. 6.6) and next we press the „Ph Diag” button, the liquidus surface projection for this system will be displayed (Fig. 6.26).

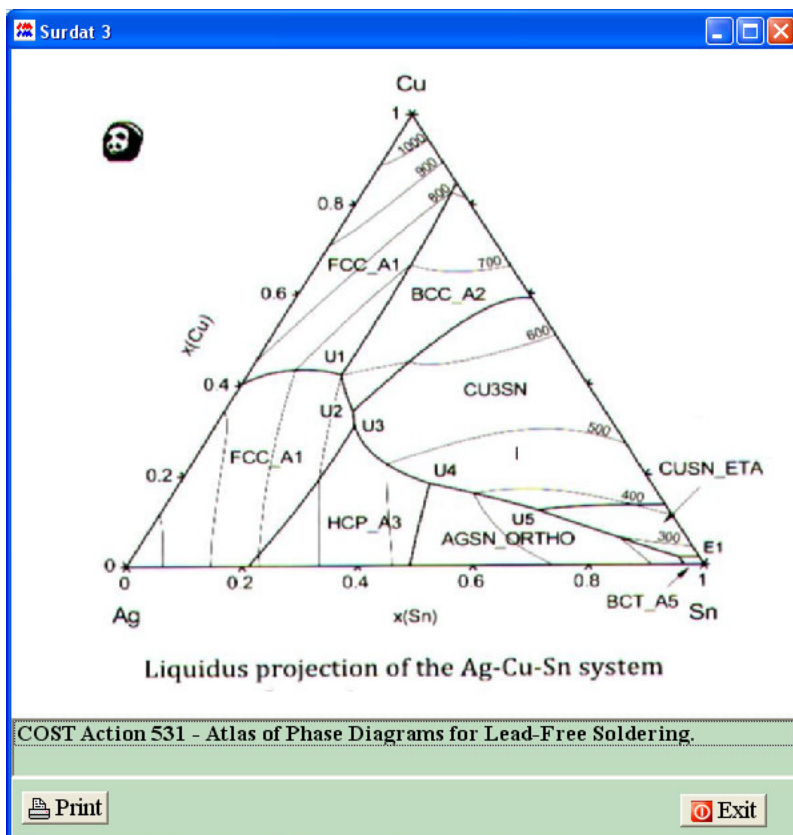


Fig. 6.26. Liquidus surface projection in Ag-Cu-Sn

The phase diagram option in the SURDAT 3 database is demonstrative in character and does not provide the possibility of phase diagram calculations.

The SURDAT 3 database is capable of presenting the results of meniscographic tests, which will be discussed on the example of the Ag-Cu-Sn system. The selection of this option is possible after the activation of the „Menisc” button (Fig. 6.6), which opens the meniscographic test window (Fig.6.27). in this window, it is possible to select the presentation mode for the meniscographic data. We can choose from either diagrams (Figure) or tables (Table). Selecting diagrams

as the presentation mode makes it possible to select the author of the meniscographic data („Select Author”). After the selection of e.g. [2006Mos1], one should also specify the type of the meniscographic data, which can be:

- contact angle,
- wetting force,
- wetting time,
- interfacial tension.

For example, after the selection of „Contact angle”, one should additionally specify the system (alloy). Selecting Ag-Sn and pressing the „Show” button will display the window informing on the availability of the meniscographic data for the given author (Fig.6.28). If we select ”Interfacial tension” and next press „Show”, the program will display the interfacial tension presented in [2006Mos1] (Fig. 6.29). If we press the „All data” button, we will be demonstrated by a graphic representation of all the collected meniscographic data for the selected system. The use of the „All data” button makes it possible to gain a brief access to the available meniscographic data for the given system provided in the graphic form. If one selects the „Interfacial tension” option and then presses „Show”, the program will display the data presented in [2006Mos1] (Fig. 6.29).

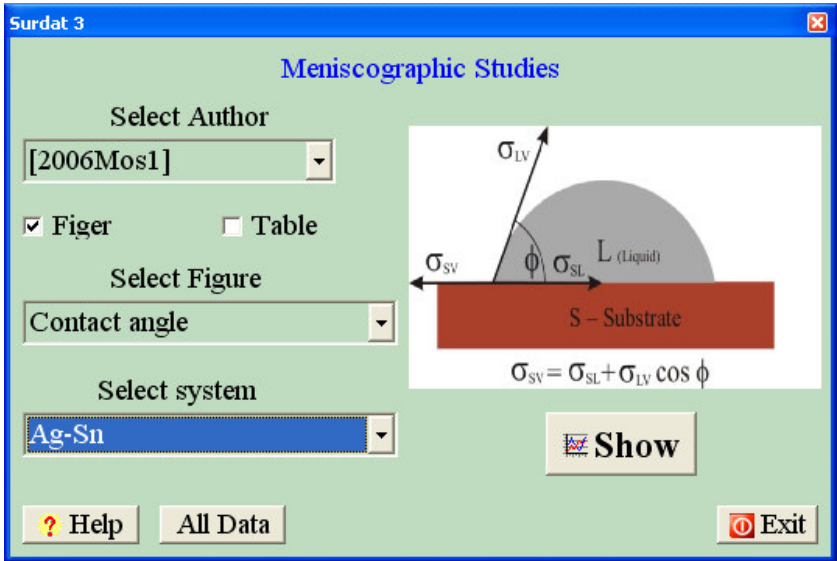


Fig. 6.27. Main meniscographic data window

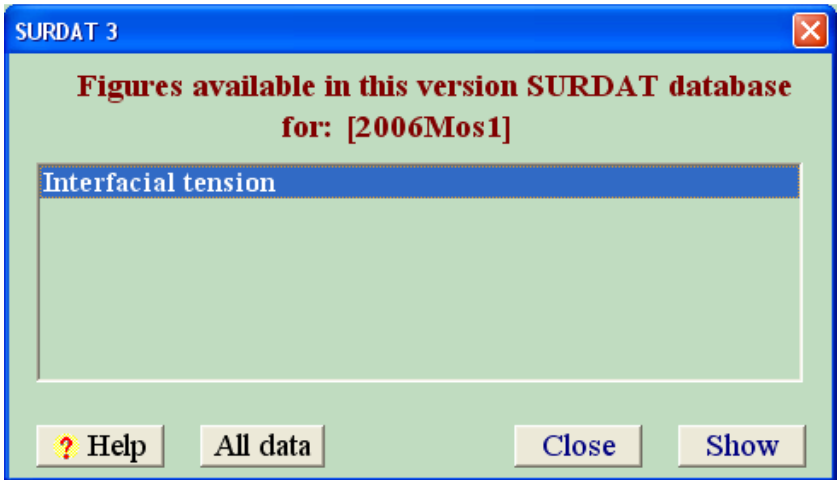


Fig. 6.28. Information window – available graphic presentation of results in [2006Mos1]

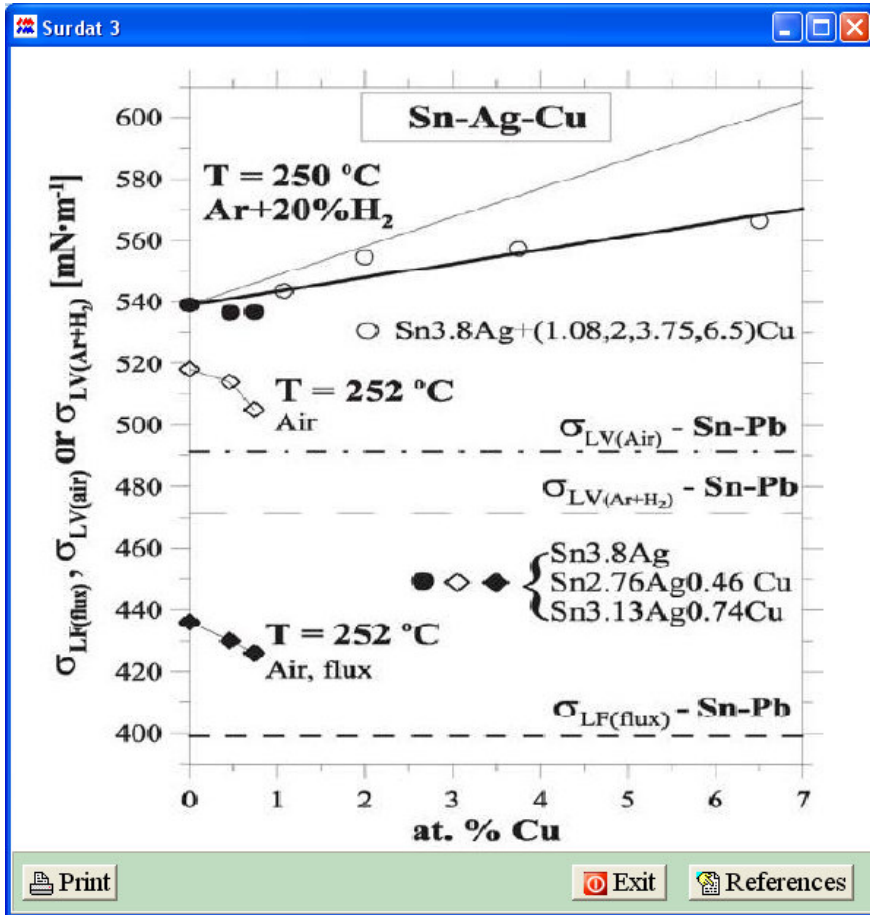


Fig. 6.29. Graphic presentation of meniscographic data in [2006Mos1]

If, in the window shown in Fig. 6.27, the „Table” option is selected followed by „Show”, the program will display the available meniscographic data for the selected system (Ag-Cu-Sn) in the form of a table (Fig.6.30), which includes such information as: the author (REFERENCES), the alloy type (SYSTEM), as well as WETTING TIME, WETTING FORCE, CONTACT ANGLES, SURFACE TENSION, INTERFACIAL TENSION), the melting point (T_m), the measurement temperature (TEMP), the substrate type (SUBSTRATE), the atmosphere in which the tests were conducted (ATMOSPHERE) and the type of the applied flux (FLUX).

REFERENCES	SYSTEM	WETTING TIME [s]	WETTING FORCE [mN]	CONTACT ANGLES [°]	SURFACE TENSION [mNm]	INTERFACIAL TENSION [mNm]	T _m [K]	TEMP [K]	SUBSTRATE	ATMOSPHERE	FLUX
[1992Wls]	Sn-4Cu-0.5Ag			34<<<51					Cu		A611, A250JF and E3508
[2004Gas1]	(SnAg)eut+0.74Cu				415(+/-)36	371(+/-)14	525	525	Cu	Air	ROL 1
[2004Gas1]	(SnAg)eut+0.46Cu				408(+/-)3	384(+/-)11	525	525	Cu	Air	ROL 1
[2004Vu1]	Sn-3.5Ag-0.7Cu	10		49(+/-)3			523	523	Cu		RMA
[2004Vu1]	Sn-2.5Ag-0.7Cu	10		53(+/-)3			523	523	Cu		RMA
[2004Vu1]	Sn-3.5Ag-0.7Cu	0.7	5	48			523	523	Cu		RMA
[2005Lop1]	95.55Sn-3.9Ag-0.6Cu			42.2(+/-)1.4		484.5(+/-)26.6	503	503	Au-Ni Kovar		RMA
[2005Lop1]	95.55Sn-3.9Ag-0.6Cu			38.6(+/-)1		443.9(+/-)16.5	518	518	OFE Cu		RMA
[2005Lop1]	95.55Sn-3.9Ag-0.6Cu			59.9(+/-)1		650.8(+/-)34.9	533	533	OFE Cu		LS
[2005Lop1]	95.55Sn-4.0Ag-0.5Cu			NW		NW	518	518	Au-Ni Kovar		R
[2005Lop1]	95.55Sn-4.0Ag-0.5Cu			72.3(+/-)35.5		804.7(+/-)383.3	518	518	Au-Ni Kovar		LS
[2005Lop1]	95.55Sn-4.0Ag-0.5Cu			55.3(+/-)30.6		641.6(+/-)21.6	533	533	Au-Ni Kovar		RMA
[2005Lop1]	95.55Sn-4.0Ag-0.5Cu			NW		NW	533	533	Au-Ni Kovar		R
[2005Lop1]	95.55Sn-3.9Ag-0.6Cu			73.7(+/-)31.7		1045.9(+/-)180.6	533	533	Au-Ni Kovar		LS
[2005Lop1]	95.55Sn-3.9Ag-0.6Cu			38.6(+/-)1		443.9(+/-)16.5	518	518	Au-Ni Kovar		RMA
[2005Lop1]	95.55Sn-3.9Ag-0.6Cu			NW		NW	503	503	Au-Ni Kovar		R
[2005Lop1]	95.55Sn-3.9Ag-0.6Cu			NW		NW	503	503	Au-Ni Kovar		LS
[2005Lop1]	95.55Sn-3.9Ag-0.6Cu			NW		NW	518	518	Au-Ni Kovar		R
[2005Lop1]	95.55Sn-3.9Ag-0.6Cu			44.0(+/-)22.2			518	518	Au-Ni Kovar		LS
[2005Lop1]	95.55Sn-3.9Ag-0.6Cu			40.4(+/-)1		496.9(+/-)15.9	533	533	Au-Ni Kovar		RMA
[2005Lop1]	95.55Sn-3.9Ag-0.6Cu			NW		NW	533	533	Au-Ni Kovar		R

REFERENCES: Z. Moser, W. Gsponer, K. Bukacik, J. Pstrus, R. Kissel, I. Ohnuma, K. Ishida, Ph - Free Solders: Part I. Wettability Testing of Sn-Ag-Cu Alloys with B Additions, 27, 133-139, (2006), J. Phase Equilib. Diffus.

Exit

Help

Fig. 6.30. Meniscographic data for Ag-Cu-Sn available as a table

The SURDAT 3 database also includes brief characteristics of some of the experimental methods often applied in the measurements of some properties. These descriptions are available in the SURDAT 3 menu after the selection of „File” and next „Experimental methods”. This opens an active window with the following specified methods (Fig. 6.31):

1. Maximum bubble pressure method,
2. Dilatometric method,
3. Meniscographic method,
4. Sessile drop method.

For example, after the selection of the „Maximum bubble pressure method” option (method of maximum pressure in gas bubbles), the program will display a window (Fig. 6.32) with the method’s scheme and description.

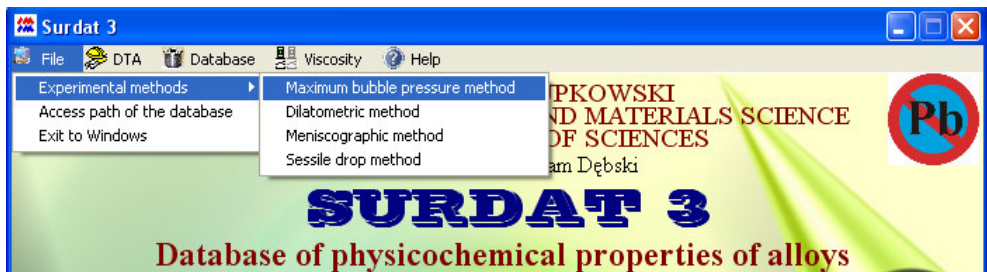


Fig. 6.31. „File” menu in SURDAT 3

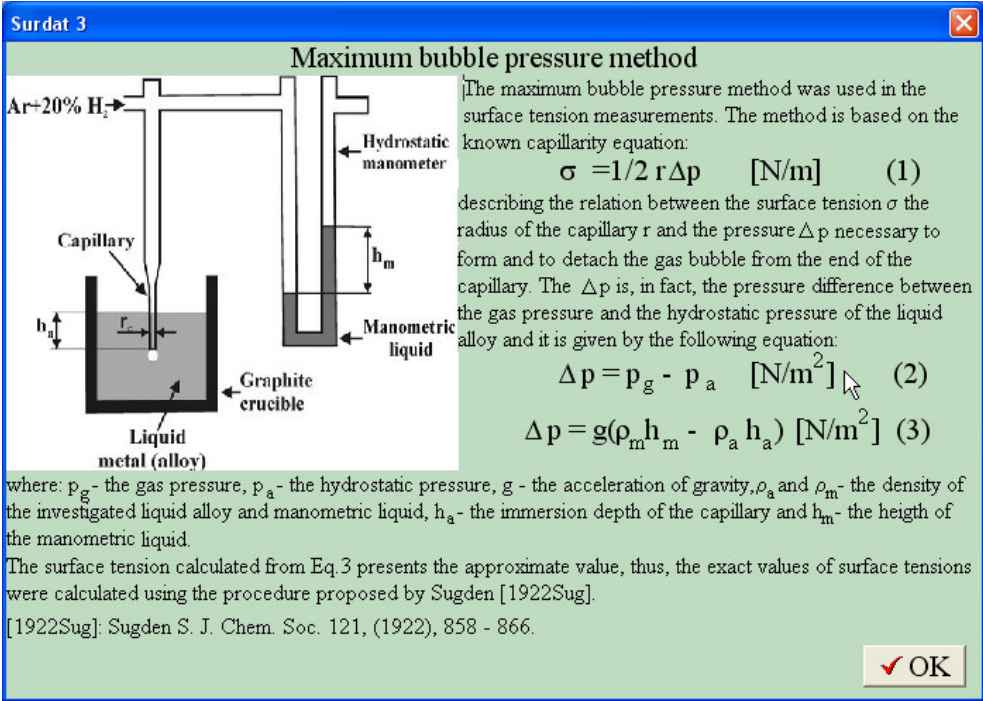


Fig. 6.32. Description of experimental methods in SURDAT 3. „Maximum bubble pressure method”



Fig. 6.33. „DTA” menu in SURDAT 3

Clicking the „DTA” menu (Fig. 6.33) will active a display of the DTA test result for the selected solders, which have been obtained in the frames of the implementation of the „Advanced soldering materials” scientific network (Fig. 6.34).

The SURDAT 3 database is supplemented by the NIST database (National Institute of Standards and Technology z Boulder (Colorado, USA)) whose activation is possible after the selection of „NIST Database (Fig .6.36) in the “Database” menu shown in Fig. 6.35.

Temperature (Solidus, Liquidus) [K]			Elemental Composition (% by Mass)									
Alloy Number	Solidus	Liquidus	Ag	Al	Au	Bi	Cu	In	Li	Sb	Sn	Zn
8943	471,5	476									89,8	9,92
8944	470	476				1,17				1,13	88,6	9,43
8945	467	473				2,27				2,17	87	9,03
8946	470	476				1,08				2,45	86,8	9,54
8947	466,5	476				2,2				1,18	87,3	9,55
9174	469	476				1,07				1,24	90,7	6,99
9175	464	476				2,25				1,25	89,5	7
9176	469	476				1,06				2,18	90	6,76
9177	463	476				2,3				2,2	88,6	6,9
9485	471,5	473,5									92,92	7,08
9486	468	468				1,1					91,71	7,19
9487	462,5	462,5				3,35					89,5	7,15
9488	471,5	475									93,59	6,41
9489	469	474,5							0,03		93,9	6,07
9490	468,5	475							0,04		93,89	6,07
9627	483	487	2,93			3,43	0,57				93,07	
9627/A	494	686	30								70	
9628	494	779	53								47	
9629	494	866	66								34	
9630	1176	1216	95,9								4,1	
9631	491	494,5	5,5				0,66				93,6	
9632	490	494	3,54				1,01				95,45	
9633	491	496	3,51				1,61				94,88	
9634	481	487	3,25				0,5	1,92			94,33	
9635	481	486,5	3,22				0,6	2,6			93,58	
9636	479	485	3,13				0,58	3,51			92,78	
9637	469	479	2,83				0,56	7,45			89,16	

Fig. 6.34 DTA test results for selected solders researched in the frames of „Advanced soldering materials” network



Fig. 6.35. „Database” menu in SURDAT 3

Database for Solder Properties with Emphasis on New Lead-free Solders Release 5.0

National Institute of Standards & Technology,
Colorado School of Mines and
Institute of Metallurgy and Materials Science Polish Academy of Sciences

File posted on: 2009 April 9

[Back to main page](#)

Properties of Lead-Free Solders

Disclaimer: In the following database, companies and products are sometimes mentioned, but solely to identify materials and sources of data. Such identification neither constitutes nor implies endorsement by NIST of the companies or of the products. Other commercial materials or suppliers may be found as useful as those identified here.

Note: Alloy compositions are given in the form "Sn-2.5Ag-0.8Cu-0.5Sb," which means: 2.5 % Ag, 0.8 % Cu, and 0.5 % Sb (percent by mass), with the leading element (in this case, Sn) making up the balance to 100 %.

Abbreviations for metallic elements appearing in this database:

Ag: silver	Cu: copper	Pt: platinum
Al: aluminum	In: indium	Sb: antimony
Au: gold	Mo: molybdenum	Sn: tin
Bi: bismuth	Ni: nickel	W: tungsten
Cd: cadmium	Pb: lead	Zn: zinc
Cr: chromium	Pd: palladium	
Sn-Ag-Cu: Refers to compositions near the eutectic		

Table of Contents:

- [Mechanical Properties](#): Elastic modulus, elongation, tensile strength, yield strength
 - [Table 1.1](#): Strength and Ductility of Low-Lead Alloys Compared with Alloy Sn-37Pb (NCMS Alloy A1), Ranked by Yield Strength (15 Alloys) and by Total Elongation (19 Alloys)
 - [Table 1.2](#): Tensile Properties of Lead-Free Solders

Fig. 6.36. Preliminary (5.0) version of NIST database combined with SURDAT database

As the SURDAT 3 database introduces the experimental and the calculated viscosity data on binary systems, it also provides brief descriptions of the applied viscosity models. They are available from the menu under „Viscosity” with the „Models” option, when the program displays an active window with the names of the authors. The following five viscosity models are available (Fig. 6.37):

1. Gašior (Gas),
2. Gašior- Moser (G-M),
3. Iida – Ueda – Morita_Gex (I-U-M_G),
4. Iida – Ueda – Morita_Hm (I-U-M_H),
5. Kaptay (Kap),
6. Kozlov – Romanov – Petrov (K-R-P),
7. Kucharski (Kuc),
8. Moelwyn – Hughes (M-H),
9. Sato (Sat),
10. Schick-Brillo-Egry-Hallstedt (S-B-E-H),
11. Seetharaman – Du Sichen (S-S),
12. Sichen-Bygden- Seetharaman (S-B-S).

After the selection of the „Iida – Ueda – Morita_Gex (I-U-M_G),” option, the program will display the window shown in Fig. 6.38.

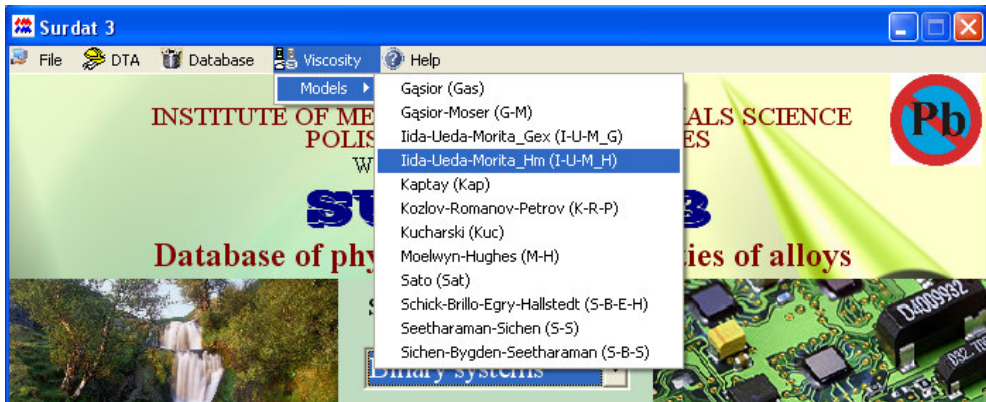


Fig. 6.37. „Viscosity” menu in SURDAT 3

The screenshot displays the 'Iida – Ueda – Morita model' dialog box. It contains the following mathematical equation for viscosity η :

$$\eta = (\eta_1 X_1 + \eta_2 X_2) \left\{ 2 \left[1 + \frac{X_1 X_2 (\sqrt{m_1} - \sqrt{m_2})^2}{(X_1 \sqrt{m_1} + X_2 \sqrt{m_2})^2} \right]^{\frac{1}{2}} - 1 - \frac{5 X_1 X_2 (d_1 - d_2)^2}{X_1 d_1^2 + X_2 d_2^2} - \Delta \right\}$$

Below the equation, the parameters Δ are defined as:

$$\Delta = 0.12 \frac{\Delta H_m}{RT} \quad \Delta = 0.12 \frac{\Delta G^E}{RT}$$

The dialog box also includes a list of parameter definitions:

- η, η_1, η_2 – viscosity of alloy and metals
- X_1, X_2 – mole fraction of metals
- d_1, d_2 – Pauling's atomic radii
- m_1, m_2 – atomic masses
- R – gas constant
- T – temperature
- ΔH_m – enthalpy of mixing
- ΔG^E – excess Gibbs free energy

An 'OK' button is located at the bottom right of the dialog box.

Fig. 6.38. Description of viscosity models in SURDAT 3. Iida – Ueda – Morita model

Clicking the „Help” menu (Fig. 6.39) will open a help window providing the user with the present monograph.

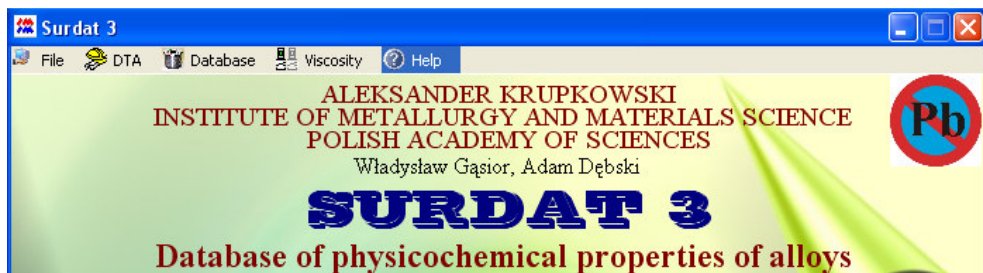


Fig. 6.39. „Help” menu in SURDAT 3

A comparison of the experimental data with those calculated from different models which use the thermodynamic properties of the liquid phase is yet another option in the SURDAT 3 database. Next to the surface tension modeling with the application of the Butler’s model, the program allows for the modeling of viscosity from the five available viscosity models. The various options for presenting these data will be discussed on the example of the Ag-Sn and Ag-Cu-Sn system. First, we will focus on the binary one.

Entering the binary system option begins in the start window (Fig. 6.5) with the selection of „Binary systems” and in the unfoldable selection windows for the system and the physical properties (Fig. 6.6). After the selection of the „Ag-Sn” system, the „Density” property and the „Isotherms” presentation mode, and after the activation of the „Next” button, the program will open a window where we can model, process and analyze the data by various authors. After the selection of the data author „SELECT AUTHOR” (Fig. 6.40), followed by the „Show” button, the program will display, in the bottom right-hand part, the density

equations by the given author. If the option „Show calculate value” is selected and the temperature values are entered (max. 4: T1, T2, T3, T4) the program will calculate the density and present it graphically in a diagram (Fig.6.41).

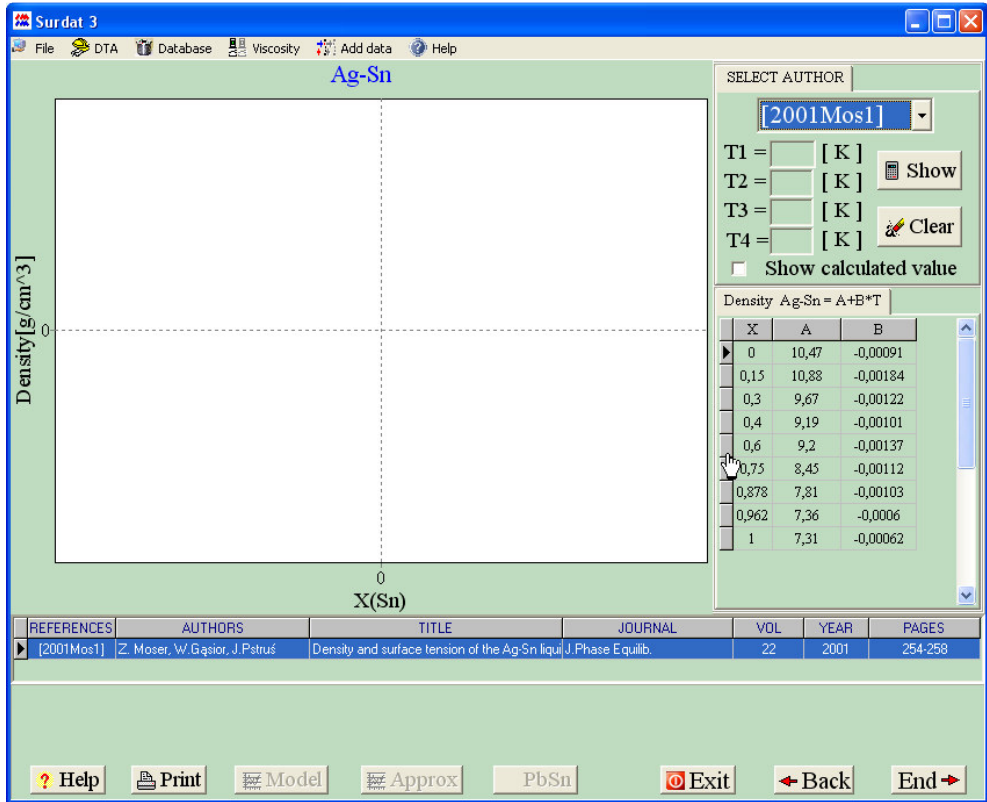


Fig. 6.40. Temperature dependences of density for Ag-Sn system elaborated by a selected author [2001Mos1]

The calculated values of density for the corresponding concentrations at a given temperature can be seen in the tables, in the bottom right-hand part of the window. This option gives us the possibility to observe the temperature dependences for the analyzed system and, if other authors’

data are available, to make a comparison of the data, by re-selecting the author („SELECT AUTHOR”). The „Approx” option presents the polynomial approximation to the experimental points. In the bottom part, we can see „References”. Pushing the „Clear” button clears the diagram and the numeric data.

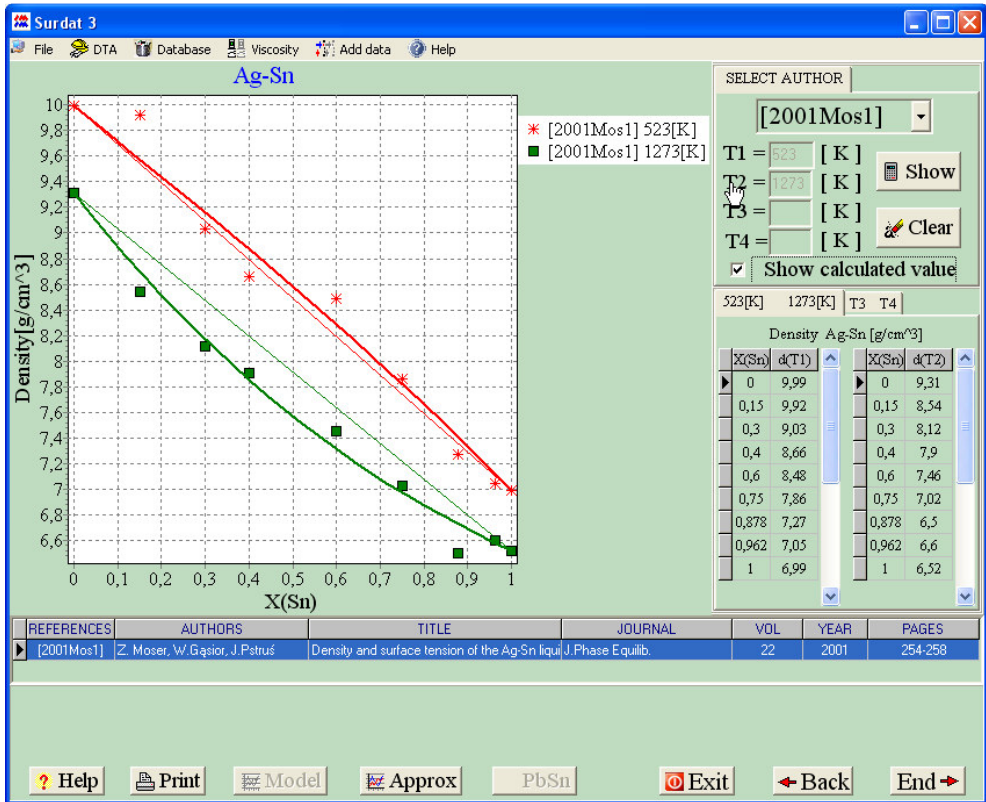


Fig. 6.41. Density isotherms of liquid Ag-Sn alloys calculated at 523K and 1273 from equations by the author of [2001Mos1]

After the selection of „Temperature relation” and the author in the previous window (Fig. 6.6), followed by „Show”, the program will display the available concentrations. It is possible to select all of them („SELECT ALL”) or those of interest. The activated „Points” button will display

the experimental points for the given concentrations (Fig. 6.42). The program will show only the points by the author selected in the upper window.

If we push the „Graph” button, the program will add the linear approximation to the experimental data. There is an option to print the diagram by means of the „Print” button, as well as to compare the density of the given system with those of the traditional tin-lead solders, which is activated by „PbSn”.

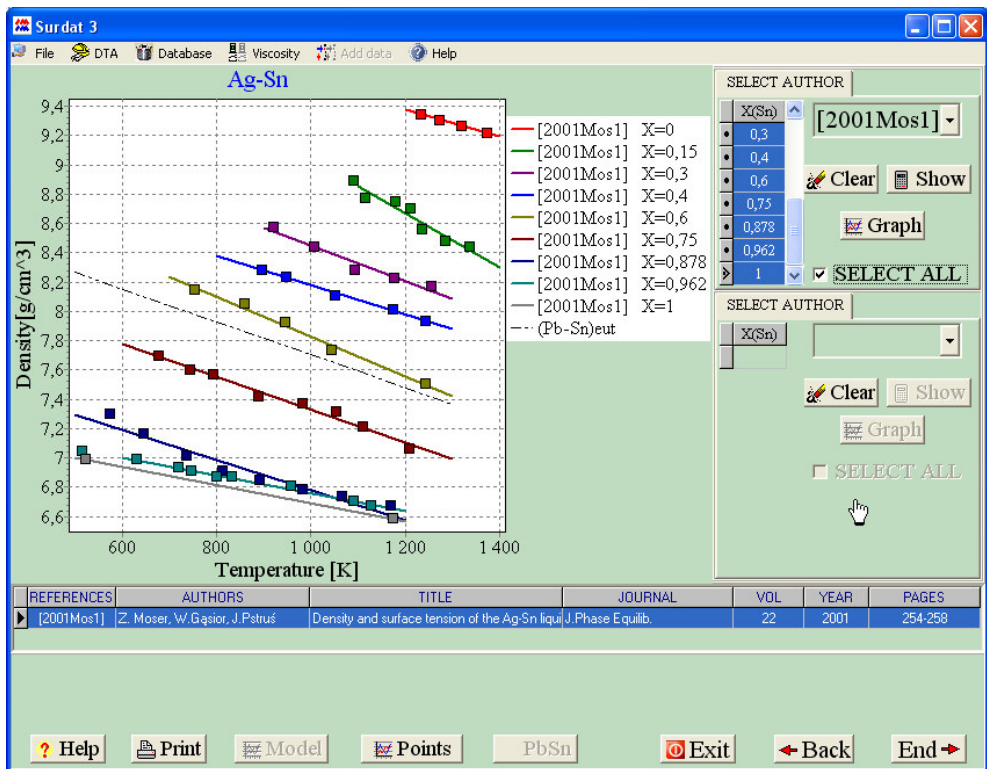


Fig. 6.42. temperature dependences of density for Ag-Sn (Sn-Pb)_{eut} liquid alloys

By going back to the window in Fig. 6.6 and selecting "Surface tension", similarly as density, we can display the following:

- the parameters A and B of the linear equations $\sigma = A + BT$ describing the temperature dependences of surface tension for different concentrations ($X_{(Sn)}$) (Fig. 6.43),
- the possibility to calculate the isotherms at any temperature and
- the possibility to compare them with the data by another author (Fig. 6.44).

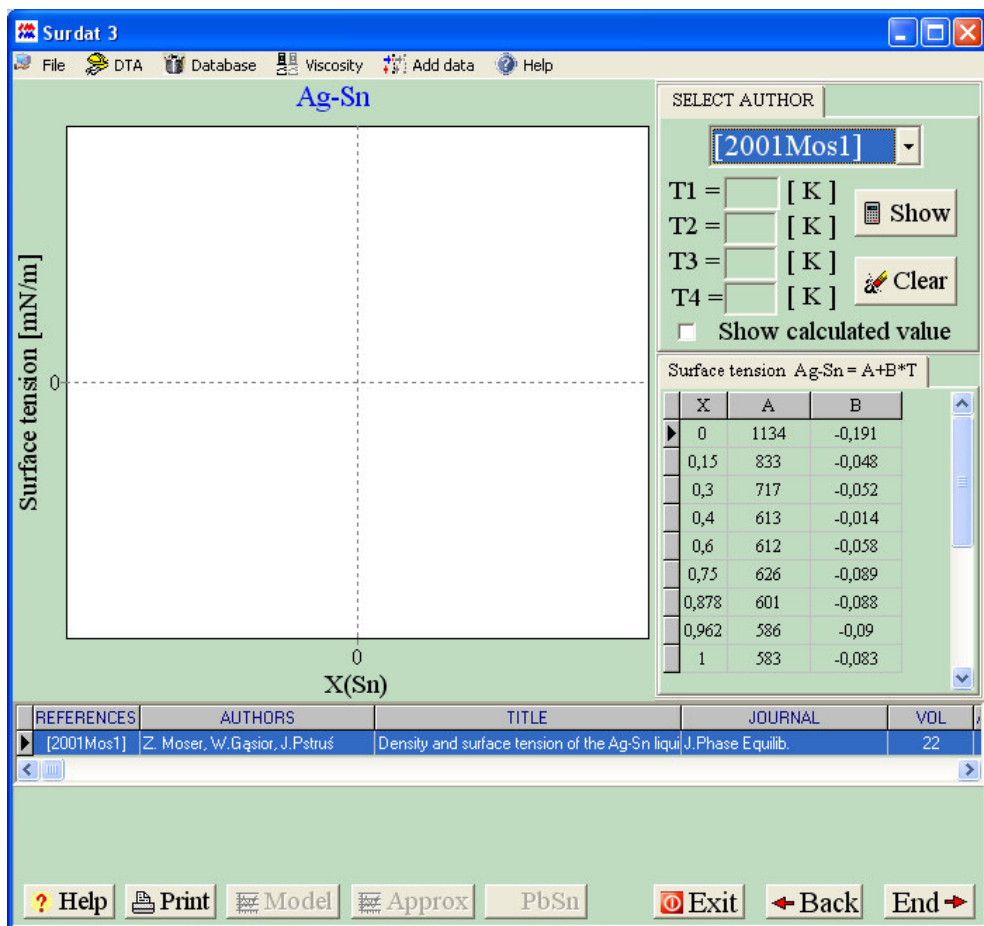


Fig. 6.43. Temperature dependences of surface tension for liquid Ag-Sn alloys elaborated by the author of [2001Mos1]



Fig. 6.44. Isotherms of surface tension for Ag-Sn system calculated at 523 K, elaborated by two authors, compared with experimental data

The „Butler model” option in the window in Fig. 6.6 makes it possible to calculate the surface tension from the Butler’s relation by pressing the „Model” button, as well as to confirm the compatibility with the data obtained in the experiment by the given author (Fig. 6.45).

The selection of the option of temperature dependence visualization „Temperature relation” and the authors makes it possible to view the temperature dependence diagram (Fig. 6.46). If experimental data by other authors are available, there is a possibility to show and compare

them in one diagram, which can be done after the selection of other authors, followed by „Show”, as well as concentrations, displayed after „Graph” is pressed. If we wish to compare the surface tension of the given system with that of the traditional tin-lead solders, we can push the „PbSn” button. Clicking the diagram with the left mouse button will zoom it in to the full screen mode (Fig. 6.47). Clicking it again will restore the previous view.

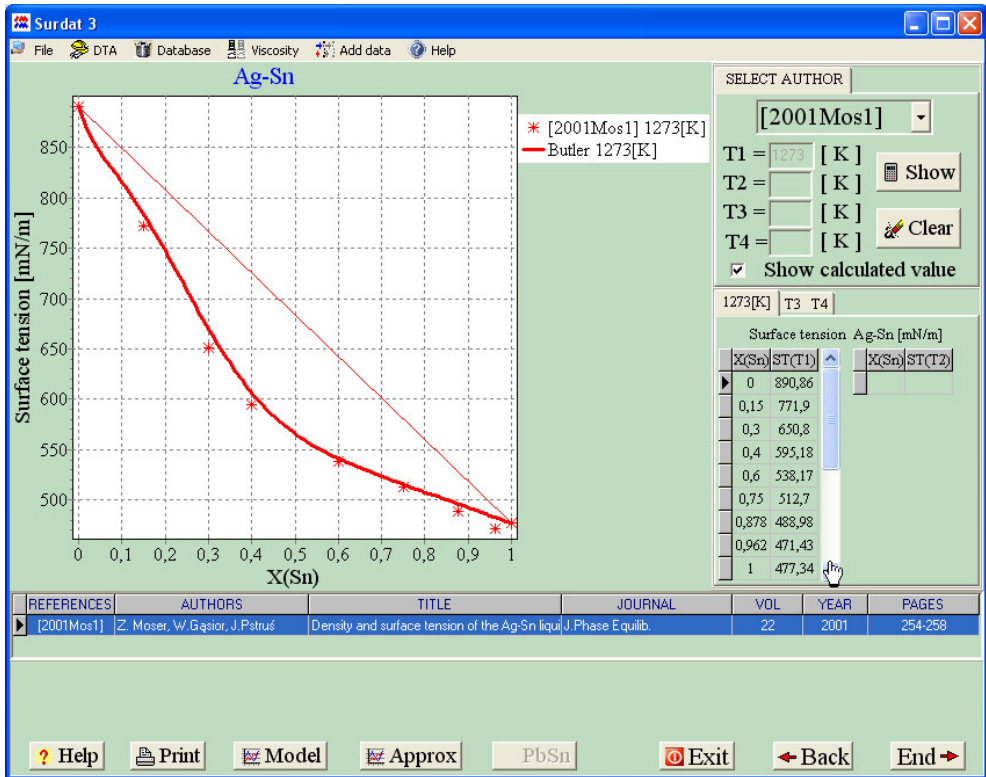


Fig. 6.45. Isotherm of surface tension for Ag-Sn system calculated from Butler’s model at 1273 K and compared with experimental data

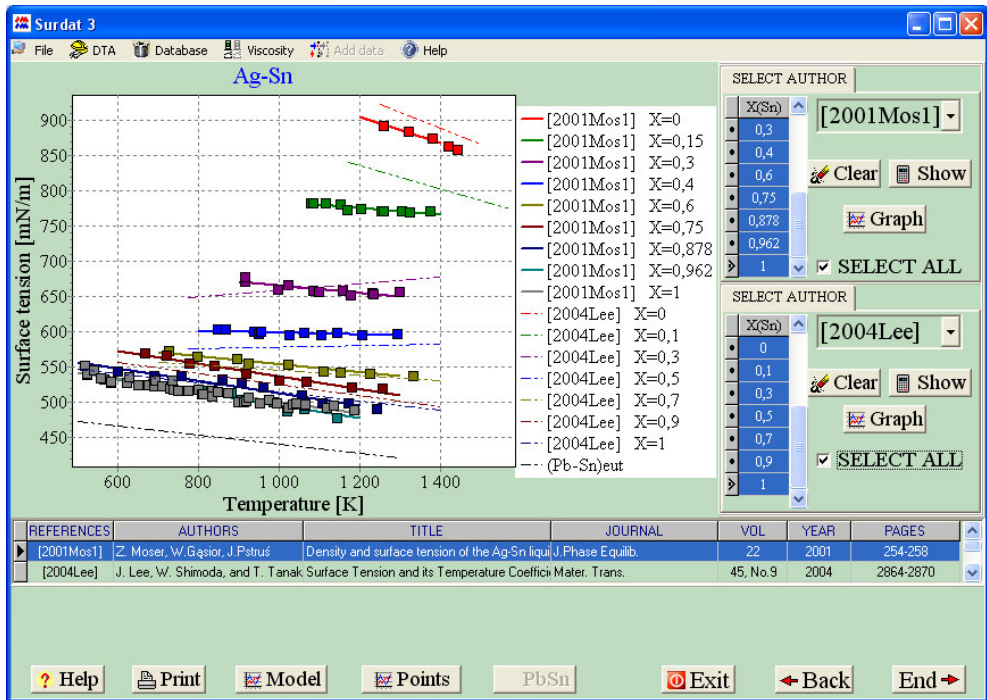


Fig. 6.46. Comparison of temperature dependences of surface tension for liquid Ag-Sn alloys by two authors with data for (Sn-Pb)_{eut}

The activation of the „Model” option will make it possible to calculate the temperature dependences from the Butler’s model. Modeling can be performed only for the concentrations available for the given authors. By selecting the authors, we can model the surface tension for all the available concentrations („SELECT ALL”) or only for the selected ones. Next, by activating the „Model” option, we can view the temperature dependences calculated from the Butler’s equations, and the „Points” button will provide the option to compare them with the experimental data for all the concentrations (Fig. 6.48) or for the selected ones (Fig. 6.49).

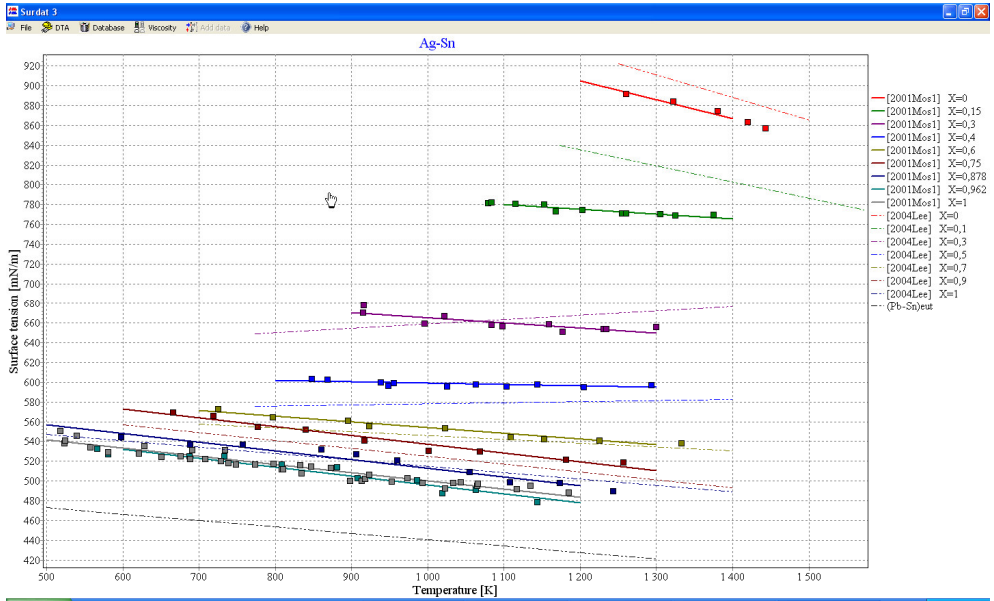


Fig. 6.47. Comparison of temperature dependences of surface tension for liquid Ag-Sn alloys by two authors with those for $(\text{Sn-Pb})_{\text{eut}}$ – zoom in



Fig. 6.48. Temperature dependences of surface tensions for liquid Ag-Sn alloy calculated from Butler's model, compared with experimental data

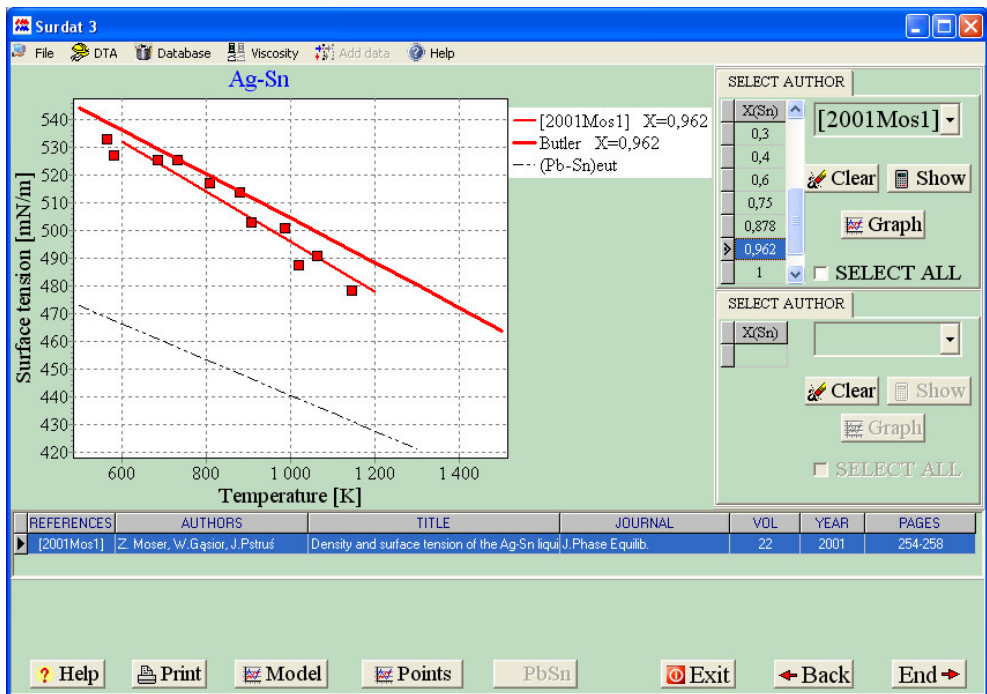


Fig. 6.49. Temperature dependence of surface tension for a selected alloy from Ag-Sn system calculated from Butler's model, compared with experimental data and with (Pb-Sn)_{eut} (dotted line)

Next to surface tension and density, SURDAT 3 provides the possibility to determine and view the dependences of solutions' molar volume in the function of concentration by way of selecting the property (Fig. 6.6) as well as the options of „Molar volume” and „Isotherms”. SURDAT 3 allows for the calculation and graphical presentation of maximum four isotherms simultaneously (Fig. 6.50).

The presentation of viscosity begins in the property selection window („Select properties”-„Viscosity”, Fig. 6.6). The SURDAT 3 database allows for both a presentation of the measured viscosity and that calculated from the relations (models) proposed by various authors.

The visualization of viscosity can be performed by the display of the following:

- a) The parameters **A** and **E** of the viscosity equations $\eta = e^{\frac{E}{RT}}$ describing the temperature dependence of viscosity for different concentrations ($\mathbf{X}_{(Sn)}$) (Fig. 6.51),
where: **R** – universal gas constant,
T – temperature,
- b) The experimental isotherms determined at any temperature (Fig. 6.52),
- c) The presentation of the temperature dependences of viscosity (experimental points) by the selected author (Fig. 6.53),
- d) The viscosity isotherms for binary systems calculated from different models (Fig. 6.54).

The modes of displaying the viscosity equations and their graphic presentation are the same as in the case of density and surface tension.

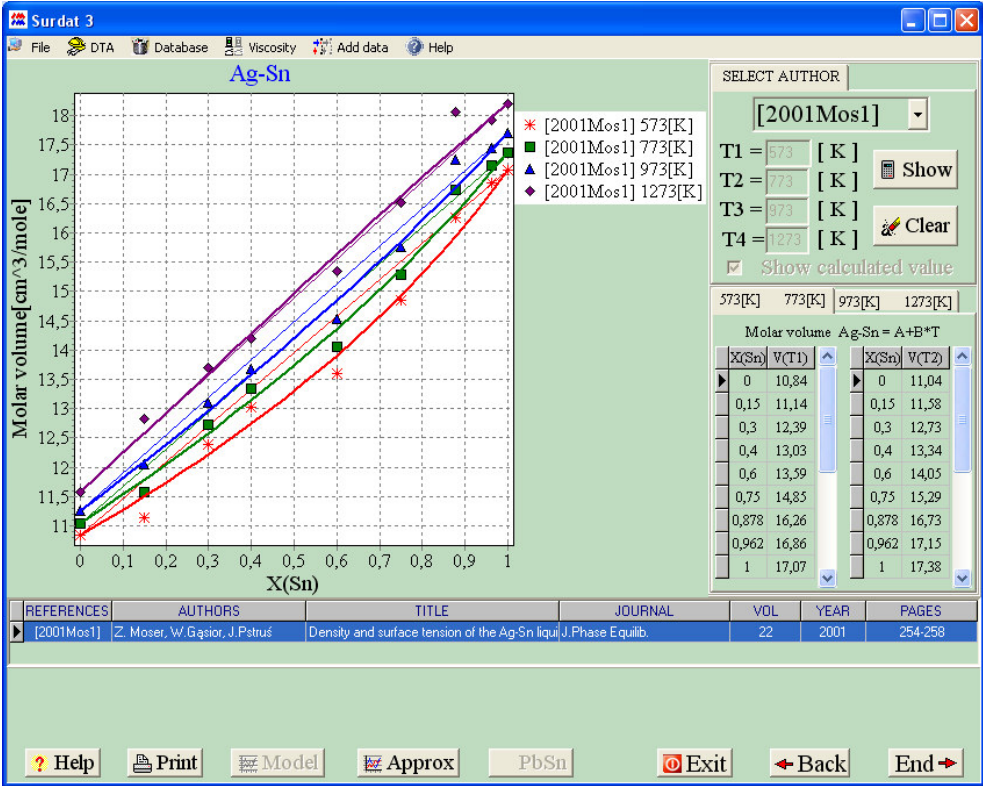


Fig. 6.50. Isotherms of molar volume of liquid Sn-Ag alloys calculated for four temperatures (523 K, 773 K, 973 K, 1273 K), compared with experimental data

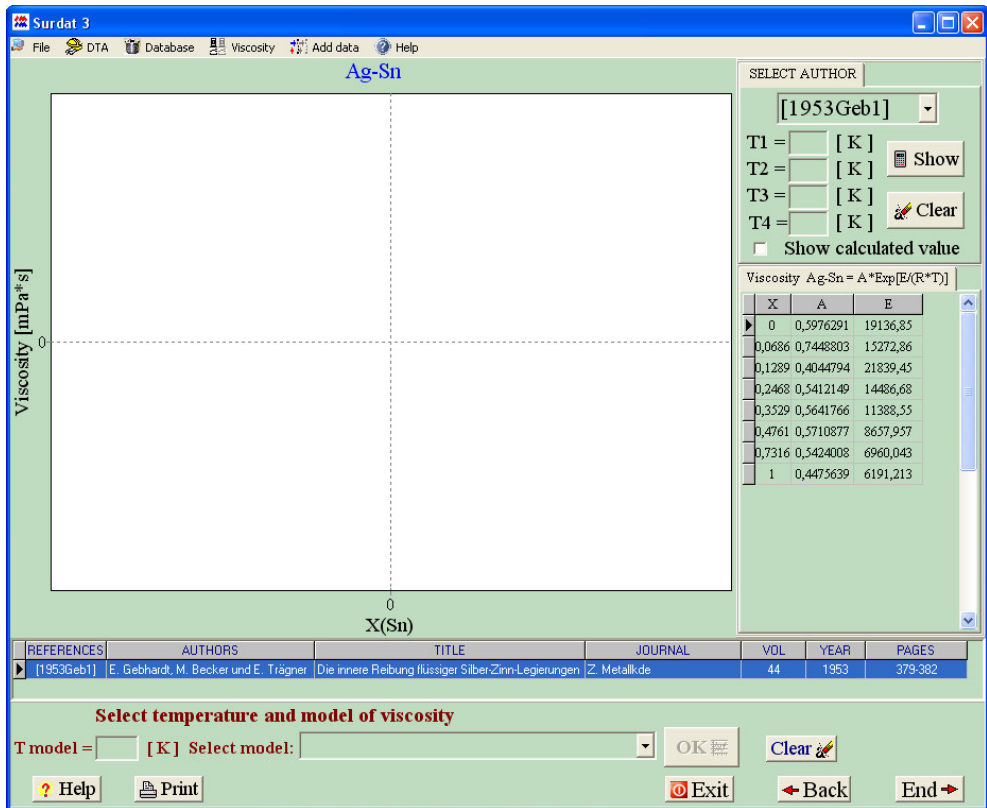


Fig. 6.51. Temperature dependences of viscosity of liquid Ag-Sn alloys elaborated by the author of [1953Geb1]

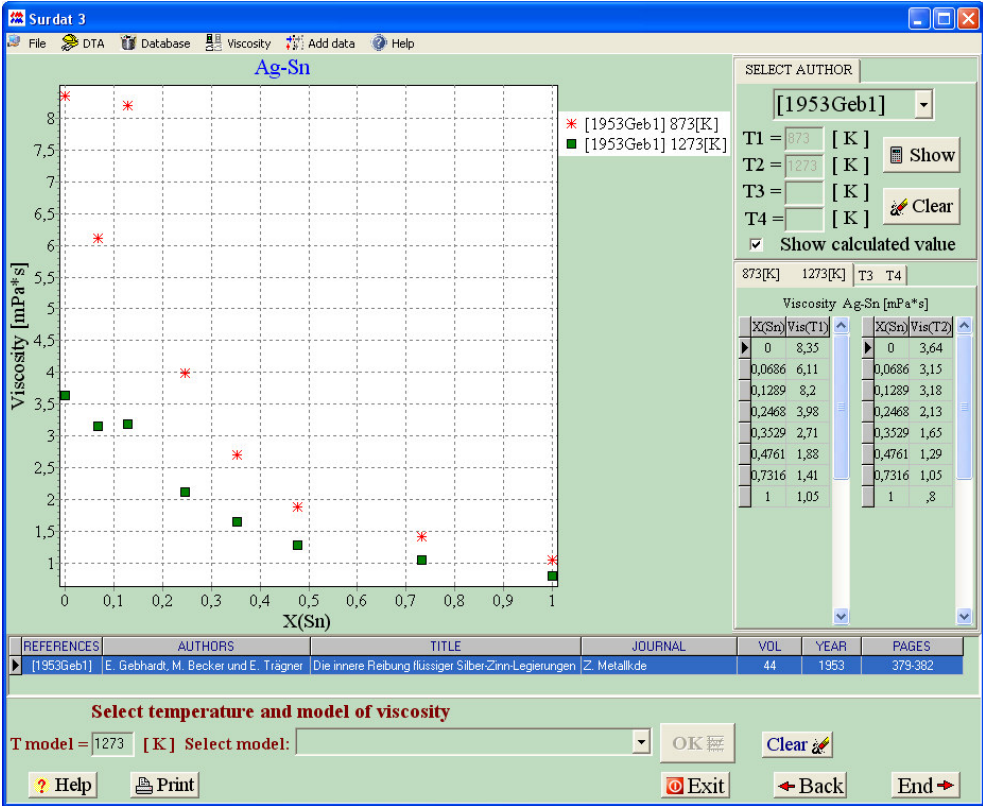


Fig. 6.52. Isotherms of viscosity of liquid Ag-Sn alloys calculated for two temperatures (experimental points)

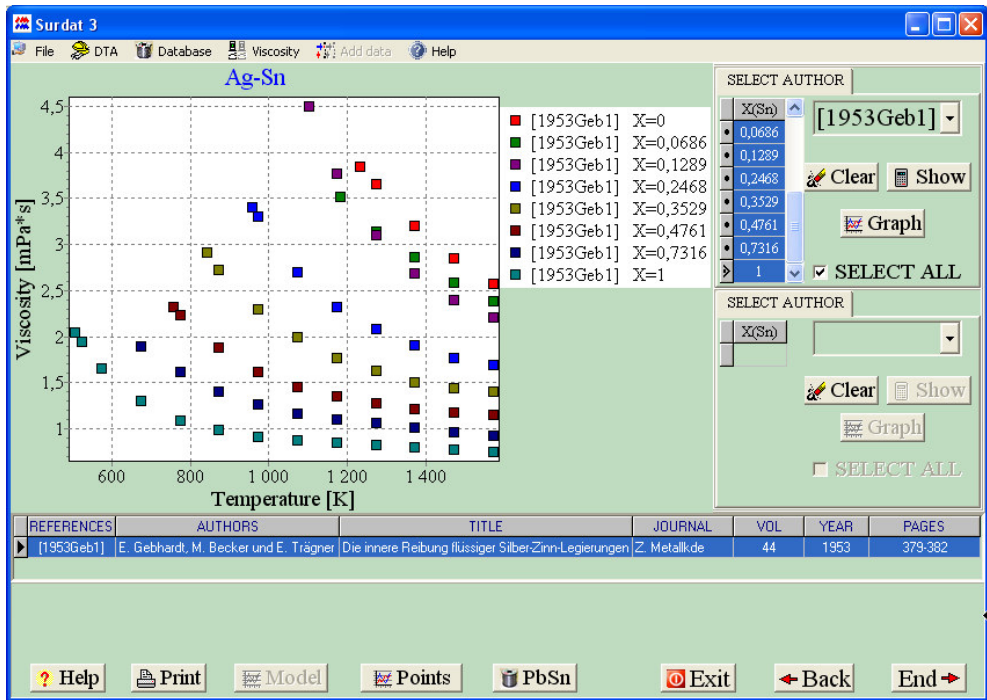


Fig. 6.53. Temperature dependences of viscosity (experimental points) by the author of [1953Geb1]

To model viscosity, we use the bottom part of the window shown in Fig. 6.51. The following viscosity models are available:

1. Gaşior,
2. Gaşior-Moser,
3. Iida-Ueda-Morita_G^{ex},
4. Iida-Ueda-Morita_H_m,
5. Kaptay,
6. Kozlov-Romanov-Petrov,
7. Kucharski,
8. Moelwyn-Hughes,

9. Sato,
10. Schick-Brillo-Egry-Hallstedt,
11. Seetharaman-Sichen,
12. Sichen-Bygden-Seetharaman.

After specifying the temperature and selecting the viscosity model, we should press „OK”. For each system, the program provides temperature ranges for which the viscosity modeling option is available. Introducing a temperature from outside the range will make the program display the window in Fig. 6.54 with the information on the temperature range for the given system and the person to contact in order to calculate the viscosity isotherms at the temperature of interest.

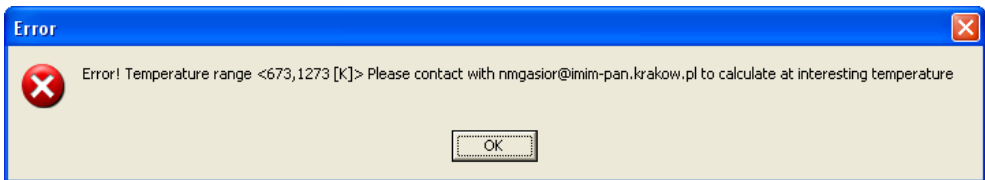


Fig. 6.54. Temperature range for Ag-Sn modeling

For example, by introducing the temperature of 1273 K and selecting the viscosity models confirmed by „OK”, we will see the window presented in Fig.6.55.

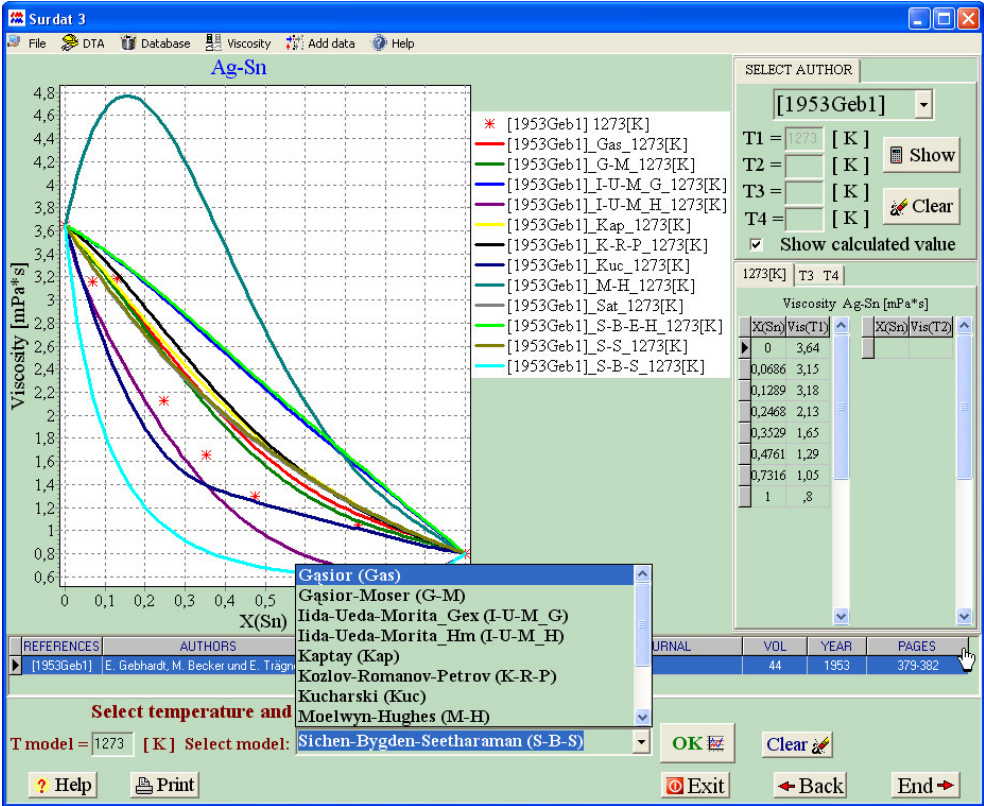


Fig. 6.55. Viscosity isotherms calculated from different models compared with literature data of [1953Geb1] at 1273 K

SURDAT 3 makes it possible to compare the own data with those provided by the base. This option is available only after the selection of isotherms as the mode of presentation. On the example of the Ag-Sn system, we will see the method of introducing the own data, for comparison's sake. The „Add data” menu (Fig. 6.56) initializes the introduction of the own data. We can enter them manually or from a text file by pressing the „Load” button (Fig. 6.57).

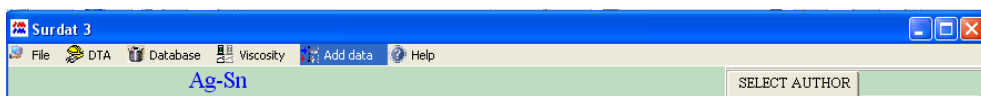


Fig. 6.56. „Add data” menu in SURDAT 3

We should remember that the format of the introduced data should be compatible with that required by SURDAT 3. By specifying the temperature and entering the reference to the own publication in the „AUTHOR” field, confirmed by „OK”, we will be able to compare the entered data with the viscosity ones calculated from various models, as well as on the background of other experimental data (Fig.6.58).

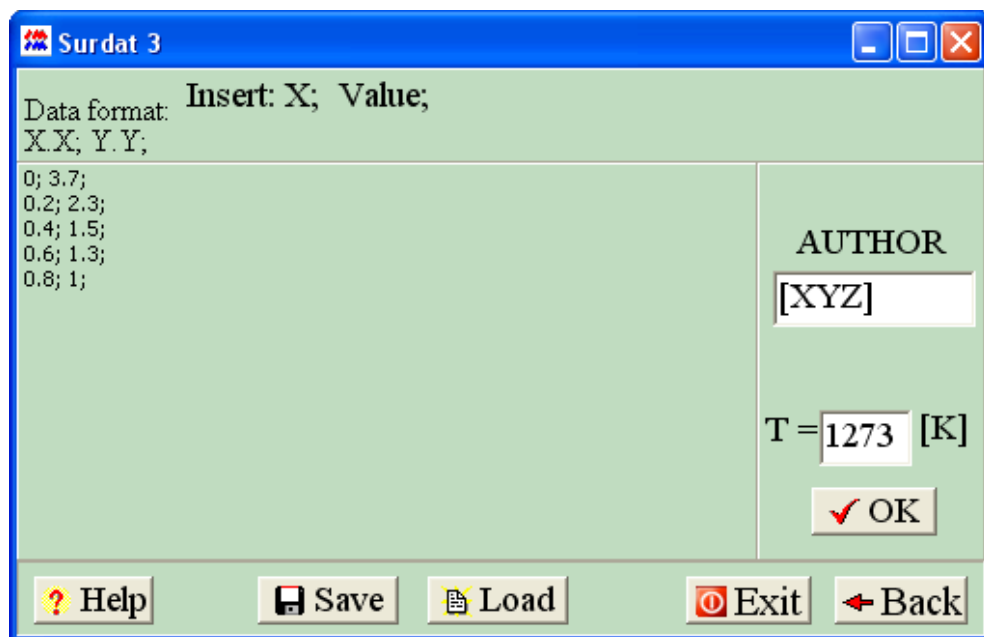


Fig. 6.57. Window for own data introduction (isotherms)

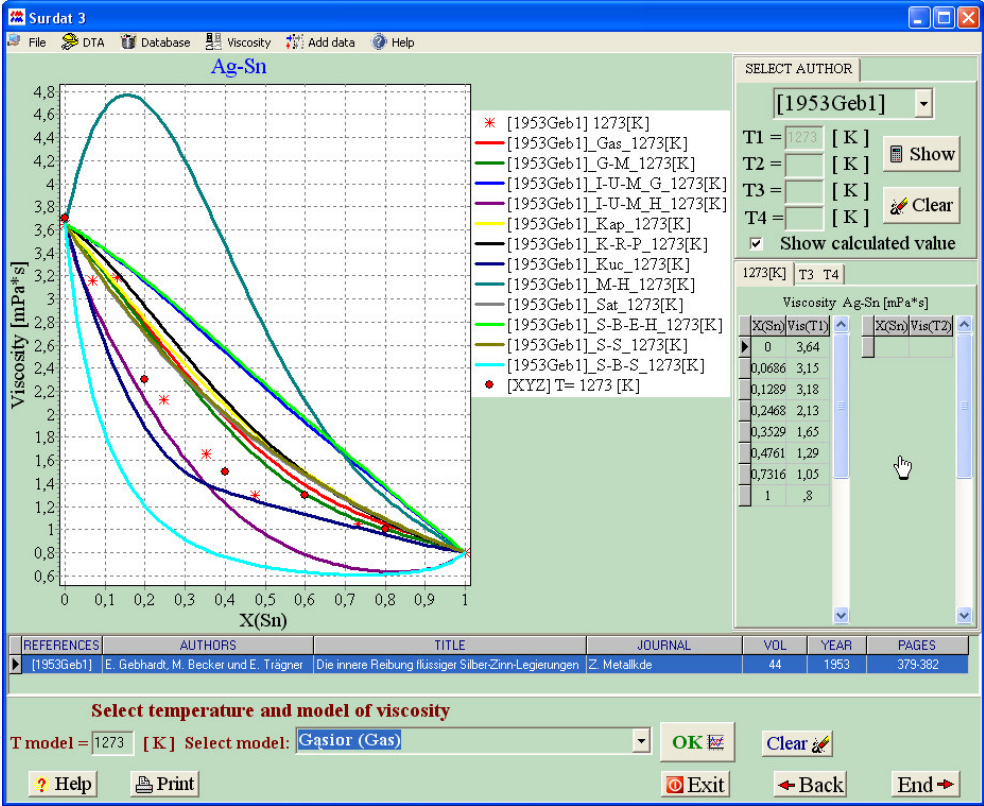


Fig. 6.58. Viscosity isotherms calculated from different models, compared with selected literature data [1953Geb1] and with the introduced own data [XYZ] at 1273 K

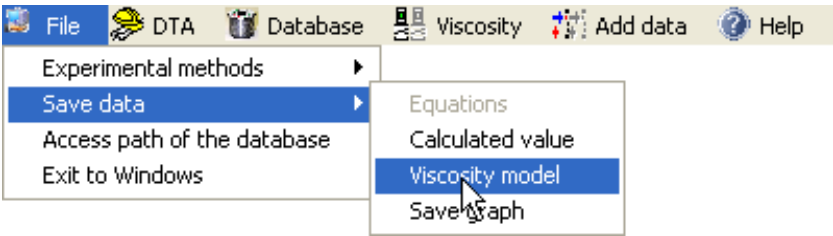
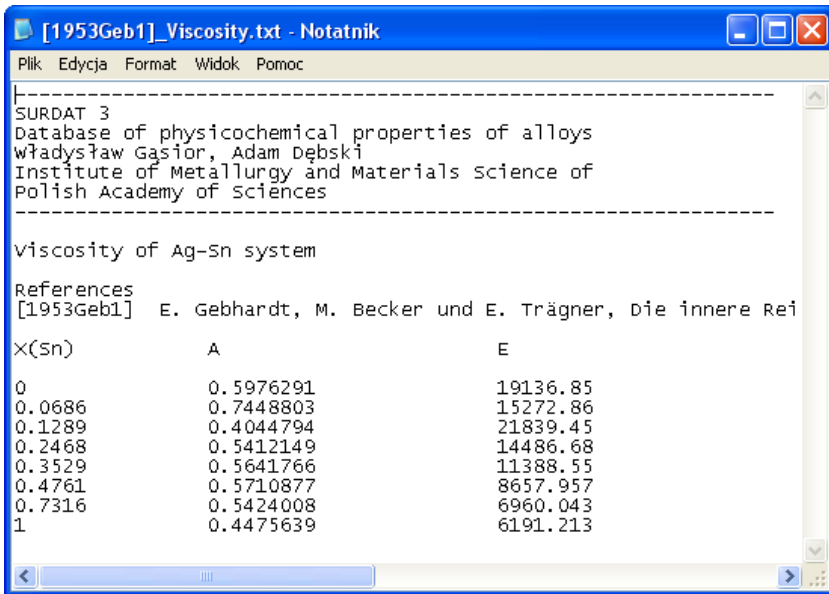


Fig. 6.59. „File” menu, „Save data” option, SURDAT 3

The program makes it possible to save the data (Fig. 6.59) in the database folder. We can save the following:

- The equation parameters by the given author (Fig.6.60),
- The values calculated for the given temperature (Fig.6.61),
- The values calculated from viscosity modeling (Fig. 6.62),
- The diagram (Fig.6.63).



```
[1953Geb1]_Viscosity.txt - Notatnik
Plik Edycja Format Widok Pomoc
-----
SURDAT 3
Database of physicochemical properties of alloys
Władysław Gasiór, Adam Dębski
Institute of Metallurgy and Materials science of
Polish Academy of sciences
-----

Viscosity of Ag-Sn system

References
[1953Geb1] E. Gebhardt, M. Becker und E. Trägner, Die innere Rei

X(Sn)          A              E
0              0.5976291      19136.85
0.0686        0.7448803      15272.86
0.1289        0.4044794      21839.45
0.2468        0.5412149      14486.68
0.3529        0.5641766      11388.55
0.4761        0.5710877      8657.957
0.7316        0.5424008      6960.043
1             0.4475639      6191.213
```

Fig. 6.60. Saved equations by the given author [1953Geb1]

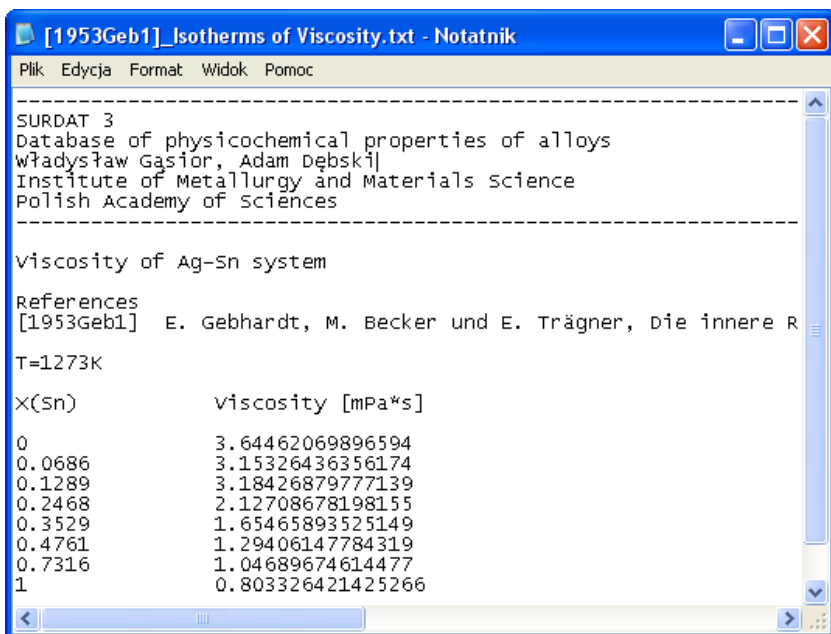


Fig. 6.61. Saved isotherms calculated from the selected author [1953Geb1]

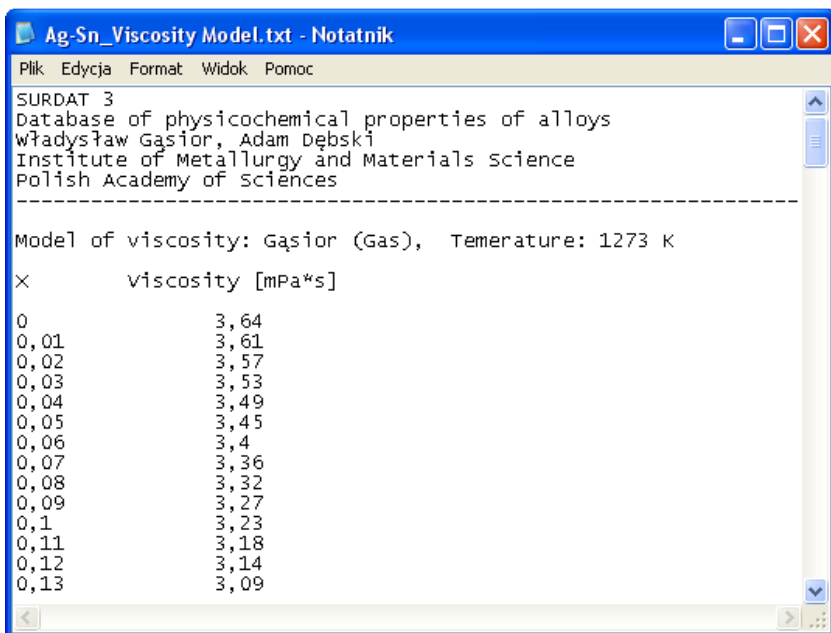


Fig. 6.62. Saved model viscosity values

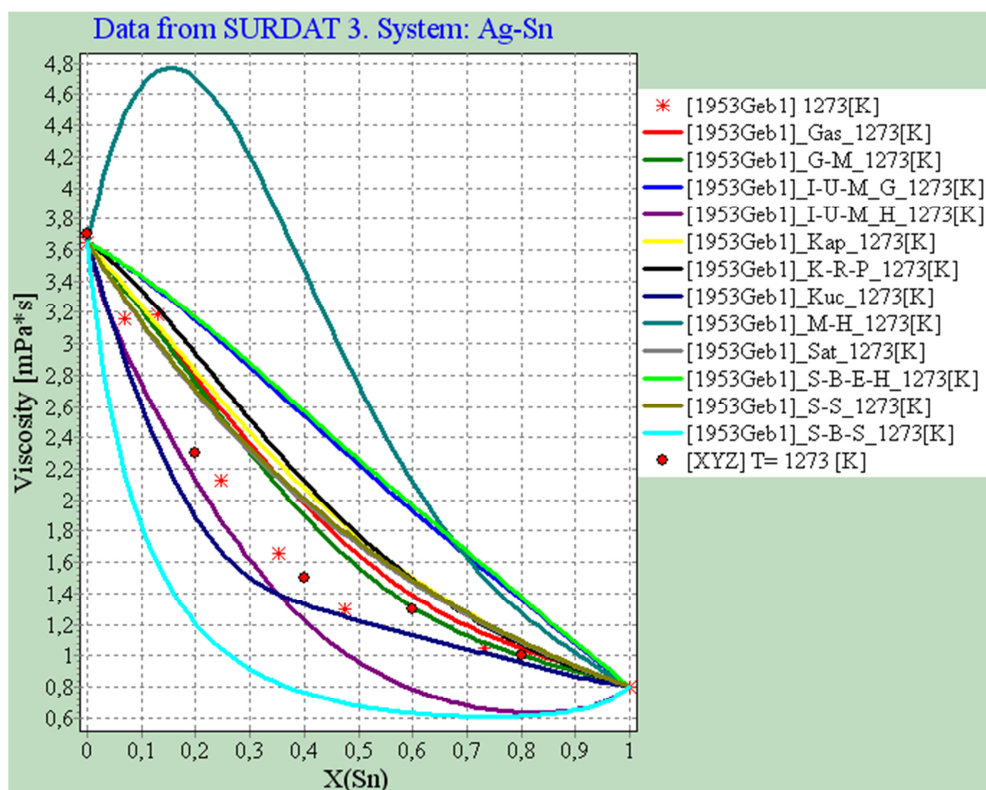


Fig. 6.63. Saved diagram

In the case of multicomponent systems, the display of the properties runs analogically to that for the binary systems. The only difference is the necessity to select the initial alloy for which we want to view the data (Fig.6.64). The data display for the multicomponent systems will be presented on the example of the Ag-Cu-Sn system. We add copper to the initial $(\text{Sn-Ag})_{\text{eut}}$ alloy. For such ternary system, Ag-Cu-Sn, we present the surface tension calculated from the Butler's model, in the function of concentration, for two random temperatures, compared with the data calculated from the linear equations by the given author (Fig. 6.65).

Figure 6.66 shows the temperature dependences of the surface tension for two selected concentrations of Cu, calculated from the Butler's relation, compared with the experimental points obtained by the given author.

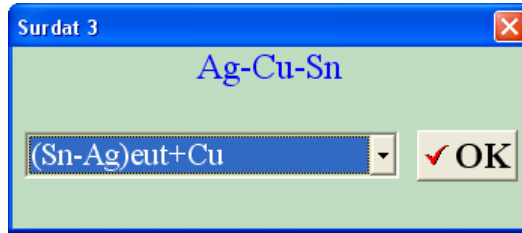


Fig. 6.64. Initial alloy selection window

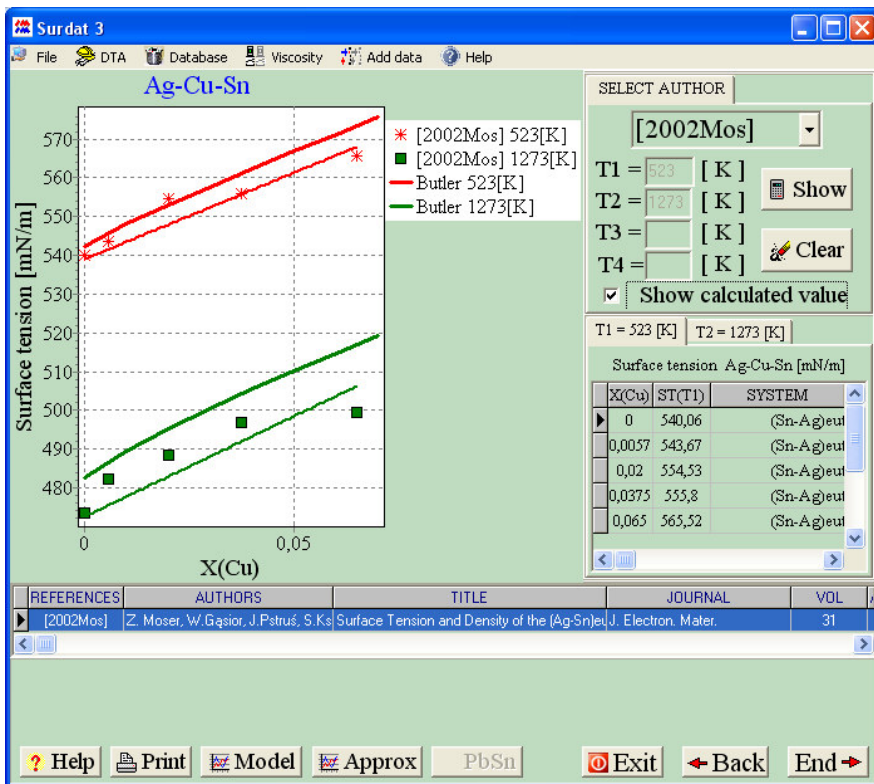


Fig. 6.65. Comparison of surface tension isotherms for liquid Ag-Cu-Sn alloys calculated from Butler's relation (bold lines) and from relations developed by authors (thin lines) with experimental data (symbols) for 523 K and 1273 K

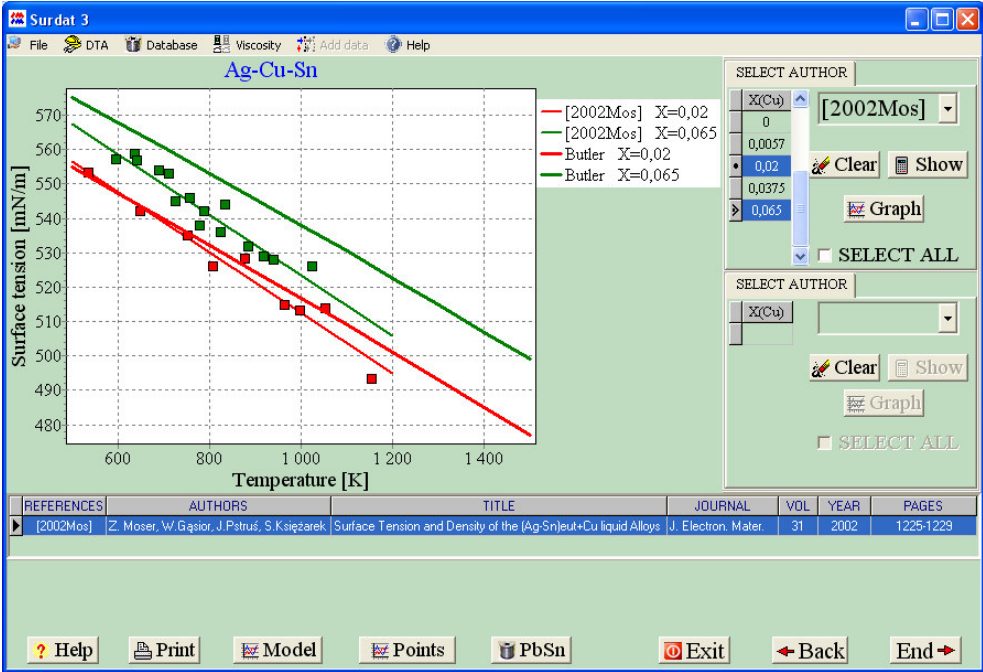


Fig. 6.66. Temperature dependences of surface tension in Ag-Cu-Sn calculated from Butler's model on the background of experimental data (symbols)

7. References

Note: The data from the reference entries marked with * have been used in the SURDAT 3 database.

- [2014Gas1] Gašior W., *Viscosity modeling of binary alloys: Comparative studies*, Calphad, 44, (2014), 119-128.
- [2012Gas1] Gašior W., *Discussion Meeting on Thermodynamic of Alloys*, September 23-28, 2012, Pula, Croatia, Book of Abstracts & Programme, p. 86.
- [2012Sic] Schick, M. Brillo, J. Egry, I. and Hallstedt, B. *Viscosity of Al-Cu liquid alloys - Measurement and thermodynamic description*. Journal of Materials Science, 47, (2012), 8145-8152.
- [2011Gas1]: Gašior W., Fima P., Moser Z., *Modeling of the thermodynamic properties of liquid Fe-Ni and Fe-Co alloys from the surface tension data*, Archs Metall. Mater. 56 (1), (2011), 13 – 23.
- *[2011Mos1] Moser Z., Fima P., Bukat K., Sitek J., Pstruś J., Gašior W., Kościelski M., Gancarz T., *Investigation of the effect of indium addition on wettability of Sn-Ag-Cu solders*, Soldering @Surface Mount Technology, 22(4), (2011), 13 – 19.
- [2011Sat] Sato Y., Japanese Journal of Applied Physics, 50 (2011) 11RD01-7.
- *[2010Buk1] Bukat K., Moser Z., Sitek J., Gasior W., Kościelski M., Pstruś J., *Investigations of Sn-Zn-Bi solders. Part I. Surface tension, interfacial tension and density measurements of the Sn-Zn-7Bi solders*, Soldering @ Surface Mount Technology, **22 No.3**, (2010), 10 – 16.

- *[2010Buk2] Bukat K., Sitek J., Kościelski M., Moser Z., Gąsior W., Pstruś J., Investigations of Sn-Zn-Bi solders. Part II. Wetting measurements of the Sn-Zn-Bi solders on copper and on PCB with lead-free finishes by using the wetting balance method, *Soldering @Surface Mount Technology*, **22 No.4**, (2010), 13 – 19.
- [2010Buk3] Bukat K., Sitek J., Moser Z., Gąsior W., Kościelski M., Pstruś J., *Influence of indium additives to SnZnBi alloys on wetting properties of different substrates used in electronic*, *Przegląd Spawalnictwa* 9/2010, 36–40.
- [2010Deb1] Dębski A., Moser Z., Gąsior W., SURDAT 3 – database of physicochemical properties of selected solders, 3 Międzynarodowa Konferencja Naukowo – Techniczna, Postęp w Technologiach Lutowania, Wrocław 20 – 22 września 2010.
- [2010Deb2] Dębski A., Moser Z., Gąsior W., *SURDAT 3 – database of physicochemical properties of selected solders*, *Przegląd Spawalnictwa* 9/2010, 63–66.
- *[2010Fim1] Fima P., Nowak R., Sobczak N., *Effect of metal purity and testing procedure on surface tension measurements of liquid tin*, *J. Mater. Sci.*, **45**, (2010), 2009 – 2014.
- [2010Fim2] Fima P., Gąsior W., Sypień A., Moser Z., *Wetting of Cu by Bi–Ag based alloys with Sn and Zn additions*, *J. Mater. Sci.*, **45** (2010) 4339–4344.
- [2010Gas1] Gąsior W., Moser Z., Dębski A., and Siewert T., *Integration of the NIST and SURDAT Databases on Physical Properties of Lead-Free Solder Alloys*, *Int. J. Thermophysics*, **31**, (2010), 502–512.
- [2010Gas2] Gąsior W., Moser Z., *Modelowanie lepkości stopów metali analiza porównawcza*, Konferencja sprawozdawcza Komitetu

- Metalurgii PAN Metalurgia 2010, Krynica-Zdrój 20-23 października 2010.
- [2010Mos1] Moser Z., Gašior W., Dębski A., *Modyfikacja bazy SURDAT*, Konferencja sprawozdawcza Komitetu Metalurgii PAN Metalurgia 2010, Krynica-Zdrój 20-23 października 2010.
- [2010Mos2] Moser Z., Gašior W., Bukat K., Fima P., Sitek J., Pstruś J., *Wetting properties of In-Sn, Sn-Ag-In and Sn-Ag-Cu-In alloys*, Przegląd Spawalnictwa 9/2010, 29-35.
- *[2009Gan1] Gancarz T., Moser Z., Gašior W., Pstruś J. Henein H., *A comparison of surface tension, viscosity and density of Sn and Sn-Ag alloys using two measurement techniques*, 17 Symposium on Thermophysical Properties, Boulder, CO, USA June 21 - 26, 2009, 59.
- [2009Gas1] Gašior W., Moser Z., Dębski A., *New data to the SURDAT-database of modelled and experimental physical properties of lead-free solder alloys*, Abstracts 17 Symposium on Thermophysical Properties, Boulder, CO, USA June 21 - 26, 2009, 59.
- [2009Gas2] Gašior W., Moser Z., Dębski A., *SURDAT- Database of the physical properties of lead-free solder alloys. New data and new experimental and modeled properties*, Book of Abstracts XI Workshop of APDTC Ljubljana, Slovenia 18 -20 September 2009.
- [2009Gas3] Gašior W., Moser Z., Dębski A., *Arch. of Metall. and Mater.*, **54**, 4/2009, 1253.
- *[2009Mos1] Moser Z., Sebo P., Gašior W., Svec P. and Pstruś J. *Effect of indium on wettability in studies of Sn-Ag-Cu solders, Experiment vs. modeling. Part I*, Calphad, **33**, (2009), 63-68.

- *[2009Mos2] Moser Z., Gaşior W., Pstruś J., Kaban I., Hoyer W., *Thermophysical Properties of Liquid In–Sn Alloys*, Int. J. Thermophys., **30**, (2009), 1811-1822.
- [2009Seb1] Sebo P., Moser Z., Svec P., Janickovic D., Dobrocka E., Gaşior W., Pstruś J., *Effect of indium on the microstructure of the interface between Sn_{3.13}Ag_{0.74}CuIn solder and Cu substrate*, J. Alloys Compd., **480**, (2009), 409-415.
- *[2009Nov1] Novakovic R., Ricci E., Giuranno D., Lanata T., Amore S., *Thermodynamics and surface properties of liquid Bi-In alloys*, Trans. JIM., **33**, (2009), 69-75.
- *[2008Amo1] Amorea S., Ricci E., Lanata T., Novakovic R., *Surface tension and wetting behaviour of molten Cu–Sn alloys*, J. Alloys Compd, **452**, (2008), 161–166.
- [2008Buk1] Bukat K., J. Sitek, R. Kisiel, Z. Moser, W. Gaşior, Kościelski M., Pstruś J., *Evaluation of the influence of Bi and Sb additions to Sn–Ag–Cu and Sn–Zn alloys on their surface tension and wetting properties using analysis of variance – ANOVA*, Soldering @ Surface Mount Technology, **20**, (2008), 9-19.
- [2008Buk2] Bukat K., Moser Z., Gaşior W., Sitek J., Kościelski M., Pstruś J., *Trends in wettability studies, of Pb-free solders. Basic and application. Part II. Relation between surface tension, interfacial tension and wettability of lead-free of Sn–Zn*, Archs. Metall. and Mater., **53**, (2008), 1065-1074.
- *[2008Din1] Dinsdale A., Watson A., Kroupa A., Vrestal J., Zemanova A., Vizdal J., COST Action 531 - Atlas of Phase Diagrams for Lead-Free Soldering, ISBN 978-80-86292-28-1.

- *[2008Fim1] Fima P., Kucharski M., *The surface tension and density of Ag-Bi-Sn alloys*, Int. J. Mat. Res. (formerly Z. Metallkd.), **99 No.2**, (2008), 159-161.
- [2008Gas1] Gąsior W., Moser Z., Dębski A., Pstruś J., SURDAT – baza eksperymentalnych i modelowych właściwości fizycznych stopów metali, potencjalnych zamienników lutów bezołowiowych, Infobazy 2008 Systemy, Aplikacje, Usługi Materiały V Krajowej Konferencji Naukowej (2008), 95-100.
- *[2008Guo1] Guo Z., Saunders N., Miodownik P., and Schillé J.P., *Modeling Material Properties of Lead-Free Solder Alloys*, J. Electron. Mater., **37 No1**, (2008), 23-31.
- *[2008Kam1] Kamal M., El Said Gouda, *Effect of zinc additions on structure and properties of Sn–Ag eutectic lead-free solder alloy*, J. Mater. Sci: Mater. Electron., **19**, (2008), 81-84.
- [2008Mos1] Moser Z., Gąsior W., Pstruś J., Dębski A., *Wettability Studies of Pb-Free Soldering Materials*, Int. J. Thermophys., **29**, (2008), 1974-1986.
- [2008Mos2] Moser Z., Gąsior W., Bukat K., Pstruś J., Sitek J., *Trends in wettability studies of Pb-free solders. Basic and application. Part I. Surface tension and density measurements of Sn-Zn and Sn-Zn-Bi-Sb alloys. Experiment vs. modeling*, Archs. Metall. and Mater., **53**, (2008), 1055-1063.
- [2008Mos3] Moser Z., Gąsior W., Pstruś J., Kaban I., Hoyer W., Novakovic R., Ricci E., Giurano D., Lanata T., *Thermophysical properties of liquid In–Sn alloys*, in Proceedings of TOFA 2008, Discussion Meeting on Thermodynamics of Alloys, Kraków 2008, Abstracts and Programs p. 30.

- *[2008Nov1] Novakovic R., Giuranno D., Ricci E., Lanata T., *Surface and transport properties of In–Sn liquid alloys*, Surf. Sci., **602**, (2008), 1957–1963.
- [2008Seb1] Šebo P., Švec P., Janičkovič D., Moser Z., *Identification of phases in Sn-Ag-Cu-In solder on Cu substrate interface*, Kovove Mater. **46**, (2008), 235–238.
- *[2008Xu1] Xu D.-X., Lei Y.-P., Xia Z.-D., Guo F., and Shi Y.-W., *Experimental Wettability Study of Lead-Free Solder on Cu Substrates Using Varying Flux and Temperature*, J. Electron. Mater., **37 No.1**, (2008), 125-133.
- [2007Bud] Budai I., Benko M. Z., Kaptay G., Materials Science Forum, 537-538 (2007) 489.
- [2007Deb1] Dębski A., Moser Z., Gąsior W., Pstruś J., Baza danych właściwości fizycznych lutowi bezołowiowy, 2 Międzynarodowa Konferencja Naukowo – Techniczna, Postęp w Technologiach Lutowania, Wrocław 24 – 26 września 2007.
- [2007Deb2] Dębski A., Moser Z., Gąsior W., Pstruś J., SURDAT - baza danych właściwości fizycznych lutowi bezołowiowych, Przegląd Spawalnictwa 9/2007, 41-44.
- *[2007Fim1] Fima P., Wiater K., Kucharski M., *The surface tension and density of the Cu–Ag–In alloys*, Surf. Sci., **601**, (2007), 3481–3487.
- [2007Gas1] Gąsior W., Moser Z., Dębski A., Pstruś J., SURDAT – A Database of Lead-Free Solder Materials, Polska Akademia Nauk, Annual Report 2007 2007, 65-66.
- *[2007Gne1] Gnecco F., Ricci E., Amore S., Giuranno D., Borzone G., Zanicchi G., Novakovic R., *Wetting behaviour and reactivity of lead*

- free Au-In-Sn and Bi-In-Sn alloys on copper substrates*, J. Adches. Adches, **27**, (2007), 409-416.
- *[2007Hou1] Hou J.X., Sun J.J., Zhan C.W., Tian X.L., and Chen X.C., *The structural change of Cu-Sn melt*, Sci China Ser G-Phys Mech. Astron., **50 No.4**, (2007), 414-420.
- *[2007Kab1] Kaban I., Gruner S., Hoyer W., *Surface tension and density in liquid Ag-Cu-Sn alloys*, J.N. Crystalline Sol., **353**, (2007), 3717–3721.
- [2007Kap1] Kaptay G., *Comparison of different theoretical models to Experimental Data*, Mater. Sci. Forum, **537-538**, (2007), 489-496. <http://www.scientific.net>.
- *[2007Lan1] Landolt-Börnstein, New Series IV, **19B**, (2007), 1-4.
- *[2007Mos1] Moser Z., Gaşior W., Bukat K., Pstruś J., Kisiel R., Sitek J., Ishida K. and Ohnuma I., *Pb-Free Solders: Part III. Wettability Testing of Sn-Ag-Cu-Bi Alloys with Sb Additions*, J. Phase Equilib. Diffus., **28/5**, (2007), 433-438.
- *[2007Mos2] Sieć Moser et all *Zaawansowane materiały lutownicze*, 2007.
- *[2007Mos3] Moser Z., Gaşior W., Dębski A., and Pstruś J., *Database of lead – free soldering materials*, Kraków 2007, ISBN 83-60768-01-3.
- [2007Mos4] Moser Z., Gaşior W., Dębski A., Pstruś J., *SURDAT – database of physical properties of lead free solders*, Journal of Mining and Metallurgy. 2007, 43 B (2), 125 – 130.
- *[2007Pst2] Pstruś J., *Influence of Indium Additions on Wettability of Sn-Zn Alloys* (Doctor Thesis, Institute of Metallurgy and Materials Science, Polish Academy of Sciences, Kraków, 2007).

- [2007Sob1] N. Sobczak, A. Kudyba, R. Nowak, W. Radziwiłł, K. Pietrzak: *Factors affecting wettability and bond strength of solder joint couples*, Pure Appl. Chem., **79** (10), (2007), 1755 – 1769.
- *[2007Tan1] Tan M., Xiufang B., Xianying X., Yanning Z., Jing G., Baoan S., *Correlation between viscosity of molten Cu–Sn alloys and phase diagram*, Physica B, **387**, (2007), 1–5.
- *[2007Ter1] Terzieff P., Li Z., Knott S., Mikula A., *Physicochemical properties of liquid Ag–Bi–Sn*, Physica B, **388**, (2007), 312–317.
- *[2007Wan1] Wang H., Wang F., Gaob F., Mac X., Qian Y., *Reactive wetting of Sn_{0.7}Cu–xZn lead-free solders on Cu substrate*, Alloys Compd., **433**, (2007), 302–305.
- *[2007Wei1] Wei X., Huang H., Zhou L., Zhang M., Liu X., *On the advantages of using a hypoeutectic Sn–Zn as lead-free solder material*, Mater., Letters, **61**, (2007), 655–658.
- *[2007Wu1] Wu C.M.L., Wong Y.W., *Rare-earth additions to lead-free electronic solders*, J. Mater. Sci.: Mater. Electron., **18**, (2007), 77–91.
- *[2007Wu2] Wu A.Q., Guo L.J., Liu C.S., Jia E.G., Zhu Z.G., *The experimental viscosity and calculated relative viscosity of liquid In–Sn alloys*, Physica B, **392**, (2007), 323–326.
- *[2007Yan1] Yan, L., Zheng S., Ding G., Xu G., Qiao Z., *Surface tension calculation of the Sn–Ga–In ternary alloy*, Computer Coup. Phase Diagrams Thermo., **31**, (2007), 112–119.
- [2006Gas1] Gąsior W., *Modeling of the Thermodynamic Properties from the Surface Tension Measurements* (in Polish), Institute of Metallurgy and Materials Science, Polish Academy of Sciences, Kraków 2006.
- [2006Gas2] Gąsior W. *Modeling of the Thermodynamic Properties from the Surface Tension. Part 1. Polarized Atoms Model of the Mono-*

- atomic Surface Layer for Modeling of the Surface Tension*, Arch. Metall. Mater., **51**, (2006), 317-326.
- [2006Gas3] Gasior W. *Modeling of the Thermodynamic Properties from the Surface Tension. Part 2. Calculations and the Comparative Studies*, Arch. Metall. Mater., **51**, (2006), 327-334.
- *[2006Kuc1] Kucharski M., Fima P., Skrzyniarz P., Przebinda-Stefanowa W., *Surface Tension and Density of Cu-Ag, Cu-In and Ag-In Alloys*, Archs. Metall. and Mater., **51**, (2006), 389-397.
- *[2006Li1] Li J., Yuan Z., Qiao Z., Fan J., Xu Y, Ke J., *Measurement and calculation of surface tension of molten Sn-Bi alloy*, J. Colloid and Interface Sci., **297**, (2006), 261–265.
- *[2006Liu1] Liu Y.H., *Density and Viscosity of Molten Zn-Al Alloys*, Metall. Mater. Trans. A, **37A**, (2006), 2767-2771.
- [2006Liu2] Liu N.-S., Lin K.-L. *The effect of Ga content on the wetting reaction and interfacial morphology formed between Sn-8.55Zn-0.5Ag-0.1Al-xGa solders and Cu*, Scr. Mater. **54** (2006), 219 – 224.
- *[2006May1] Mayappan R., Ismail A. B., Ahmad Z.A., Ariga T., Hussain L.B., *Effect of sample perimeter and temperature on Sn-Zn based lead-free solders*, Mater. Letters, **60**, (2006), 2383–2389.
- [2006Mos1] Moser Z., Gasior W., Bukat K., Pstruś J., Kisiel R., Ohnuma I., Ishida K., *Pb – free Solders: Part I. Wettability Testing of Sn-Ag-Cu Alloys with Bi Additions*, J. Phase Equilib. Diffus., **27 No 2**, (2006), 133-139.
- *[2006Mos2] Moser Z., Gasior W., Pstruś J., Ohnuma I., Ishida K., *Influence of Sb additions on surface tension and density of Sn-Sb, Sn-Ag-Sb and Sn-Ag-Cu-Sb alloys: Experiment vs. Modeling*, Z. Metallkd., **97**, (2006), 365-370.

- [2006Mos3] Moser Z., Gasior W., Pstruś J., *Influence of In additions on surface tension and density of In-Sn, Sn-Ag-In and Sn-Ag-Cu-In liquid solders. Experiment vs. modeling*, COST Action 531, Lead – free Solder Materials, Mid-Term Meeting, February 23 & 24, 2006, 29.
- [2006Mos4] Moser Z., Gasior W., Pstruś J., Dębski A., Application of thermodynamics in Pb-free soldering materials, Abstracts 16 Symposium on Thermophysical Properties, Boulder, CO, USA, July 30 – August 4, 2006, 205-207.
- *[2006Nov1] Novakovic R., Ricci E., Gnecco F., *Surface and transport properties of Au-In liquid alloys*, Surf. Sci., **600**, (2006), 5051-5061.
- *[2006Nov2] Novakovic R., Ricci E., Amore S., Lanata T., *Surface and transport properties of Cu-Sn-Ti liquid alloys*, Rare Metals **25**, (2006), 457-468.
- [2006Ohn] Ohnuma I., Ishida K., Moser Z., Gasior W., Bukat K., Pstruś J., Kisiel R., Sitek J., *Pb – free solders. Application of ADAMIS data base in modeling of Sn – Ag – Cu alloys with Bi additions. Part II. J. Phase Equilib. Diffus.* **27 No 3**, (2006), 245-254.
- *[2006Pra1] Prasad L.C., Mikula A., *Surface segregation and surface tension in Al-Sn-Zn liquid alloys*, Physica B, **373**, (2006), 142–149.
- *[2006Yin1] Yin L., Murray B.T., Singler T.J., *Dissolutive wetting in the Bi-Sn system*, Acta Mater., **54**, (2006), 3561 – 3574.
- *[2006Ziv1] Živković D., *Estimation of the viscosity for Ag-In and In-Sb liquid alloys using different models*, Z. Metallkde., **97**, (2006), 89-93.
- *[2005Anu1] Anusionwua B.C., Ilo-Okeke E.O., *Temperature effect on demixing and surface properties of Sn-Zn liquid alloys*, J. Alloys Compd., **397**, (2005), 79–84.

- *[2005Fuj1] Fujii H., Matsumoto T., Ueda T., Nogi K., *A new method for simultaneous measurement of surface tension and viscosity*, *J. Mater. Sci.*, **40**, (2005), 2161 – 2166.
- [2005Hen] Henein H., *The Transition from Free Stream Flow to Dripping in Draining Vessels*, *Canadian Metallurgical Quarterly*, **44** (2), (2005), 261-264.
- *[2005Kab1] Kaban I.G., Gruner S., and Hoyer W., *Experimental and Theoretical Study of the Surface Tension in Liquid Ag–Cu–Sn Alloys*, *Mona. Chemie*, **136**, (2005), 1823–1828.
- [2005Kap] Kaptay G., *Z. Metalkde*, 96 (2005) 24.
- [2005Kis] Kisiel R., Gaşior W., Moser Z., Pstruś J., Bukat K., Sitek J., *Electrical and Mechanical Studies of the Sn-Ag-Cu-Bi and Sn-Ag-Cu-Bi-Sb Lead Free Soldering Materials*, *Archs. Metall. and Mater.*, **50**, (2005), 1065-1071.
- *[2005Kuc] Kucharski M. and Fima P., *The Surface Tension and Density of Liquid Ag–Bi, Ag–Sn, and Bi–Sn Alloys*, *Monatshefte fur Chemie.*, **136**, (2005), 1841–1846.
- *[2005Lop1] Lopez E.P., Vianco P.T., and Rejent J.A., *Solderability Testing of Sn-Ag-XCu Pb-Free Solders on Copper and Au-Ni-Plated Kovar Substrates*, *J. Electron. Mater.*, **34 No. 3**, (2005), 299 – 310.
- [2005Mos1] Moser Z., Gaşior W., Ishida K., Ohnuma I., Liu X.J., Bukat K. et al, *Experimental Wettability Studies Combinied With the Related Properties from Data Base for Tin Based Alloys With Silver, Copper, Bismuth and Antimony Additions*. TMS, 134th Annual Meeting & Exhibition, Book of Final Program, San Francisco, USA, February 13 - 17, 2005.

- *[2005Mos2] Moser Z., Gaşior W., Pstruś J., *Influence of Sb additions on surface tension and density of Sn-Sb, Sn-Ag-Sb and Sn-Ag-Cu-Sb alloys. Experiment vs. modeling*, Calphad XXXIV May 22-27, 2005 Maastricht, The Netherlands, Programme and Abstracts, 64.
- *[2005Nov1] Novakovic R., Ricci E., Giuranno D., Passerone A. *Surface and transport properties of Ag-Cu liquid alloys*, , Surf. Sci., **576**, (2005), 175-187.
- *[2005Nov2] Novakovic R., Ricci E., Gnecco F., Giuranno D., Borzone G., *Surface and transport properties of Au-Sn liquid alloys*, Surf. Sci., **599**, (2005), 230-247.
- *[2005Ple1] Plevachuka Y., Sklyarchuka V., Yakymovycha A., Willersb B., Eckertb S., *Electronic properties and viscosity of liquid Pb-Sn alloys*, J. Alloys Compd., **394**, (2005), 63–68.
- *[2005Sun1] Sun C., Geng H., Yang Z., Zhang J., Wang R., *Viscous and structural behaviors of molten In-Sn alloys*, Mater. Character., **55**, (2005), 383–387.
- *[2005Ter1] Terzieff P., *Concentration fluctuations and surface tension in liquid Au-Sn-Zn*, J. Mater. Sci., **40**, (2005), 3759 – 3763.
- *[2005Wan1] Wang L. and AXian.P., *Density Measurement of Sn-40Pb, Sn-57Bi, and Sn-9Zn by Indirect Archimedean Method*, J. Electron. Mater., **34 No.11**, (2005), 1414-1419.
- *[2005Woo1] Woo H.C.B, in MSc Thesis of "Solderability & Microstructure of Lead-free Solder in Leadframe Packaging", Department of Physics and Materials Science, City University of Hong Kong (2005).

- *[2004Gas1] Gašior W., Moser Z., Pstruś J., Bukat K., Kisiel R., Sitek J., *(Sn-Ag)_{eut} + Cu Soldering Materials, Part I: Wettability Studies*, J. Phase Equilib. Diffus., **24** (2004), 115-121.
- *[2004Gas2] Gašior W., Moser Z., Pstruś J., *SnAgCu+Sb Measurements of the Surface Tension and Density of Tin Based Sn-Ag-Cu-Sb Liquid Alloys*, Arch. Metall. and Mater., **49**, (2004), 155-167.
- [2004Kis] Kisiel R., Gašior W., Moser Z., Pstruś J., Bukat K., Sitek J., *(Sn-Ag)_{eut} + Cu Soldering Materials, Part II: Electrical and Mechanical Studies*, J. Phase Equilib. Diffus., **24** (2004), 122-124.
- [2004Kuc1] Kucharski M, Fima P, *The Surface Tension and Density of Cu-Pb-Fe Alloys*, Arch. Metall. Mater., **49** (2004) 565 – 573.
- *[2004Lee] Lee J., Shimoda W., and Tanaka T., *Surface Tension and its Temperature Coefficient of Liquid Sn-X (X=Ag, Cu) Alloys*, Mater. Trans., **45, No.9**, (2004), 2864-2870.
- *[2004Liu1] Liu X.J., Hamaki T., Ohnuma I., Kainuma R. and Ishida K., *Thermodynamic Calculations of Phase Equilibria, Surface Tension and Viscosity In the In-Ag-X (X=Bi, Sb) System*, Mater. Trans., **45 No3**, (2004), 637-645.
- *[2004Mos] Moser Z., Gašior W., Pstruś J., Ishida K., Ohnuma I., Bukat K., Sitek J., Kisiel R., *Experimental Wettability Studies Combined with the Related Properties from Data Base for Lead – free Soldering Materials*, CALPHAD XXXIII, May 30 - June 4, 2004, Kraków, Poland, Program of Abstracts, , 81.
- *[2004Mos2] Moser Z., Gašior W., Pstruś J., Ishida K., Ohnuma I., Kainuma R., Ishihara S., and Liu X. J., *Surface Tension and Density Measurements of Sn-Ag-Sb Liquid Alloys and Phase Diagram*

- Calculations of the Sn-Ag-Sb Ternary System*, Mater. Trans., **45**, (2004), 652-660.
- *[2004Pst] Pstruś J, Moser Z., Gašior W., *Surface Tension and Density Measurements of Liquid Zn-Sn and Zn-In Alloys*, TOFA 2004, Discussion Meeting on thermodynamics of Alloys, Book of Abstracts, Program, Vienna, Austria, September 12-17.
- *[2004Smi] Gale W.F., Totemeier T.C, *Smithells Metals Reference Book Eighth Edition*, (2004), ASM International.
- [2004Sob] N. Sobczak: *Wpływ temperatury, dodatków stopowych i modyfikacji powierzchni na zwilżalność, strukturę granic podziału i wytrzymałość połączenia w układzie Al/Al₂O₃*, *Odlewnictwo – Nauka i Praktyka*, **4**, (2004), 3 – 21.
- *[2004Wu1] Wu C.M.L., Yu D.Q., Law C.M.T., Wang L., *Materials Science and Engineering Reports*, R44/1 pp. 1, April 2004.
- *[2004Yu1] Yu D.Q., Zhao J., Wang L., *Improvement on the microstructure stability, mechanical and wetting properties of Sn–Ag–Cu lead-free solder with the addition of rare earth elements*, *J. Alloys Compd.*, **376**, (2004), 170–175.
- *[2004Yu2] Yu D.Q., Xie H.P., Wang L., *Investigation of interfacial microstructure and wetting property of newly developed Sn–Zn–Cu solders with Cu substrate* *J. Alloys Compd.*, **385**, (2004), 119–125.
- *[2003Alc1] Alchagirov B. B., Chochaeva A. M., Bekulov V. B., and Khokonov Kh. B., *The Surface Tension of Melts of Aluminum–Indium Binary System*, *High Temperature*, **41 No4**, (2003), 472–476.
- *[2003Gas1] Gašior W., Moser Z., Pstruś J., Krzyżak B., Fitzner K., *Surface Tension and Thermodynamic Properties of the Liquid Ag-Bi Solutions*, *J. Phase Equilib.*, **24**, (2003), 40-49.

- *[2003Gas2] Gaşior W., Moser Z., Pstruś J., *Density and Surface Tension of Sb-Sn Liquid Alloys. Experiment vs. Modeling*, J. Phase Equilib., **24**, (2003), 504-510.
- *[2003Kap1] Kaptay G., Proc. of microCAD, Int. Conf. Section: Metallurgy, Univ. of Miskolc, Hungary, (2003), 23-28.
- *[2003Lin1] Lin C.T., Lin K.L., *Contact angle of 63Sn–37Pb and Pb-free solder on Cu plating*, Applied Surf., Sci., **42**, (2003), 243–258.
- *[2003Wu1] Wu C.M.L., Yu D.Q., Law C.M.T., Wang L., J. Electron. Mater., **32 (29)**, (2003), 63.
- *[2002Aki1] Akinlade O., Singh R.N., *Bulk and surface properties of liquid In–Cu alloys*, J. Alloys Compd., **333**, (2002), 84–90.
- *[2002Liu] Liu X.J., Inohana Y., Ohnuma I., Kainuma R., Ishida K., Moser Z., Gaşior W., Pstruś J., *Experimental Determination and Thermodynamic Calculation of the Phase Equilibria and Surface tension of the Ag-Sn-In System*, J. Electron. Mater., **31**, (2002), 1139-1151.
- *[2002Mos] Moser Z., Gaşior W., Pstruś J., Księżarek S., *Surface Tension and Density of the (Ag-Sn)_{eut}+Cu liquid Alloys*, J. Electron. Mater., **31**, (2002), 1225-1229.
- *[2002Oka1] Okamoto H., Cu-Ti, J. Phase Equilib. **26 No. 3**, (2002), 549.
- *[2002Wu1] Wu C.M.L., Yu D.Q., Law C.M.T., and Wang L., *The Properties of Sn-9Zn Lead-Free Solder Alloys Doped with Trace Rare Earth Elements*, J. Electron. Mater., **31No.9**, (2002), 921-927.
- *[2002Wu2] Wu C.M.L., Yu D.Q., Law C.M.T., Wang L., J. Mater. Res, **31(9)**, (2002), 3146.
- *[2002Wu3] C.M.L. Wu, D.Q. Yu, C.M.T. Law, L. Wang, J. Electron. Mater., **31(9)**, (2002), 928.

- *[2001Gas1] Gaşior W., Moser Z., Pstruś J., Kucharski M., *Viscosity of the Pb-Sn Liquid Alloys*, Arch. of Metall., **46 (1)**, (2001), 23-32.
- *[2001Gas2] Gaşior W., Moser Z., Pstruś J., *Surface Tension and Density of the Pb-Sn Liquid Alloys*, J.Phase Equilib., **22**, (2001), 20-25.
- *[2001Lee1] Lee J.H. and Lee D. N., *Use of Thermodynamic Data to Calculate Surface Tension and Viscosity of Sn-based Soldering Alloy Systems*, J. Electron. Mater., **30No.9**, (2001), 1112-1119.
- *[2001Mos1] Moser Z., Gaşior W., Pstruś J., *Density and surface tension of the Ag-Sn liquid alloys*, J. Phase Equilib., **22**, (2001), 254-258.
- *[2001Mos2] Moser Z., Gaşior W., Pstruś J., Zakulski W., Ohnuma I., Liu X.J., Inohana Y., Ishida K., *Density and surface tension of the Ag-In liquid alloys*, J. Electron. Mater., **30**, (2001), 1120-1128.
- *[2001Mos3] Moser Z., Gaşior W., Pstruś J., *Surface tension measurements of the Sn-Bi and Sn-Bi-Ag liquid alloys*, J. Electron. Mater., **30**, (2001), 1104-1111.
- *[2001Pra1] Prasad L.C., Mikula A., *Effect of temperature on the surface properties of Cu-Sn liquid alloys*, J. Alloys Compd., **314**, (2001), 193-197.
- *[2001Tan] Tanaka T., Matsuda M., Nakao K., Katayama Y., Kaneko D., Hara S., Xing X., Qiao Z., *Measurement of Surface Tension of Liquid Ga-Base Alloys by a Sessile Drop Method*, Z. Metallkd., **92**, (2001), 1242-1246.
- *[2000Che1] Chen Y-Y., Duh J.-G., *The effect of substrate surface roughness on the wettability of Sn-Bi solders*, J. Mater. Sci.: Materials in Electronics, **11**, (2000), 1279-1283.
- [2000Moo] Moon K.-W., Boettinger W.J., Kattner U.R., Biancaniello F.S. and Hadwerker C.A., *Experimental and Thermodynamic*

- Assessment of Sn-Ag-Cu Solder Alloys*, J. Electron. Mater., **29**, (2000), 1122-1136.
- *[2000Ohn1] Ohnuma I., Cui Y., Liu X.J., Inohana Y., Ishihara S., Ohtani H., Kainuma R., and Ishida K., *Phase Equilibria of Sn-In Based Micro-Soldering Alloys*, J. Electron. Mater., **29 No10**, (2000), 1113-1121.
- *[2000Par1] Park J.Y., Ha J.S., Kang C.S., Shin K.S., Kim M.I., Jung J.P., *Study on the soldering in partial melting state. Analysis of surface tension and wettability*, J. Electron. Mater., **29No.10**, (2000), 1145-1152.
- *[2000Tu1] Tu C.C., Natishan M.E., *Solder. Surf. Mt. Technol.*, **12(2)**, (2000), 10.
- *[2000Yu1] Yu S.-P., Liao C.-L., Hon M.-H., Wang M.-C., *The Effects of Flux on the Wetting Characteristics of Near-Eutectic Sn-Zn-In Solder on Cu Substrate*, J. Mater. Sci., **35**, (2000), 4217 – 4224.
- [1999Mos] Moser Z., Fitzner K., *The use experimental thermodynamic data in the phase equilibria verification*, Termochim. Acta, **332**, (1999), 1-19.
- *[1999Ohn1] Ohnuma I., Liu X.J., Ohtani H., and Ishida K., *Thermodynamic Database for Phase Diagrams in Micro-Soldering Alloys*, J. Electron. Mater., **28 No11**, (1999), 1164-1171.
- *[1999Pra1] Prasad L.C., Xie Y., Mikula A., *Lead free solder materials In-Sn-Zn system*, J. Non-Crystalline Solids., **250-252** (1999), 316-320.
- [1999Tan] Tanaka T., Hack K., Hara S., *Use of Thermodynamic Data to Determine Surface Tension and Viscosity of Metallic Alloys*, MRS Bulletin, **24**, (1999), 45 – 50.

- *[1999Yoo1] Yoon S.W., Cho W.K., and Lee H.M., *Calculation of surface tension and wetting properties of Sn-based solder alloys*, *Scrip. Mater.*, **40No.3**, (1999), 297–302.
- *[1998Lan1] Landolt-Börnstein, New Series IV(5) Vol 5J, (1998), 1-3.
- [1998Lee] Lee H. M. Yoon S. W. and Lee B – J: *Thermodynamic Prediction of Interface at Cu/Solder Joints*, *J. Electron. Mater.*, **27**, (1998), 1161-1166.
- *[1998Yos1] Yost F.G. and Otoole E.J., *Metastable and Equilibrium Wetting States in the Bi-Sn System*, *Acta mater.*, **46 No.14**, (1998), 5143-5151.
- *[1997Hua] Hua F., Glazer J., *Lead-free solders for electronic assembly, design and reliability of solders and solder interconnections*, (1997), 65-74.
- [1997Lee] Lee B.J, Lee H.M., *Alloy Design Sn – Ag – In – Ni – Sb Solders System Using Thermodynamic Calculations in Design and Reliability of Solders and Solder Connections*, ed. R.K. Mahidhara, D.R. Frear, S.M.L. Sastry, K.L. Murty, P.K. Liaw and K. Winterbottom, The Minerals, Metals and Materials Society, (1997), 129 – 136.
- [1997Miy] Miyazaki M., Mitutani M., Takemoto T & Matsunawa A., *Conditions for Measurement of Surface Tension of Solders with a Wetting Balance Tester*, *Trans. of JWRI*, **26(1)**, (1997) 81-84.
- [1996Tan] Tanaka T., Hack K., Iida T., Hara S., *Applications of Thermodynamic Database to the Evaluation of Surface Tension of Molten Alloys, Salt Mixtures and Oxide Mixtures*, *Z. Metallkde.*, **87**, (1996), 380-389.

- *[1996Via1] Vianco P.T., Claghorn A.C., *Solder. Surf. Mt. Technol.*, **8(3)**, (1996), 12.
- *[1996Xie] Xie Y., Qiao Z., *J. Phase Equilibria*, **17**, (1996), 208 – 217.
- *[1995Art] Artaki I., Finley D.W., Jackson A.M., Ray U., Vianco P.T., Wave soldering with lead-free solders, in: *Proceedings of the Technical Program on Advanced Electronics Manufacturing Technologies*, SMI Surface Mount International, San Jose, CA, 495-510, 1995.
- [1995Gla] J. Glazer: *Metallurgy of low temperature Pb-free solders for electronic assembly*, *Int. Materials Rev.*, 40 (1995) 65 – 93.
- *[1995Lee] Lee N.C, Slattery J., Sovinsky J., Artaki I., Vianco P., *A novel lead-free solder replacement*, *Circuits Assembly* **6**, (1995) 36-44.
- *[1995See] Seelig K., *A study of lead-free solder alloys*, *Circuits Assembly* **6 (10)**, (1995) 46-48.
- *[1995Vil1] Villars P., Prince A., Okamoto H., *Handbook of Ternary Alloy Phase Diagrams*, (1995), ASM International.
- *[1994Art] Artaki I., Jackson A.M., Vianco P.T., *Evaluation of lead-free joints in electronic assemblies*, *J. Electron. Mater* **23**, (1994), 757-764.
- *[1994Jac] Jackson A.M, Vianco P.T., Artaki I., Manufacturing feasibility of several lead-free solders for electronic assembly, in: *Proceedings of the 7th International SAMPE Electronics Conference*, 20-23 June 1994, Parsippany, NJ, 381-391.
- *[1994Loo] Loomans M.E., Vaynman S., Ghosh G., Fine M.E., *Investigation of multi-component lead-free solders*, *J. Electron. Mater.***23**, (1994), 741-746.

- *[1994Pan] Pan T.-Y., Nicholson J., Blair H., Poulson R., Cooper R., Mitlin D., Cheung M.F., Dynamic wetting characteristics of some lead-free solders, in: Proceedings of the 7th International SAMPE Electronics Conference. 20-23 June 1994.
- [1994Sic] Sichen Du, Bygden J., Seetharaman S., Metall. Mater. Trans., 25B (1994) 519.
- [1994See] Seetharaman S., Sichien D., *Estimation of the Viscosities of Binary Metallic Melts Using Gibbs Energies of Mixing*, Metall. Mater. Trans. **25B**, (1994), 589-595.
- [1993Iid1] Iida T., Ghutrie R. I. L., The Physical Properties of Liquid Metals. Clarendon Press, Oxford 1993.
- [1993Kar] Karakaya I., Thompson W.T., *The Ag – Bi (Silver – Bismuth) System*, J. Phase Equilibria, **14**, (1993), 525 – 529.
- *[1993Kee] Keene B.J., *Review of Data for the Surface Tension of Pure Metals*, Int. Mater. Rev., **38**, (1993), 157-192.
- *[1993Via1] Vianco P.T., Frear D.R., *Issues in the replacement of lead-bearing solders*, JOM, **45**, (1993), 14-19.
- *[1993Via2] Vianco P.T., Frear D.R., JOM, **23(7)**, (1993), 14.
- *[1993Vin] Vincent J.H., Richards B.P., *Part2: UK Progress and Preliminary Trials*, Circuit World, **19**, (1993), 32-38.
- *[1992Fel] Felton L.E., Raeder C.H., Havasy C.K., Knorr D.B., Pb-free soldering alternatives for fine pitched electronics packaging, in: Proceedings of the 13th IEEE/CHMT International Symposium on Electronics Manufacturing Technology, (1992), 300-304.
- [1992Lee] Lee H.-K., Hajra J.P., Frohberg M.G., *Calculations of Surface Tensions in Liquid Ternary Metallic Systems*, Z. Metallkde, **83**, (1992), 638 – 643.

- [1992Muk] K. Mukai: *Wetting and Marangoni Effect in Iron and Steelmaking Processes*, ISIJ Intern., 32 (1992) 19 – 25.
- *[1992Via] Vianco P.T., Hosking F.M., Rejent J.A., Wettability analysis of tin-based, lead-free solders, in: Proceedings of the Technical Program - National Electronic Packaging and Production Conference, **3**, (1992), 1730-1738.
- *[1990Mas1] Massalski T.B., *Binary Alloy Phase Diagrams S.E.*, 1990, Editors: Okamoto H., Subramanian P.R., Kacprzak L., (1990), ASM International.
- *[1990Pas] Passerone A.P., Ricci F., Sangorgi R., *Influence of oxygen contamination on the surface tension of liquid tin*, J.Mater.Sci., **25**, (1990), 4266-4272.
- [1989Kle] Klein Wassink R. J., *Soldering in Electronics*, Second Edition. Electrochemical Publications, ISBN 0 901150 24 X, (1989).
- *[1989Nog] Nogi K., Oshino K., Ogino K., *Wettability of Solid Oxides by Liquid Pure Metals*, Mater. Trans. JIM, **30 No. 2**, (1989), 137-145.
- *[1989Yeu] Yeum K.S., Speiser R., Poirier D.R., *Estimation of the Surface Tension of Binary Liquid Alloys*, Metall. Trans., **20B**, (1989), 693 – 703.
- [1988Che] Chevalier P.Y., *A Thermodynamic Evaluation of the Ag – Sn System*, Termochim. Acta, **136**, (1988), 45 – 54.
- *[1988Dar] Ownby, P.D. and Liu, J., *Surface Energy of Liquid Copper and Its Wetting Behavior on Sapphire Substrates*, J. Adhes Sci. Tech., **2 (4)**, (1988), 255-269.
- *[1988Iid] Iida T. and Guthrie R.I.L., *The Physical Properties of Liquid Metals*, Clarendon Press, Oxford, (1988).

- [1988Kar] Karakaya I., Thompson W.T, *The Pb – Sn (Lead – Tin) System*, Bull. Alloy Phase Diagrams, **9**, (1988), 144 – 152.
- *[1988Wal1] Walsdorfer H., Arpshofen I.und Predel B., *Viscositat und spezifischer elektrischer Widerstand flussiger Legierungen der Systeme In-Sn und In-Bi*, Z. Metallkde., **79**, (1988), 503-512.
- *[1987Boj] Bojarski Z., Gigla M., Stróż K., Surowiec M., *Krystalografia, Podręcznik Wspomagany Komputerowo*, PWN, Warszawa 2001, 257.
- [1987Kuc] Kucharski M., Lepkość Roztworów Metali, Soli Stopionych o Wspólnym Jonie i Żuzli, Zeszyty Naukowe AGH, Metalurgia i Odlewnictwo, 109 (1987) 31.
- [1987Spe] Speiser R., Poirier D.R., Yeum K., *Surface Tension of Binary Liquid Alloys*, Scripta Metall., **21**, (1987), 348 – 375.
- [1986Mos] Moser Z., Gąsior W., Sommer F., Schwitzgebel G., Predel B., *Calorimetric and Emf Studies on Liquid Li-Sn Alloys*, Metall.Trans., **17 B**, (1986), 791-796.
- [1986Wea] Weast R.S., Astle M.J., Beyer W.H., CRC Handbook of Chemistry and Physics 1985-1986, CRC Press, Inc.Boca Raton, Florida, ISBN-0-8493-0466-0.
- *[1985Som] Somol V., Berenek M., *Surface Tension Measurements of Liquid Pb- Sn Alloys (in Czech)*, Hutn.Listy, **4**, (1985), 278-280.
- *[1984Pam] Pamies A., Garcia-Cordovilla C., Louis E., *Measurements of Surface Tension of Liquid Aluminium by Means of the Maximum Bubble Pressure Method : the Effect of Surface Oxidation*, Scr. Metall., **18**, (1984), 869-872.
- *[1984Som] V. Somol, M. Beranek, Sb.Vysk.Sk.Chem.-Technol.Praze Anorg.Chem. Technol., **B30**, (1984), 199-205.

- *[1983Bra] Brandes E.A., Smithells Metals Reference Book, Sixth Edition (Editor E.A. Brandes BSc, ARCS, CEng, FIM In association with Fulmer Research Institute Ltd), (1983).
- [1983Koz1] Kozlov L. Y., Romanov L. M., Petrov N. N., *Prognozirovaniye Vjaskosti Multikomponentnyh metalicheskikh razplavov*, Izv. Vuzov. Chernaya Metall., **3**, (1983), 7-11.
- [1983Rot1] Rotenberg Y, Boruvka L, Neumann AW J Colloid Interface Sci., *Determination of surface tension and contact angle from the shapes of axisymmetric fluid interfaces*, **93** (1983) 169 – 183.
- *[1982Sen] Sengiorgi R., Muolo M.L., Passerone A., *Surface Tension and Adsorption in Liquid Silver – Oxygen Alloys*, Acta Metall., **30**, (1982), 1597-1604.
- *[1981Fro1] Froberg M.G. und Özbagi K., *Die Viskosität flüssiger Kupfer-Wismut-Legierungen*, Z. Metallkde., **72**, (1981), 630-636.
- *[1979Lep] Lepinskikh B.M., Doc. VINITI, USSR, **4/5**, (1979), 1813-1879.
- *[1979Zad] Zadumkin S.N., Ibrachimov Ch.I. and Ozniev D.T., *Surface tension and density measurements overcooled Sn, In, Bi, and Pb (in Russian)*, Izv.VUZ, Cvet. Metall., **22**, (1979), 82-85.
- *[1977Bru] Brunet M., Joud J.C., Eustathopoulos N., Desre P., *Surface Tension of Germanium and Silver – Germanium Alloys in the Liquid State*, J. Less Common Met., **51**, (1977), 69-77.
- [1977Iid] Morita Z., Iida T., Ueda M., Liquid Metals, Ins. Phys. Conf. Ser. No 30, Bristol (1977), 600.
- *[1977Kuc] Kucharski M., *Density and Surface Tension of Sn-Cd Alloys*, Arch. Hut., **22**, (1977), 181-194.

- *[1977Lan] Lang G., Laty P., Joud J.C. and Desre P., *Measurement of the surface tension of some fluid metals with different methods (in German)*, Z. Metallkd., **68**, (1977), 113-115.
- *[1977Par] Paramonov V.A., Karamyshev E.P., Ukhov V.F., *Colloq. on physics and chemistry of surface melts*, In Fiz. khim. poverkh. rasp, Tbilisi, Metsniyerba, (1977), 155.
- *[1977Seb1] Sebo P., Gallois B., and Lupis C.H.P., *The Surface Tension of Liquid Silver-Copper Alloys*, Metall. Trans., **8B**, (1977), 691-693.
- *[1976Kas] Kasama A., Iida T., Morita Z., *Temperature Dependence of Surface Tension of Liquid Pure Metals*, J. Japan Inst. Metals, **40**, (1976), 1030-1038.
- [1976Mor1] Morita Z., Iida T., Ueda M., *Tetsu-to-Hagane*, **64**, (1976), 629.
- *[1976Nak1] Nakajima H., *Viscosities of Liquid In-, Sn- and Sb-Ag Binary Systems*, Trans. JIM., **17**, (1976), 403-407.
- [1976Sha] Shannon R.D., *Revised Effective Ionic Radii and Systematic Studies of Interatomic Distances in Halides and Chacogenides*, Acta Cryst. **A32**, (1976), 751 – 767.
- *[1975Abd] Abdel-Azis A.K., Kirshak H.R., *Surface Tension of Molten Tin and an Estimate of its Critical Temperature*, Z. Metallkde., **66**, (1975), 183-184.
- *[1974Lan] Lang G., *The Influence of Alloying Elements to The Surface Tension of Liquid Super Purity Aluminum*, Aluminium, **50**, (1974), 731-734.
- [1973Bar] Barin I., Knacke O., *Thermochemical Properties of Inorganic Substances*, Springer-Verlag, Berlin, Heilderberg, new York, Verlag Stahleisen m.b.H Duesseldorf, 1973.

- *[1973Bri1] Bricard A., Eustathopoulos N., Joud J.C., Desré P., *Tension superficielle de l'alliage liquide Ag-Cu par la méthode de la goutte posée*, C.R.Acad. Sci.Paris., **276C**, (1973), 1613-1616.
- *[1972Ada] Adachi A., Morita Z., Kita Y., Kasama A., *Surface Tension of Liquid Lead – Tin Alloys Measured by the Maximum Bubble – Pressure Method*, Technol.Rep.Osaka Univ., **22**, (1972), 1027-1052.
- [1972Ran] Randles J.E.B., Behr B., *Adsorption at Fluid Interfaces. I. Surface Tension at the Interface between Binary Liquid Mixtures and its Vapour*, J. Electroanal. Chem., **35**, (1972), 389 – 404.
- *[1972Cra1] Crawley A. F., *Densities and Viscosities of Some Liquid Alloys of Zinc and Cadmium*, Metall. Trans., **3**, (1972), 971-975.
- *[1972Yat] Yatsenko S.P., Kononenko W.I., Schukman A.L., *Experimental studies of the temperature dependence of the surface tension and density of tin, indium, aluminium and gallium*, Teplofiz. Vys. Temp., **10**, (1972), 55-66.
- *[1971Ber] Bernard G., Lupis C.H.P., *The Surface Tension of Liquid Silver Alloys: Part I. Silver – Gold Alloys*, Metall. Trans., **2**, (1971), 555-559.
- *[1971Lan] Lang G., *The Surface Tension of Mercury and Liquid Lead, Tin, and Bismuth*, J.Inst.Metals., **104**, (1971), 300-308.
- *[1971Whi] White D.W.G., *The Surface Tension of Pb, Sn, and Pb – Sn Alloys*, Metall.Trans., **2**, (1971), 3067-3071.
- *[1970Rhe] Rhee S.K., *Wetting of AlN and TiC by Liquid Ag and Liquid Cu*, J. Am. Ceram. Soc., **53**, (1970), 639-641.
- *[1968Thr] Thresh H.R., Crawley A.F., White D.W.G., *The Densities of Liquid Tin, and Tin – Lead Alloys*, Trans. TMS-AIME, **242**, (1968), 819-822.

- [1967Tea] Teatum E., Gschneider K., Waber J., *Compilation of Calculated Data Useful in Predicting Metallurgical Behaviour of the Elements in Binary Alloy Systems*, 1962, La-2345 Los Alamos Scientific Laboratory, <http://www.iumsc.indiana.edu/radii.html>.
- *[1965Bud1] Budde J. und Sauerwald F., *Die Viskosität der schmelzflüssigen E- (Entmischungs-) - Systeme Blei-Zink und Wismut-Zink, Ermittlung von Mischungslücken*, Z. Phys.Chem., **230**, (1965), 42-47.
- *[1964Lau] Lauerman I., Sauerwald F., *Measurements of the surface tension of melted metals X. Surface tension measurements of molten metals copper, silver, antimony, copper-tin, copper-antimony and silver-antimony (in German)*, Z. Metallkd., **55 (10)**, (1964), 605-612.
- *[1964Laz] Lazarev V.B., *Experimental Studies of the Surface Tension of Liquid In-Sb Alloys*, Russ.J.Phys. Chem., **38**, (1964), 325-330.
- *[1961Lau] Lauerman I., Metzger G., Sauerwald F., *Surface tensions of molten silver, tin and silver-tin alloys(in German)*, Z. für Phys. Chem., **216**, (1961), 42-49.
- [1961Moe1] Moelwen-Hughes E. A., 1961. *Physical Chemistry*. Pergamon Pres, Oxford·London·New·York·Paris.
- *[1959Pok] Pokrowski N.L., *Investigations of the surface – active films of the liquid metallic surface (in Russian)*, P.S.Dok.Akad.Nauk SSSR, **128**, (1959), 1228-1231.
- *[1957Hoa] Hoar T.P., Melford D.A., *The Surface Tension of Binary Liquid Mixtures: Lead + Tin and Lead + Ind Alloys*, Trans. Faraday Soc., **53**, (1957), 315-326.
- *[1956Geb1] Gebhardt E., Becker M., Köstlin K., *Über die Eigenschaften metallischer Schmelzen*, Z. Metallkde., **47(10)**, (1956), 684-687.

- *[1956Mel] Melford D.A., Hoar T.P., *Determination of the Surface Tension of Molten Lead, Tin, and Indium by an Improved Capillary Method*, J. Inst. of Metals, **85**, (1956), 197-205.
- *[1957Geb1] Gebhardt E. und Köstlin K., *Die innere Reibung flüssiger Blei-Zinn- und Blei-Antimon-Legierungen*, Z. Metallkde., **48**, (1957), 636-641.
- [1954Sat] Sato T., Munakata S., Bull. Res. Inst. Min. Met. Tohoku Univ., 10, (1954), 173.
- *[1956Tay] Taylor J.W., *The Surface Tension of Liquid – Metal Solutions*, Acta Metall., **4**, (1956), 460-468.
- *[1954Geb1] Gebhardt E., Becker M. und Dorner S., *Die innere Reibung flüssiger Aluminium-Zink- Legierungen*, Z. Metallkde., **45**, (1954), 83-85.
- *[1953Geb1] Gebhardt E., Becker M. und Trägner E., *Die innere Reibung flüssiger Silber-Zinn-Legierungen*, Z. Metallkde., **44**, (1953), 379-382.
- *[1953Kin] Kingery W.D., Humenik M., *Surface Tension at Elevated Temperatures. I. Furnace and Method for use of the Sessile Drop Method; Surface Tension of Silicon, Iron and Nickel*, J. Phys. Chem., **57**, (1953), 359-363.
- *[1952Geb1] Gebhardt E., Becker M. und Schäfer S., *Die innere Reibung flüssiger Kupfer-Zinn- Legierungen*, Z. Metallkde., **43**, (1952), 292-296.
- *[1951Geb1] Gebhardt E. und Wörwag G., *Die innere Reibung Flussinger Legierungen aus Kupfer-Silber und Gold-Kupfer*, Z. Metallkde., **42**, (1951), 358-361.
- *[1951Geb2] Gebhardt E., Becker M., *Über die innere Reibung flüssiger Gold-Silber-Legierungen*, Z. Metallkde., **42**, (1951), 111-117.

- *[1949Pel] Pelzer E., Berg – und Hüttenmännische. Monatshefte, *Surface tensions of liquid metals and alloys II (in German)*, **94**, (1949), 10-17.
- [1945Gug] Guggenheim E.A., *Statistical Thermodynamics of the Surface of Regular Solutions*, Trans. Faraday Soc., **41**, (1945), 150-156.
- *[1934Bir] Bircumshaw L.L., Phil. Mag, **17**, (1934), 181-192.
- [1932But] Butler J.A. V., *The Thermodynamics of the Surfaces of Solutions*, Proceedings of the Royal Society of London series A, **85**, (1932), 348-375.
- *[1929Kra] Krause W., Sauerwald F., Micalke M., *Density measurements at high temperature. About the density of liquid gold and liquid gold-copper and silver- copper alloys (in German)*, **181**, Z. Anorg. Chem., (1929), 347-352.
- *[1928Lib] Libman E.E., Bull. Ill. Univ. Eng. Exp. Sta., **187**, (1928).
- *[1927Dra] Drath G. and Sauerwald F., *Surface tensions of molten metals and alloys II (in German)*, Z. anorg. u. allg. Chem., **162**, (1927), 301-320.
- [1923Gold] Goldschmidt V.M., *Geochemische Verteilungsgesetze der Elementen*, Oslo, 1923: Kristallchemie in Hand Woerterbuch den Naturwiessensch, Jena, 1934: Smithells Metals Reference Book, sixth edition, London, Boston, Sngapur, Sydney, Wellington, Durban, Toronto, Butterworth and Co (Publishers) Ltd, 1923.
- [1922Sug] Sugden, S. *Determination of surface tension from the maximum pressure in bubbles*, J. Am. Chem. Soc., **121**, (1922), 858-866.

- *[1921Hog] Hognes T.R., *The Surface Tension and Density of Liquid Mercury, Cadmium, Zinc, Lead, Tin and Bismuth*, J. Am. Chem. Soc., **43**, (1921), 1621-1628.
- [1915Sch] Schrödinger E., Ann. Physik, **46**, (1915), 413.
- [1869Dup] Dupré A., *Theorie Mechnique de la Chaleur*, Paris, (1869), 207.
- [1805You] Young T., Phil. Trans. Roy. Soc. London 95, (1805), 65; reprinted with additions in Works of Dr. Young (Peacock, ed.) London, **1**, (1855), 418.

8. The abstracts of the most important publications

In this chapter are reported the abstracts of the most important publications used in preparation of SURDAT 3 database.

[2011Mos1] Moser Z., Fima P., Bukat K., Sitek J., Pstruś J., Gaşior W., Kościelski M., Gancarz T., *Investigation of the effect of indium addition on wettability of Sn-Ag-Cu solders*, Soldering @Surface Mount Technology (in print).

Abstract

Purpose – The purpose of this work is to investigate the influence of In additions on the wetting properties of the Sn_{2.86}Ag_{0.40}Cu (in wt.%) eutectic-based alloys on a copper substrate in the presence of the flux. Four independent methods, namely wetting balance (WB), sessile drop (SD), maximum bubble pressure (MBP) and dilatometric method are applied for contact angle, surface tension and interfacial tension, wetting force and wetting time, and density measurements. The main goal of these investigations is to gather results that enable to find correlations between the results of wetting balance and sessile drop method in relation to contact angles.

Design/methodology/approach – The authors applied the WB method for the wetting measurements at 250°C in air atmosphere in the presence of the flux. SD measurements were conducted at the same temperature in the presence of the same flux, but in Ar atmosphere, while the MBP and dilatometric measurements were conducted in Ar+H₂ atmosphere.

The density data from dilatometric method were used for surface tension determination with MBP as well as surface tension and interfacial determination with WB method, and the surface tension data from these two methods were compared. WB data were used to calculate contact angles and the obtained indirect data were compared with the results of direct SD measurements of the contact angle.

Findings – As the authors had expected, a higher In content in the alloy resulted in lower contact angle on copper, and the wetting balance results agree well with the results of sessile drop experiments. It was confirmed that in liquid In-Sn and alloys containing In and Sn (Ag-In-Sn, Sn-Ag-Cu-In, Sn-Zn-In) the improvement of wettability is indicated only by the increase of contact angle with increasing In content.

Research limitations/implications – It is suggested that further studies are necessary for the confirmation of the practical application, but they should be directed to the soldering of high indium alloys on PCBs with different finishes and the quality of solder joint performance.

Practical implications – Taking into account contact angle data, from WB and SD method the best results of SAC-In alloy on copper were obtained for the alloy of the highest In content. It was found, that the contact angles from SD after 4 s are higher (non-equilibrium conditions) than the values calculated from WB method after 3 s. Contrary, contact angles from SD after 10 min (equilibrium conditions) are lower than those from WB after 3 s. The comparison suggests, that the contact angles from WB are situated within the data from SD, showing the same lowering tendency with increasing content of In, and they may be well accepted for practical purposes. On the other hand, sample of the solder in SD method after

prolonged time to get equilibrium contact angle, may be used to study interfacial phenomena with Cu substrate.

Originality/value – The WB and the SD method were used for contact angle determination of a wide range of solder compositions under the same temperature and flux conditions. Also the surface tension for these alloys was determined with two independent methods, i.e., MBP and WB method. The obtained results allowed to draw conclusions regarding correlation between the output of different methods and the conditions under which a comparison of results can be made. It is supposed that these observation apply to many other alloy systems.

[2010Buk1] Bukat K., Moser Z., Sitek J., Gasior W., Kościelski M., Pstruś J., *Investigations of Sn-Zn-Bi solders. Part I. Surface tension, interfacial tension and density measurements of the Sn-Zn-7Bi solders*, *Soldering @ Surface Mount Technology*, 22 No.3, (2010), 10 – 16.

Abstract

Purpose – The purpose of Part I is to investigate the influence of Bi additions on the surface tension, the interfacial tension and the density of the SnZn7Bi alloys (Bi =1 and 3 % by mass) as a continuation of similar previous studies on Bi and Sb additions to the binary Sn-Zn. The main aim of Part I is to indicate that the lowering of the surface tensions and interfacial tension is not sufficient for the practical application. However, the knowledge of the interfacial tension between the soldering flux and the solder is necessary to convert the wetting force into the contact angle. It will be documented in Part II.

Design/methodology/approach – The authors applied the maximum bubble method for the surface tension and the Miyazaki method for the surface tension and the interfacial tension, using the density values from the dilatometric technique. The experimental surface tension results are compared with the Butler's thermodynamic modeling and are discussed by means of the analysis of variance (ANOVA).

Findings – On the basis of the previous studies on the Sn-Zn-Bi-Sb alloys, the addition of Bi to SnZn7 slightly decreases the surface tension measured in Ar + H₂ atmosphere, similarly to the Butler's modeling results. Also, a similar slight decrease of the surface tension from the Miyazaki method measured in air and in nitrogen is observed, as well as a more significant

lowering of the interfacial tension with the use of a flux in nitrogen. There is also a slight influence of the temperature on the numerical values of the surface tensions and the interfacial tension. In the ANOVA, taking into account the Bi content, the temperature of measurements, the atmosphere and the flux, the used flux was shown as the most important, and, to a lesser extent, the atmosphere as well.

Research limitations/implications – It is intended (the purpose of Part II) to verify the positive influence of Bi additions in the SnZn7 alloys on the surface tensions and the interfacial tension by the contact angles from the interaction with the Cu substrate on PCBs with different lead-free finishes.

Practical implications – It is suggested that further studies on more efficient fluxes are necessary for the practical application being in agreement with the ANOVA and the literature information.

Originality/value – A slight improvement of the wettability with the use of Bi additions in the SnZn7Bi alloys in the course of various experimental techniques was proven, similarly to various references. The obtained results will enlarge the SURDAT database of the lead-free soldering materials.

[2010Buk2] Bukat K ., Sitek J., Kościelski M., Moser Z., Gašior W., Pstruś J., *Investigations of Sn-Zn-Bi solders. Part II. Wetting measurements of the Sn-Zn-7Bi solders on copper and on PCB with lead-free finishes by using the wetting balance method*, *Soldering @Surface Mount Technology*, 22 No.4, (2010), 13 – 19.

Abstract

Purpose – The purpose of this Part II is to investigate the influence of Bi additions on the wetting properties of the SnZn7Bi alloys (Bi =1 and 3 % by mass) on a copper substrate and PCBs with lead-free finishes (SnCu, Sn_{imm}, Ni/Au, OSP) in the presence of fluxes. The practical aspect of the obtained results is the main goal of these investigations.

Design/methodology/approach – The authors applied the wetting balance method for the wetting measurements at 230 and 250°C in nitrogen and air atmospheres in the presence of the ORM0 or ROL0 type fluxes. The PCBs were investigated in the state “as received” and after accelerated aging. The ANOVA analysis was performed in order to explain how the main factors of the experiments (the Bi content in the alloy (1 or 3 %), the test temperature and the test atmosphere) influence the wetting ability of SnZn7Bi on Cu substrate.

Findings – As the authors had expected, a higher temperature and a higher Bi content in the alloy favored the wetting process of the copper substrate in the presence of the ORM0 type flux in a nitrogen atmosphere. These results were confirmed by the ANOVA analysis. We obtained also very good results of the SnZn7Bi3 alloy's wettability on “tin coatings” on the PCBs (SnCu and Sn_{imm}.) in the state “as received” and after aging, alike,

in the presence of the ORM0 type flux, for all the applied testing conditions (in both temperatures and N₂ and air atmospheres). The less active flux (ROL0) causes a worsening of the alloy's wettability properties; however, the PCB with SnCu and Sn_{imm.} finishes keep their wettability, even after aging, still on a very good or good level, respectively.

Research limitations/implications – It is suggested that further studies are necessary for the confirmation of the practical application, but they should be limited to the soldering of SnZnBi₃ on PCBs with “tin coating” and the quality of solder joint performance.

Practical implications – The best results of SnZn₇Bi₃ wetting on the PCBs with “tin coatings” (SnCu and Sn_{imm.}) at 230 and 250°C and nitrogen and air atmospheres suggest a possibility of a practical usage of the tin-zinc-bismuth alloys for soldering in electronics using the ORM0 type flux and the even less active ROL0 type flux, which are currently applied in the industry lead-free soldering processes.

Originality/value – The wetting balance method combined with the analysis of variance (ANOVA) was used as the quickest way to determine the wettability properties of SnZn₇Bi on the Cu substrate. A wettability measurement of the SnZn₇Bi and SnZn₇Bi alloys with different lead-free finishes, in different experimental conditions, was also performed.

[2010Fim2] Fima P., Gašior W., Sypień A., Moser Z., *Wetting of Cu by Bi–Ag based alloys with Sn and Zn additions*, *J Mater Sci.*, **45** (2010) 4339–4344.

Abstract

Contact angles on copper substrate of Bi–Ag–Sn and Bi–Ag–Zn ternary alloys containing 3, 6, and 9 at.% of Sn and Zn, respectively, were studied with the sessile drop method. Wetting tests were carried out at 573 and 603 K with or without the use of a flux. Without the flux, the examined alloys do not wet copper, i.e., the observed contact angles are higher than 90°. However, in the presence of the flux wetting of copper is observed. In the case of alloys with Sn, the contact angles decrease with increasing content of Sn, while in the case of alloys with Zn no such tendency is observed. Solidified solder–substrate couples were cross-sectioned and examined with scanning electron microscopy coupled with electron dispersive X-ray analysis.

[2009Seb1] Sebo P., Moser Z., Svec P., Janickovic D., Dobrocka E., Gašior W., Pstruś J., *Effect of indium on the microstructure of the interface between Sn_{3.13}Ag_{0.74}CuIn solder and Cu substrate*, *J. Alloys Compd.*, **480**, (2009), 409-415.

Abstract

Influence of indium in Sn_{3.13}Ag_{0.74}Cu solder containing 4, 15, 30, 50 and 75 at.% In on the microstructure at the solder/Cu interface after wetting at 523K for 1800 s was studied. The scanning electron microscopy (SEM) combined with energy-dispersive X-ray spectroscopy (EDX), standard and spatially resolved X-ray diffraction (XRD) techniques were used to determine the phases present at the solder/Cu interface. It was found that for In concentration up to 30 at.% the interface is formed by Cu₆Sn₅ phase. For higher In content (50 and 75 at.% In) interface consists of copper rich Cu₄₁Sn₁₁ phase.

[2009Mos1] Moser Z., Sebo P., Gašior W., Svec P., Pstruś J., *Effect of indium on wettability of Sn-Ag-Cu solders. Experiment vs. modeling, Part I*, Int. Calphad, 33, (2009), 63-68.

Abstract

The density and surface tension measurements of the Sn_{3.13}Ag_{0.74}Cu liquid alloys with 2, 3, 4, 15, 30, 50 and 75 at.% In additions were conducted in the temperature range from 431 K up to 1209 K by dilatometric technique and the maximum bubble pressure method, respectively. The results obtained in both techniques exhibited 2%-3% scattering of experimental errors, similarly to the previously investigated In-Sn and Sn-Ag-In systems. This was due to the very similar surface tension and density values of pure indium and tin. The experimental surface tensions were compared with calculated ones using data of the constituent systems, (a) by means of thermodynamic method of Butler, and (b) by the temperature and concentration relation of the surface tension. The improvement of wettability in liquid alloys containing different In additions was confirmed with a sessile drop method in the temperature interval 523 K-593 K up to 1800 s. The wetting angles decreased with temperature and increasing In concentrations in the solders from ~ 37 for the solder without In at 523 K down to ~ 22 for the solder with 75 at.% In at 593 K. In the following Part II, the structure investigations of the interface between relevant solder and Cu substrate of the same liquid solders after contact angle measurements will be carried out.

[2009Mos2] Moser Z., Gašior W., Pstruś J., Kaban I., Hoyer W.,
Thermophysical Properties of Liquid In–Sn Alloys, *Int. J. Thermophys.*, **30**, (2009), 1811-1822.

Abstract

The surface tension of liquid In–Sn alloys was measured with three experimental techniques carried out in a protective atmosphere of a mixture of argon and hydrogen: tensiometric (in Chemnitz), and maximum bubble pressure and sessile drop (in Kraków). Attempts were undertaken to confirm the correlation of surface tension with electrical conductivity and viscosity and to compare them with literature data. The lack of such correlation or a weak one was observed, probably due to a slight negative departure of thermodynamic properties of liquid In–Sn alloys from ideal behavior. Both resistivity and viscosity correlated with the existence of In-rich β and Sn-rich γ phases of the In–Sn phase diagram. The mutual correlations of thermodynamic and physical properties, structure, and the type of phase diagram were confirmed previously for Li–Sn and Mg–Sn systems with evident negative thermodynamic departures from ideal behavior and with the occurrence of intermetallic compounds (IMCs) in the phase diagrams. Due to nearly the same values of surface tension and density of pure In and Sn, the concentration dependence on the surface tension and density was practically unchanged within an extensive range of temperatures in studies on Pb-free solders of binary and multicomponent alloys containing both metals. Thus, the beneficial influence of In on the wettability of In–Sn alloys was observed solely by the lowering of the contact angle.

[2008Buk1] Bukat K., J. Sitek, R. Kisiel, Z. Moser, W. Gąsior, Kościelski M., Pstruś J., *Evaluation of the influence of Bi and Sb additions to Sn-Ag-Cu and Sn-Zn alloys on their surface tension and wetting properties using analysis of variance – ANOVA*, *Soldering @ Surface Mount Technology*, 20, (2008), 9-19.

Abstract

Purpose - The purpose of this paper is a comparable evaluation of the influence of a particular element (Bi and Sb) added to Sn-Ag-Cu and Sn-Zn alloys on their surface and interfacial tensions, as well as the wetting properties on the Cu substrate expressed by the wetting angle.

Design/methodology/approach - The authors applied the U orthogonal Taguchi array to carry out the experiments and discussed the results using analysis of variance (ANOVA).

Findings - It was expected, on the base of previous studies, the decrease of the surface and interfacial tensions and thus improving wettability after the Bi and Sb addition to Sn-Ag-Cu and Sn-Zn alloys. Unfortunately, the obtained results on the quinary Sn-Ag-Cu-Bi-Sb alloys and the quaternary Sn-Zn-Bi-Sb alloys do not confirm these trends. The performed analyses suggest that the compositions of the quinary Sn-Ag-Cu-Bi-Sb alloys, as well as the quaternary Sn-Zn-Bi-Sb alloys, do not have optimal compositions for practical application. The Cu, Bi and Sb elements in the case of the Sn-Ag-Cu-Bi-Sb alloys and the Zn, Bi and Sb elements in the case of the Sn-Zn-Bi-Sb alloys show mutual interaction and, in consequence, there is no correlation between the tendency of the surface and interfacial tensions changes and the wettings of the Cu substrate.

Research limitations/implications - It is suggested that further studies are necessary for the purpose of the practical application, but they should be limited mainly to the Sn-Ag-Cu-Bi and the Sn-Zn-Bi alloys with the optimal compositions.

Practical implications - The performed analysis suggests that none of the investigated compositions of the quinary Sn-Ag-Cu-Bi-Sb alloys, as well as the quaternary Sn-Zn-Bi-Sb alloys, have the optimal compositions for practical application.

Originality/value - The quickest way to determine which element of the alloy composition influences the surface tension and the wetting properties, and how, is to apply orthogonal analysis. After choosing the orthogonal array, the experiments were performed and analysis of variance (ANOVA) was used to perform the quantifiable analysis of the measured and calculated results of surface and interfacial tensions, as well as the wetting properties on the Cu substrate.

[2008Buk2] Bukat K., Moser Z., Gašior W., Sitek J., Kościelski M., Pstruś J., *Trends in wettability studies, of Pb-free solders. Basic and application. Part II. Relation between surface tension, interfacial tension and wettability of lead-free of Sn-Zn*, *Archs. Metall. and Mater.*, **53**, (2008), 1065-1074.

Abstract

The surface tension of a molten alloy plays an important role in determining the wetting behavior of solders. The systematic measurements of surface tension by the maximum bubble pressure method, in Ar + H₂ atmosphere, were performed at the Institute of Metallurgy and Materials Science, Polish Academy of Sciences in Krakow (IMIM PAS). In parallel, the surface tension and interfacial tension were measured by the Miyazaki method, using wetting balance technique, in air and in N₂ atmospheres, at the Tele and Radio Research Institute (ITR) in Warsaw. Both of these methods were used for a comparative analysis of the Sn-Zn and Sn-Zn-Bi-Sb alloys manufactured by Institute of Non-Ferrous Metal in Gliwice (INMET INM). The authors would like to know how the addition of Bi and Sb elements to the eutectic Sn-Zn alloy influences the changes of the surface tension and wettability on copper substrate. It has been found that addition of Bi and Sb to the Sn-Zn alloy decreases surface tension. A more evident decreasing tendency of surface tension was noted in wetting balance(meniscographic) measurements, especially of an interfacial tension measured in presence of a flux. The results of the surface tension from both methods are comparable. Strong interaction between Bi and Sb elements in the Sn-Zn-Bi-Sb alloys was demonstrated by variance analysis (ANOVA). The wettability results of investigated zinc alloys on Cu substrate were unexpected: the better

wettability of eutectic Sn-Zn alloy than this modified by addition of Bi and Sb Sn-Zn was obtained. It appeared therefore that modified Sn-Zn-Bi-Sb solders were useless for soldering from technological point of view. So, the next wettability investigation will concentrate on new Sn-Zn-Bi alloy compositions with small amount of Zn. The surface tension of this alloy is not known.

[2008Mos1] Moser Z., Gašior W., Pstruś J., Dębski A., *Wettability Studies of Pb-Free Soldering Materials*, *Int. J. Thermophys.*, **29**, (2008), 1974-1986.

Abstract

The surface tension of liquid In–Sn alloys was measured with three experimental techniques carried out in a protective atmosphere of a mixture of argon and hydrogen: tensiometric (in Chemnitz), and maximum bubble pressure and sessile drop (in Kraków). Attempts were undertaken to confirm the correlation of surface tension with electrical conductivity and viscosity and to compare them with literature data. The lack of such correlation or a weak one was observed, probably due to a slight negative departure of thermodynamic properties of liquid In–Sn alloys from ideal behavior. Both resistivity and viscosity correlated with the existence of In-rich β and Sn-rich γ phases of the In–Sn phase diagram. The mutual correlations of thermodynamic and physical properties, structure, and the type of phase diagram were confirmed previously for Li–Sn and Mg–Sn systems with evident negative thermodynamic departures from ideal behavior and with the occurrence of intermetallic compounds (IMCs) in the phase diagrams. Due to nearly the same values of surface tension and density of pure In and Sn, the concentration dependence on the surface tension and density was practically unchanged within an extensive range of temperatures in studies on Pb-free solders of binary and multicomponent alloys containing both metals. Thus, the beneficial influence of In on the wettability of In–Sn alloys was observed solely by the lowering of the contact angle.

[2008Mos2] Moser Z., Gašior W., Bukat K., Pstruś J., Sitek J., *Trends in wettability studies of Pb-free solders. Basic and application. Part I. Surface tension and density measurements of Sn-Zn and Sn-Zn-Bi-Sb alloys. Experiment vs. modeling*, *Archs. Metall. and Mater.*, **53**, (2008), 1055-1063.

Abstract

Surface tension and density measurements by maximum bubble pressure and dilatometric techniques were carried out in 1 extensive range of temperature on liquid alloys close to binary eutectic Sn-Zn composition with small Bi and Sb additions. It is been found that the addition of Bi and Sb decreases the surface tension and density. The values of the surface tension were so calculated by the Butler model using ADAM1S database from Tohoku University and this of COST 531 program for excess Gibbs energies of liquid components. For modeling, surface tension and density of pure components from SURDAT database ere accepted . Calculated surface tension is close to experimental results. Values at 523 K were compared with results om meniscographic/wetting balance studies undertaken in cooperation with industrial institutes in the frame of net-work: advanced soldering materials" financed by Polish sources 2006/2007.

The main aim of these joint studies combining basic research with application is to search for substitute materials of traditional solders based on Sn-Pb eutectics and to propose the metric of wettability suitable for different Pb-free materials.

[2008Seb1] Šebo P. Švec P., Janičkovič D., Moser Z., *Identification of phases in Sn-Ag-Cu-In solder on Cu substrate interface*, *Kovove Mater.* **46**, (2008), 235–238.

Abstract

Determination of the phases arising at the interface between lead-free Sn_{3.5}Ag_{0.4}Cu_{29.5}In solder and copper substrate after wetting of copper at 280 °C for 1800 s is presented. Compared are results obtained with methods of scanning electron microscopy (SEM) equipped with EDX analyzer, X-ray diffraction and X-scan X-ray diffraction method. Standard X-ray diffraction profile shows the existence of four phases In_{0.2}Sn_{0.8}, Cu₆Sn₅, In₃Sn and Ag₃Sn. X-scan X-ray diffraction profile shows the presence of two phases at the interface In_{0.2}Sn_{0.8} and Cu₆Sn₅ and adjacent phase to the copper substrate is In_{0.2}Sn_{0.8} phase. Comparison of both methods is discussed.

[2007Mos1] Moser Z., Gašior W., Bukat K., Pstruś J., Kisiel R., Sitek J., Ishida K. and Ohnuma I., *Pb-Free Solders: Part III. Wettability Testing of Sn-Ag-Cu-Bi Alloys with Sb Additions*, *J. Phase Equilib. Diffus.*, **28** (No 5), (2007), 433-438.

Abstract

Maximum bubble pressure, dilatometric, and meniscographic methods were used in the investigations of the surface tensions, densities, wetting times, wetting forces, contact angles, and solder-flux interfacial tensions of liquid Sn-Ag-Cu-Bi alloys with various additions of Sb. Density and surface tension measurements were conducted in the temperature range 230 to 900 °C. Surface tensions at 250 °C were measured in air and under a protective atmosphere of Ar-H₂ and were combined with data from meniscographic studies done under air or with a protective flux. Meniscographic data with a nonwetted Teflon substrate provided data on solder-flux interfacial tensions, and meniscographic data with a Cu substrate allowed determinations of wetting times, wetting forces, and calculations of contact angles. Additions of Sb to quaternary Sn-Ag-Cu-Bi alloys improve wettability, move the parameters closer to those of traditional solders, and affirm, as found in previous studies of Bi additions to the Sn-Ag-Cu near-eutectic compositions, that interfacial tensions and contact angles are the two parameters most important as a metric of wettability. However, in contrast to results found in studies of quaternary Sn-Ag-Cu-Bi alloys, the changes in quinary Sn-Ag-Cu-Bi-Sb alloys of interfacial tensions and contact angles do not correlate with decreasing wetting time and increasing wetting force.

[2006Mos1] Moser Z., Gasior W., Bukat K., Pstruś J., Kisiel R., Ohnuma I., Ishida K., *Pb – free solders - Wettability Testing of Sn-Ag-Cu Alloys with Bi Additions. Part I*, *J. Phase Equilib. Diffus.*, 27 (No 2), (2006), 1-6.

Abstract

Maximum bubble pressure, dilatometric, and meniscographic methods were used in the investigations of the surface tension, density, wetting time, wetting force, contact angle, and interfacial tension of liquid alloys of Sn-Ag-Cu eutectic composition with various additions of Bi. Density and surface tension measurements were conducted in the temperature range 250-900 °C. Surface tensions at 250 °C measured under a protective atmosphere of Ar-H₂ were combined with data from meniscographic studies done under air or with a protective flux. The meniscographic data with a nonwetted teflon substrate provided data on interfacial tension (solder-flux), surface tension in air, and meniscographic data with a Cu substrate allowed determinations of wetting time, wetting force, and calculation of contact angle. The calculated wetting angles from meniscographic studies for binary Sn-Ag eutectic and two ternary Sn-Ag-Cu alloys were verified by separate measurements by the sessile drop method under a protective atmosphere with a Cu substrate. Additions of Bi to both ternary alloys improve the wettability and move the parameters somewhat closer to those of traditional Sn-Pb solders.

[2006Mos2] Moser Z., Gasior W., Pstruś J., Ohnuma I., Ishida K.,
Influence of Sb additions on surface tension and density.
Experiment vs. Modeling. Z. Metallkd., 97 No. 4, (2006), 365-370.

Abstract

Surface tension and density measurements by the maximum bubble pressure and dilatometric techniques were carried out in an extensive range of temperature on liquid alloys close to the ternary eutectic Sn_{3.3}Ag_{0.76}Cu with different Sb content. It has been found that the addition of Sb to Sn, Sn-Sb, to binary eutectic Sn-Ag and to Sn_{3.3}Ag_{0.76}Cu decreases the surface tension and density. The values of the surface tension calculated by the Butler model and by the method based on the binary alloys surface tension data with the ternary and quaternary correction factors were compared with the experimental results. The best agreement between the measured and the calculated values was observed for the model comprising the binary data with the correction factors.

[2006Ohn] Ohnuma I., Ishida K., Moser Z., Gasior W., Bukat K., Pstruś J., Kisiel R., Sitek J., *Pb – free solders. Application of ADAMIS data base in modeling of Sn – Ag – Cu alloys with Bi additions. Part II. J. Phase Equilib. Diffus., 27 No 3, (2006), 245-254.*

Abstract

The ADAMIS data base was used for calculation of the surface tension of the quaternary Sn – Ag – Cu – Bi liquid alloys by the Butler model. The obtained data were compared with those from the maximum bubble pressure measurements from Part 1. The same thermodynamic data base was next applied for the calculation of various phase equilibria. It was established that the Bi addition to the ternary Sn – Ag – Cu alloys (Sn – 2.6Ag – 0.46Cu and Sn – 3.13Ag – 0.74Cu in at.% (Sn – 2.56Ag – 0.26 Cu and Sn – 2.86Ag – 0.40Cu in mass %)) causes lowering of the melting temperature and the surface tension to make the tested alloys closer to traditional Sn – Pb solders. The simulation of the solidification by the Scheil's model showed that the alloys with the higher Bi concentration are characterized by the lifting-off failure because of the segregation of Bi at the solder/substrate boundary. Thus, in modeling of new Pb - free solders, a compromise among various properties should be taken into consideration.

[2005Kis] Kisiel R., Gašior W., Moser Z., Pstruś J., Bukat K., Sitek J., *Electrical and Mechanical Studies of the Sn-Ag-Cu-Bi and Sn-Ag-Cu-Bi-Sb Lead Free Soldering Materials*, *Archs. Metall. and Mater.*, 50, (2005), 1065-1071.

Abstract

The electrical resistivity and the tensile strength of two near ternary eutectic Sn-Ag-Cu and four solder alloys close to ternary eutectic Sn-Ag-Cu with different Bi contents as well as eight Sn- Ag-Cu-Bi with different Sb contents in the form of wires were investigated. The four-probe technique was used for electrical parameter measurements. Equipment of the author's own construction for the tensile strength measurement was applied. It was found that the additions of Bi and Sb to Sn-Ag-Cu near eutectic alloys increase the resistivity and the tensile strength and that the resistivity of the Sn-Ag-Cu-Bi and Sn-Ag-Cu-Bi-Sb alloys is comparable with those of Pb-Sn solders for the bismuth and antimony content of about 3 atomic percent.

[2004Gas1] Gašior W., Moser Z., Pstruś J., Bukat K., Kisiel R., Sitek J.,
(Sn-Ag)_{eut} + Cu Soldering Materials, Part I: Wettability Studies, J. Phase Equilib. Diffus., 24 (2004), 115-121.

Abstract

The maximum bubble pressure, dilatometric, and meniscographic methods were used in investigations of the surface tension, density, wetting time, wetting force, contact angles, and interfacial tension of liquid (Sn-Ag)_{eut} and two (Sn-Ag)_{eut} + Cu alloys (Cu at.% = 0.46 and 0.74). The density and surface tension measurements were conducted in the temperature range from 230 to 950 °C, and the meniscographic investigations were carried out at 252 °C. The resultant values of surface tension were compared with those calculated from Butler's model based on optimized thermodynamic parameters and our data from earlier investigations. In an earlier study, experimental data for all investigated compositions (Cu at. % = 1.08 to 6.5) exhibit an increase in the surface tension with increasing temperature, while both ternary alloys of this study show a slight lowering tendency in comparison to (Sn-Ag)_{eut}. A more evident decreasing tendency of surface tension and interfacial tension was noted in meniscographic measurements, noting that data of interfacial tension are always lower than surface tension due to the role of the flux. Eight different fluxes were tested to select the lowest interfacial tension for the (Sn-Ag)_{eut}. ROLI (3% solids), which is the alcoholic solution of organic compounds and rosin activated by halogens, was recommended. In (Sn-Ag)_{eut} + Cu Soldering Materials, Part II: Electrical and Mechanical Studies, for the same (Sn-Ag)_{eut} and (Sn-Ag)_{eut} + Cu alloys (Cu at. % = 0.46 and 0.74), the electrical resistance and strength measurements will be presented in parallel with printed-circuit boards in wave soldering at 260 °C.

[2004Gas2] Gašior W., Moser Z., Pstruś J., Ishida K., Ohnuma I., *Surface Tension and Density Measurements of Sn-Ag-Sb Liquid Alloys and Phase Diagram Calculations of the Sn-Ag-Sb Ternary System*, Mater. Trans., 45, (2004), 652-660.

Abstract

The maximum bubble pressure method has been used to measure the surface tension of pure antimony and the surface tension and density (dilatometric method) of Sn-3.8at%Ag eutectic base alloys with 0.03, 0.06 and 0.09 mol fraction of antimony at a temperature range from 550 to 1200K. The linear dependencies of surface tension and density on temperature were observed and they were described by straight-line equations. Moreover, experimental determination of phase diagram and thermodynamic calculations in the Sn-Ag-Sb system were performed and the resulting optimized thermodynamic parameters were used for modeling of the surface tension. In addition, a non-equilibrium solidification process using the Scheil model was simulated and compared with the equilibrium solidification behavior of a Sn-Ag-Sb alloy.

[2004Gas3] Gasior W., Moser Z., Pstruś J., *SnAgCu+Sb Measurements of the Surface Tension and Density of Tin Based Sn-Ag-Cu-Sb Liquid Alloys*, *Archs. Metall. and Mater.*, **49**, (2004), 155-167.

Abstract

The maximum bubble pressure method for the determination of the surface tension and dilatometric technique for density measurements were applied in the studies of liquid quaternary Sn-Ag-Cu-Sb alloys close to the ternary eutectic (Sn-Ag-Cu). The investigations of the density were conducted in the temperature range from 513 K to 1186 K and those of the surface tension from 513 K to 1177 K. The experiments were carried out for the liquid alloy of composition close to the ternary eutectic (Sn_{3.3}Ag_{0.76}Cu) and for four quaternary liquid alloys (Sn-3.3Ag-0.76Cu) + Sb alloys ($X_{sb} = 0.03, 0.06, 0.09, 0.12$ mol fractions). It has been found that both surface tension and density show linear dependence on temperature. The relations describing the dependence of the surface tension and density on concentration were determined. The surface tension, density and molar volume isotherms calculated at 673 K and 1273 K have shown that the antimony addition to the ternary alloy (Sn-3.3Ag-0.76Cu) decreases the surface tension and the density while increase of the molar volume is observed. The maximal decrease of surface tension is slightly higher than 50 mN/m and that for density is about 0.15 g·cm³. The observed increase of molar volume is about 2.5 cm³ at the maximal Sb addition equal to 0.12 mole fraction.

[2004Kis] Kisiel R., Gąsior W., Moser Z., Pstruś J., Bukat K., Sitek J.,
*(Sn-Ag)_{eut} + Cu Soldering Materials, Part II: Electrical and
Mechanical Studies, J. Phase Equilib. Diffus., 24 (2004), 122-124.*

Abstract

Electrical (solder resistivity and solder joint resistance) and mechanical (tensile strength and shear strength of solder joints) parameters of the binary eutectic Sn-Ag and two alloys close to the ternary eutectic Sn-Ag-Cu composition were investigated. The four-probe technique was used for the measurement of electrical parameters. Special equipment was constructed for the tensile strength measurements and also for determination of the shear strengths of solder joints between a typical circuit component and a Cu contact on a printed circuit board (PCB). It was found that electrical and mechanical properties of the three alloys studied are comparable to data in the literature for traditional Pb-Sn solders. A joint resistance below 0.3 mΩ (Ω =ohm) and shear strength of above 20 MPa were found for an individual solder joint between a circuit component (in the current study a "jumper" resistor) and a copper surface on a PCB.

[2003Gas1] Gašior W., Moser Z., Pstruś J., Krzyżak B., Fitzner K.,
*Surface Tension and Thermodynamic Properties of the Liquid
Ag-Bi Solutions*, *J. Phase Equilib.*, 24, (2003), 40-49.

Abstract

With the maximum bubble pressure method, the density and surface tension were measured for five Ag-Bi liquid alloys ($X_m = 0.05, 0.15, 0.25, 0.5,$ and 0.75), as well as for pure silver. The experiments were performed in the temperature range 544-1443 K. Linear dependences of both density and surface tension versus temperature were observed, and therefore the experimental data were described by linear equations. The density dependence on concentration and temperature was derived using a polynomial method. A similar dependence of surface tension on temperature and concentration is presented. Next, the Gibbs energy of formation of solid Bi_2O_3 as well as activities of Bi in liquid Ag-Bi alloys, were determined by a solid-state electromotive force (emf) technique using the following galvanic cells: $\text{Ni}, \text{NiO}, \text{Pt}/\text{O}^{2-}/\text{W}, \text{Ag}_x\text{Bi}_{(1-x)}, \text{Bi}_2\text{O}_3(\text{s})$. The Gibbs energy of formation of solid Bi_2O_3 from pure elements was derived: $\Delta G_{f(\alpha\text{-Bi}_2\text{O}_3)}^0 = -598\,148 + 309.27T$ [$\text{J} \cdot \text{mol}^{-1}$] and $\Delta G_{f(\delta\text{-Bi}_2\text{O}_3)}^0 = -548\,009 + 258.94T$ [$\text{J} \cdot \text{mol}^{-1}$]; the temperature and the heat of the $\alpha \rightarrow \delta$ transformation for this solid oxide were calculated as 996 K and $50.14 \text{ J} \cdot \text{mol}^{-1}$. Activities of Bi in the liquid alloys were determined in the temperature range from 860-1075 K, for five Ag-Bi alloys ($X_{\text{Ag}} = 0.2, 0.35, 0.5, 0.65, 0.8$), and a Redlich-Kister polynomial expansion was used to describe the thermodynamic properties of the liquid phase. Using Thermo-Calc software, the Ag-Bi phase diagram was calculated. Finally, thermodynamic data were used to predict surface tension behavior in the Ag-Bi binary system.

[2003Gas2] Gašior W., Moser Z., Pstruś J., *Density and Surface Tension of Sb-Sn Liquid Alloys. Experiment vs. Modeling*, *J. Phase Equilib.*, **24**, (2003), 504-510.

Abstract

Through the application of the maximum bubble pressure and dilatometric methods, density and surface tension were investigated. The experiments were conducted in the temperature range from $583 \text{ K} \leq T \leq 1257 \text{ K}$. The surface tension was measured for pure antimony and for six liquid Sb-Sn alloys (mole fractions $X_{\text{Sn}} = 0.2, 0.4, 0.6, 0.8, 0.9, \text{ and } 0.935$ mm²) and measurements of-the density were only for alloys. It has been observed that both surface tension and density show linear dependence on temperature. The temperature-concentration relations were of both surface tension and density determined with minimization procedures. The surface tension isotherms calculated at 873 K and 1273 K show slight negative deviations from linearity changes, but the observed maximal differences did not exceed $30 \text{ mN} \cdot \text{m}^{-1}$. The surface tension calculated from Butler's model was higher than the experimental value for most concentrations and also showed curvilinear temperature dependence. The experimental densities and the molar volumes of the Sb-Sn liquid alloys conform very closely to ideal behavior with differences comparable to the experimental errors.

[2002Liu] Liu X.J., Inohana Y., Ohnuma I., Kainuma R., Ishida K., Moser Z., Gašior W., Pstruś J., *Experimental Determination and Thermodynamic Calculation of the Phase Equilibria and Surface tension of the Ag-Sn-In System*, *J. Electron. Mater.*, **31**, (2002), 1139-1151.

Abstract

The phase equilibria of the Sn-Ag-In system were investigated by means of differential scanning calorimetry (DSC) and metallography. The isothermal sections at 180-600 °C, as well as some vertical sections were determined. Thermodynamic assessment of this system was also carried out based on the experimental data of thermodynamic properties and phase equilibria using the CALPHAD method, in which the Gibbs energies of the liquid, fcc and hcp phases are described by the subregular solution model and those of compounds are represented by the sublattice model. The thermodynamic parameters for describing the phase equilibria were optimized, and reasonable agreement between the calculated and experimental results was obtained.

The maximum bubble - pressure and dilatometric method have been used in measurements of the surface tension and density of the binary In-Sn and the ternary (Sn-3.8Ag)_{eut}+In (5 and 10% at.) liquid alloys, respectively. The experiments were performed in the temperature range from 160 °C to 930 °C. The experimental data of the surface tension were compared with those obtained by the thermodynamic calculation of the Butler model.

[2002Mos] Moser Z., Gašior W., Pstruś J., Książek S., *Surface Tension and Density of the (Ag-Sn)_{eut}+Cu liquid Alloys*, *J. Electron. Mater.*, **31**, (2002), 1225-1229.

Abstract

The maximum bubble-pressure method has been used to measure the surface tension and density of liquid alloys (Ag-Sn)_{eut} + Cu ($X_{Cu} = 0.005, 0.020, 0.0375, \text{ and } 0.065$ (mole fraction)). The surface tension and density measurements were carried out in the temperature ranges of 262-942°C and 264-937°C, respectively. The linear dependencies of surface tensions and densities on temperature were observed, and they were described by straight-line equations. It has been found that the additions of Cu to the Ag-Sn eutectic alloy increase the surface tension. Experimental data of the surface tension were compared with those from modeling based on Butler method, using the optimized-thermodynamic parameters from the literature, and a slight tendency contrary to the experimental results was observed.

[2001Gas1] Gašior W., Moser Z., Pstruś J., Kucharski M., *Viscosity of the Pb-Sn Liquid Alloys*, *Archs. Metall.*, **46** (1), (2001), 23-32.

Abstract

The capillary method was used in the measurements of the viscosity of the lead-tin liquid alloys. The experiments were performed for the lead, tin and five lead-tin alloys of the concentration 0.1, 0.261 (eutectic), 0.5, 0.7 and 0.9 mole fraction of lead and between 521 K and 871 K. The experimental data on viscosity of pure components and liquid Pb-Sn alloys were described by the exponential equation $\eta = A \exp(E/RT)$. The dependence of viscosity on temperature and concentration was modeled by the K u c h a r s k i' method considered in the calculations the activity coefficients, the partial molar volume of components and the molar volume of liquid alloys. Obtained isotherms of viscosity at 623 K and 823 K have shown nearly linear changes with the concentration and a reasonable agreement with the experimental data. The observed differences when compared with data from the literature do not exceed 15 %.

[2001Gas2] Gašior W., Moser Z., Pstruś J., *Surface Tension and Density of the Pb-Sn Liquid Alloys*, *J.Phase Equilib.*, 22, (2001), 20-25.

Abstract

The maximum bubble pressure and the dilatometric method were used respectively in measurements of surface tension and density of Pb-Sn liquid alloys. The experiments were carried out in the temperature range from 573 K to 1200 K for the pure Pb, pure Sn and 7 alloys of the composition 0.1, 0.2, 0.26, 0.36, 0.5, 0.7 and 0.9 mole fraction of Pb. A straight-line dependence on temperature was observed and fitted by the method of least squares both for the densities and the surface tension. The calculated density isotherm at 673 K showed a positive deviation from the linearity over the entire range of composition, and the same tendency was seen at 1173 K for compositions higher than $X_{Pb}=0.26$. At the lower concentration of Pb a nearly linear character of isotherm was noted. In the case of the surface tension, both at the lowest and the highest temperatures (673 K, 1173 K), the deviation from linearity with composition was negative, but deviation decreased with increasing temperature. The isotherms of the compositional dependence of surface tension calculated from the Butler model exhibit good agreement with the experimental data.

[2001Mos1] Moser Z., Gašior W., Pstruś J., *Density and surface tension of the Ag-Sn liquid alloys*, *J. Phase Equilib.*, **22**, (2001), 254-258.

Abstract

The maximum bubble pressure method has been used to measure the surface tension of pure tin and seven binary alloys with concentrations of 15,30,40, 60, 75,87.8, and 96.2 at.% Sn. Measurements were performed at the temperature range from 500 to about 1400 K depending on the composition of the investigated alloy. Densities of the Ag-Sn alloys were measured dilatometrically. The linear dependencies of densities and surface tensions on temperature were observed, and they are described by a straight-line equation.

Experimental data of the surface tensions were compared with calculations using Butler's model, which assumes an equilibrium between the bulk phase and the monolayer surface phase. Excess Gibbs energies of silver and tin necessary in calculations were taken from the optimized thermodynamic parameters reported recently from Tohoku University. It is shown that the calculated surface tension data from the optimized thermodynamic parameters of the liquid phase of the Ag-Sn are in good agreement with the experimental results.

[2001Mos2] Moser Z., Gašior W., Pstruś J., Zakulski W., Ohnuma I., Liu X.J., Inohana Y., Ishida K., *Density and surface tension of the Ag-In liquid alloys*, *J. Electron. Mater.*, **30**, (2001), 1120-1128.

Abstract

The phase boundaries of the Ag-In binary system were determined by the diffusion couple method, differential scanning calorimetry (DSC) and metallographic techniques. The results show that the region of the ζ (hcp) phase is narrower than that reported previously. Thermodynamic calculation of the Ag-In system is presented by taking into account the experimental results obtained by the present and previous works, including the data on the phase equilibria and thermochemical properties. The Gibbs energies of liquid and solid solution phases are described on the basis of the sub-regular solution model, and that of the intermetallic compounds are based on the two-sublattices model. A consistent set of thermodynamic parameters has been optimized for describing the Gibbs energy of each phase, which leads to a good fit between calculated and experimental results. The maximum bubble pressure method has been used to measure the surface tension and densities of liquid In, Ag, and five binary alloys in the temperature range from 227°C to about 1170°C. On the basis of the thermodynamic parameters of the liquid phase obtained by the present optimization, the surface tensions are calculated using Butler's model. It is shown that the calculated values of the surface tensions are in fair agreement with the experimental data.

[2001Mos3] Moser Z., Gašior W., Pstruś J., *Surface tension measurements of the Sn-Bi and Sn-Bi-Ag liquid alloys*, *J. Electron. Mater.*, **30**, (2001), 1104-1111.

Abstract

The maximum bubble pressure method has been used to measure the surface tension of pure Bi, surface tension and density of liquid binary Bi-Sn alloys ($X_{\text{Bi}} = 0.2, 0.4, 0.6, \text{ and } 0.8$ molar fractions) at the temperature range from about 500 K to 1150 K. Similarly, there were investigated ternary alloys adding to the eutectic (3.8 at. %Ag-Sn) 0.03, 0.06, 0.09, and 0.12 molar fractions of Bi. The linear dependencies of densities and surface tensions on temperature were observed and they were described by straight-line equations. It has been confirmed that the additions of Bi to liquid Sn and to the eutectic alloy (3.8 at. %Ag-Sn) markedly reduce the surface tension. Experimental data of the surface tension of liquid Bi-Sn were compared with modeling based on Butler's method and a reasonable agreement was observed.

Authors:

Prof. Władysław Gąsior, PhD. DSc. Eng. is an employee at A. Krupkowski Institute of Metallurgy and Materials Science of the Polish Academy of Sciences. At present, he is the head of the Metallurgic Processes Theory Laboratory. He specializes in studies of the thermodynamic and physical properties of alloys and modelling of surface tension and viscosity. He has developed a mono-atomic surface layer model, which well correlates the surface tension with the excess Gibbs free energy, as well as an entropic viscosity model. He is author and co-author of over 190 publications and over 120 presentations showed at domestic and international conferences. He has participated in studies realized within international scientific programs COST 531, COST 535 and COST MP 0601. He is a reviewer of articles published in journals included in the Institute of Scientific Information list, a member of Technical Science Committee of the Polish Academy of Arts and Sciences, National Committee for the Cooperation with the Committee on Data for Science and Technology ICSU (CODATA) and National Committee for the Cooperation with the Alloy Phase Diagram Committee (APDIC). He was a Member of the External Expert Group for Delphi Analyses of the National Program Foresight Poland 2020 as well as co-executor of a series of research projects of Ministry of Science and Higher Education. He is co-author of the first and second book edition (SURDAT and SURDAT 2) as well as the computer version of the database.

Adam Dębski, PhD. DSc. Eng. is an employee at A. Krupkowski Institute of Metallurgy and Materials Science of the Polish Academy of Sciences. At present, he is the head of the Physico-Chemical Research Laboratory. He specializes in studies of the thermodynamic and physical properties of alloys. He is author and co-author of 90 publications, including 59 from the JCR list. He has participated in research works realized within international scientific programs COST 535 and COST MP 0601. He is a reviewer of articles published in journals included in the JCR list. He is a co-executor of a series of research projects of Ministry of Science and Higher education and National Science Centre. He is co-author of the first and second book edition (SURDAT and SURDAT 2) as well as the computer version of the database.

Reviewer:

John „Jack” F. Smith†, PhD, died on Sept. 26, 2015. He was a long-time MSE professor and an Ames Laboratory scientist. He began his 40-year career at Iowa State University and Ames Laboratory in 1948, where he was a professor of metallurgy and a senior scientist. He served as chairman of ISU's Department of Metallurgy from 1966 to 1970, and a section chief for the Metallurgy and Ceramics department. He was elected a Fellow of the American Institute of Chemists in 1969 and the American Society of Metals (ASM) in 1984. Smith worked for 24 years as the editor of the ASM Journal of Phase Equilibria and Diffusion. In 2007, Smith was named an International Member of the Polish Academy of Arts and Sciences. He authored more than 180 technical papers as well as a book on thorium. His research focused on multicomponent diffusion and phase diagrams, phase transformations, heat treatment, high temperature coatings, gas/solid reactions and irradiation damage.

John „Jack ” F. Smith was a pilot for the U.S. Navy during World War II and served on the Pacific on the carrier USS Suwannee. In 1995, he published a book about his time on the Suwannee entitled "Hellcats over the Philippine Deep". Smith was an avid pilot, taking up gliding later on in his life.

ISBN 978-83-60768-08-2